SYNTHESES AND PHYSICAL STUDIES OF DINUCLEAR RHENIUM COMPLEXES AS PRECURSORS FOR POTENTIAL MOLECULAR WIRE APPLICATIONS

DISSERTATION

zur

Erlangung der naturwissenschaftlichen Doktorwürde

(Dr. sc. nat.)

Vorgelegt der

Mathematisch-naturwissenschaftlichen Fakultät

der

Universität Zürich

von

YAN LI

aus

V. R. China

Promotionskomitee

Prof. Dr. Heinz Berke (Vorsitz und Leitung)

Prof. Dr. Roland K. O. Sigel

Prof. Dr. Roger Alberto

Prof. Dr. Eva Freisinger

Prof. Dr. Greta R. Patzke

Zurich 2011

CONTENT

LIST OF ABBREVIATIONS

A	acceptor
AFM	atomic force microscopy
AFMBJ	Atomic-force-microscopy break junction
B	bridge
Cp	cyclopentadienyl
Cp*	pentamethylcyclopentadienyl
CV	cyclic voltammetry
D	donor
DBU	1,8-Diazabicycloundec-7-ene
DIEPA	*N*,*N*-Diisopropylethylamine
depe	1,2-Bis(diethylphosphinoethane))
dmpe	1,2-Bis(dimethylphosphinoethane))
DFT	density functional theory
e^-	electron
EPR	electron paramagnetic resonance
g	*g* factor
ΔG^*	free energy of activation
h	planck constant
H_{ab}	electronic coupling energy
HSAB	Hard-soft acid-base theory
IVCT	inter valence charge transfer
IR	infrared

K_c	comproportionation constant
λ	reorganization energy
L	ligand
LDA	lithium diisopropylamide
LICKOR	KO*t*Bu/*n*-BuLi mixture
M	metal
MCBJ	mechanically controllable break junction
MLCT	metal-to-ligand charge transfer
MMCT	metal-to-metal charge transfer
MoSI	$Mo_6S_{9-x}I_x$
MV	mixed valence
MWNT	multi-wall nanotube
NIR	near infrared
NMR	nuclear magnetic resonance
OPEs	oligi(1,4-phenylene ethylene)s
OPVs	oligi(1,4-phenylene vinylene)s
OTEs	oligi(2,5-thiophene ethynylene)s
OTf	triflate
Ox.	oxidation
Ψ	wave function
quint	quintet (spectral)
Red.	reduction
Ref.	reference (in tables)
r.t.	room temperature

s	singlet (spectral)
S_{ab}	overlap integral
sept	septet (spectral)
STM	scanning tunneling microscopy
STMBJ	scanning tunneling microscopy break junction
SWNT	single-walled carbon nanotube
THF	tetrahydrofuran
t	triplet (spectral)
TBD	triazabicyclodecene
Γ	delocalization parameter
UHV	Ultra-high vacuum
UV-vis	Ultraviolet-visible spectroscopy
X	Reaction coordinate
χ_m	molar magnetic susceptibility

LIST OF PREPARED METAL COMPLEXES

Dinitrogen rhenium complex

trans-[$ReCl(N_2)(PMe_3)_4$] (**1**)

Mononuclear rhenium vinylidene complexes

trans-[$ReCl(=C=CHSiMe_3)(PMe_3)_4$] (**2**)

trans-[$ReCl(=C=CH_2)(PMe_3)_4$] (**3**)

trans-[$Re(=C=CH_2)(C\equiv CSiMe_3)(PMe_3)_4$] (**7**)

Mononuclear rhenium carbyne complexes

trans-[$ReCl(\equiv C\text{-}CH_3)(PMe_3)_4$]Cl (**4**)

trans-[$ReCl(\equiv C\text{-}CH_3)(PMe_3)_4$][$PF_6$] (**5**)

trans-[$Re(C\equiv CSiMe_3)(\equiv C\text{-}CH_3)(PMe_3)_4$][$PF_6$] (**6**)

trans-[$Re(C\equiv CSiMe_3)(\equiv C\text{-}CH_3)(PMe_3)_4$]Cl (**8**)

Dinuclear rhenium Complexes

trans-[$Cl(PMe_3)_4Re\equiv C\text{-}CH_2\text{-}CH_2\text{-}C\equiv Re(PMe_3)_4Cl$][$PF_6$]$_2$ (**9**)

trans-[$(Me_3SiC\equiv C)(PMe_3)_4Re\equiv C\text{-}CH_2\text{-}CH_2\text{-}C\equiv Re(PMe_3)_4(C\equiv CSiMe_3)$][$PF_6$]$_2$ (**10**)

trans-[$Cl(PMe_3)_4Re=C=CH\text{-}CH=C=Re(PMe_3)_4Cl$] (**11**)

trans-[$Cl(PMe_3)_4Re\equiv C\text{-}CH=CH\text{-}C\equiv Re(PMe_3)_4Cl$][$PF_6$] (**11[$PF_6$]**)

trans-[$Cl(PMe_3)_4Re\equiv C\text{-}CH=CH\text{-}C\equiv Re(PMe_3)_4Cl$][$PF_6$] (**11[$PF_6$]**)

trans-[$(Me_3SiC\equiv C)(PMe_3)_4Re=C=CH\text{-}CH=C=Re(PMe_3)_4(C\equiv CSiMe_3)$] (**12**)

trans-[$(Me_3SiC{\equiv}C)(PMe_3)_4Re{\equiv}C$-CH=CH-$C{\equiv}Re(PMe_3)_4(C{\equiv}CSiMe_3)][PF_6]$ (**12[PF_6]**)

trans-[$(Me_3SiC{\equiv}C)(PMe_3)_4Re{\equiv}C$-CH=CH-$C{\equiv}Re(PMe_3)_4(C{\equiv}CSiMe_3)][PF_6]_2$ (**12[PF_6]$_2$**)

trans-[$Cl(PMe_3)_4Re{\equiv}C$-$C{\equiv}C$-$C{\equiv}Re(PMe_3)_4Cl][OTf]_2$ (**13**)

trans-[$Cl(PMe_3)_4Re$=C=C=C=$Re(PMe_3)_4Cl]$ (**14**)

trans-[$Cl(PMe_3)_4Re{\equiv}C$-$C{\equiv}C$-$C{\equiv}Re(PMe_3)_4Cl][PF_6]_2$ (**14[PF_6]$_2$**)

trans-[$(Me_3SiC{\equiv}C)(PMe_3)_4Re$=C=C=C=$Re(PMe_3)_4(C{\equiv}CSiMe_3)]$ (**15**)

trans-[$Me_3SiC{\equiv}C)(PMe_3)_4Re{\equiv}C$-$C{\equiv}C$-$C{\equiv}Re(PMe_3)_4(C{\equiv}CSiMe_3)][PF_6]_2$ (**15[PF_6]$_2$**)

trans-[$I(PMe_3)_4Re$=C=CH-CH=C=$Re(PMe_3)_4I]$ (**16**)

trans-[$I(PMe_3)_4Re{\equiv}C$-CH=CH-$C{\equiv}Re(PMe_3)_4I][PF_6]_2$ (**16[PF_6]$_2$**)

1. Introduction

1.1 Research background and scopes

In 1965, based on empiric observation, Intel co-founder Gordon Moore predicted that the number of transistors on a microchip would double every 1 to 2 years (Moore's Law). At that time there were just 30 transistors on a chip.[1-2] Since then, Moore's Law has gained a stunning success. The number of transistors in Intel microprocessors has grown substantially over time. In 2008, Intel reported that there were 2 billion transistors on the 65-nanometer Tukwila Itanium chip and the downsizing of silicon chips would continue to hold good through 2029.[3] However, it is becoming increasingly apparent that the ability to cram more transistors onto silicon chip will rapidly face its fundamental limits.[4-5] To further proceed toward miniaturization, science and technology will have to find new ways. An alternative and promising strategy is the "bottom-up" molecular-by-molecular approach, which starts from molecules with distinct shapes and properties and builds up to nanostructures.[6-7] In the last two decades chemists, who have always been working at atoms and molecules, have taken up this challenge. At the same time, the new powerful techniques, such as scanning tunneling microscopy (STM)[8-10] and atomic force microscopy (AFM)[11-13], make the "seeing" and "manipulating" single molecules more convenient. Starting from molecules, chemists have shown abilities to design and construct artificial molecular-level devices and machines.[14-19] The fancy idea of utilizing single molecules as an individual device is no longer an unreachable task. It is predicted that the progressive miniaturization will not only reduce the size and increase the power of computers, but also open the way to new technologies capable of revolutionizing medicine, producing a wealthy of new materials, providing renewable energy sources, and solving the problem of environmental pollution.[7,20]

Molecular-level devices and machines can be defined as an assembly of a discrete number of molecular components designed to achieve specific functions. Like macroscopic devices and machines, they also need energy to operate and signal to communicate with the operator.[21] During the recent years, in the pursuit of miniaturization of electronic components, the field of molecular electronics has greatly expanded in chemistry, physics, and materials science.[22-23] Molecular electronics can be defined as any devices utilizing molecular properties to perform electronic functions.[19] The pioneering effort in this field began in 1974 with the work of Aviram

and Ratner. They prepared and characterized an organic donor-σ-acceptor (D-σ-A) species, which they believed would function as a molecular rectifier.[24] A significant effort is currently being devoted to the design and construction of single molecular electrical devices[25-28] and the fabrication of simple molecular-scale circuits[20,29-30]. However, molecular electronics is still in its infancy. There is a lot remains to be learned, such as the electrical properties of molecules and how these properties correlate with the structures, the nature of metal-molecule-metal junctions and how to control the geometry of the junction and so on.[31-36] There are also difficulties concerning the means of manipulating, bonding, and ordering molecules in circuit-like structures and how molecular components may be combined to realize useful electronic functions.[37-42]

Molecular electronics is a very large field including many components, such as wires, switches, transistors, memories, diodes and rectifiers and so on. Molecular wire is one of the basic components of a molecular-level electrical circuit. Many sophisticated devices are based on molecular wires. A molecular wire is a "One dimensional molecule allowing a through-bridge exchange of an electron or hole between its remote ends or terminal groups, themselves able to exchange electrons with the outside world".[43] Based on this definition, the fabrication of wire-like molecule capable to "wire-up" to the other components, the evaluation of the electron conduction capability of the molecule and its ability to convey electrons to the contacts such as electrodes is very crucial. Therefore much effort has been devoted to devising experimental methods to fabricate reliable wire-like or rod-type compounds and developing theoretical and experimental tools to evaluate and test the electronic conductivity of a molecule. During the last two decades, there are mainly three types of wire-like compounds that have drawn much attention of the research community: nanotubes,[44-46] organic molecular wires[22] and organometallic molecular wires.[19] Although great progress has been made in this field, it has to be pointed out that the ongoing investigations are fundamental and there is still much work left for their real application as a "wire".

Due to the scope and limitation of this thesis, the first two topics will only be mentioned briefly, whereas the last one will be discussed in depth.

Nanotubes, such as carbon nanotubes and transition metal chalcogenide-halide nanowires, are one of the interesting areas for molecular scale wires. Carbon nanotubes (Figure 1-1) were discovered by Iijima in 1991,[47] since then the investigation on the syntheses and the propertie have improved dramatically.[48-49] It has been observed that the largest resistance in a nanotube

wire arises from the contact resistance between an electrode and the nanotube, which suggests that carbon nanotubes will make very efficient wires in nanoscale systems, if they can be connected well.[19] Unfortunately, the functionalized ends of carbon nanotubes are typically not conducting due to the non-covalent contact, which limits their usefulness as molecular connectors. Although, individual carbon nanotube can be soldered in an electron microscope, the poor dispersion characteristics makes them difficult to be self-assembled.[50]

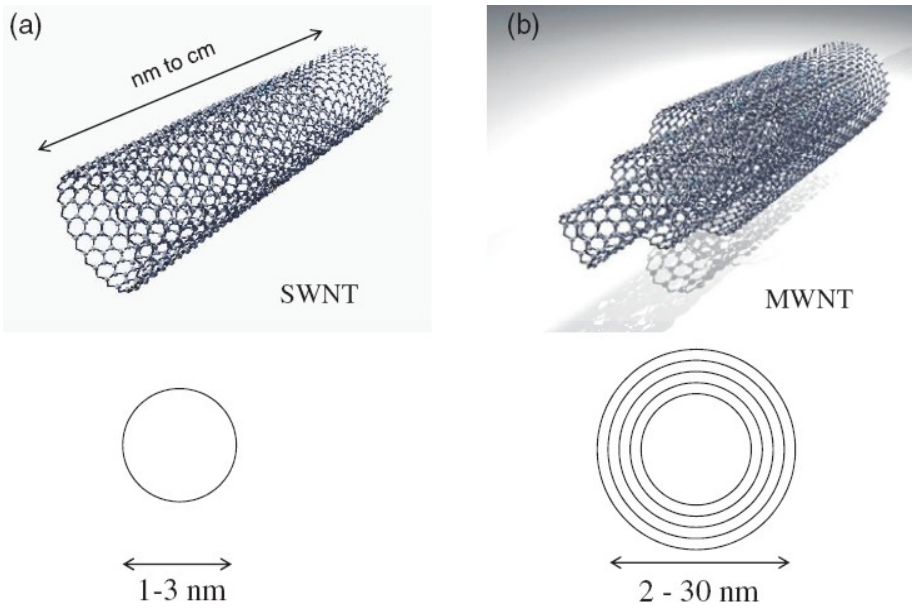

Figure 1-1. Schematic view and typical size of (a) a single-walled carbon nanotube (SWNT); (b) a multi-wall nanotube (MWNT)[51]

Since the discovery of an air-stable nanowire with the formula $Mo_6S_3I_6$ in 2004,[52] the $Mo_6S_{9-x}I_x$ ($4 < x < 6$) (or MoSI) nanowires have been considered as a potential replacement for carbon nanotubes. The material with superior dispersion characteristics is relatively easily synthesized and isolated. It is reported that a single 0.9 nm diameter MoSI molecular wire is reproducibly obtained with lengths up to 100 μm. They conduct electrically and the measurements of the single-bundle longitudinal conductivity have shown metallic behavior in the ohmic regime. The very good dispersion characteristics in a variety of solvents including water makes the assembly of circuits involving single nanowires or thin bundles by self-assembly possible. The molecular wires have S atoms at the ends, allowing covalent bonds to gold surfaces or to thiol groups on larger molecules, which are commonly used for connecting molecules to contacts. These

properties make MoSI molecular wires a promising breakthrough in molecular-scale connectors for making large-scale self-assembled circuits.[50,53]

Organic molecular wire is a rapidly expanding field following the early work of Aviram and Ratner. Most research in this field has concentrated on the syntheses and the electronic behaviors of linear, conjugated oligomers. A variety of wire-like organic compounds have been available (Figure 1-2 and Figure 1-3).

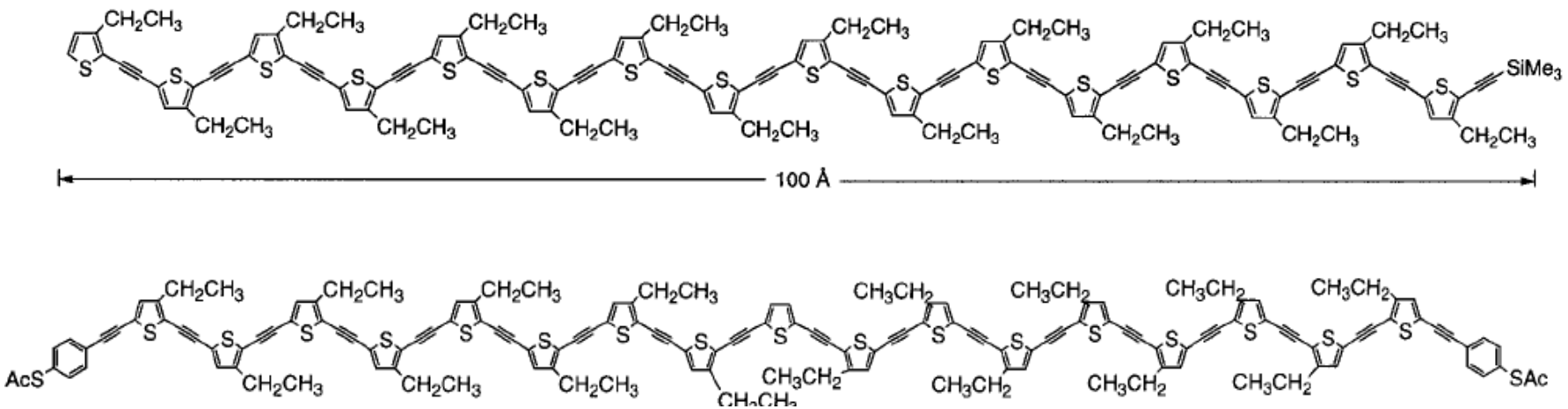
SiMe3
100 Å
AcS
SAc

(a)

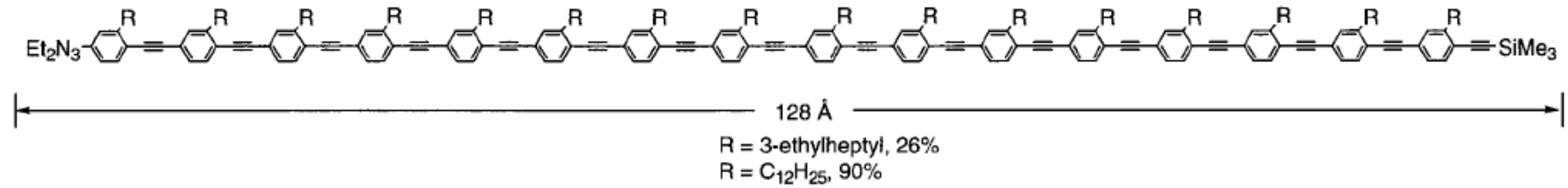
Et2N3
SiMe3
128 Å
R = 3-ethylheptyl, 26%
R = C12H25, 90%

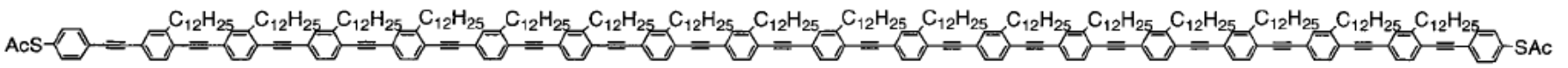
AcS
SAc

(b)

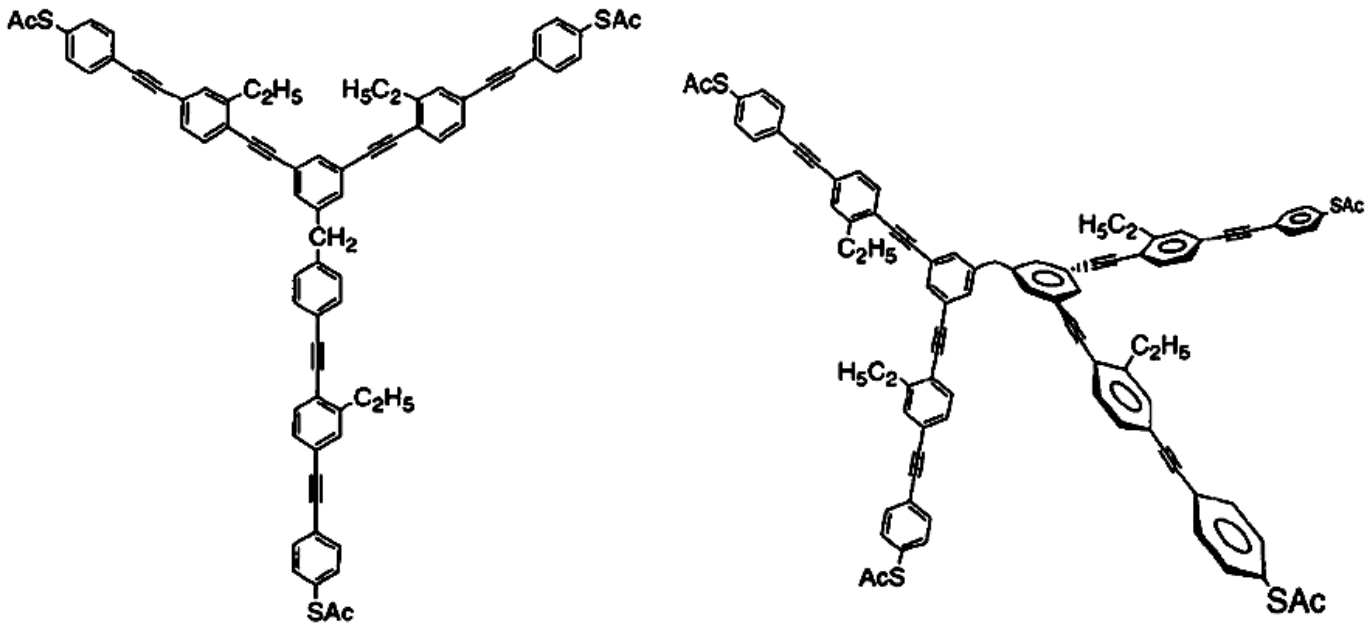

(c)

Figure 1-2. Examples of some of the organic molecular wires: (a) oligo(thiophene ethynylene); (b) oligo(phenylene ethylene); (c) oligo(phenylene ethylene)s with three and four terminals;[23]

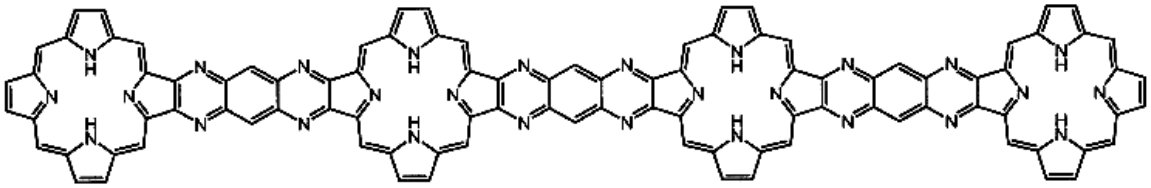

Figure 1-3. Example of porphyrin-based molecular wire[19]

One class of compounds synthesized are oligo(2,5-thiophene ethynylene)s (OTEs). Many wire-like molecules of this type have been synthesized and the longest one was 12.8 nm in length with thioester group at one or both ends. The *in-situ* deprotection of the thioester group to the thiol group enables the molecules to adhere to Au or other metals surfaces. The second class of molecules that has been studied are the oligo(1,4-phenylene ethylene)s (OPEs). In a series of syntheses of molecules in OPE subclasses, Tour and coworker have made products with more than 2 terminals. A variety of compounds such as U-shaped OPE-based molecules, OPEs with C_{60} stoppers and OPEs with different alligator clips have also been synthesized. The third class of compounds are the olig(1,4-phenylene vinylene)s (OPVs) with protected thiol groups at one side or both sides. Aromatic ladder oligomers with a defined length, rigidity, extended π-conjugation for good electron transfer and good electronic coupling with metallic contacts have also been studied. Oligophenylenes and polyphenylenes class of molecules, possessing continuous overlap of molecular orbitals through extended conjugation without intervening groups such as alkynes or olefins have been an active area of research. Acetylene oligomers synthesized by Diederich and coworkers consist of another class of organic molecular wires. Potential molecular wires composed of fused porphyrin rings have also been constructed.[19,22]

For years, intensive research has been oriented towards the central issue the electronic conductivity of these fabricated wire-like organic compounds. Recent research indicate that the "conductance" of organic wire-like molecules decrease exponentially with molecular length and the charge transport mechanism changes from direct tunneling to hopping, as evidenced by a change in the length dependence of the electron transfer rate constant.[54-57]

Organometallic molecular wires consisting of a "conducting" conjugated organic bridge with redox-active metal end-groups have drawn much attention in the last two decades. Incorporation of redox-active metal centers into rigid-rod π-conjugated organic backbones seems to be a useful strategy to obtain long and highly "conductive" molecular wires, which has been verified by

several studies.[58-59] Various organometallic wire-like molecules consisting of diverse transition metal fragments bridged by different conjugated chains have been expanded quickly. Ceccon and coworkers[60] and O'Hare and coworkers[61] have published reviews on hetero- and homobimetallic systems in 2004 and 2010, respectively. The complexes reviewed by them depended chiefly on the nature of the unsaturated hydrocarbon bridges. Herein, the survey will be carried out according to the group of the transition metal. In view of limitation of the scope, only group 7 transition metal (manganese and rhenium) complexes with symmetric unsaturated hydrocarbon bridges will be reviewed in detail. Prior to the literature overview, the theories and techniques adopted to investigate the electron transfer properties of the mixed-valence systems and the molecular conductance will be introduced.

1.2 Organometallic molecular wires

As a molecular wire, the most important characteristic is its conductivity. Namely, how effective is the charge transfer from one end of the molecule to the other? An ideal molecular wire would transfer charge over long distances at very fast rates.[19] Therefore, the evaluation of the ability of a compound to conduct electrons is very necessary before the consideration of it as a "wire".

1.2.1 ET in MV systems

The conductivity property of a compound is related greatly to the field of electron transfer (ET). The simplest model systems for studying electron transfer (ET) and delocalization are mixed-valence (MV) species.[62] MV systems (Figure 1-4) containing electron donor (D) and electron acceptor (A) sites separated by a bridge began to attract great interest in the late 1960s because of the new properties exhibited when significant electron coupling between the donor and acceptor sites is presented and because of the relationships between the optical properties and electron transfer rates of the species.[63-64]

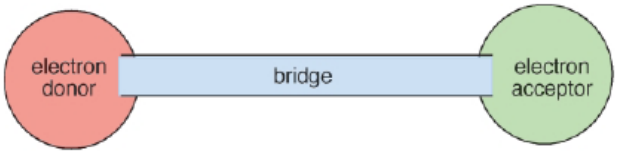

Figure 1-4. Mixed-valence (MV) molecules contain donor (D) and acceptor (A) sites separated by a bridge[63]

In MV systems, donors (D) and acceptors (A) sites could be metal centers or organic groups, such as quinone and amine etc.[65-66] Bimetallic complexes shown in Figure 1-5a, where two metal centers linked by a bridging ligand, are often precursors of stable MV species because of a pronounced through-bridge electronic interaction. If such a complex is oxidized or reduced by one electron, it forms species where the unpaired electron could be delocalized between metal centers to a different extent.[67-76] A classical example of the MV complexes is a Creutz–Taube ion shown in Figure 1-5b.[77]

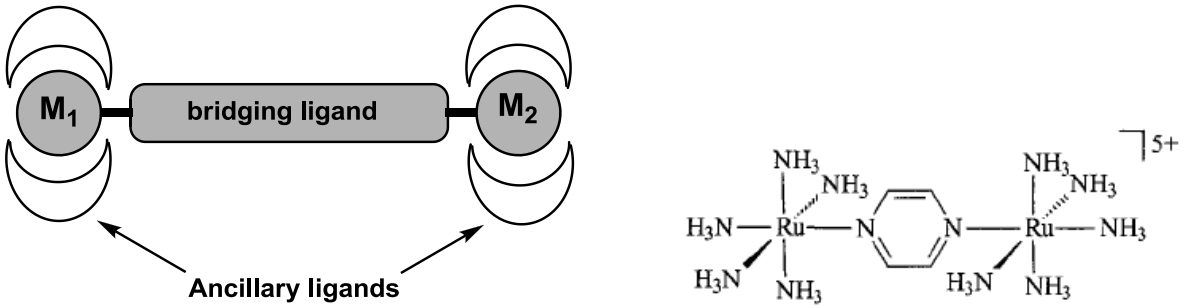

(a) (b)

Figure 1-5. (a) Representation of a bimetallic metal complex; (b) Structure of Creutz-Taube ion

The strength of the electronic interaction between the metal centers exerts great influences on the magnetic, optical, and redox properties of a wire-like complex. *Vice versa*, a complete investigation of these properties would give us a comprehensive picture of the electronic interaction. The frequently used physical techniques to investigate electronic interaction of MV systems are listed in Table 1-1, some of them will be discussed in more detail.

Table 1-1. Techniques used to investigate the valence trapping in the [M]-(bridge)-[M] mixed-valence systems

Techniques	Objects	Features	Time scales[64] (s)
Near IR (IVCT)	MV complexes	Based on the energy, intensity and half-height bandwidth of the IVCT absorption band to classified MV complexes.	10^{-11}
Cyclic voltammetry (CV)	Complexes with any oxidation state	Extraction of ΔE (or K_c) form redox couples. ΔE is an indicator of the stability and electronic coupling of MV complexes.	/
X-ray crystallography	MV complexes	Identification of MV complexes from the structure information, such as the variation of the M-C bond lengths.	/
NMR	Complexes with any oxidation state	It is useful for the diamagnetic system, but difficult to extract information from paramagnetic MV complexes.	$10^{-3} \sim 10^{-8}$
IR	Complexes with any oxidation state	IR strengths for groups connected to isolated oxidation state metal or with delocalized electron.	10^{-13}
EPR	MV complexes	Identification of the location of the unpaired electron in MV system from hyperfine splitting and g anisotropy.	$10^{-7} \sim 10^{-11}$
^{57}Fe-Mössbauer Spectroscopy	MV complexes containing Fe	It is helpful to place a time scale on the electron exchange.	$10^{-7} \sim 10^{-9}$
Magnetization measurement	Complexes with any oxidation state ($J \neq 0$)	Investigation of antiferromagnetic or ferromagnetic interactions between spins	/
DFT calculation	MV complexes	Providing accurate description of the ground- and excited-state, but tending to overdelocalize the unpair electron.[61]	/

1.2.1.1 ET theory and NIR spectroscopy

The electronic interaction between two metal centers within a system can be investigated using the Marcus theory of ET, which is restricted to weakly coupled systems.[60] Consider a MV molecule that has a symmetric bridge and two identical redox sites (the donor D and acceptor A sites) except for their oxidation states (a $\Delta G^{\circ} = 0$ symmetrical system), there is a difference in the intramolecular equilibrium and the solvent configurations at the donor and acceptor sites. As a result, the two sites are not equivalent and with a barrier for their interconversion. Because electron motion is much faster than nuclear motion, energy conservation requires that, prior to the actual electron transfer, the nuclear configurations of the reactants and the surrounding medium adjust from their equilibrium values to an intermediate configuration in which there is no energy change when the electron transfers from the donor to the acceptor. For metal complexes in a polar solvent, the nuclear configuration changes involve adjustments in the metal–ligand and intraligand bond lengths and angles, and changes in the orientations of the surrounding solvent molecules. Depending on the interplay between the nuclear and electronic frequencies, ET reactions are categorized to be weakly coupled when a non-adiabatic ET occurs and strongly coupled when an adiabatic transfer happens.

Similar to common chemical reactions, the intramolecular ET reaction can be described by the parabolic free energy plots, *i.e.*, the motion of the system on an energy surface from the initial to the final state *via* transition state. The interconversion of the two states of a weakly coupled MV system is both an isomerization and a charge transfer reaction.

$$\text{D-B-A} \rightleftharpoons \text{D}^{+}\text{-B-A}^{-} \quad (1)$$

In either case the distortions of the initial and final states of the MV system can be described in terms of displacements on harmonic free-energy curves with identical force constants. The free energy of the initial state (D-B-A) plus surrounding medium (Curve G_a, wave function Ψ_a) and the free energy of the final state (D^{+}-B-A^{-}) plus surrounding medium (Curve G_b, wave function Ψ_b) of a symmetric mixed-valence system ($\Delta G^{\circ} = 0$) are plotted *vs.* the reaction coordinate X in Figure 1-6. X varies from 0 to 1 as the reaction proceeds. E_{op} is the energy of the donor–acceptor (metal-to-metal MMCT or intervalence IVCT) charge-transfer transition. The reorganization parameter λ is the vertical difference between the free energies of the non-interacting reactants and the products at the reactants' equilibrium configuration. According to Hush theory, in a

symmetrical MV system, $E_{op} = h\nu_{max} = \lambda$. H_{ab} is the electronic coupling matrix element between the two diabatic states.

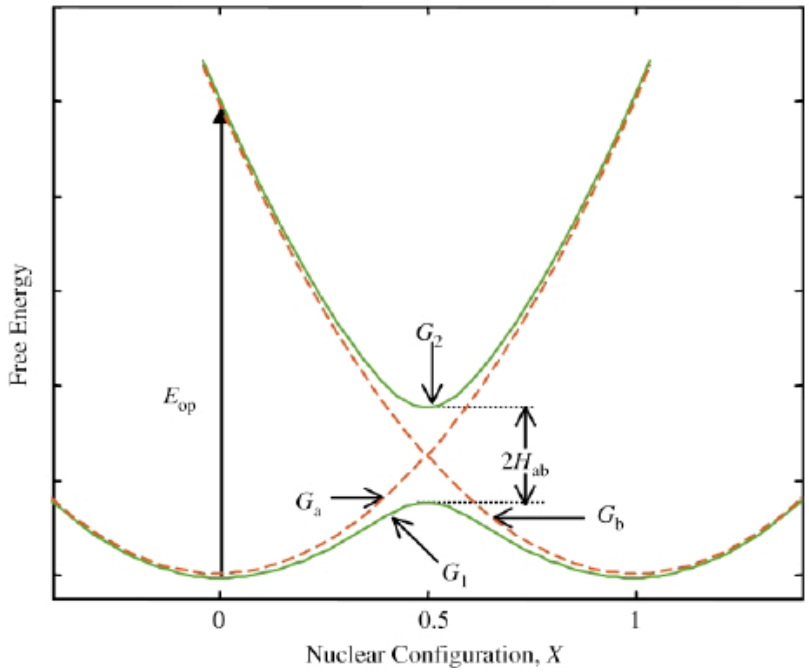

Figure 1-6. Plots of the free-energies of the initial (left-hand parabola, G_a) and final (right-hand parabola, G_b) diabatic states and the lower (G_1) and upper (G_2) adiabatic states of a symmetric mixed-valence system *vs.* the reaction coordinate X.[63]

The free energies G_a and G_b are the energies of the zero-order or diabatic states of the system and are related to X by

$$G_a = \lambda X^2 \qquad (1)$$

$$G_b = \lambda (X-1)^2 \qquad (2)$$

The interaction of the zero-order states gives rise to two linear combinations, the first-order or adiabatic states,

$$\Psi_1 = c_a\Psi_a + c_b\Psi_b \qquad (3)$$

$$\Psi_2 = c_a\Psi_b - c_b\Psi_a \qquad (4)$$

where Ψ_1 is the wave function for the lower (ground) adiabatic state and Ψ_2 is the wave function for the upper (excited) adiabatic state (energies G_1 and G_2, respectively), and the mixing coefficients are normalized, *i.e.*, $c_a^2 + c_b^2 = 1$. The overlap integral S_{ab} is neglected (or is zero by construction). The energies of the adiabatic states, obtained by solving the two-state secular determinant, are given by

$$G_1 = 0.5\{(G_b + G_a) - [(G_b - G_a)^2 + 4H_{ab}^2]^{1/2}\} \quad (5)$$

$$G_2 = 0.5\{(G_b + G_a) + [(G_b - G_a)^2 + 4H_{ab}^2]^{1/2}\} \quad (6)$$

Utilizing eq. 5 and eq. 6, the difference between the adiabatic energies is given by

$$(G_2 - G_1) = [(G_b - G_a)^2 + 4H_{ab}^2]^{1/2} = \{[\lambda(1 - 2X)]^2 + 4H_{ab}^2\}^{1/2} \quad (7)$$

As shown in Figure 1-5, the splitting at the intersection is $2H_{ab}$ and the barrier to electron transfer is lowered by H_{ab}. The free energy of activation for interconversion of the sites is then

$$\Delta G^* = (\lambda - 2H_{ab})^2/4\lambda \quad (8)$$

The corresponding kinetic rate constant is given by

$$k_{ET} = A\exp(-\Delta G^*/k_B T) = A\exp[-(\lambda - 2H_{ab})^2/4\lambda k_B T] \quad (9)$$

where k_B is the Boltzman constant and T is temperature. The prefactor A is dependent on the electronic coupling. For weak coupling (non-adiabatic ET), A is an electron-hopping frequency equal to $(2H_{ab}^2/h)(\pi^3/\lambda RT)^{1/2}$, while for strong coupling (adiabatic ET), A is determined by a nuclear vibration frequency ν_n ($\sim 10^{13} s^{-1}$).

Marcus theory was extended to inner sphere ET transition by Hush, which can be applied to stable MV systems.[78-79] The MV species often present an intervalence charge transfer (IVCT) band characteristic of the optically induced intramolecular ET,[80-81] typically in the near-infrared (NIR) spectral area, which is absent in the spectra of the reduced and oxidized states. Experimental studies of the IVCT bands on dinuclear MV complexes provide a sensitive and powerful probe to elucidate aspects of intramolecular ET processes. The energies (ν_{max}), intensities (ε_{max}), and bandwidths at half-height ($\Delta\nu_{1/2}$) of the absorption bands may be quantitatively related to the factors that govern electronic delocalization and the activation barrier to intramolecular ET according to the classical theory developed by Hush.[82] In other word, from the IVCT bands observed in the UV-vis/NIR spectrum, Hush theory allows the extraction of the two most important ET parameters-the reorganization energy λ and the electronic coupling energy H_{ab}.

According to Hush theory, there are several factors that contribute to the reorganization energy λ:

$$\lambda = \lambda_i + \lambda_o + \Delta E_0 + \Delta E' \quad (10)$$

The Franck-Condon factors λ_i and λ_o correspond to the reorganization energies within the inner- and outer-sphere, respectively. λ_i represents the energy required for reorganization of the metal-ligand and intra-ligand bond lengths and angles, and λ_o is the energy required for

reorganization of the surrounding solvent medium. The redox asymmetry ΔE_0 is the energy difference between the vibrationally-relaxed initial and final states in the hypothetical absence of electronic coupling, and $\Delta E'$ reflects any additional energy contributions due to spin-orbit coupling and ligand field asymmetry.

In the Robin and Day classification,[83] mixed-valence systems are characterized as class I, II or III depending on the strength of the electronic interaction between the oxidized and reduced sites, ranging from essentially zero (class I), to moderate (class II), to very strong electronic coupling (class III). The interplay between H_{ab} and λ determines the class to which the system belongs.

A class I complex with zero or very weak electronic coupling has a completely localized charge ($H_{ab} \approx 0$) and no IVCT band is observed. The free energy of activation for interconversion of two sites ΔG^* equals $\lambda/4$.

A valence-trapped or charge localized Class II species with a moderate strength electronic interaction, H_{ab} value ($0 < H_{ab} < \lambda/2$, or from nonadiabatic $H_{ab} < 10$ cm^{-1} to strongly adiabatic $H_{ab} > 200$ cm^{-1}) is large enough to result in an observable IVCT band and ΔG^* is given by $(\lambda - 2H_{ab})^2/4\lambda$, which holds as long as the ground state is described by a double-well potential, *i.e.*, as long as the system remains valence trapped. In a symmetric homobimetallic MV system, the H_{ab} value can be extracted from the IVCT band by using the Mulliken-Hush expression for a class II compound: [61,78-79]

$$H_{ab}\,(\text{cm}^{-1}) = (0.0206/d)(\lambda \Delta \nu_{1/2} \varepsilon_{max})^{1/2} \qquad (11)$$

where the reorganization energy λ is equal to the energy of the band maximum ν_{max} (cm^{-1}), $\Delta\nu_{1/2}$ is the bandwidth at half height for a Gaussian-shaped IVCT band (cm^{-1}), ε_{max} is the absorption coefficient at band maximum (M^{-1}cm^{-1}), and d is the electron transfer distance in Å. A problem of using eq. 8 is in defining the appropriate value of the non-adiabatic ET distance d. d is often considered as the geometric distance between the redox centers in the absence of electronic coupling, which is true for weakly coupled species. However the delocalization of the charge will lead to reduce the d value and H_{ab} will be underestimated.

In a class III system the interaction of the donor and acceptor sites has become so large that the ground state has only a single minimum at $X = 1/2$ and the odd electron is completely delocalized between two metal centers. This delocalized case occurs when $H_{ab} \geq \lambda/2$ that gives the zero barrier limit ($\Delta G^* = 0$). The IVCT band can no longer be considered as the transfer from one metal center to the other because the electron is shared equally between the two metal centers.

For very strongly coupled system with one energy minimum in the ground state the electronic coupling energy H_{ab} (cm^{-1}) is simply related to the energy of IVCT band. [67,84]

$$H_{ab}\,(cm^{-1}) = \nu_{max}/2 \qquad (12)$$

For symmetric species, the bandwidth at half height predicted by Hush theory is given by eq. 13, which is derived from class II species in the Robin and Day classification of the MV systems:

$$\Delta\nu_{1/2}(cm^{-1}) = (16RT\ln 2\lambda)^{1/2} \qquad (13)$$

At room temperature, this eq. 13 reduces to eq. 14:

$$\Delta\nu_{1/2}(cm^{-1}) = (2310\nu_{max})^{1/2} \qquad (14)$$

Comparison between the calculated and observed $\Delta\nu_{1/2}$ is useful to distinguish class II and class III species, as class III species typically exhibit IVCT bands with bandwidths at half height narrower than the Hush limits calculated from eq. 13 or 14, while the bands of class II species are typically broader than the theoretical limit.

The delocalization parameter Γ (eq. 15) is also a useful tool to evaluate the coupling of a complex. Weakly coupled class II systems display values of $0 < \Gamma < 0.1$, moderately coupled class II, $0 < \Gamma < 0.5$; borderline class II/III, $\Gamma \approx 0.5$; and class III $\Gamma > 0.5$.[61,63]

$$\Gamma = 1\text{-}\Delta\nu_{1/2}/(2310\nu_{max})^{1/2} \qquad (15)$$

In accordance with eq. 10, the IVCT band is sensitive to solvent variation, which is often employed as a criterion for the class of a MV species. For a valence-trapped class II system the absorption band maximum is predicted to show the full solvent dependency regardless of the value of H_{ab}. While the optical transition in a symmetric class III system, although intense, no longer involves charge transfer and is therefore not accompanied by a net dipole-moment change and should show no solvent dependence.[63,85]

Examples of energy-coordinate curves for three principally different situations related to the Robin and Day classification are illustrated on Figure 1-7. Plot (a) shows class I species that have non-interacting centers with the electron localized. Plot (b) describes strongly interacting class II system, but still with two minimum for the ground state. The situation (c) is a fully delocalized class III system with only one minimum on the ground surface.

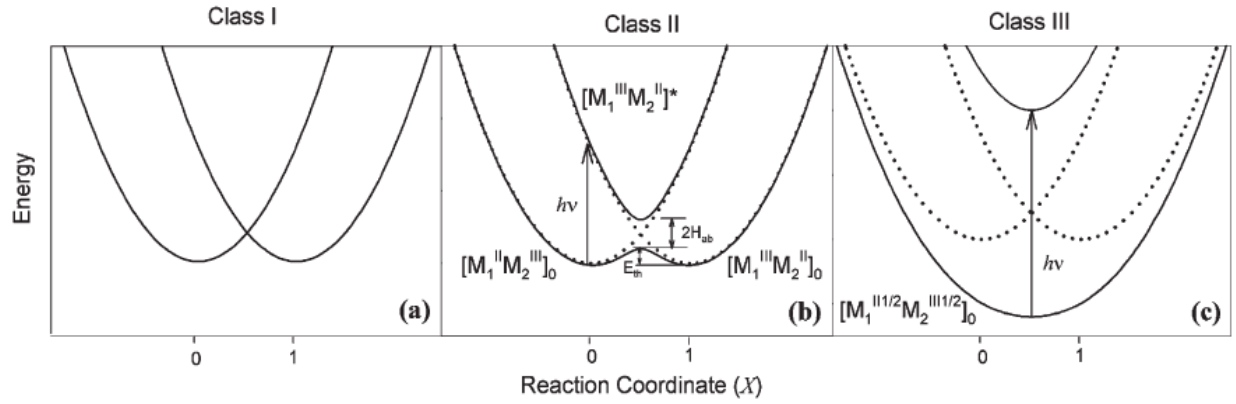

Figure 1-7. Potential energy curves for electron transfer in ligand-bridged dinuclear complexes with (a) negligible, (b) weak ($H_{ab} = \lambda/4$) and (c) strong ($H_{ab} = 3\lambda/4$) electronic coupling. The dotted and solid curves represent the diabatic and adiabatic surfaces, respectively.[85]

1.2.1.2 Cyclic votammetry (CV)

The easiest way to look at the electronic interactions between two active sites of a molecule is by using cyclic voltammetry (CV). In a complex containing two redox-active metal centers and in the case of a strong interaction, at least two reversible electrochemistry events should be observed (Scheme 1).

Scheme 1

$$[M_1]^n\text{-L-}[M_2]^n \underset{+e^-}{\overset{-e^-}{\rightleftharpoons}} [M_1]^{n+1}\text{-L-}[M_2]^n \underset{+e^-}{\overset{-e^-}{\rightleftharpoons}} [M_1]^{n+1}\text{-L-}[M_2]^{n+1}$$

(Red.) (E_1) (MV) (E_2) (Ox.)

The potential difference ($\Delta E = E_2 - E_1$) between the two reversible waves (E_1 and E_2) is representative of the thermodynamic stability of the corresponding MV state relative to the other redox states. The equilibrium 1 in Scheme 2 can be used to represent the comproportionation reaction of the formation of MV compound with redox centers strongly coupled.

Scheme 2

$$[M_1]^n\text{-L-}[M_2]^n + [M_1]^{n+1}\text{-L-}[M_2]^{n+1} \underset{}{\overset{K_c}{\rightleftharpoons}} 2[M_1]^{(n+1)/2}\text{-L-}[M_2]^{(n+1)/2} \qquad (16)$$

$$K_c = ([M_1]^{(n+1)/2}\text{-L-}[M_2]^{(n+1)/2})^2/([M_1]^n\text{-L-}[M_2]^n)([M_1]^{n+1}\text{-L-}[M_2]^{n+1}) \qquad (17)$$

The comproportionation constant K_c given in eq. 17 is proportional to the potential difference (ΔE) between two reversible redox couples observed in the CV spectrum. Using the Nernst equation, K_c which is readily calculated from the separation of the redox processes:[76,86]

$$K_c = [MV]^2/[Ox.][Red.] = \exp(\Delta G_0/RT) \quad (18)$$

$$\Delta G_0 = nF\Delta E,\ n = 1 \quad (19)$$

$$K_c = \exp(F\Delta E/RT) \quad (20)$$

where the F is Faraday constant 96485.33 C/mol, R is the universal gas constant 8.314 $J \cdot mol^{-1} \cdot K^{-1}$, and T is temperature (K). The free energy of comproportionation ΔG_0 responsible for stabilization of MV complex consists of many contributions.[76,84,87]

$$\Delta G_0 = \Delta G_{stat} + \Delta G_{coul} + \Delta G_{iduct} + \Delta G_{reson} + \Delta G_{af} + \Delta G_{ip} \quad (21)$$

where ΔG_{stat} represents the statistical distribution; ΔG_{coul} the electrostatic repulsion of the two similarly charged metal centers linked by the bridging ligand; ΔG_{iduct} an inductive factor related to the competitive coordination of the bridging ligand by the metal ions, especially to decrease of π acceptor properties of bridged ligand in reduced form of complex; ΔG_{reson} the resonance stabilization factor due to electronic delocalization; ΔG_{af} the antiferromagnetic exchange stabilization, for example for biradical form; and ΔG_{ip} the ion-pairing effects depending on the charges of the complexes. It was shown by different studies that a solvation and an ion pairing have very often dominant contribution, and that K_c strongly depends on the solvent and the supporting electrolyte used in the experiment.[88-89] Of the contributions, none except ΔG_{reson} is the component that represents the actual metal-metal coupling in a MV complex, and is related to H_{ab} by eq. 22 and eq. 23 for localized and delocalized systems, respectively.

$$-\Delta G_{reson} = 2H_{ab}^2/\lambda = 2H_{ab}^2/\nu_{max} \quad (22)$$

$$-\Delta G_{reson} = 2(H_{ab} - \lambda/4) = \nu_{max} - \lambda/2 \quad (23)$$

In general, a large ΔE value (or K_c value) indicates a high possibility to isolate the MV compound. In symmetrical homobimetallic complexes, ΔE value (or K_c value) is an indicator of the interactions between two metal centers (assuming that both waves are reversible). If the ΔE value is close to zero, the metals are non-interacting either because of the great distance between them or because the ligand does not provide and electronic coupling pathway. Usually these systems belong to class I species. A small ΔE separation represents a weak interaction between the metals with a small K_c. This situation is commonly assigned to trapped-valence systems

(class II). A larger value of ΔE corresponds to a totally delocalized system with a very large K_c (Scheme 2), and there is a stabilization of the MV species, normally assigned to class III.[60] The redox centers are so strongly coupled that the lone-electron is delocalized and only a single average valence state can be assigned to the two centers ($M_1^{(n+1)/2} = M_2^{(n+1)/2}$). However, some class III compounds may present very small ΔE values. This is contrary to what is expected as systems with large values of ΔE normally present large H_{ab} values. According to eq. 6, ΔE can be influenced by other factors such as electrostatic interactions, solvation, ion pairing with the electrolyte and structural distortions from oxidation or reduction processes and so on. Therefore ΔE should not be used on its own to classify MV species. Table 1-2 summarizes the general characteristic properties for the classification of MV systems.

Table 1-2. Summary of the properties for each class of MV systems[61]

	Electronic interaction	H_{ab}	Γ	IVCT bands	ΔE or K_c
Class I	zero or little	0	no	no	small
Class II	moderate	$< \lambda/2$	$0 < \Gamma < 0.1$ (weakly coupled) $0 < \Gamma < 0.5$ (moderately coupled)	$\Delta\nu_{1/2(calc)} < \Delta\nu_{1/2(obs)}$ broad and weak	Inter-mediate
Borderline Class II/III	Intermediate properties		$\Gamma \approx 0.5$	Intermediate properties between class II and class III	
Class III	strong	$\geq \lambda/2$	$\Gamma > 0.5$	$\Delta\nu_{1/2(calc)} > \Delta\nu_{1/2(obs)}$ narrow and intense	large

1.2.1.3 X-ray crystallography and NMR spectroscopy

X-ray crystallography provides useful structural information. A system presenting two metal centers in the same oxidation state is expected to generally show equivalent M-C bond distances, whereas a complex with both metal centers in different oxidation states is predicted to display two distinctive M-C bond lengths. This variation is caused by the different environments around each of the metal centers. Still, it might be difficult to distinguish between apparent equivalence arising from delocalization and those from static or dynamic disorder. On the other hand, an unsymmetric crystal environment may lead to a localization of the cation structure that is not

necessarily found in solution. Nuclear magnetic resonance (NMR) spectroscopy is a useful technique when the system studied is diamagnetic. However, most of mixed-valence bimetallic organometallic complexes are paramagnetic. They display typically broad peaks because of electron-nuclear dipolar coupling from which is difficult to extract information.

1.2.1.4 IR spectroscopy

Infrared (IR) spectroscopy is also a useful technique in distinguishing between localized and delocalized MV systems via the extent of averaging of the characteristic absorptions strongly affected by the oxidation state of the metal centre. In some cases, it can be used to establish the rates of intramolecular ET in class II systems. Two slightly different applications of IR spectroscopy can be established. First, the IR activity of a mode of the bridging ligand in the MV state, which is IR-inactive in the fully oxidized and reduced states, indicates a breaking of the symmetry in the MV species down to the time scale of a single vibration (e.g., on the time scale of $\sim 6 \times 10^{13}$ s^{-1} for a C≡C stretching), that is, indicating that the cation belongs to classes I or II. On the other hand, in class III systems, modes of this type are expected to be IR-inactive. The spectrum of IR-localized species present bands characteristic of both oxidation states of the redox units, whereas IR-delocalized systems show only new bands corresponding to the averaged MV unit. Thus, the rates of intramolecular ET are respectively small and large compared to the differences in frequency ($\sim 1 \times 10^{12}$ s^{-1}). In some cases, the temperature dependence of IR bands that act as redox state markers (typically the stretches of CO groups) have been used to determine the rates of ET at multiple temperatures and, hence, to provide estimates for the barrier to ET (ΔG^*).

1.2.1.5 EPR spectroscopy

Electron paramagnetic resonance (EPR or electron spin resonance, ESR) is a major technique allowing to distinguish between ligand centered radicals, metal centered radicals and radicals with a mixed metal-ligand characters and also an attractive method to obtain important information about the extent of electronic and nuclear interactions.[64] It is a powerful tool to identify electron delocalization. In certain cases it gives a direct information about the electron localization from hyperfine splitting and *g* factor anisotropy.[75] The ideal situation for EPR studies occurs when the paramagnetic species have non-degenerate ground-states and hyperfine

coupling can be observed. When degenerate ground-states are analyzed, the situation is more difficult as low temperatures are often required to obtain EPR spectra.

1.2.1.6 Magnetization measurement

Measurements of temperature dependence of sample magnetization could give important information about coupling of the electronic states for systems with more than one unpaired electron. Analysis of molar magnetic susceptibility χ_m *vs* T curve gives information about interaction of unpaired electrons in the system. Most important case is the binuclear complexes with one unpaired electron on each metal center. Such complexes can have antiferromagnetic or ferromagnetic interaction of spins, dependent from electronic structure of metal center and bridge. The π-conjugated bridges with even number of atoms mostly provide the antiferromagnetic coupling while bridges with odd number of atoms mediate ferromagnetic coupling. Spin-polarization mechanism was used to explain these behaviors.[90]

1.2.2 Techniques for measuring single-molecule conductance and the selection of anchor group

Understanding electronic transport through a single molecule is an interesting scientific challenge.[24,26,91-92]

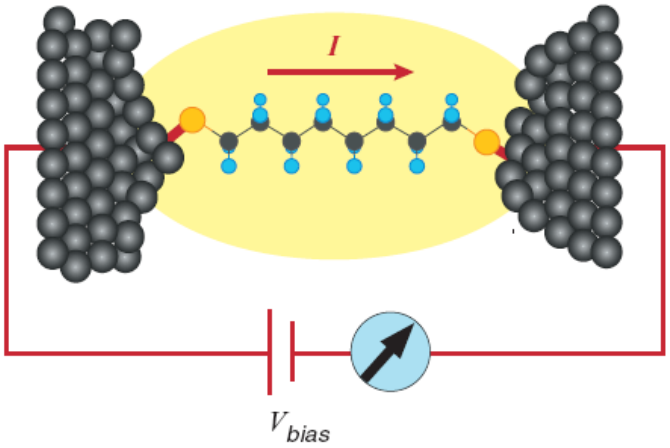

Figure 1-8. Current through a molecule covalently bound to two electrodes[93]

Many experimental techniques have been developed to measure and control current through molecules, which can be divided into two broad categories: the measurements of single molecules covalently bound to two electrodes (Figure 1-8) and the approaches to measure the conductance of molecular thin film sandwiched between two electrodes.[93] The techniques that allow to measure single molecule conductance are scanning probe methods (Figure 1-9), fixed electrodes (Figure 1-10), and mechanically controlled molecular junctions.

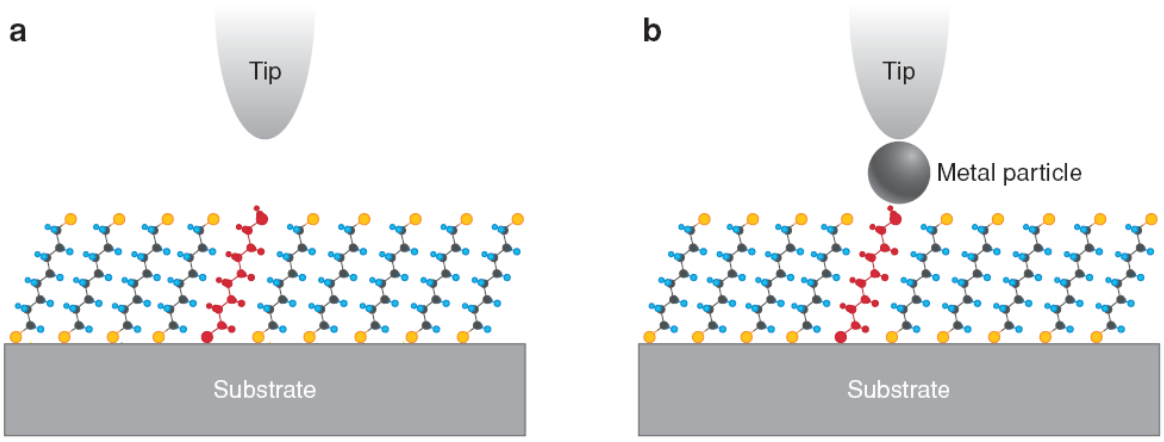

Figure 1-9. Scanning probe techniques[93]

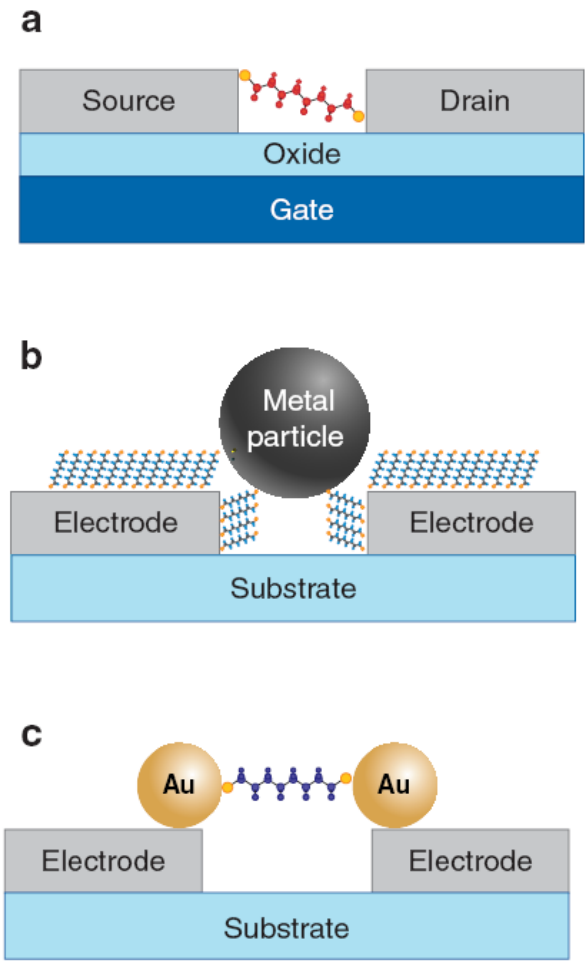

Figure 1-10. Fixed electrodes techniques[93]

The mechanically controlled molecular junctions including scanning tunneling microscopy break junction (STMBJ, Figure 1-11), conducting atomic-force-microscopy break junction (c-AFMBJ, Figure 1-12), and mechanically controllable break junction (MCBJ, Figure 1-13) are of great interest to us, especially MCBJ. Because the charge transport studies of our molecules will be conducted using the MCBJ technique, which has been proven to enable charge transport measurements through individual molecule.[94]

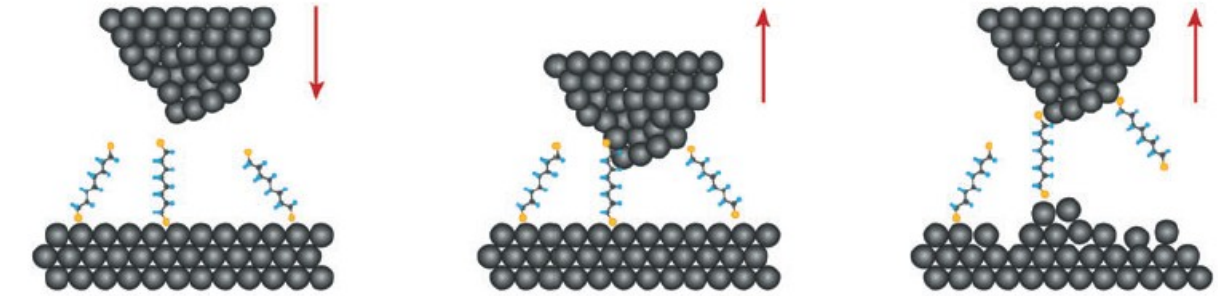

Figure 1-11. STM break junction method.[93]

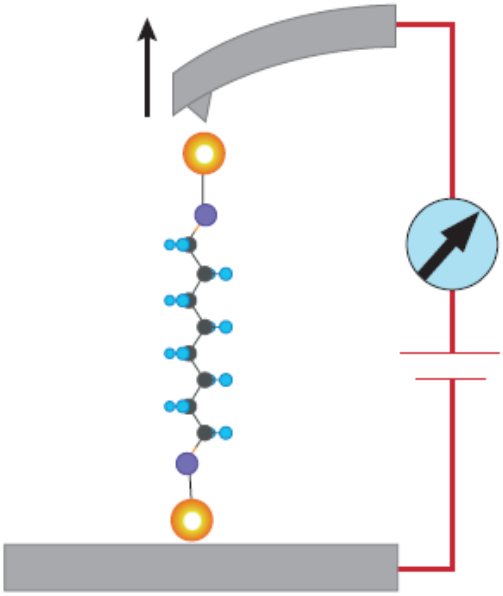

Figure 1-12. AFM break junction method.[93]

The basic principle of the MCBJ method is to break a thin Au metal bridge (typically 50 nm × 50 nm) into a pair of atomic-sized electrode opposite to each other in a three-point bending mechanism.[95-96] Electron-beam lithography and reactive ion etching are used to fabricate a

freestanding metal bridge on the top of a flexible substrate (Figure 1-13a). Distance between the electrodes and the breaking process is controlled by bending of the solid substrate. Bending is achieved by fixing two ends of the substrate while pushing the middle part of the substrate vertically, with a very high accuracy due to the low transmission ratio between pushing rod translation (Δh) and resulting electrode separation (Δd) in the order of 1×10^{-5}.

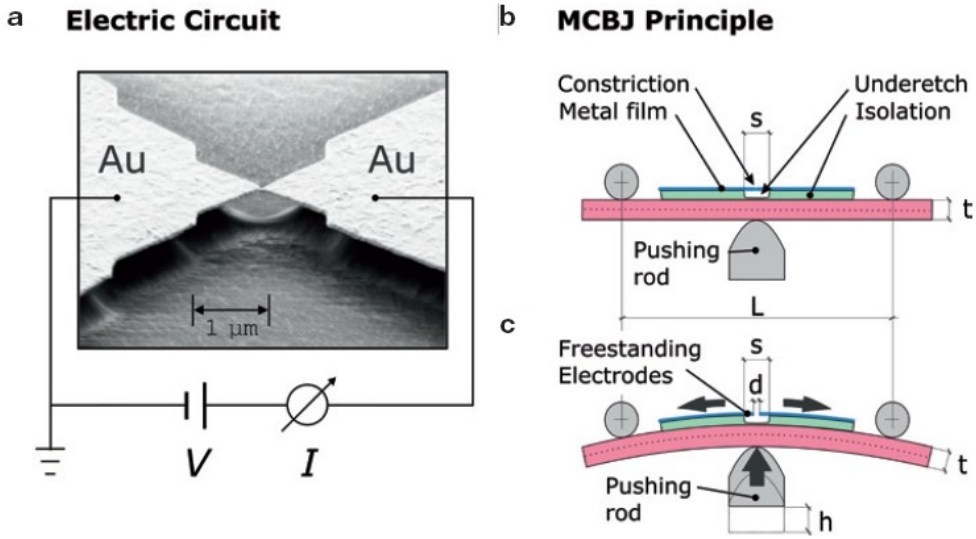

Figure 1-13. Principle of MCBJ method[94]

For the application of molecules, the distance between the electrodes is set to be longer than the length of the molecule to be studied. The molecules are deposited from a highly diluted solution (typically 4×10^{-5} mol/L) and adsorb to one of the two electrode surfaces while the solvent evaporates. Ultra-high vacuum condition (UHV, pressure $p < 10^{-8}$ mbar) is a prerequisite to preserve the integrity of the molecular system from unwanted contaminations. Electrodes are slowly moved closer to each other, during which the molecules can bridge the gap of the electrodes and I/V curve is measured. Usually, several hundreds or thousands of closing and opening curves are measured under the same condition and the statistical analysis of the data was carried out to eliminate the effect of the actual microscopic configuration of the junction dependence on the gap distance, the geometric shape of the electrodes, the resulting electrical field distribution and the specific bonding of the molecule-metal interfaces.[97]

To determine the conductance of a molecule, one must bring it into reliable contact with two electrodes. It is important to deepen insight into the chemical nature of the metal-molecule link and establish guidelines for selecting optimal anchor groups.[98] Up to now, several terminal

groups have been studied such as thiol,[99-102] thioacetyl,[103-105] isothiocyanate,[106-109] carbodithioate,[110] methyl sulfide,[111] fullerene,[112] isonitrile,[113-115] pyridyl,[116-117] dimethyl phosphine,[118] amine[102,118] and carboxylic acid groups[102] (Figure 1-14).

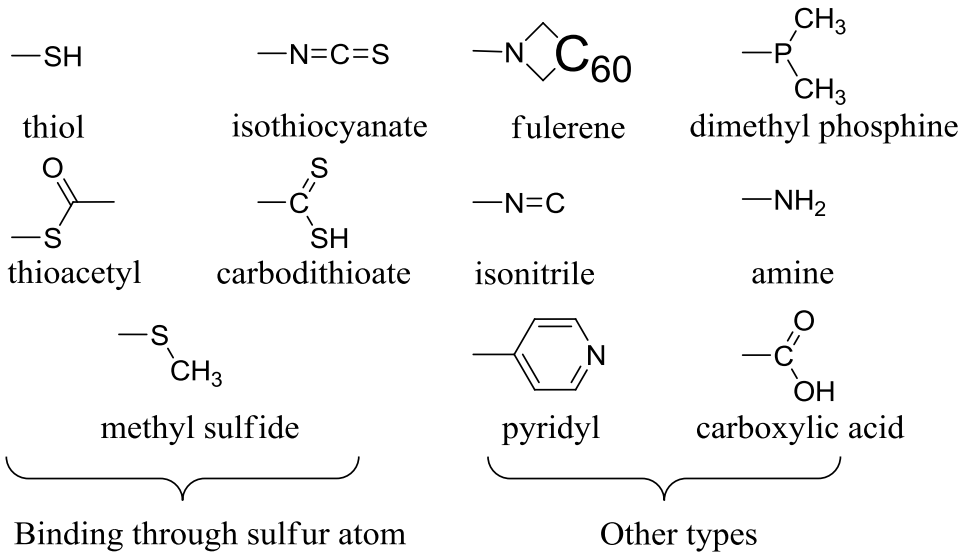

Figure 1-14. Examples of anchor groups[90]

The conductance values are influenced by many experimental details, a systematic and thorough examination from a homologous series of molecules appears necessary to derive the intrinsic properties of the head group-electrode contact.[107] Since most common electrode material is gold and the high affinity of sulfur to gold, our molecules can be equipped with appropriate anchor groups containing sulfur to guarantee strong contact to the gold surface. Thiol group and its protected form-thioacetyl group are frequently used anchor group in organic systems. These groups are favorable owing to the possibility of comparison with the organic species. The thioacetyl group is especially interesting to us due to its relative low reactivity and its easy conversion to thiol group by *in-situ* deprotenction.

1.2.3 Literature overview on Group 7 transition metal (manganese and rhenium) complexes

As mentioned above, organometallic wire-like molecules consisting of transition metal fragments bridged by different π-conjugated chains are attracting considerable interest. The through-bridge electronic interaction of the metal centers exerts significant effect on the chemical and physical properties of these complexes, which greatly depend on the metal centers, the ancillary ligands and the bridging ligands.[60-61,119-122] Therefore, the investigation on the series of

group 7 transition metal complexes will deepen the understanding on the influence of the metal centers in comparison with the complexes bearing other metal centers. The published symmetric manganese and rhenium complexes with π-conjugated hydrocarbon chain bridges are summarized in Figure 1-15, Figure 1-16, and Figure 1-17.

General routes to $L_nM\text{-}C\equiv C\text{-}ML_n$ (M = Mn and Re) complexes and the full characterized complexes of these types are rare.[123] The reported manganese and rhenium complexes with π-conjugated C_2 bridges are listed in Figure 1-15.

$(OC)_5Mn{-}C{\equiv}C{-}Mn(CO)_5$ $(OC)_5Re{-}C{\equiv}C{-}Re(CO)_5$

$[(MeC_5H_4)(dmpe)Mn{-}C{\equiv}C{-}Mn(dmpe)(C_5H_4Me)]^{n+}$ (n = 0, 1, 2) **1**

Figure 1-15. Manganese and rhenium complexes with π-conjugated C_2 bridges

Beck and coworkers reported the synthesis of the σ,σ-acetylide bridged complex $(OC)_5ReC{\equiv}CRe(CO)_5$ by the reaction of $(OC)_5ReFBF_3$ with $HC{\equiv}CSiMe_3$ to form the σ,π-ethynide bridged complex $[(OC)_5Re(\mu\text{-}\eta^1\text{:}\eta^2\text{-}C{\equiv}CH)Re(CO)_5][BF_4]$, which upon deprotonation gave $(OC)_5ReC{\equiv}CRe(CO)_5$ in good yields. This complex is not formed by metathesis of $NaC{\equiv}CNa$ (or $LiC{\equiv}CLi$) with $(OC)_5ReFBF_3$. Similarly the reaction of $NaC{\equiv}CNa$ (or $LiC{\equiv}CLi$) with $Mn(CO)_5Br$ gave $Mn_2(CO)_{10}$ instead of $(OC)_5MnC{\equiv}CMn(CO)_5$. The CV studies carried out on $(OC)_5ReC{\equiv}CRe(CO)_5$ showed two irreversible oxidation processes with E values of 1.12 V and 1.35 V in CH_2Cl_2.[124] The investigation by Davies and coworkers on the reactions of $Mn(CO)_5^-$ and $Re(CO)_5^-$ with $IC{\equiv}CI$ demonstrated different results. In the reaction involving manganese, $(OC)_5MnC{\equiv}CMn(CO)_5$ formed in 15% yield along with $Mn_2I_2(CO)_8$ and some insoluble black residue, while in the reaction of rhenium compound, $ReI(CO)_5$, $Re_2I_2(CO)_8$ and some insoluble black residue were produced. The author believed that the difference in reactivity between $Re(CO)_5^-$ and $Mn(CO)_5^-$ can be explained by simple hard-soft acid-base (HSAB) theory. The iodines in $IC{\equiv}CI$ are electrophilic sites due to the low electronegativity. Attack of the third-row, strongly basic anion, $Re(CO)_5^-$, occurs exclusively at this site. With the first-row, less basic anion, $Mn(CO)_5^-$, attack directly at iodine will be less favored on HSAB grounds and that at the harder carbon site becomes competitive.[125]

Berke and coworkers successfully prepared a series of half sandwich manganese complexes of the type $[(MeC_5H_4)(dmpe)Mn\text{-}C{\equiv}C\text{-}Mn(dmpe)(C_5H_4Me)]^{n+}$ (**1**, n = 0, 1, and 2) starting from a substituted mangnocene $[(MeC_5H_4)_2Mn]$, 1.2-bis(dimethylphosphino)ethane (dmpe) or the dmpe

adducts [$(MeC_5H_4)_2$(dmpe)Mn]) and $Me_3SnC{\equiv}CSnMe_3$.[126] The paramagnetic MV complex [(MeC_5H_4)(dmpe)Mn-C≡C-Mn(dmpe)(C_5H_4Me)]$^+$ (**1**$^+$) was isolated from the reaction, which was reduced by Na/Hg in THF to the neutral complex [(MeC_5H_4)(dmpe)Mn-C≡C-Mn(dmpe)(C_5H_4Me)] (**1**) or was oxidized with one equiv. of $[Cp_2Fe][PF_6]$ in CH_2Cl_2 to the diamagnetic dicationic complex [(MeC_5H_4)(dmpe)Mn-C≡C-Mn(dmpe)(C_5H_4Me)]$^{2+}$ (**1**$^{2+}$). The neutral complex **1** was highly reducing and very sensitive towards oxygen and moisture and decomposed in solution within 24 h. An unusual paramagnetic behavior was observed in the NMR spectra of **1**. The DFT calculations of the neutral model complex suggested a small energy gap between the singlet and triplet electronic states. Therefore a singlet/triplet spin equilibrium is very likely to exist for **1**, which might be one of the interpretations for the unusual paramagnetic behavior (The other explanation might be the antiferromagnetic coupling).

The X-ray diffraction studies on this series of compounds [(MeC_5H_4)(dmpe)Mn-C≡C-Mn(dmpe)(C_5H_4Me)]$^{n+}$ (n = 0, 1, and 2) revealed the structural variation from the cumulenic resonance form (Mn=C=C=Mn) to the biscarbyne type (Mn≡C-C≡Mn) upon the oxidation of **1** to [**1**]$^{2+}$ (M-C bond distances of 1.872(2) Å for **1**, 1.792(3) Å for [**1**]$^+$ and 1.733(2) Å for [**1**]$^{2+}$) and two equivalent Mn centers for the MV complex [**1**]$^+$ as evidence from the same M-C distances. The CV spectrum of **1[PF$_6$]$_2$** displayed three fully reversible waves. The two potential differences $\Delta E_{1/2}$ between the three redox processes are the same value of 0.988 V resulting in a large K_c value of 8.6×10^{16} (Table 1-1). The UV-vis/NIR spectra of the complexes **1**, **1[PF$_6$]** and **1[PF$_6$]$_2$** in CH_2Cl_2 clearly showed intense bands with a shoulder at the range of 300~600 nm for all complexes. One additional band of very low intensity ($\varepsilon < 500$ $M^{-1}cm^{-1}$) at ~1300 nm for **1** and **1[PF$_6$]** could be assigned to the IVCT band. The variable-temperature magnetic susceptibility measurements at 5~300 K for **1** and **1[PF$_6$]** suggested an antiferromagnetic coupling for **1** and a one-electron paramagnetism for **1[PF$_6$]**.

Berke and coworkers have contributed to the symmetric π-conjugated C_4-bridged manganese complexes (Figure 1-16).

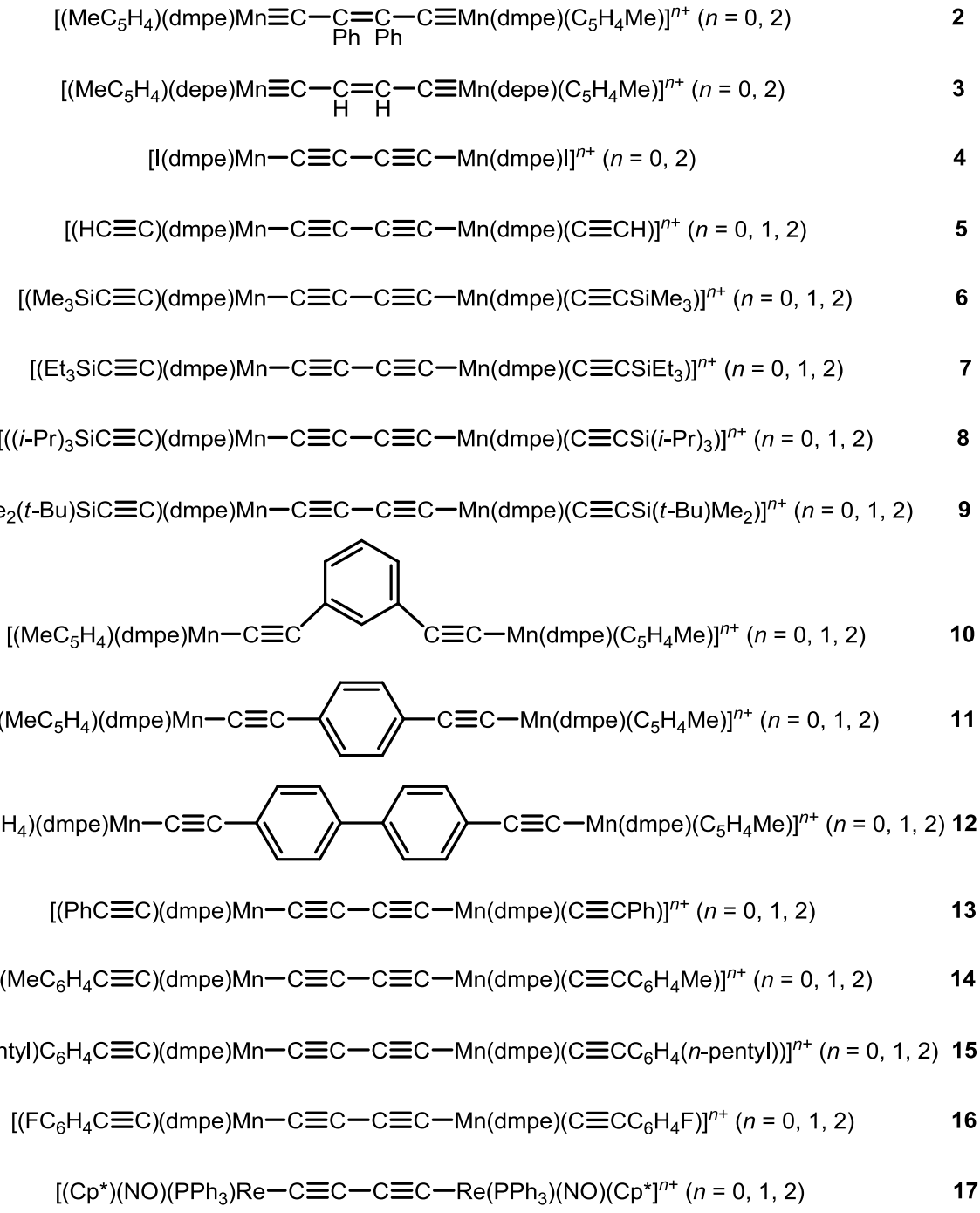

Figure 1-16. Manganese and rhenium complexes with π-conjugated hydrocarbon chain bridges

They reported the dinuclear manganese vinylidene-bridged biscarbyne complexes $[(MeC_5H_4)(dmpe)Mn{\equiv}C\text{-}CPh{=}CPh\text{-}C{\equiv}Mn(dmpe)(C_5H_4Me)]^{2+}$ ($\mathbf{2}^{2+}$)[127] and $[(MeC_5H_4)(depe)Mn{\equiv}C\text{-}CH{=}CH\text{-}C{\equiv}Mn(depe)(C_5H_4Me)]^{2+}$ ($\mathbf{3}^{2+}$)[123,128]. The former was obtained

by the slow dimerization of the cationic species $[(MeC_5H_4)(dmpe)Mn\text{-}C{\equiv}CPh]^+$ and the latter was isolated by the oxidation of the reaction mixture of $(MeC_5H_4)_2Mn$, bis(diethylphosphino)ethane (depe) and an excess of $Bu_3Sn\text{-}C{\equiv}C\text{-}H$ with $[Cp_2Fe][PF_6]$. The reduction of the dicationic complexes with two equiv. of $Cp_2{}^*Co$ gave the corresponding bisvinylidene complexes $[(MeC_5H_4)(dmpe)Mn{=}C{=}CPh\text{-}CPh{=}C{=}Mn(dmpe)(C_5H_4Me)]$ (**2**) and $[(MeC_5H_4)(depe)Mn{=}C{=}CH\text{-}CH{=}C{=}Mn(depe)(C_5H_4Me)]$ (**3**). The neutral complex **2** were also produced in moderate yield by the reaction of $[(MeC_5H_4)(dmpe)Mn\text{-}C{\equiv}CPh]$ with *n*-Bu_3SnH as H· source[127] The neutral complex **2** and the dicationic complex $\mathbf{2}^{2+}$ are thermally stable, and $\mathbf{2}^{2+}$ is even air-stable.

Both CV spectra of **2** and $\mathbf{3}^{2+}$ displayed two fully reversible waves with the potential differences $\Delta E_{1/2}$ of 0.211 V and 0.576 V, which resulted in the comproportionation constants K_c of 8×10^3 and 6.6×10^9, respectively (Table 1-1).[123,127] The huge difference observed between the K_c values of these two quite similar compounds suggests that the communication between the metal centers may be reduced in the case of the phenylated compound, which might be derived from the stabilizing perpendicular orientation of the metal fragments. The NIR spectrum of the MV complex **2[PF$_6$]** in CH_2Cl_2 clearly showed the IVCT band at the 1018 nm (with a shoulder at ~900 nm) with the intensity ε of 3.3×10^3 $M^{-1}cm^{-1}$. The observed bandwidths of the band at half height ($\Delta\nu_{1/2}$ = 3120 cm^{-1}) are narrower than the predicted width of 4765 cm^{-1} from the Hush's theory for the weakly coupled MV compounds indicated a class III character. The EPR spectrum measured at 83 K in CH_2Cl_2 glass showed an undecet with broad individual lines of *g* value of 2.018 and $A_{iso,Re}$ value of 60 G, which is half of those of related mononuclear manganese complexes. This result might suggest that an electron delocalization over the two Mn centers or a very rapid electron transfer.

A series of symmetric dinuclear manganese complexes of the type $[(X)(dmpe)Mn\text{-}C{\equiv}C\text{-}C{\equiv}C\text{-}Mn(dmpe)(X)]^{n+}$ (X = I, **4**; C≡CH, **5**; $C{\equiv}CSiMe_3$, **6**; $C{\equiv}CSiEt_3$, **7**; $C{\equiv}CSi(i\text{-}Pr)_3$, **8**; $C{\equiv}CSi(t\text{-}Bu)Me_2$, **9**; n = 0, 1, 2) were also reported by Berke and coworkers. These compounds were prepared either by the reaction of two equiv. of $[MnI(dmpe)(MeC_5H_4)]$ with $Me_3Sn\text{-}C{\equiv}C\text{-}C{\equiv}C\text{-}SnMe_3$ and dmpe[129] or by an in situ C-C coupling of $[Mn(dmpe)_2(C{\equiv}CX)(C{\equiv}C\cdot)]$ radicals[130-131]. However, their attempts to synthesize $[(MeC_5H_4)(dmpe)Mn\text{-}C{\equiv}C\text{-}C{\equiv}C\text{-}Mn(dmpe)(C_5H_4Me)]$ were unsuccessful.[123] As shown in Table 1-3, $\Delta E_{1/2}$ values of complexes **4**-**9** are large and very close to each other. Single crystal X-ray diffractions revealed two equivalent Mn centers for the

MV complexes $\mathbf{4}^+$, $\mathbf{5}^+$, $\mathbf{6}^+$ and $\mathbf{7}^+$, suggesting a strong communication between the two metal sites. In the NIR spectrum of the MV complex $\mathbf{4}^+$, the IVCT band appeared at the 1610 nm with the intensity ε of 2.5×10^3 $M^{-1}cm^{-1}$ and the observed bandwidths of the band at half height $\Delta\nu_{1/2}$ is 2070 cm^{-1} indicating a class II character. The electronic coupling energy H_{ab} derived from the Hush's theory for the class II MV complex is 500 cm^{-1}. In the EPR spectrum a broad feature without detectable hyperfine structure is observed at *g* value of 1.83 leading to the interpretation that the system is in the fast exchange regime in the EPR time scale.[129] In the UV-vis/NIR spectra of the neutral complexes **5** and **6** and the MV complexes $\mathbf{5}^+$ and $\mathbf{6}^+$, an additional band of very low intensity ($\varepsilon < 500$ $M^{-1}cm^{-1}$) at 800~900 nm could be assigned to the IVCT band. The variable-temperature magnetic susceptibility measurements at 5~300 K indicated an antiferromagnetic coupling for the neutral complexes **5** and **6** and a one-electron paramagnetism for the MV complexes $\mathbf{5}^+$ and $\mathbf{6}^+$.[131]

They also investigated the influence of the incorporating aromatic spacer groups. Complexes of the type $[[(MeC_5H_4)(dmpe)Mn\text{-}C{\equiv}C\text{-}X\text{-}C{\equiv}C\text{-}Mn(dmpe)(C_5H_4Me)]^{n+}$ (X = 1,3-C_6H_4, **10**; 1,4-C_6H_4, **11**; 4,4-$(C_6H_4)_2$, **12**; n = 0, 1, 2) were prepared in very good yield by the treatment of $[(MeC_5H_4)_2(dmpe)Mn]$ with 0.5 equiv. of the corresponding acetylides 1,3-$C_6H_4(C{\equiv}CSnMe_3)_2$, 1,4-$C_6H_4(C{\equiv}CSnMe_3)_2$ and 4,4-$(C_6H_4)_2(C{\equiv}CSnMe_3)_2$ in THF for 72 h.[132] However, their attempts to synthesize $[(MeC_5H_4)(dmpe)Mn\text{-}C{\equiv}C\text{-}C{\equiv}C\text{-}Mn(dmpe)(C_5H_4Me)]$ were unsuccessful because of its lability.[123] The CV studies of the dicationic complexes in CH_3CN showed reversible redox processes except for the complex $\mathbf{10}^{2+}$. The K_c values (Table 1-3) for the complexes $\mathbf{11}^{2+}$ and $\mathbf{12}^{2+}$ were 1.8×10^4 and 1.4×10^9, respectively, indicating that the electronic communication might be lowered by the incorporating cyclic groups.

The further functionalization of the terminal iodide end groups of the complex [I(dmpe)Mn-C≡C-C≡C-Mn(dmpe)I] (**4**) have also been accomplished by Berke and coworkers. They utilized simple metathesis reactions of the complex [I(dmpe)Mn-C≡C-C≡C-Mn(dmpe)I] (**4**) with various lithium acetylides $LiC{\equiv}CC_6H_4X$ (X = H, **13**; Me, **14**; *n*-pentyl, **15**; F, **16**; n = 0, 1, 2) to obtain the corresponding alkyne terminated dinuclear complexes $[(XC_6H_4C{\equiv}C)(dmpe)Mn\text{-}C{\equiv}C\text{-}C{\equiv}C\text{-}Mn(dmpe)(C{\equiv}CC_6H_4X)]^{n+}$ (X = H, **13**; Me, **14**; *n*-pentyl, **15**; F, **16**; n = 0, 1, 2) in good yields.[133]

Table 1-3. Electrochemical data for the dinuclear manganese in leterature, E vs $Fc^{0/+}$

Complexes	Couple 1 $E_{1/2}$ (V)	Couple 2 $E_{1/2}$ (V)	$\Delta E_{1/2}$ (V)	K_c	H_{ab} (cm^{-1})	Ref.
1	-0.847	-1.835	0.988	8.6×10^{16}	/	123
2	-0.445	-0.656	0.211	8.0×10^{3}	/	127
$\mathbf{3}^{2+}$	-0.820	-1.386	0.576	6.6×10^{9}	/	123
4	-0.021	-0.651	0.630	1.1×10^{10}	500	
5	+0.124	-0.451	0.575	7.5×10^{9}	/	131
6	-0.271	-0.816	0.545	2.2×10^{9}	/	
7	-0.286	-0.843	0.557	3.5×10^{9}	/	134
8	-0.293	-0.857	0.564	4.4×10^{9}	/	
9	-0.289	-0.849	0.560	4.0×10^{9}	/	
$\mathbf{10}^{2+}$	Irreversible redox processes				/	123
$\mathbf{11}^{2+}$	/	/	/	1.8×10^{4}	/	
$\mathbf{12}^{2+}$	/	/	/	1.4×10^{9}	/	
17	0.06	0.59	0.53	1.1×10^{9}	5663 (band A) 5000 (band B) 4166 (band C)	135

Research on symmetric π-conjugated hydrocarbon chain bridged rhenium complexes is relatively rare. Gladysz and co-workers prepared a series of dinuclear rhenium complexes [(Cp*)(NO)(PPh_3)Re-$(C\equiv C)_x$-Re(PPh_3)(NO)(Cp*)] with carbon chains of up to ten alkynyl units (x = 10).[121-122] The CV studies of these compounds revealed the dependence of K_c value on the

distance between the rhenium metal centers (K_c are on the order of 10^9 for x = 2, 10^6 for x = 3, 10^3 for x = 5, 6 and 8).[121] In other words, the longer the chain length, the smaller the extent of delocalization between two metal centers. Their studies also showed that when the polyynediyl chain was extended, even to six carbons, the oxidized counterparts became dramatically less stable.

Complex $[(Cp^*)(NO)(PPh_3)Re\text{-}C{\equiv}C\text{-}C{\equiv}C\text{-}Re(PPh_3)(NO)(Cp^*)]^{n+}$ (**17**, n = 0, 1, 2) was produced in 88% yield as a 50:50 diastereomer mixture by the reaction of the rhenium ethynyl complex $[(Cp^*)(NO)(PPh_3)Re(C{\equiv}CH)]$ with 1.5 equiv. of $Cu(OAc)_2$ in pyridine. The CV studies carried out on the neutral complex **17** in CH_2Cl_2 showed two reversible couples with a large K_c value of 1.1×10^9. ESR spectrum of the MV complex $\mathbf{17}^+$ showed a undecet with $A_{iso,Re}$ values of 98 G, which is half of those of related monorhenium radical cations, indicating spin delocalization over two rhenium (I = 5/2) centers. The IR spectrum gave only one ν_{NO} band, positioned between those of **17** and $\mathbf{17}^{2+}$. Near IR spectra showed three Gaussian-shaped IVCT bands at the range of 883~1200 nm, which are solvent-independent. The observed bandwidths of the bands at half height (1800 cm^{-1} band A, 1200 cm^{-1} band B, 1500 cm^{-1} band C) are much narrower than the predicted widths (5115 cm^{-1} band A, 4806 cm^{-1} band B, 4387 cm^{-1} band C clearly indicated a class III character.

Based on the literature survey, the following conclusions could be drawn:

- From the consideration of synthetic ease and the extent of the electronic communication between the metal centers, the C_4-bridged complex is more favorable than the C_2-brigded complexes and the complexes with longer chains;
- Most efforts are devoted to the manganese complexes, but the work on rhenium complexes is much rare. Although the reported manganese complexes showed large K_c values, the energies, intensities and half-height bandwidths of the IVCT bands indicate a weakly coupled class II system.
- Reported rhenium complexes show strong electronic communication between the metal centers. However, these complexes are stopper-type, which prevents further functionalization for fixation of the electrode “anchor” groups and extension to oligonuclears;

- Bisvinylidene sp^2 C_4H_2-bridge seems to be a promising linkage for electronic communication but there is no report on this kind of rhenium complexes;
- There is still no measurement of single-molecular conductance for the reported manganese and rhenium complexes.

1.3 Goal of work

- ❖ Development of synthetic methods for the electron-rich $Re(PMe_3)_4$ fragment based C_4-bridged molecules with end groups, such as halide and acetylide compatible for further functionalization;
- ❖ Study of electronic communication between the metal centers on the synthesized compounds by various physical methods;
- ❖ Substitution of the end groups of the synthesized compounds with the thioacetyl end groups for the measurement of single-molecule conductance.

1.4 References

(1) Schaller, R. R. *Ieee. Spectrum.* **1997**, *34*, 52-59.

(2) Lundstrom, M. *Science.* **2003**, *299*, 210-211.

(3) See the International Technology Roadmap for Semiconductors (ITRS), 2009 edition, available at http://www.itrs.net/reports.html.

(4) Thompson, S. E.; Parthasarathy, S. *Mater. Today.* **2006**, *9*, 20-25.

(5) Balzani, V. *Chemphyschem.* **2009**, *10*, 21-21.

(6) Balzani, V.; Credi, A.; Venturi, M. *Nano. Today.* **2007**, *2*, 18-25.

(7) Balzani, V.; Credi, A.; Venturi, M. *Molecular Devices and Machines: Concepts and Perspectives for the Nanoworld*; 2nd ed.; Wiley-VCH Verlag GmbH & Co. KGaA: Weinheim, **2008**.

(8) Binning, G.; Rohrer, H.; Gerber, C.; Weibel, E. *Phys. Rev. Lett.* **1982**, *49*, 57-61.

(9) Binnig, G.; Rohrer, H. *Rev. Mod. Phys.* **1999**, *71*, S324-S330.

(10) Binnig, G.; Rohrer, H. *Rev. Mod. Phys.* **1987**, *59*, 615-625.

(11) Binnig, G.; Quate, C. F.; Gerber, C. *Phys. Rev. Lett.* **1986**, *56*, 930-933.

(12) Greene, M. E.; Kinser, C. R.; Kramer, D. E.; Pingree, L. S. C.; Hersam, M. C. *Microsc. Res. Tech.* **2004**, *64*, 415-434.

(13) Meyer, E.; Glatzel, T. *Science.* **2009**, *324*, 1397-1398.

(14) Jones, R. A. L. *Soft Machines, Nanotechnology and Life*; Oxford University Press: Oxford, **2004**.

(15) Schliwa, M. *Molecular Motor*; Wiley-VCH Verlag GmbH: Weinheim, **2003**.

(16) Goodsell, D. S. *Bionanotechnology*; Wiley-Liss: Hboken, **2004**.

(17) Cramer, F. *Chaos and Order. The Complex Structure of Living Systems*; VCH: Weinheim, **1993**.

(18) Zhang, Q.; Tu, Y. Q.; Tian, H.; Zhao, Y. L.; Stoddart, J. F.; Agren, H. *J. Phys. Chem. B.* **2010**, *114*, 6561-6566.

(19) Carroll, R. L.; Gorman, C. B. *Angew. Chem. Int. Ed.* **2002**, *41*, 4379-4400.

(20) Heath, J. R. *Annu. Rev. Mater. Res.* **2009**, *39*, 1-23.

(21) Balzani, V. *Pure. Appl. Chem.* **2008**, *80*, 1631-1650.

(22) Chen, J.; Reed, M. A.; Dirk, S. M.; Price, D. W.; Rawlett, A. M.; Tour, J.; Grubisha, D. S.; Bennett, D. W. In *Molecular Nanoelectronics*; Reed, M. A., Lee, T., Eds.; American Scientific Publishers: **2003**.

(23) Tour, J. M. *Acc. Chem. Res.* **2000**, *33*, 791-804.

(24) Aviram, A.; Ratner, M. A. *Chem. Phys. Lett.* **1974**, *29*, 277-283.

(25) Metzger, R. M. *Chem. Rev.* **2003**, *103*, 3803-3834.

(26) Nitzan, A.; Ratner, M. A. *Science.* **2003**, *300*, 1384-1389.

(27) James, D. K.; Tour, J. M. *Chem. Mater.* **2004**, *16*, 4423-4435.

(28) Tran, E.; Duati, M.; Ferri, V.; Mullen, K.; Zharnikov, M.; Whitesides, G. M.; Rampi, M. A. *Adv. Mater.* **2006**, *18*, 1323-1328.

(29) Green, J. E.; Choi, J. W.; Boukai, A.; Bunimovich, Y.; Johnston-Halperin, E.; DeIonno, E.; Luo, Y.; Sheriff, B. A.; Xu, K.; Shin, Y. S.; Tseng, H. R.; Stoddart, J. F.; Heath, J. R. *Nature.* **2007**, *445*, 414-417.

(30) Mendes, P. M.; Flood, A. H.; Stoddart, J. F. *Appl. Phys. A-Mater.* **2005**, *80*, 1197-1209.

(31) Service, R. F. *Science.* **2003**, *302*, 556-559.

(32) Venkataraman, L.; Klare, J. E.; Nuckolls, C.; Hybertsen, M. S.; Steigerwald, M. L. *Nature.* **2006**, *442*, 904-907.

(33) Kaiser, F. J.; Hanggi, P.; Kohler, S. *New J. Phys.* **2008**, *10*, 065013.

(34) Solomon, G. C.; Andrews, D. Q.; Van Duyne, R. P.; Ratner, M. A. *J. Am. Chem. Soc.* **2008**, *130*, 7788-7789.

(35) Galperin, M.; Ratner, M. A.; Nitzan, A.; Troisi, A. *Science.* **2008**, *319*, 1056-1060.

(36) McCreery, R. L.; Bergren, A. J. *Adv. Mater.* **2009**, *21*, 4303-4322.

(37) Chen, Y.; Jung, G. Y.; Ohlberg, D. A. A.; Li, X. M.; Stewart, D. R.; Jeppesen, J. O.; Nielsen, K. A.; Stoddart, J. F.; Williams, R. S. *Nanotechnology.* **2003**, *14*, 462-468.

(38) Srivastava, N.; Banerjee, K. *Jom-Us.* **2004**, *56*, 30-31.

(39) Chung, S. W.; Ginger, D. S.; Morales, M. W.; Zhang, Z. F.; Chandrasekhar, V.; Ratner, M. A.; Mirkin, C. A. *Small.* **2005**, *1*, 64-69.

(40) Pingree, L. S. C.; Martin, E. F.; Shull, K. R.; Hersam, M. C. *Ieee. T. Nanotechnol.* **2005**, *4*, 255-259.

(41) Cerofolini, G. F.; Arena, G.; Camalleri, C. M.; Galati, C.; Reina, S.; Renna, L.; Mascolo, D. *Nanotechnology.* **2005**, *16*, 1040-1047.

(42) Huang, J.; Momenzadeh, M.; Lombardi, F. *Ieee. Des. Test. Comput.* **2007**, *24*, 304-311.

(43) Lehn, J. M. *Supramolecular Chemistry: Concepts and Perspectives*; Wiley-VCH Verlag GmbH: Weinheim, **1995**.

(44) Schnabel, M.; Nicholls, R. J.; Salzmann, C. G.; Vengust, D.; Mihailovic, D.; Nellist, P. D.; Nicolosi, V. *Phys. Chem. Chem. Phys.* **2010**, *12*, 433-441.

(45) Mihailovic, D. *Prog. Mater. Sci.* **2009**, *54*, 309-350.

(46) Zhang, R. Y.; Hummelgard, M.; Dvorsek, D.; Mihailovic, D.; Olin, H. *J. Colloid. Interf. Sci.* **2010**, *348*, 299-302.

(47) Iijima, S. *Nature.* **1991**, *354*, 56-58.

(48) Campidelli, S.; Meneghetti, M.; Prato, M. *Small.* **2007**, *3*, 1672-1676.

(49) Fan, H. J.; Gosele, U.; Zacharias, M. *Small.* **2007**, *3*, 1660-1671.

(50) Ploscaru, M. I.; Kokalj, S. J.; Uplaznik, M.; Vengust, D.; Turk, D.; Mrzel, A.; Mihailovic, D. *Nano. Lett.* **2007**, *7*, 1445-1448.

(51) Bourgoin, J. P.; Campidelli, S.; Chenevier, P.; Derycke, V.; Filoramo, A.; Goffman, M. F. *Chimia.* **2010**, *64*, 414-420.

(52) Vrbanic, D.; Remskar, M.; Jesih, A.; Mrzel, A.; Umek, P.; Ponikvar, M.; Jancar, B.; Meden, A.; Novosel, B.; Pejovnik, S.; Venturini, P.; Coleman, J. C.; Mihailovic, D. *Nanotechnology.* **2004**, *15*, 635-638.

(53) Uplaznik, M.; Bercic, B.; Strle, J.; Ploscaru, M. I.; Dvorsek, D.; Kusar, P.; Devetak, M.; Vengust, D.; Podobnik, B.; Mihailovic, D. D. *Nanotechnology.* **2006**, *17*, 5142-5146.

(54) Peng, G.; Strange, M.; Thygesen, K. S.; Mavrikakis, M. *J. Phys. Chem. C.* **2009**, *113*, 20967-20973.

(55) Luo, L.; Frisbie, C. D. *J. Am. Chem. Soc.* **2010**, *132*, 8854-+.

(56) Choi, S. H.; Kim, B.; Frisbie, C. D. *Science.* **2008**, *320*, 1482-1486.

(57) Choi, S. H.; Risko, C.; Delgado, M. C. R.; Kim, B.; Bredas, J. L.; Frisbie, C. D. *J. Am. Chem. Soc.* **2010**, *132*, 4358-4368.

(58) Surridge, N. A.; Jernigan, J. C.; Dalton, E. F.; Buck, R. P.; Watanabe, M.; Zhang, H.; Pinkerton, M.; Wooster, T. T.; Longmire, M. L.; Facci, J. S.; Murray, R. W. *Faraday. Discuss.* **1989**, *88*, 1.

(59) Tuccitto, N.; Ferri, V.; Cavazzini, M.; Quici, S.; Zhavnerko, G.; Licciardello, A.; Rampi, M. A. *Nat. Mater.* **2009**, *8*, 41-46.

(60) Ceccon, A.; Santi, S.; Orian, L.; Bisello, A. *Coord. Chem. Rev.* **2004**, *248*, 683-724.

(61) Aguirre-Etcheverry, P.; O'Hare, D. *Chem. Rev.* **2010**, *110*, 4839-4864.

(62) Lancaster, K.; Odom, S. A.; Jones, S. C.; Thayumanavan, S.; Marder, S. R.; Bredas, J. L.; Coropceanu, V.; Barlow, S. *J. Am. Chem. Soc.* **2009**, *131*, 1717-1723.

(63) Brunschwig, B. S.; Creutz, C.; Sutin, N. *Chem. Soc. Rev.* **2002**, *31*, 168-184.

(64) Astruc, D. *Electron Transfer and Radical Processes in Transition-Metal Chemstry*; VCH Publishers, Inc.: New York, **1995**.

(65) Aviram, A.; Roland, P. *Molecular Electronics: Science and Technology* **1998**, *852*, 339-348.

(66) Renz, M.; Theilacker, K.; Lambert, C.; Kaupp, M. *J. Am. Chem. Soc.* **2009**, *131*, 16292-16302.

(67) Demadis, D. D.; Hartshorn, C. M.; Meyer, T. J. *Chem. Rev.* **2001**, *101*, 2655-2685.

(68) Kaim, W.; Klein, A.; Glockle, M. *Acc. Chem. Res.* **2000**, *33*, 755-763.

(69) Paul, F.; Lapinte, C. *Coord. Chem. Rev.* **1998**, *178-180*, 431-509.

(70) Richardson, D. E.; Taube, H. *Coord. Chem. Rev.* **1984**, *60*, 107-129.

(71) Ward, M. D.; McCleverty, J. A. *Dalton Trans.* **2002**, 275.

(72) Astruc, D. *Acc. Chem. Res.* **1997**, *30*, 383-391.

(73) Ward, M. D. *Chem. Soc. Rev.* **1995**, 121-134.

(74) Benniston, A. C. *Chem. Soc. Rev.* **2004**, *33*, 573-578.

(75) Barlow, S.; O'Hare, D. *Chem. Rev.* **1997**, *97*, 637-669.

(76) Kaim, W.; Lahiri, G. K. *Angew. Chem. Int. Ed.* **2007**, *46*, 1778-1796.

(77) Creutz, C.; Taube, H. *J. Am. Chem. Soc.* **1969**, *91*, 3988-3989.

(78) Hush, N. S. *Prog. Inorg. Chem.* **1967**, *8*, 391-444.

(79) Hush, N. S. *Coord. Chem. Rev.* **1985**, *64*, 135-157.

(80) Lay, P. A.; Magnuson, R. H.; Taube, H. *Inorg. Chem.* **1988**, *27*, 2364-2371.

(81) Creutz, C.; Taube, H. *J. Am. Chem. Soc.* **1973**, *95*, 1086-1094.

(82) D'Alessandro, D. M.; Keene, F. R. *Pure. Appl. Chem.* **2008**, *80*, 1-16.

(83) Robin, M. B.; Day, P. *Adv. Inorg. Chem. Radiochem.* **1967**, *10*, 247 – 422.

(84) Brunschwig, B. S.; Sutin, N. *Coord. Chem. Rev.* **1999**, *187*, 233-254.

(85) D'Alessandro, D. M.; Keene, F. R. *Chem. Soc. Rev.* **2006**, *35*, 424-440.

(86) Ernst, S.; Kasack, V.; Kaim, W. *Inorg. Chem.* **1988**, *27*, 1146-1148.

(87) Salaymeh, F.; Berhane, S.; Yusof, R.; de la Rosa, R.; Fung, E. Y.; Matamoros, R.; Lau, K. W.; Zheng, Q.; Kober, E. M.; Curtis, J. C. *Inorg. Chem.* **1993**, *32*, 3895-3908.

(88) Barriere, F.; Geiger, W. E. *J. Am. Chem. Soc.* **2006**, *128*, 3980-3989.

(89) Geiger, W. E.; Barriere, F. *Acc. Chem. Res.* **2010**, *43*, 1030-1039.

(90) Semenov, S. N. *PhD Dissertation.* **2010**.

(91) Joachim, C.; Gimzewski, J. K.; Aviram, A. *Nature.* **2000**, *408*, 541-548.

(92) Mayor, M.; Weber, H. B.; Reichert, J.; Elbing, M.; von Hanisch, C.; Beckmann, D.; Fischer, M. *Angew. Chem. Int. Ed.* **2003**, *42*, 5834-5838.

(93) Chen, F.; Hihath, J.; Huang, Z. F.; Li, X. L.; Tao, N. J. *Annu. Rev. Phys. Chem.* **2007**, *58*, 535-564.

(94) Lortscher, E.; Riel, H. *Chimia.* **2010**, *64*, 376-382.

(95) Moreland, J.; Ekin, J. W. *J. Appl. Phys.* **1985**, *58*, 3888-3895.

(96) Muller, C. J.; Vanruitenbeek, J. M.; Dejongh, L. J. *Phys. Rev. Lett.* **1992**, *69*, 140-143.

(97) Lortscher, E.; Weber, H. B.; Riel, H. *Phys. Rev. Lett.* **2007**, *98*, 176807.

(98) Tsutsui, M.; Taniguchi, M.; Kawai, T. *J. Am. Chem. Soc.* **2009**, *131*, 10552-10556.

(99) Stapleton, J. J.; Harder, P.; Daniel, T. A.; Reinard, M. D.; Yao, Y. X.; Price, D. W.; Tour, J. M.; Allara, D. L. *Langmuir.* **2003**, *19*, 8245-8255.

(100) Huang, Z. F.; Chen, F.; Bennett, P. A.; Tao, N. J. *J. Am. Chem. Soc.* **2007**, *129*, 13225-13231.

(101) Tour, J. M.; Rawlett, A. M.; Kozaki, M.; Yao, Y. X.; Jagessar, R. C.; Dirk, S. M.; Price, D. W.; Reed, M. A.; Zhou, C. W.; Chen, J.; Wang, W. Y.; Campbell, I. *Chem. Eur. J.* **2001**, *7*, 5118-5134.

(102) Chen, F.; Li, X. L.; Hihath, J.; Huang, Z. F.; Tao, N. J. *J. Am. Chem. Soc.* **2006**, *128*, 15874-15881.

(103) Stuhr-Hansen, N.; Sorensen, J. K.; Moth-Poulsen, K.; Christensen, J. B.; Bjornholm, T.; Nielsen, M. B. *Tetrahedron.* **2005**, *61*, 12288-12295.

(104) Haiss, W.; Wang, C. S.; Grace, I.; Batsanov, A. S.; Schiffrin, D. J.; Higgins, S. J.; Bryce, M. R.; Lambert, C. J.; Nichols, R. J. *Nature Mater.* **2006**, *5*, 995-1002.

(105) Vonlanthen, D.; Mishchenko, A.; Elbing, M.; Neuburger, M.; Wandlowski, T.; Mayor, M. *Angew. Chem. Int. Ed.* **2009**, *48*, 8886-8890.

(106) Han, W. H.; Li, S. M.; Lindsay, S. M.; Gust, D.; Moore, T. A.; Moore, A. L. *Langmuir.* **1996**, *12*, 5742-5744.

(107) Ko, C. H.; Huang, M. J.; Fu, M. D.; Chen, C. H. *J. Am. Chem. Soc.* **2010**, *132*, 756-764.

(108) Fu, M. D.; Chen, W. P.; Lu, H. C.; Kuo, C. T.; Tseng, W. H.; Chen, C. H. *J. Phys. Chem. C* **2007**, *111*, 11450-11455.

(109) Han, W. H.; Durantini, E. N.; Moore, T. A.; Moore, A. L.; Gust, D.; Rez, P.; Leatherman, G.; Seely, G. R.; Tao, N. J.; Lindsay, S. M. *J. Phys. Chem. B* **1997**, *101*, 10719-10725.

(110) Xing, Y. J.; Park, T. H.; Venkatramani, R.; Keinan, S.; Beratan, D. N.; Therien, M. J.; Borguet, E. *J. Am. Chem. Soc.* **2010**, *132*, 7946-7956.

(111) Park, Y. S.; Whalley, A. C.; Kamenetska, M.; Steigerwald, M. L.; Hybertsen, M. S.; Nuckolls, C.; Venkataraman, L. *J. Am. Chem. Soc.* **2007**, *129*, 15768-15769.

(112) Villares, A.; Martin, S.; Giner, I.; Diaz, J.; Lydon, D. P.; Low, P. J.; Cea, P. *Soft. Matter.* **2008**, *4*, 1508-1514.

(113) Kiguchi, M.; Miura, S.; Hara, K.; Sawamura, M.; Murakoshi, K. *Appl. Phys. Lett.* **2006**, *89*, 213104.

(114) Angelici, R. J.; Lazar, M. *Inorg. Chem.* **2008**, *47*, 9155-9165.

(115) Chen, J.; Calvet, L. C.; Reed, M. A.; Carr, D. W.; Grubisha, D. S.; Bennett, D. W. *Chem. Phys. Lett.* **1999**, *313*, 741-748.

(116) Xu, B. Q.; Tao, N. J. J. *Science.* **2003**, *301*, 1221-1223.

(117) Wang, C. S.; Batsanov, A. S.; Bryce, M. R.; Martin, S.; Nichols, R. J.; Higgins, S. J.; Garcia-Suarez, V. M.; Lambert, C. J. *J. Am. Chem. Soc.* **2009**, *131*, 15647-15654.

(118) Park, Y. S.; Whalley, A. C.; Kamenetska, M.; Steigerwald, M. L.; Hybertsen, M. S.; Nuckolls, C.; Venkataraman, L. *J. Am. Chem. Soc.* **2007**, *129*, 15768-+.

(119) Adams, H.; Costa, P. J.; Newell, M.; Vickers, S. J.; Ward, M. D.; Felix, V.; Thomas, J. A. *Inorg. Chem.* **2008**, *47*, 11633-11643.

(120) Balzani, V.; Juris, A.; Venturi, M.; Campagna, S.; Serroni, S. *Chem. Rev.* **1996**, *96*, 759-833.

(121) Dembinski, R.; Bartik, T.; Bartik, B.; Jaeger, M.; Gladysz, J. A. *J. Am. Chem. Soc.* **2000**, *122*, 810-822.

(122) Jiao, H. J.; Costuas, K.; Gladysz, J. A.; Halet, J. F.; Guillemot, M.; Toupet, L.; Paul, F.; Lapinte, C. *J. Am. Chem. Soc.* **2003**, *125*, 9511-9522.

(123) Venkatesan, K.; Blacque, O.; Berke, H. *Dalton. Trans.* **2007**, 1091-1100.

(124) Heidrich, J.; Steimann, M.; Appel, M.; Beck, W.; Phillips, J. R.; Trogler, W. C. *Organometallics.* **1990**, *9*, 1296-1300.

(125) Davies, J. A.; Elghanam, M.; Pinkerton, A. A.; Smith, D. A. *J. Organomet. Chem.* **1991**, *409*, 367-376.

(126) Kheradmandan, S.; Venkatesan, K.; Blacque, O.; Schmalle, H. W.; Berke, H. *Chem. Eur. J.* **2004**, *10*, 4872-4885.

(127) Unseld, D.; Krivykh, V. V.; Heinze, K.; Wild, F.; Artus, G.; Schmalle, H.; Berke, H. *Organometallics.* **1999**, *18*, 1525-1541.

(128) Venkatesan, K. *PhD Dissertation.* **2003**.

(129) Kheradmandan, S.; Heinze, K.; Schmalle, H. W.; Berke, H. *Angew. Chem. Int. Ed.* **1999**, *38*, 2270-2273.

(130) Fernandez, F. J.; Blacque, O.; Alfonso, M.; Berke, H. *Chem. Commun.* **2001**, 1266-1267.

(131) Fernandez, F. J.; Venkatesan, K.; Blacque, O.; Alfonso, M.; Schmalle, H. W.; Berke, H. *Chem. Eur. J.* **2003**, *9*, 6192-6206.

(132) Venkatesan, K.; Fox, T.; Schmalle, H. W.; Berke, H. *Eur. J. Inorg. Chem.* **2005**, 901-909.

(133) Fritz, T.; Schmalle, H. W.; Blacque, O.; Venkatesan, K.; Berke, H. *Z. Anorg. Allg. Chem* **2009**, *635*, 1391-1401.

(134) Venkatesan, K.; Fox, T.; Schmalle, H. W.; Berke, H. *Organometallics.* **2005**, *24*, 2834-2847.

(135) Brady, M.; Weng, W. Q.; Zhou, Y. L.; Seyler, J. W.; Amoroso, A. J.; Arif, A. M.; Bohme, M.; Frenking, G.; Gladysz, J. A. *J. Am. Chem. Soc.* **1997**, *119*, 775-788.

2. C_4-bridged Dinuclear Rhenium Complexes from Oxidative C-C Coupling of Mononuclear Vinylidene Complexes

ABSTRACT. The preparation of the mononuclear rhenium carbyne complex *trans*-[ReCl(≡C-CH_3)(PMe_3)$_4$]Cl (**4**) was achieved in 80% yield by the protonation of the vinylidene complex *trans*-[ReCl(=C=CHSiMe_3)(PMe_3)$_4$] (**2**) with HCl in THF. **2** was obtained by irradiation of the dinitrogen complex *trans*-[ReCl(N_2)(PMe_3)$_4$] (**1**) with sunlight in the presence of an excess of HC≡CSiMe_3 in THF. The carbyne complex *trans*-[Re(C≡CSiMe_3)(≡C-CH_3)(PMe_3)$_4$][PF_6] (**6**) was prepared in 90% yield by heating a mixture of the dinitrogen complex **1**, TlPF_6, and an excess of HC≡CSiMe_3 in a 1:1 mixture of *N*,*N*-Diisopropylethylamine (DIPEA)/THF at 95 °C for 24 h. Both the carbyne complexes **4** and **6** can be deprotonated with KO*t*Bu to the corresponding vinylidene complexes *trans*-[XRe(=C=CH_2)(PMe_3)$_4$] (X = Cl, **3**; C≡CSiMe_3, **7**) in excellent yields. The oxidation of the vinylidene complexes **3** and **7** with 1.2 equiv. of [Cp_2Fe][PF_6] at -78 °C gave the C_β-C_β' coupled dinuclear rhenium biscarbyne complexes *trans*-[X(PMe_3)$_4$Re≡C-CH_2-CH_2-C≡Re(PMe_3)$_4$X][PF_6] (X = Cl, **9**; C≡CSiMe_3, **10**) in 90% and 92%, respectively. X-ray diffraction analyses have been carried out on the complexes **2**, **3**, **4**, **5**, **6**, **9** and **10**.

KEYWORDS. Oxidative coupling reaction; Rhenium carbyne complex; Rhenium vinylidene complex; Cyclic voltammetry; X-ray diffraction analysis

2.1 Introduction

Organometallic rigid-rod type dinuclear complexes consisting of a "conducting" π-conjugated organic bridge with redox-active metal end-groups of the type [$L_nMC_xML_n$] (M = metal; L = ligand, C_x = carbon chain), have recently received considerable attention due to their potential to function as electrical devices in molecular electronics. The simplest of such devices is the molecular wire providing single-electron-conductance between the remote ends.[1-14] More sophisticated devices are based on molecular wires. Gladysz and co-workers had prepared a series of dinuclear rhenium complexes with carbon chains of up to ten alkynyl units (x = 20).[15-16] They found that with increasing chain length, the potential difference (Δ*E*) between the two redox peaks in the CV spectra decreases and the oxidation becomes increasingly irreversible. In

other words, the longer the chain length, the smaller the extent of delocalization between two metal centers. In a classical view the through-bridge travel of an electron from one side to the other can be viewed as a redox process with oxidation of one side and concomitant reduction of the other side. This ability of single-electron-conductance is mainly dependent on the through-bridge electronic communication, which can be determined by cyclic voltammetry (CV) and UV-vis NIR spectroscopy. Generally speaking, the two redox waves of the two redox-active metal centers show increase in the potential difference (ΔE) with increasing through-bridge communication. Depending on the extent of the through-bridge communication between two metal centers, the mixed-valence systems have been classified into three groups by Robin & Day.[17] While the complexes belonging to class I have no or very weak through-bridge communication between redox sites, the class II species show moderate through-bridge communication between the metal centers. In the case of class III compounds, the redox centers are strongly coupled and the lone-electron of the mixed-valence species is fully delocalized. In other words the molecular wires can be differentiated by their varying degrees of barriers for electron transfer such as wires with barriers, moderate barriers and no barriers for electron transfer.

Based on the synthetic ease, stability and favorable electronic properties, polyynediyl with x = 4 carbon chain was thought to be the ideal bridge for electronic communication between the metal centers.[15-16] Therefore many studies have focused on complexes of the type $[L_nMC_4ML_n]$ with various transition metal centres, such as Mn,[18-20] Fe,[16,21] Re,[22-24] Ru,[25-26] Pt,[27] W and Mo[28-30]. However, most of these complexes have stopper-type termini that prevent further functionalization for fixation of "anchor" groups to electrodes and/or the eventual extension of these systems to form oligonuclears.[30] Our group's research efforts over the years were directed towards the construction of C_4-bridged dinuclear and oligonuclear transition metal complexes with replaceable ligands at the termini. The through-bridge electronic communication between the metal centers was investigated by various physical methods.

The C_4-bridged dinuclear manganese complexes reported by our group showed interesting electronic properties, but were relatively unstable in organic solvents for prolonged periods of time. The fact that heavier transition elements possess higher barriers for ligand exchange reactions and would render complexes more stable, provided the impetus for the development of

rhenium based molecular fragment that is structurally analogous to the manganese compounds. The relatively low delocalization energy of the poly-acetylenic unit and a higher π-interaction energy between the internal C-C bonds of bisvinylidene, an isomer of diacetylene, prompted us to investigate the bisvinylidene (|C=CH-CH=C|) ligand as a bridging unit. Physical investigation on this type of complexes has been limited.[28,31-32] In addition, it should be mentioned that according to the canonical form of a C_4 bridged [M]C4[M] system (Scheme 1), the bridge delocalization energy might be increased, if the metal centered end groups are capable of stabilizing the biscarbynic form. The interaction energy of two acetylene units is close to nil and therefore is the delocalization energy of a butadiyne moiety low. While the carbyne carbons of transition metal complexes are expected to have considerably higher interactions with an acetylenylidene moiety.

Scheme 1

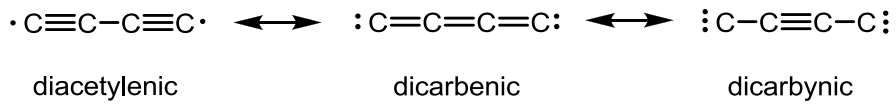

Oxidative C-C coupling reactions of mononuclear rhenium $C_2H_{n/2}$ (n = 0, 2 or 4) complexes was sought as the strategy to construct C_4H_n (n = 0, 2 or 4) dinuclear rhenium complexes. Our work on such manganese complexes[19,33-38] and others work on niobium,[39] tungsten,[28] molybdenum,[28,40] manganese,[31,41] rhenium,[42] iron,[21,43] and ruthenium[44] demonstrates that oxidative coupling of metal alkynyls or oxidative dehydro-dimerization of metal vinylidenes (eq. 24, eq. 25, and eq. 26) is one of the most effective methods to access dinuclear bis(acetylide) or bis(vinylidene) complexes.[32,45-48]

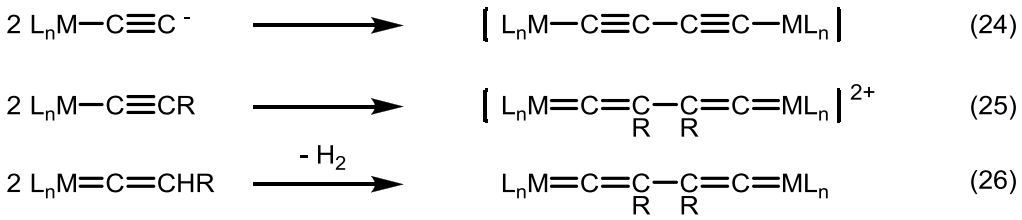

Metal vinylidene complexes can be prepared by converting terminal alkyne complexes into their vinylidene tautomers via the acetylene-vinylidene rearrangement. To obtain dinuclear rhenium C_4-bridged complexes with replaceable substituents, the dinitrogen rhenium complex *trans*-[$ReCl(N_2)(PMe_3)_4$] (**1**) was chosen as a suitable starting material, since neutral vinylidene

complexes were expected to be prepared by using a reported method.[49] In this work, we report the investigation on the C-C coupling reactions of the vinylidene complexes *trans*-[XRe(=C=CH_2)(PMe_3)$_4$] (X = Cl, **3**; C≡$CSiMe_3$, **7**) and their coupled products *trans*-[X(PMe_3)$_4$Re≡C-CH_2-CH_2-C≡Re(PMe_3)$_4$X][PF_6] (X = Cl, **9**; C≡$CSiMe_3$, **10**).

2.2 Syntheses of the mononuclear rhenium vinylidene complexes

2.2.1 Syntheses of the mononuclear rhenium vinylidene complexes **2** and **3**

The complex *trans*-[ReCl(=C=$CHSiMe_3$)(PMe_3)$_4$] (**2**) was prepared by sunlight irradiation of the dinitrogen complex *trans*-[ReCl(N_2)(PMe_3)$_4$] (**1**) in the presence of an excess of HC≡$CSiMe_3$ in THF at room temperature (Scheme 1). This reaction proceeded with the substitution of the N_2 ligand by HC≡$CSiMe_3$, followed by a 1, 2-hydrogen shift to give the vinylidene complex **2**. **2** shows good solubility in non-polar solvents, such as pentane, diethyl ether, benzene and toluene and is sparingly soluble in acetonitrile, but reacts with CH_2Cl_2 resulting in the corresponding carbyne complex *trans*-[ReCl(≡C-CH_3)(PMe_3)$_4$]Cl (**4**). The crude product was directly used for desilylation without further purification.

Scheme 1

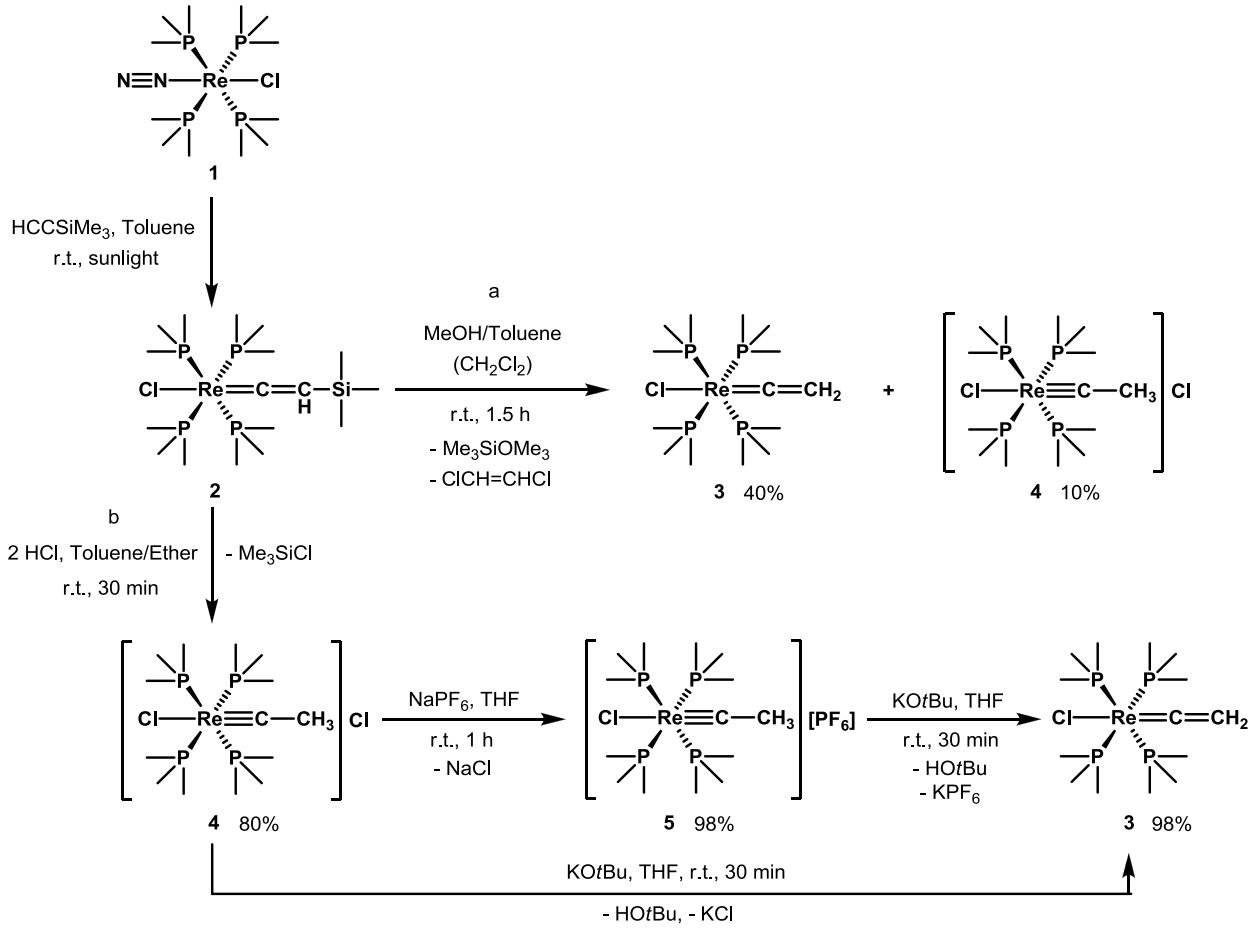

Our initial attempts to effect desilylation of the vinylidene complex **2** with methanol in toluene and trace amount of CH_2Cl_2 gave a mixture of the vinylidene complex *trans*-[ReCl(=C=CH_2)(PMe_3)$_4$] (**3**) and the carbyne complex *trans*-[ReCl(≡C-CH_3)(PMe_3)$_4$]Cl (**4**) in 40% and 10% yield, respectively (Scheme 1a). A vinylidene ligand bound to a metal complex has shown to be polarized with the C_α being electron poor (δ+) and the C_β is electron rich (δ-).

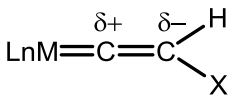

Attack of electrophiles usually occurs at the C_β atom and the addition of nucleophiles exclusively on the C_α atom.[32,47] The reason for the formation of the carbyne complex **4** can be attributed to the electron-rich C_β of the vinylidene complex **3**, which undergoes an electrophilic attack by H^+ from methanol. The electron-rich C_β of the vinylidene complexes **2** and **3** imparts

greater reactivity towards CH_2Cl_2 to produce the carbyne complex *trans*-[ReCl(≡C-CH_3)$(PMe_3)_4$]Cl (**4**). As shown in Scheme 2, presumably, the electron-rich C_β atom of the vinylidene complexes **2** and **3** abstracts a H^+ from CH_2Cl_2 (α-H elimination) to give a carbanion and a carbyne complex. The loss of the chloride anion from the carbanion creates a chlorocarbene that dimmers to 1,2-dichloroethene and in the process results in the trimethylsilyl chloride and producing the vinylidene complex **3** that reacts further with CH_2Cl_2 giving the carbyne complex **4**.

Scheme 2

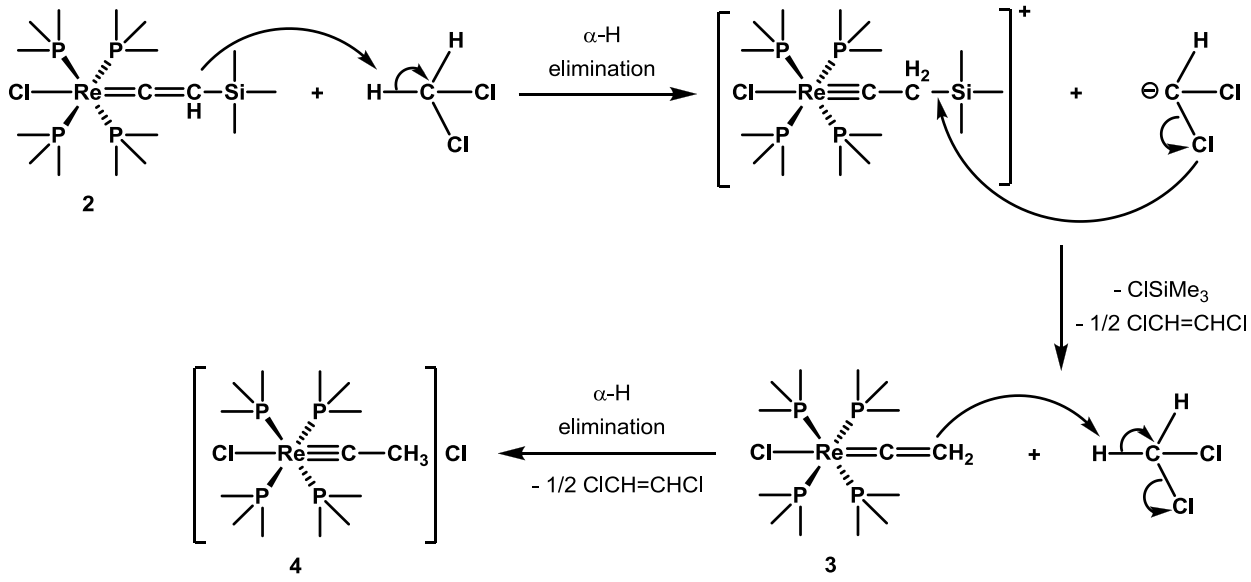

Another proton transfer from CH_2Cl_2 was observed in the oxidation of [Fe(Cp*)(dppe)(C≡CH)] with $[Cp_2Fe][PF_6]$ in CH_2Cl_2, resulting in the formation of the vinylidene complex $[Fe(Cp^*)(dppe)(=C=CH_2)][PF_6]$.[21] They attribute this result to a 17-electron intermediate $[Fe(Cp^*)(dppe)(C\equiv CH)][PF_6]$ that abstracts a proton radical from CH_2Cl_2 resulting in the vinylidene complex.

The deprotonation of the carbyne complexes is the formal reverse of the addition of a proton to the vinylidene (eq. 27 and eq. 28).[50] Pombeiro and co-workers have earlier shown that the resulting vinylidene complex *trans*-$[ReCl(dppe)_2(=C=CHSiMe_3)]$ was susceptible to protonation of the C_β to give the corresponding carbyne product *trans*-$[ReCl(dppe)_2(\equiv C\text{-}CH_3)]$ and

desilylation could be achieved by treatment of the trimethylsilyl vinylidene complex with acid.[49,51-52]

The carbyne complex is easier to purify and handle in comparison with the vinylidene complex. Therefore protonation of complex **2** with HCl in THF was sought, which afforded the carbyne complex *trans*-[ReCl(≡C-CH_3)(PMe_3)$_4$]Cl (**4**) in 80% yield. The anion exchange of Cl^- with PF_6^- was easily accomplished by reacting **4** with $NaPF_6$ in THF. The resulting complex *trans*-[ReCl(≡C-CH_3)(PMe_3)$_4$][PF_6] (**5**) was deprotonated with KO*t*Bu in THF to give the *trans*-[ReCl(=C=CH_2)(PMe_3)$_4$] (**3**) product in 98% yield (Scheme 1b).

2.2.2 Preparation of the mononuclear rhenium vinylidene complex **7**

Preparation of the complex *trans*-[Re(C≡C$SiMe_3$)(≡C-CH_3)(PMe_3)$_4$][PF_6] (**6**) was achieved in 90% yield by heating a mixture of the dinitrogen rhenium (I) complex *trans*-[$ReClN_2$(PMe_3)$_4$] (**1**), $TlPF_6$, and an excess of HC≡C$SiMe_3$ in a 1:1 mixture of *N*,*N*-Diisopropylethylamine (DIPEA)/THF at 95 °C for 24 h. Longer reaction times were required when the reaction was carried out at 60 °C (62 h). An inseparable mixture of the rhenium (III) chloro carbyne complex *trans*-[ReCl(≡C-CH_3)(PMe_3)$_4$][PF_6] (**5**) and the rhenium (III) carbyne acetylide complex *trans*-[Re(C≡C$SiMe_3$)(≡C-CH_3)(PMe_3)$_4$][PF_6] (**6**) was obtained with shorter reaction times. The mechanism leading to the formation of these complexes is still unclear. However it can be postulated that the reaction involves the release of N_2 to form the vinylidene complex **2** that reacts with residual water from the starting materials. This reaction results in the formation of the monosubstituted carbyne complex **5**, which is followed by the substitution of Cl^- with $Me_3SiC{\equiv}C^-$ to give the disubstituted carbyne acetylide complex **6** (Scheme 3). It is important to note that the monosubstituted complex **5** is the initial product generated during the reaction that gradually transforms to the disubstituted complex **6** during the course of the reaction.

Scheme 3

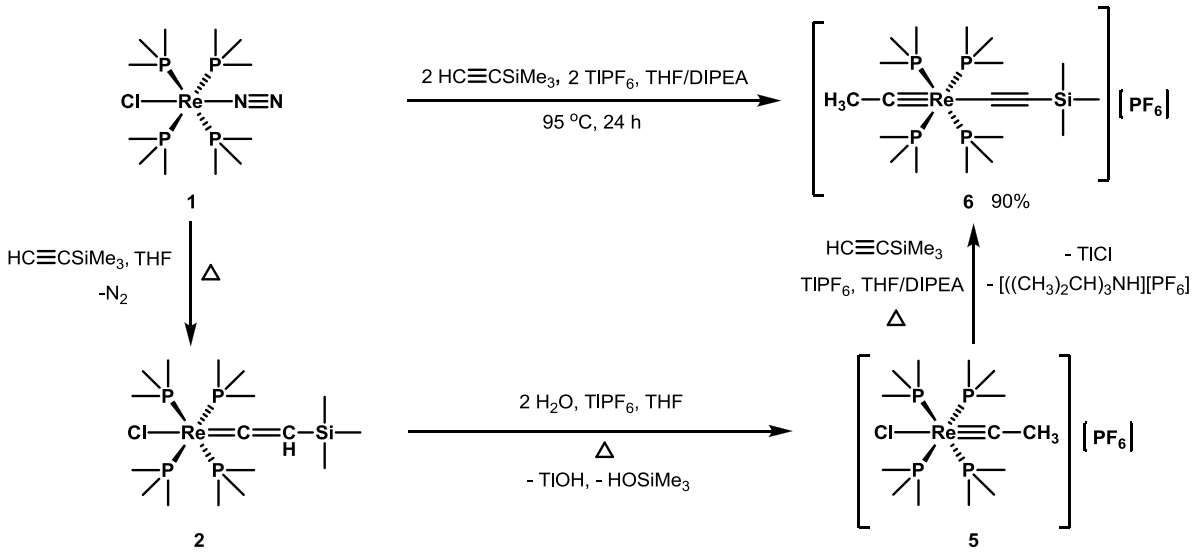

Deprotonation of **6** with an excess of DBU did not proceed, however, **6** underwent deprotonation readily with an excess of KO*t*Bu in THF to form the corresponding rhenium (I) vinylidene complex *trans*-[Re(C≡CSiMe$_3$)(=C=CH$_2$)(PMe$_3$)$_4$] (**7**) in 98% yield (Scheme 4). The protonation of the β carbon atom of **6** with HCl afforded the corresponding carbyne complex *trans*-[Re(C≡CSiMe$_3$)(≡C-CH$_3$)(PMe$_3$)$_4$]Cl (**8**) as well, which could be deprotonated with KO*t*Bu effectively to regenerate the vinylidene complex **7**.

Scheme 4

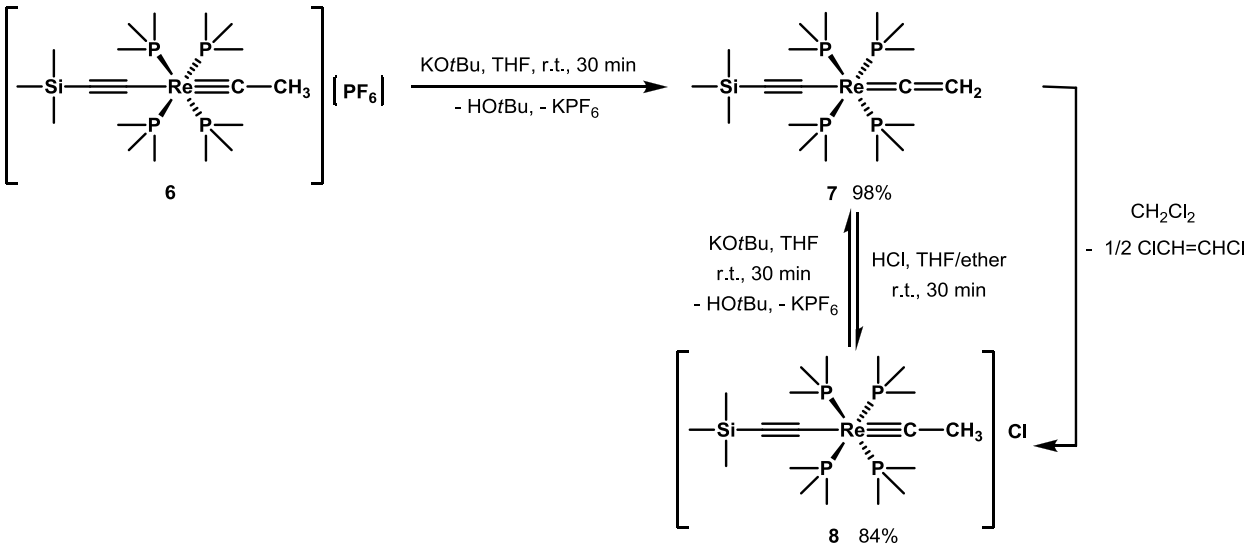

When the deprotonation was carried out in a competitive experiment with a mixture of *trans*-[Re(C≡CSiMe$_3$)(≡C-CH$_3$)(PMe$_3$)$_4$][PF$_6$] (**6**) and *trans*-[ReCl(≡C-CH$_3$)(PMe$_3$)$_4$][PF$_6$] (**5**), it was found that **6** reacted with KO*t*Bu prior to **5** to form the corresponding vinylidene complex, attributing **6** a higher kinetic acidity than **5**.

2.2.3 Characterization of the vinylidene complexes **2**, **3** and **7** and the carbyne complexes **4**, **5**, **6** and **8**

The vinylidene complexes **2**, **3** and **7** and the carbyne complexes **4**, **5, 6** and **8** were characterized by NMR, IR, elemental analyses and mass spectroscopy. Selected ^{1}H NMR and ^{31}P NMR data for the complexes **2-8** are listed in Table 2-1for comparison.

Table 2-1. Selected ^{1}H NMR and ^{31}P NMR data for the vinylidene complexes **2**, **3**, and **7** measured in C_6D_6 and for the carbyne complexes **4, 5, 6,** and **8** measured in CD_2Cl_2

Complexes	^{13}C NMR (δ, ppm)		^{1}H NMR (δ, ppm)	^{31}P NMR (δ, ppm)
	C_α	C_β	H (C_β)	PMe_3
[ReCl(=C=CHSiMe$_3$)(PMe$_3$)$_4$] (**2**)	287.5	82.0	0.75	-34.8
[ReCl(=C=CH$_2$)(PMe$_3$)$_4$] (**3**)	291.4	80.8	1.22	-34.4
[Re(=C=CH$_2$)(C≡CSiMe$_3$)(PMe$_3$)$_4$] (**7**)	301.6	87.8	1.35	-41.4
[ReCl(≡C-CH$_3$)(PMe$_3$)$_4$]Cl (**4**)	260.0	37.4	1.50	-34.8
[ReCl(≡C-CH$_3$)(PMe$_3$)$_4$][PF$_6$] (**5**)	272.6	36.4	1.40	-35.0
[Re(C≡CSiMe$_3$)(≡C-CH$_3$)(PMe$_3$)$_4$][PF$_6$] (**6**)	284.5	38.4	1.27	-41.6
[Re(C≡CSiMe$_3$)(≡C-CH$_3$)(PMe$_3$)$_4$]Cl (**8**)	284.9	38.7	1.31	-41.5

The ^{1}H NMR spectra of the vinylidene complexes *trans*-[ReCl(=C=CHSiMe$_3$)(PMe$_3$)$_4$] (**2**) and *trans*-[ReCl(=C=CH$_2$)(PMe$_3$)$_4$] (**3**) revealed resonances for the vinylidene protons as quintets at 0.75 ppm ($^4J_{PH}$ = 4.6 Hz) and 1.22 ppm ($^4J_{PH}$ = 4.4 Hz), respectively, due to coupling with the four equivalent phosphorus nuclei. The ^{13}C{^{1}H} NMR spectra showed two characteristic signals for the vinylidene C_α and C_β atoms of **2** at 287.5 ppm ($^2J_{PC}$ = 10.0 Hz) and 82.0 ppm, and those

of **3** at 291.4 ppm ($^2J_{PC}$ = 10.8 Hz) and 80.8 ppm. In the IR spectra, the strong ν(C=C) vibrations at 1504 cm^{-1} and 1550 cm^{-1} confirm the presence of the vinylidene unit of **2** and **3**. The IR spectrum of **7** showed a strong ν(C=C) band at 1558 cm^{-1} and a ν(C≡C) band at 1982 cm^{-1}. The ^{1}H NMR spectrum of **7** displayed a characteristic quintet for the vinylidene protons at 1.35 ppm ($^4J_{PH}$ = 3.5 Hz). In the $^{13}C\{^1H\}$ NMR spectrum two resonances were found at 301.6 ppm ($^2J_{PC}$ = 11.9 Hz) and 87.8 ppm that could be assigned to the C_α and C_β atoms of vinylidene group. The other two resonances at 150.1 ppm and 67.8 ppm were attributed to the C_α' and C_β' atoms of the acetylide group. By comparing the vinylidene complexes presented in Table 2-1, one observes that the replacement of chloride ligand with trimethylacetylide ligand results in a downfield shift for the H, C_α, and C_β resonances. This could be attributed to the strong π electron-donating property of the Cl^- ligand, while the $Me_3SiC{\equiv}C^-$ ligand being a relatively better π acceptor, which is also the same reason for the low ν(C=C) of **2**. According to Table 2-2, the vinylidene H, C_α and C_β resonances observed in **2**, **3** and **7** undergo an upfield shift in comparison with those resonances of the reported manganese and rhenium vinylidene complexes in the literature.

Table 2-2. Selected ^{1}H NMR and ^{13}C NMR data measured in C_6D_6 for the reported vinylidene complexes and the vinylidene complexes **2**, **3**, and **7**

Complexes	^{13}C NMR (δ, ppm)		^{1}H NMR (δ, ppm)	Ref.
	C_α	C_β	H (C_β)	
(η^5-C_5H_5)$(CO)_2$Mn=C=C(H)Ph	379.54	123.54	/	41
(η^5-C_5Me_5)$(CO)_2$Mn=C=C(H)Ph	377.9	134.5	6.59	31
(η^5-C_5H_5)$(CO)_2$Re=C=C(H)Ph	326.2	116.0	4.47	42
($Me_3SiC\equiv C$)$(dmpe)_2$Mn=C=CH_2	345.1	170.4	3.55	37-38
(η^5-C_5H_5)(dmpe)Mn=C=CH_2 (THF-d_8)	341.9	97.3	3.77	19
(η^5-C_5H_4Me)(dmpe)Mn=C=CH_2	341.9	97.2	4.34	
(η^5-C_5H_5)(depe)Mn=C=CH_2 (THF-d_8)	341.3	98.2	3.77	
(η^5-C_5H_4Me)(dmpe)Mn=C=C(H)Ph	342.5	142.2	5.81	
(η^5-C_5H_4Me)(depe)Mn=C=C(H)Ph	340.5	120.8	5.82	
(η^5-C_5H_4Me)(depe)Mn=C=CH_2	341.9	97.6	4.25	
(η^5-C_5H_5)(dmpe)Mn=C=C(H)Ph	342.4	141.9	6.00	
(η^5-C_5H_5)(dmpe)Mn=C=C(H)PhCH_3	339.4	138.9	5.98	
(η^5-C_5H_4Me)(dmpe)Mn=C=C(H)PhCH_3	341.5	141.9	5.98	
(η^5-C_5H_4Me)(dmpe)Mn=C=C(H)(Si(*t*Bu)$(CH_3)_2$)	332.4	142.3	4.05	
[ReCl(=C=C$HSiMe_3$)$(PMe_3)_4$] (**2**)	287.5	82.0	0.75	Present work
[ReCl(=C=CH_2)$(PMe_3)_4$] (**3**)	291.4	80.8	1.22	
[Re(=C=CH_2)(C≡C$SiMe_3$)$(PMe_3)_4$] (**7**)	301.6	87.8	1.35	

In the ^{1}H NMR spectra, the carbyne complexes *trans*-[ReCl(≡C-CH_3)(PMe_3)$_4$]Cl (**4**), *trans*-[ReCl(≡C-CH_3)(PMe_3)$_4$][PF_6] (**5**), *trans*-[Re(C≡C$SiMe_3$)(≡C-CH_3)(PMe_3)$_4$][PF_6] (**6**) and *trans*-[Re(C≡C$SiMe_3$)(≡C-CH_3)(PMe_3)$_4$]Cl (**8**) exhibited a characteristic quintet for the carbyne protons at 1.50 ppm ($^4J_{PH}$ = 4.0 Hz), 1.40 ppm ($^4J_{PH}$ = 4.0 Hz), 1.27 ppm ($^4J_{PH}$ = 4.0 Hz), and 1.31 ppm ($^4J_{PH}$ = 4.0 Hz), respectively. The ^{13}C{^{1}H} NMR spectra displayed resonances for the C_α and C_β atoms of **4** at 260.0 ppm and 37.4 ppm; those of **5** at 272.6 ppm and 36.4 ppm**,** those of **6** at 284.5 ppm and 38.4 ppm, and those of **8** at 284.9 ppm and 38.7 ppm, respectively (the ^{13}C{^{1}H} NMR spectra showed signals of low intensities for these complexes which did not allow to extract the J_{PC} values). The C_α and C_β resonance of the carbyne ligand in **6** displays upfield shifts in comparison with those (314.3 ppm and 38.8 ppm) of the manganese analog *trans*-[Mn(C≡C$SiMe_3$)(≡C-CH_3)(dmpe)$_2$]$^+$.[38] In comparison to the chemical shifts of the carbyne complexes in Table 2-1, downfield shifts of the H, C_α, and C_β resonances were also observed from the Cl^- complexes **4** and **5** with respect to the $Me_3SiC{\equiv}C^-$ complexes **6** and **8**. The anion exchange of Cl^- with PF_6^- did not alter the ^{1}H and the ^{13}C chemical shift significantly, especially for **6** and **8** with the trimethylacetylide ligand. Two additional resonances for **6** at 134.7 ppm and 125.7 ppm and for **8** at 135.0 ppm and 125.8 ppm confirmed the presence of the acetylide group. In the IR spectra, the diagnostic ν(C≡C) vibrations for **6** and **8** were observed at 2029 cm^{-1} and 2025 cm^{-1}, respectively. The carbyne structure of **6** was corroborated by ^{13}C-DEPT and long-range (^{1}H, ^{13}C) correlation NMR. The characteristic up signal of the CH_3 was observed at 38.4 ppm in ^{13}C-DEPT NMR spectrum (CH and CH_3 up; CH_2 down) and the long-range (^{1}H, ^{13}C) correlation spectrum displayed a characteristic cross peak from carbyne C_α atom to the carbyne proton, which allowed the assignment of the resonance for CH_3 group. The *trans*-arrangement of all the vinylidene and carbyne complexes was unambiguously confirmed by the singlet resonance observed in their ^{31}P{^{1}H} NMR spectra and further corroborated by X-ray diffraction studies of complexes **2**-**6** (Figure 2-1). The selected bond distances and bond angles for **2**-**6** are summarized in Table 2-3 and Table 2-4.

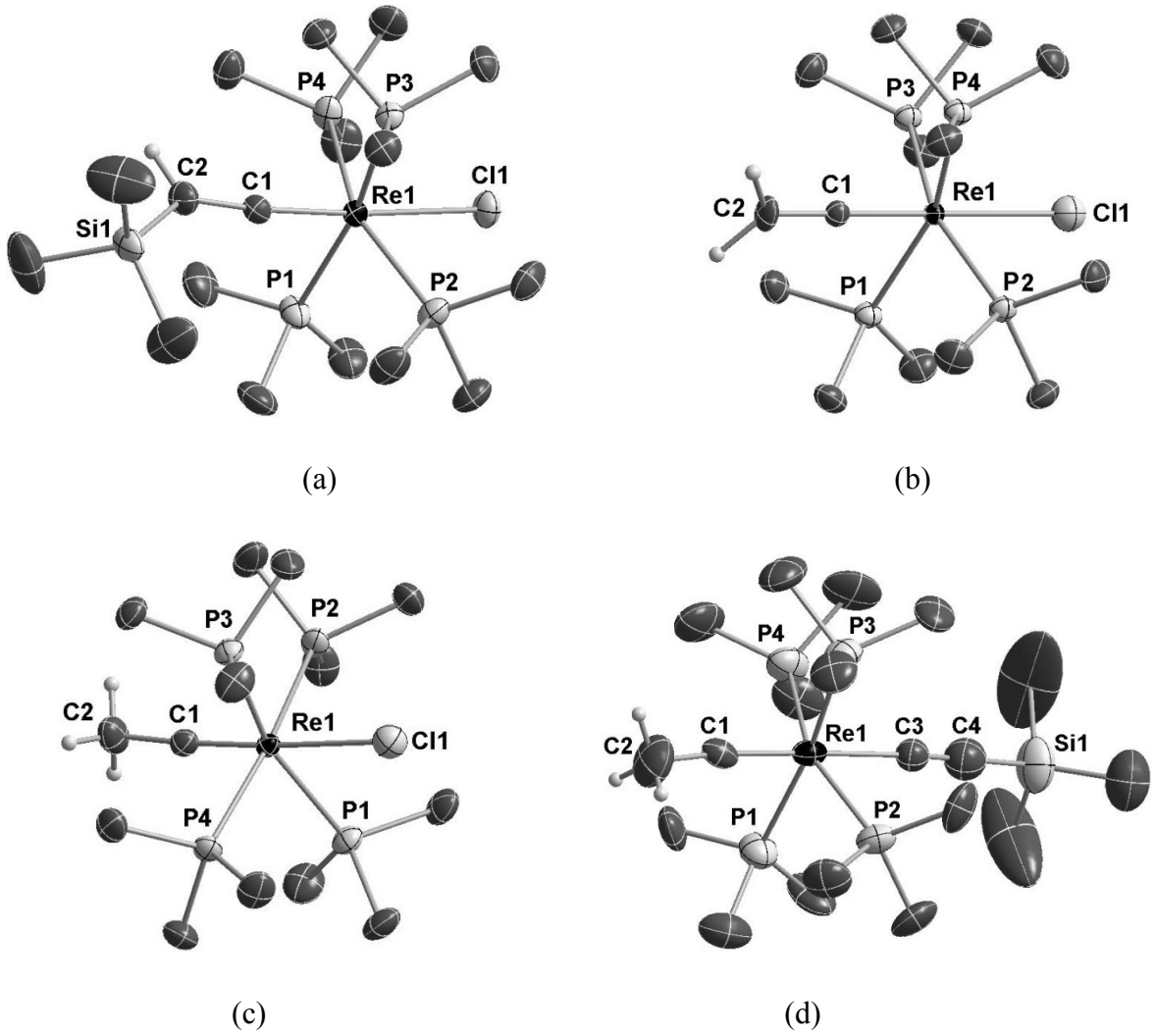

Figure 2-1. Molecular structure of (a) *trans*-**[**$ReCl(=C=CHSiMe_3(PMe_3)_4]$ **2**; (b) *trans*-$[ReCl(=C=CH_2(PMe_3)_4]$ **3**; (c) *trans*-**[**$ReCl(\equiv C\text{-}CH_3)(PMe_3)_4][PF_6]$ **5**; (d) *trans*-$[Re(C\equiv CSiMe_3)(\equiv C\text{-}CH_3)(PMe_3)_4][PF_6]$ **6** (thermal ellipsoids drawn at the 50% probability level, solvent, counter ion and selected hydrogen atoms are omitted for clarity)

Table 2-3. Selected bond lengths [Å] for complexes **2**, **3**, **4**, **5,** and **6**

Complexes	Selected bond lengths [Å]			
	Re-C1	C1-C2	Re-Cl1	C3-C4
[ReCl(=C=CHSiMe$_3$)(PMe$_3$)$_4$] (**2**)	1.854(3)	1.347(14)	2.5707(7)	/
[ReCl(=C=CH$_2$)(PMe$_3$)$_4$] (**3**)	1.861(9)	1.353(16)	2.576(3)	/
[ReCl(≡C-CH$_3$)(PMe$_3$)$_4$]Cl (**4**)	1.818(6)	1.355(9)	2.5132(15)	/
[ReCl(≡C-CH$_3$)(PMe$_3$)$_4$][PF$_6$] (**5**)	1.753(2)	1.475(4)	2.5239(6)	/
[Re(C≡CSiMe$_3$)(≡C-CH$_3$)(PMe$_3$)$_4$][PF$_6$] (**6**)	1.862(8)	1.427(12)	2.134(9) (Re-C3)	1.186(12)

Table 2-4. Selected bond angles [º] for complexes **2**, **3**, **4**, **5,** and **6**

Complexes	Selected angles [º]		
	Re-C1-C2	C1-Re-C11	C1-C2-Si
[ReCl(=C=CHSiMe$_3$)(PMe$_3$)$_4$] (**2**)	172.1(3)	174.19(9)	132.4(3)
[ReCl(=C=CH$_2$)(PMe$_3$)$_4$] (**3**)	180.000(1)	180.0	/
[ReCl(≡C-CH$_3$)(PMe$_3$)$_4$]Cl (**4**)	179.1(5)	178.68(15)	/
[ReCl(≡C-CH$_3$)(PMe$_3$)$_4$][PF$_6$] (**5**)	176.5(2)	178.80(8)	/
[Re(C≡CSiMe$_3$)(≡C-CH$_3$)(PMe$_3$)$_4$][PF$_6$] (**6**)	174.1(8)	178.6(3) (C1-Re-C3)	/

The Re-C1 distances in the vinylidene complexes *trans*-[ReCl(=C=CHSiMe$_3$)(PMe$_3$)$_4$] (**2**) and *trans*-[ReCl(=C=CH$_2$)(PMe$_3$)$_4$] (**3**) are 1.854(3) Å and 1.861(9) Å, which are shorter than the 2.046(8) Å Re=C distance found in *trans*-[ReCl(=C=CHPh)(dppe)$_2$],[53] but naturally longer than

the 1.782(4) Å Mn=C distance in *trans*-[Mn(C≡CSiMe$_3$)(=C=CH$_2$)(dmpe)$_2$].[38] The C1-C2 bond distances in **2** and **3** are 1.347(14) Å and 1.353(16) Å, which fall into the distance range of C=C bond (1.33-1.38 Å). The Re-C1 distances for the carbyne complexes **4** and **5** are 1.818(6) Å and 1.753(2) Å, respectively. They are longer than the expected distance range (1.75-1.72 Å) of the triple-bonded covalent radii of Re≡C(sp).[53] Complex **6** revealed a Re≡C distance 1.862(8) Å that is close to the Re=C distance found in the vinylidene complexes **2** and **3**. The C1-C2 bond distances of **4**, **5** and **6 [**1.355(9) Å, 1.475(4) Å and 1.427(12) Å] are shorter than the bond distance range of a C-C bond (1.47-1.54 Å). The ReC1C2 bond angles are nearly 180° in the complexes **2**-**6**.

2.2 Oxidative C-C coupling reactions of the mononuclear rhenium vinylidene complexes 3 and 7

Although oxidative C-C coupling reaction has been shown to be an effective method for the syntheses of dinuclear biscarbyne and bisvinylidene complexes, the mechanism of such processes is still not completely understood. The following mechanism (Scheme 5) was proposed by Ustynyuk and co-workers.[32,46] In the absence of base, the oxidation of vinylidene complex leads to a radical cation that further dimerizes through two competitive routes (A and C):

Route A: radical cation C_β-C_β self-couples to the corresponding dinuclear biscarbyne complex.

Route C: the radical cation undergoes homolysis of the C_β-H bond to give the mononuclear carbyne complex and the dinuclear ethylenidene biscarbyne complex.

In the presence of a base the reaction goes through route B, where the radical cation is deprotonated by the base, followed by a direct coupling to yield the neutral dinuclear bisvinylidene complex that can be further oxidized to the dicationic species.

Scheme 5

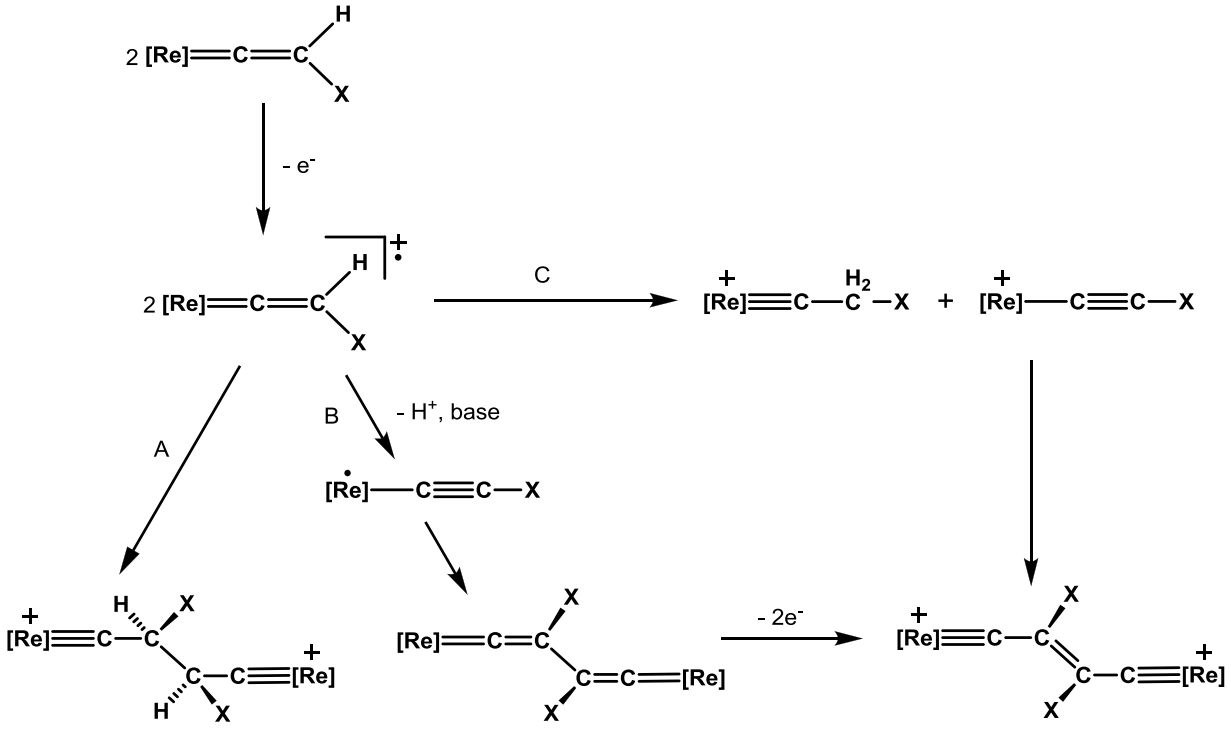

In order to obtain the μ-bisvinylidene dinuclear rhenium complex, we initially tried the coupling reaction in the presence of base following oxidation with an oxidizing agent, which is similar to the reported reaction conditions.[19,31,37-38,41-42] However, the oxidation of the mononuclear rhenium vinylidene complexes *trans*-[XRe(=C=CH_2)(PMe_3)$_4$] (X = Cl, **3**;C≡C$SiMe_3$, **7**) with 2 equiv. of [Cp_2Fe][PF_6] in the presence of 1.2 equiv. of base, such as quinuclidine, DBU and KO*t*Bu, always resulted in a mixture of the corresponding mononuclear rhenium carbyne complexes *trans*-[XRe(≡C-CH_3)(PMe_3)$_4$][PF_6] (X = Cl, **5;** C≡C$SiMe_3$, **6**), the dinuclear rhenium biscarbyne complexes *trans*-[X(PMe_3)$_4$Re≡C-CH_2-CH_2-C≡Re(PMe_3)$_4$X][PF_6] (X = Cl, **9**; C≡C$SiMe_3$, **10**), and the dinuclear rhenium vinylidene-bridged biscarbyne complexes *trans*-[X(PMe_3)$_4$Re≡C-CH=CH-C≡Re(PMe_3)$_4$X][PF_6] (X = Cl, **11[PF_6]$_2$**; C≡C$SiMe_3$, **12[PF_6]$_2$**. This could be attributed to the highly basic nature of the vinylidene complexes *trans*-[XRe(=C=CH_2)(PMe_3)$_4$] (X = Cl, **3**;C≡C$SiMe_3$, **7**) in the reactions. The bases that were used in these reactions were not strong enough to effect deprotonation of the resulting radical cation (Scheme 4, route B) and as a consequence the reaction proceeds through route B along with the

other two competitive routes A and C. Ustynyuk and co-workers reported that the radical cation of $[(\eta^5\text{-}C_5H_5)(CO)_2Mn{=}C{=}C(H)Ph]$ is stable in solution at -50 °C for at least 10-15 min and the process C is still noticeable even at -30 °C.[41] We anticipated that a better control of the resulting products could be achieved by performing the reaction at lower temperature in the absence of a base.

It is worth mentioning that partial oxidation of the vinylidene complex would also result in a mixture of mononuclear carbyne complex, dinuclear biscarbyne complex, and dinuclear vinylidene-bridged biscarbyne complex, owing to the unreacted vinylidene complex that can function as a base and deprotonate the resulting radical cation (Scheme 6).[19]

Scheme 6

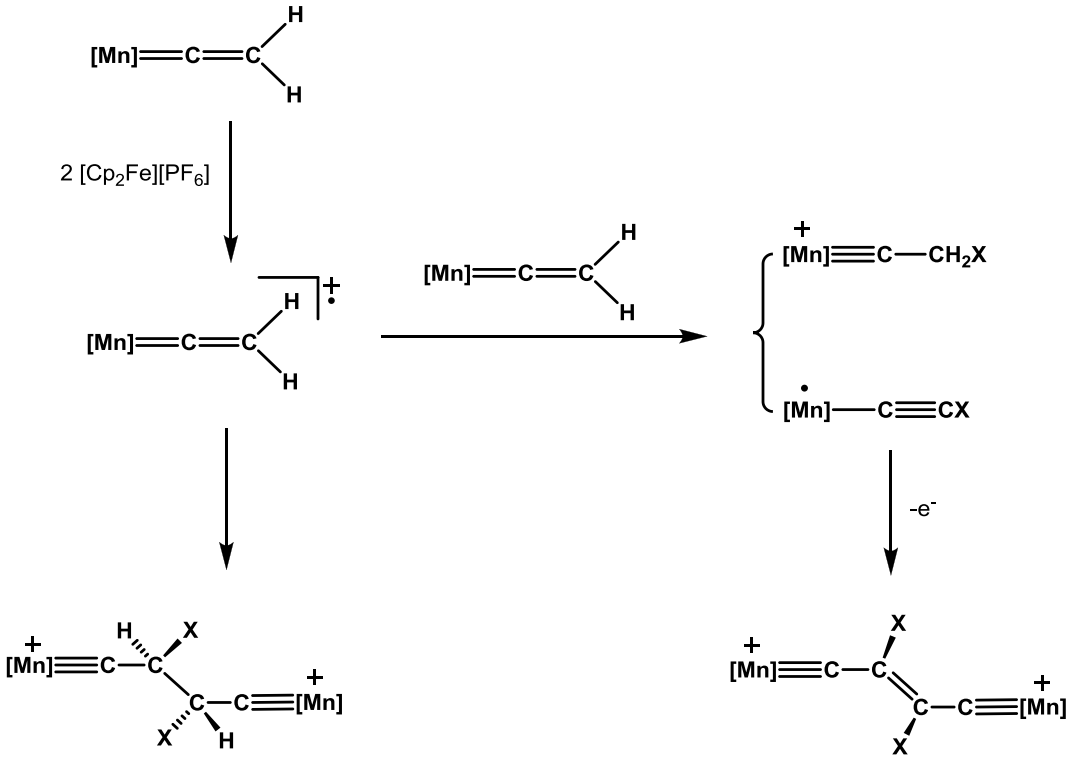

Due to the solubility of the oxidizing agent and the side products associated with this reaction, the order of addition plays a determining role. In order to avoid the presence of the unoxidized vinylidene complexes in the reaction mixture, dilute solution of the vinylidene complex was added into a solution containing an excess of the oxidizing agent $[Cp_2Fe][PF_6]$. The vinylidene complexes **2**, **3** and **7** are sensitive towards CH_2Cl_2 and produce the corresponding carbyne

complexes *trans*-[ReCl(≡C-CH_3)(PMe_3)$_4$][PF_6] (**4**) and *trans*-[Re(C≡C$SiMe_3$)(≡C-CH_3)(PMe_3)$_4$][PF_6] (**6**), respectively. Due to the susceptibility of the C_β atom of these vinylidene complexes towards electrophilic attack by electrophiles, the C-C coupling reactions of the vinylidene complexes **3** and **7** should be carried out under an atmosphere devoid of CH_2Cl_2 and other protic solvents, such as methanol and ethanol, to avoid the formation of the mononuclear rhenium carbyne complexes. Because of the low solubility of [Cp_2Fe][PF_6] in THF, a 1:3 mixture of CH_3CN/THF was used as the solvent for the reactions. The vinylidene complex *trans*-[XRe(=C=CH_2)(PMe_3)$_4$] (X = Cl, **3**; C≡C$SiMe_3$, **7**) in THF was added to a 1:3 CH_3CN/THF solution of [Cp_2Fe][PF_6] at -78 °C. The directly coupled dinuclear rhenium biscarbyne complexes *trans*-[X(PMe_3)$_4$Re≡C-CH_2-CH_2-C≡Re(PMe_3)$_4$X][PF_6]$_2$ (X = Cl, **9**; C≡C$SiMe_3$, **10**) were isolated in 90% and 92% yield respectively (Scheme 7).

Scheme 7

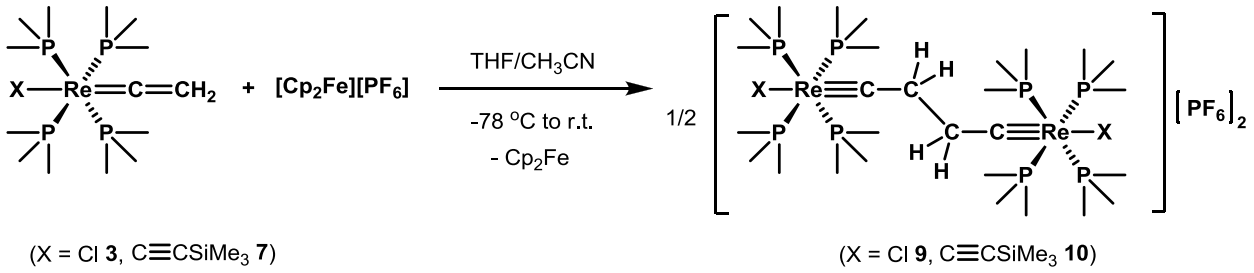

(X = Cl **3**, C≡C$SiMe_3$ **7**) (X = Cl **9**, C≡C$SiMe_3$ **10**)

The dinuclear rhenium biscarbyne complexes *trans*-[X(PMe_3)$_4$Re≡C-CH_2-CH_2-C≡Re(PMe_3)$_4$X][PF_6]$_2$ (X = Cl, **9**; C≡C$SiMe_3$, **10**) were characterized by NMR, IR, elemental analysis, mass spectroscopy. Selected ^{1}H NMR and ^{31}P NMR data for **9** and **10** are summarized in Table 2-5.

Table 2-5. Selected ^{1}H NMR and ^{31}P NMR data measured in CD_2Cl_2 for **9** and **10**

Complexes	^{13}C NMR (δ, ppm)		^{1}HNMR (δ, ppm)	^{31}P NMR (δ, ppm)
	C_α	C_β	H_β	PMe_3
[Cl(PMe_3)$_4$Re≡C-CH_2]$_2$[PF_6]$_2$ (**9**)	267.3	44.8	1.75	-35.8
[(Me_3SiC≡C)(PMe_3)$_4$Re(≡C-CH_2]$_2$[PF_6]$_2$ (**10**)	279.9	46.4	1.56	-42.2

The ^{1}H NMR spectrum for **9** showed a singlet at 1.75 ppm for the $P(CH_3)_3$ and CH_2 protons. A characteristic quintet at 267.3 ppm ($^{2}J_{PC}$ = 13.0 Hz) and a singlet at 44.8 ppm observed in the $^{13}C\{^{1}H\}$ NMR spectrum for the C_α and C_β atoms. The signal at -35.8 ppm in the ^{31}P NMR spectrum was assigned to the $P(CH_3)_3$ ligand and the characteristic signal at -143.9 ppm for the PF_6^- anion. The ^{1}H NMR spectrum of **10** displayed three signals. The one at 1.56 ppm was ascribed to the CH_2 protons and the other two at 1.75 ppm and 0.05 ppm were attributed to protons of the $P(CH_3)_3$ group and the $Si(CH_3)_3$ group, respectively. In the $^{13}C\{^{1}H\}$ NMR spectrum, the C_α and C_β carbyne resonances, appeared at 279.9 ppm ($^{2}J_{PC}$ = 13.8 Hz) and 46.4 ppm, which is a upfield shift in contrast to **9** with Cl^- ligand. In comparison to the carbyne resonances of the H, C_α and C_β atoms (2.72 ppm, 330.0 ppm and 46.4 ppm) in the manganese analog $[(C_5H_4CH_3)(dmpe)Mn{\equiv}CCH_2\text{-}CH_2C{\equiv}Mn(dmpe)(C_5H_4CH_3)][PF_6]_2$,[34] an upfield shift was observed in the rhenium complex. For **10**, two additional resonances at 134.0 ppm ($^{2}J_{PC}$ = 19.4 Hz) and 126.6 ppm in the $^{13}C\{^{1}H\}$ NMR spectrum and the diagnostic ν (C≡C) vibration displayed at 2027 cm^{-1} in the IR spectrum confirmed the presence of the acetylide group. In the ^{31}P NMR spectrum, the resonance for the $P(CH_3)_3$ ligand appears at -42.2 ppm and a septet at -146.6 ppm for the PF_6^- anion. X-ray diffraction analyses (Figure 2-3) were carried out on **9** and **10** and the selected bond distances and bond angles are summarized in Table 2-6 and Table 2-7.

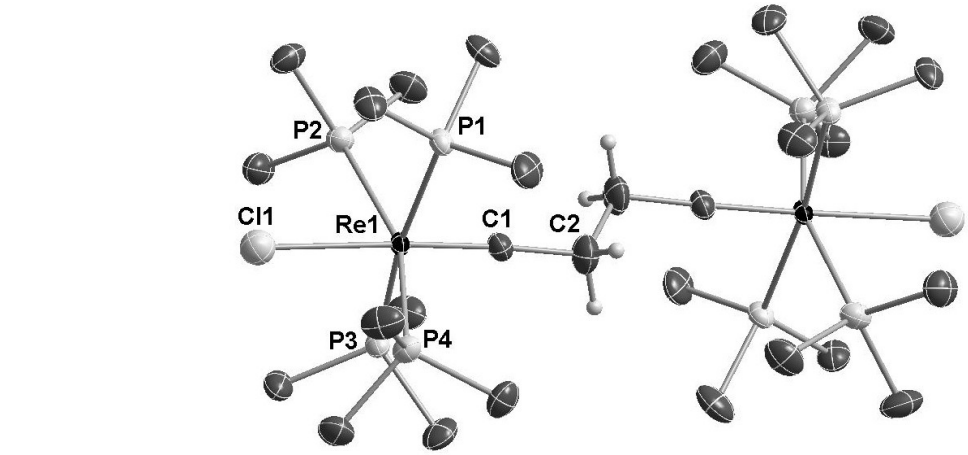

(a)

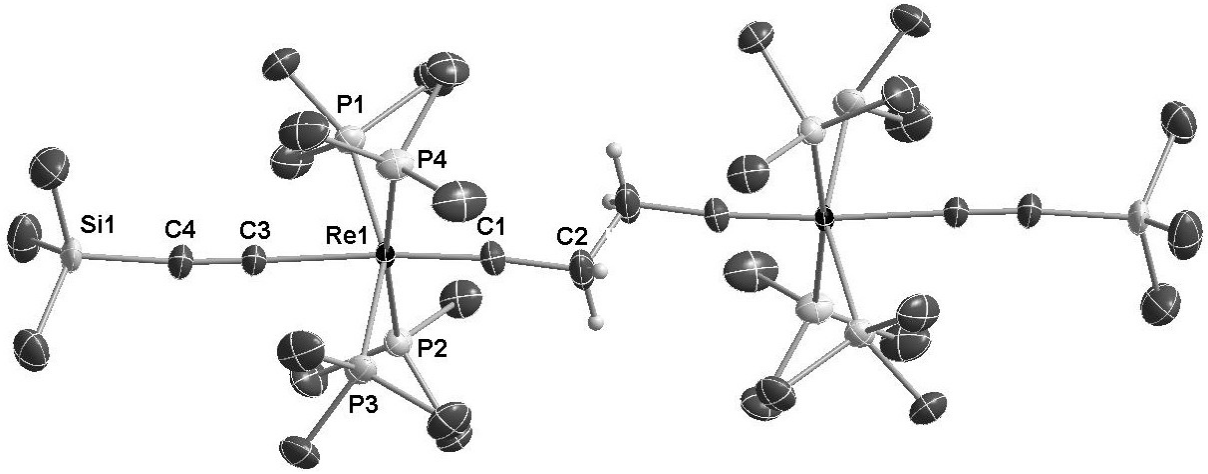

(b)

Figure 2-3. Molecular structure of *trans*-[X(PMe_3)$_4$Re≡C-CH_2-CH_2-C≡Re(PMe_3)$_4$X][PF_6]$_2$ (X = Cl, **9**, a; C≡C$SiMe_3$, **10**, b) (Ellipsoids are 50%, solvent, counter ion PF_6^- and selected hydrogen atoms are omitted for clarity)

Table 2-6. Selected bond lengths [Å] for **9** and **10,** assignment of the bond lengths in the C_4 bridge according to the following notation: [Re]C1C2C2'C1'[Re']

Complexes	Selected bond lengths [Å]						
	C2-C2'	C1-C2	C1-Re1	Cl1-Re1	C3-Re1	C3-C4	C4-Si1
9	1.463(6)	1.476(5)	1.755(3)	2.5175(8)	/	/	/
10	1.513(4)	1.491(3)	1.7834(19)	/	2.183(2)	1.217(3)	1.823(2)

Table 2-7. Selected bond angles [º] for **9** and **10,** assignment of the bond lengths in the C_4 bridge according to the following notation: [Re]C1C2C2'C1'[Re']

Complexes	Selected angles [º]					
	C1-C2-C2'	C2-C1-Re1	C1-Re1-Cl1	C1-Re1-C3	Re1-C3-C4	C3-C4-Si1
9	116.0(4)	175.5(3)	176.61(12)	/	/	/
10	112.7(2)	174.31(18)	/	175.44(8)	177.3(2)	174.7(2)

The Re1-C1, C1-C2 and C2-C2' bond distances for **9** and **10** are 1.755(3) Å and 1.7834(19) Å, 1.476(5) Å and 1.491(3) Å, and 1.463(6) Å and 1.513(4) Å respectively. The Re1-C1 bond distances are longer than the expected distance range (1.75-1.72 Å) of the triple-bonded covalent radii of Re≡C(sp) and the C1-C2 and C2-C2' bond distances fall into the range of a C-C bond (1.47-1.54 Å). The lengthening of the Re1-C1 distance in the Cl^- complex **9** to the $Me_3SiC{\equiv}C^-$ complex **10** can be ascribed to the higher *trans* effect of the $Me_3SiC{\equiv}C^-$ ligand relative to the Cl^- ligand. The Re1-C3 and C3-C4 distances for **10** are 2.183(2) Å and 1.217(3) Å, respectively, similar to the Re-C [2.037(5) Å] and C≡C [1.202(7) Å] distances in the complex $[(C_5Me_5)(NO)(PPh_3)Re\text{-}C{\equiv}C\text{-}C{\equiv}C\text{-}Re(PPh_3)(NO)(C_5Me_5)]$.[22] The C1-C2-C2' bond angles are close to 120° and the Re-C-C and C-Re-Cl(C)-bond angles are close to 180° for **9** and **10**.

In our previous study on dinuclear manganese biscarbyne complex *trans*-$[(C_5H_4CH_3)(dmpe)Mn{\equiv}C\text{-}CH_2\text{-}CH_2\text{-}C{\equiv}Mn)(dmpe)(C_5H_4CH_3)][PF_6]_2$, the reduction of the

biscarbyne complex with cobaltocene resulted in the cleavage of the C-C bond in the complex and giving back the starting vinylidene complex.[19,35] But a similar reaction carried out on the rhenium complexes **9** and **10** did not result in the corresponding starting vinylidene complexes. It was assumed that a stronger reducing agent should be used, since the cobaltocene does not possess a strong enough reduction potential. However, the experiment carried out on the complex *trans*-[$(Me_3SiC{\equiv}C)(PMe_3)_4Re{\equiv}C\text{-}CH_2\text{-}CH_2\text{-}C{\equiv}Re(PMe_3)_4C{\equiv}CSiMe_3][PF_6]_2$ **10** with sodium benzophenone ketyl in THF resulted in the neutral dinuclear rhenium bisvinylidene complex *trans*-[$(Me_3SiC{\equiv}C)(PMe_3)_4Re{=}C{=}CH\text{-}CH{=}C{=}Re(PMe_3)_4C{\equiv}CSiMe_3$] (**12**, chapter 3) in 80% yield (Scheme 8), while complex **9** with chloride end groups decomposed under the same reaction condition. It has to be mentioned that the reaction of **9** or **10** with sodium in THF did not proceed at room temperature for 2 days and then benzophenone was added to initiate it.

Scheme 8

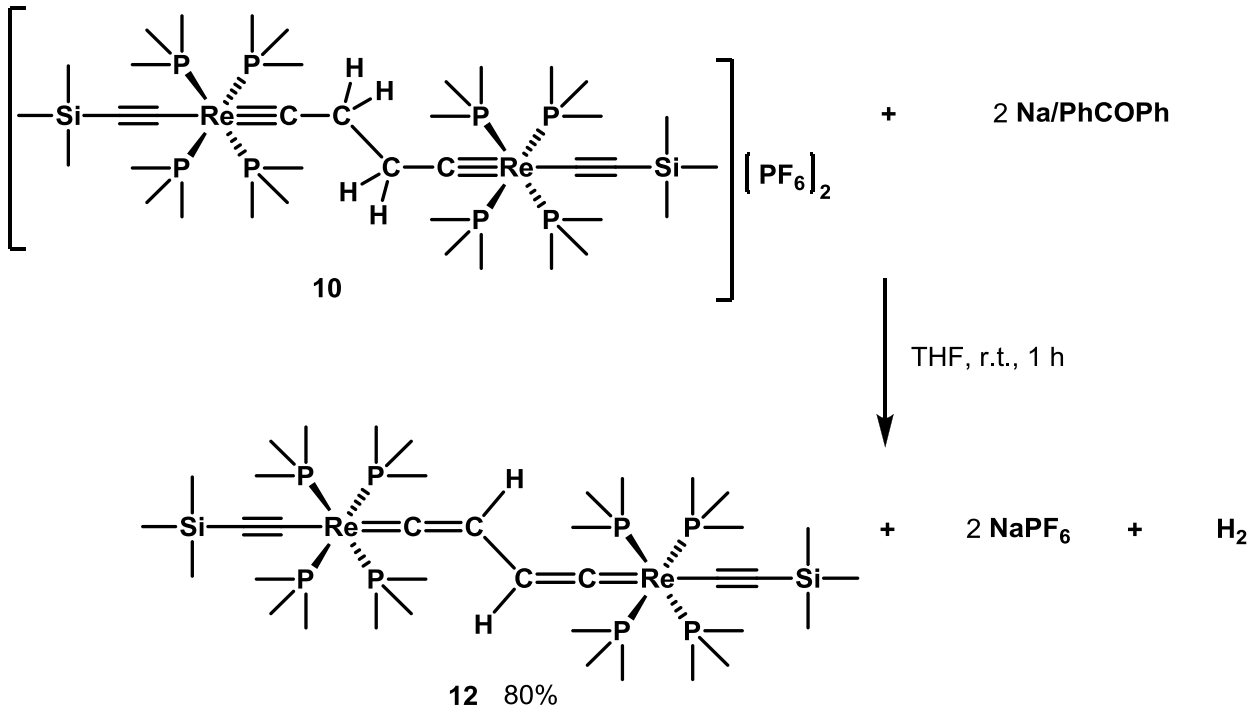

The final product formed in the reaction of **10** is similar to that of the reduction of the dinuclear manganese biscarbyne complex [$Cp(CO)(Ph_3P)Mn{\equiv}C\text{-}CHPh\text{-}CHPh\text{-}C{\equiv}Mn(PPh_3)(CO)Cp][BF_4]_2$ with $(\eta_5\text{-}C_6H_6)_2Cr$ reported by Ustynyuk and co-workers. The authors believed that the reduction

led to the homolysis of the C_β-H bonds and the corresponding bisvinylidene complex [Cp(CO)(Ph_3P)Mn=C=CPh-CPh=C=Mn(PPh_3)(CO)Cp] was formed.[31] Presumably, the same explanation can be assigned to our reaction.

2.3 Conclusion

Two mononuclear rhenium vinylidene complexes *trans*-[XRe(=C=CH_2)(PMe_3)$_4$] (X = Cl, **3**; C≡C$SiMe_3$, **7**) were prepared and the oxidative coupling reaction of them were explored. The oxidation of **3** and **7** at room temperature gave an inseparable mixture, while the reaction at -78 °C in the absence of base resulted in the exclusive formation of the C_β-C_β' coupled products *trans*-[X(PMe_3)$_4$Re≡C-CH_2-CH_2-C≡Re(PMe_3)$_4$X][PF_6] (X = Cl, **9**; C≡C$SiMe_3$, **10**) in excellent yields. The factors such as temperature, solvent and the order of reagent addition significantly affect the formation of the final product, from a mixture to the directly coupled products biscarbyne complexes **9** and **10**. The chemical reduction of **10** with sodium benzophenone ketyl in THF results in the corresponding neutral bisvinylidene complex.

2.4 Experimental section

General procedures: All the manipulations were carried out under a nitrogen atmosphere using Schlenk techniques or a glove box (M. Braun150B-G-II). Reagent grade benzene, toluene, hexane, pentane, diethyl ether and tetrahydrofuran were dried and distilled from sodium benzophenone ketyl prior to use. Dichloromethane and acetonitrile were distilled from CaH_2. Complex [$ReCl_2$(N_2COPh)(PPh_3)$_2$][54] was prepared by literature procedure. Complex [ReCl(N_2)(PMe_3)$_4$][55-56] was prepared by using similar procedure described in literature. All other chemicals were directly used as obtained from commercial suppliers. IR spectra were obtained on a Bio-Rad FTS-45 instrument. NMR spectra were measured on a Varian Mercury spectrometer at 200 MHz for ^{1}H NMR, 81 MHz for ^{31}P{^{1}H} NMR, 188 MHz for ^{19}F{^{1}H} NMR, Varian Gemini-2000 spectrometer at 300 MHz for ^{1}H NMR and 75 MHz for ^{13}C{^{1}H} NMR, and on a Bruker-DRX-500 spectrometer at 500 MHz for ^{1}H NMR, 125.8 MHz for ^{13}C{^{1}H} NMR, 202.5 MHz for ^{31}P{^{1}H} NMR, and 99.4 MHz for ^{29}Si{^{1}H} NMR. Chemical shift for ^{1}H NMR, ^{31}P NMR, ^{13}C NMR, and ^{29}Si NMR is given in ppm relative to TMS and that for ^{31}P NMR relative to phosphoric acid.

X-ray diffraction studies on 2, 3, 4, 5, 6, 9 and 10: Data collection for all crystals were carried out on Stoe IPDS diffractometer (Imaging Plate Detector System with graphite-

monochromated MoK radiation, λ = 0.71073 Å)[57] and for others on Oxford Diffraction Xcalibur R diffractometer (4-circle kappa platform, Ruby CCD detector and a single wavelength Enhance X-ray source with MoK radiation, λ = 0.71073 Å) at 183(2) K using a cold N_2-gas stream from an Oxford Cryogenic System. Pre-experiment, data collection and data reduction (unit cell determination, intensity data integration and empirical absorption correction) were carried out with the Oxford *CrysAlisPro* software.[58] The structures were solved with the unique data sets using the Patterson method of the program SHELXS-97. The structure refinement was performed with the program SHELXL-97.[59] Non-hydrogen atoms were refined anisotropically by full-matrix least-squares techniques based on F^2. The hydrogen atoms of the organic groups were placed in calculated positions and refined with a riding model with a fixed temperature factor. The program PLATON[60] was used to check the result of the X-ray analysis.

***trans*-[ReCl(N_2)(PMe_3)$_4$] (1).** [N-Benzoylhydrazido (3-) N', O]dichlorobis (triphenylphosphine)rhenium (V) [$ReCl_2(N_2COPh)(PPh_3)_2$] (1.007 g, 1 mmol) and PMe_3 (0.7 mL, 6.6 mmol) in 1:1 benzene-methanol (6 mL) were heated at 70 °C for 2 h. The clear yellow solution was dried *in vacuo* and extracted with CH_2Cl_2. To the CH_2Cl_2 solution, a large amount of ether was added to precipitate off the impurities. After filtration, the pale orange solution was evaporated to dryness, washed with -30 °C cold ether (3 × 2 mL), and dried *in vacuo*. Yield: 0.364 g (0.066 mmol, 66% based on [$ReCl_2(N_2COPh)(PPh_3)_2$]. Anal. Calcd for $C_{12}H_{36}ClN_2P_4Re$ (553.98 g/mol): C, 26.02; H, 6.55; N, 5.06. Found: C, 26.19; H, 6.34; N, 4.99. IR (ATR, cm^{-1}): ν = 1914 (N≡N), 921 (C-P). MS (ESI): *m/z* (100%): 554.1 [M]. ^{1}H NMR (THF-d_8, 200 MHz, 22 °C): δ = 1.54 (s, 12H, PMe_3). ^{31}P NMR (THF-d_8, 81 MHz, 22 °C): δ = -33.7 (s, PMe_3). ^{13}C NMR (C_6D_6, 75 MHz, 22 °C): δ = 15.6 (s, PMe_3).

***trans*-[ReCl(=C=CHSiMe_3)(PMe_3)$_4$] (2).** T*rans*-[$ReClN_2(PMe_3)_4$] (**1**) (0.079 g, 0.143 mmol), HC≡C$SiMe_3$ (0.123 mL, 0.856 mmol) and toluene (5 mL) was mixed in glove box, then N_2 was removed by freeze-pump-thaw cycles. The mixture was irradiated with sunlight until no further color change was observed. After filtration, the solvent was removed *in vacuo*. The dark brown oily residue was extracted with pentane and filtered. Removal of the solvent *in vacuo* gave crude product *trans*-[ReCl(=C=CHSiMe_3)(PMe_3)$_4$] (**2**), which was directly used to synthesize the carbyne complex *trans*-[ReCl(≡C-CH_3))(PMe_3)$_4$]Cl (**4**). This compound reacts with silca gel and aluminum oxide and hence was not purified by chromatography. Fine brown red crystals suitable

for single crystal X-ray diffraction measurement, were obtained from benzene/pentane solution cooled at -30 °C for 10 d. IR (ATR, cm^{-1}): ν = 1504 (C=C), 930 (C-P). MS (ESI): *m/z* (100%): 553.1 [M-$SiMe_3$+2H]. ^{1}H NMR (C_6D_6, 200 MHz, 22 °C): δ = 1.46 (s, 36H, PMe_3), 0.75 (quint, $^4J_{PH}$ = 4.6 Hz, 1H, CH), 0.27 (s, 9H, $SiMe_3$); ^{13}C (C_6D_6, 125.8 MHz, 10 °C): δ = 287.5 (quint, $^2J_{PC}$ = 10.0 Hz, C_α), 82.0 (quint, $^3J_{PC}$ = 1.4 Hz, C_β), 19.7 (s, PMe_3), 3.0 (t, $SiMe_3$); ^{31}P NMR (C_6D_6, 81 MHz, 22 °C): δ = -34.8 (s, PMe_3); ^{29}Si (C_6D_6, 125.8 MHz, 10° C): δ = -20.9 (quint, $^4J_{PSi}$ = 2.7 Hz, $SiMe_3$).

***trans*-[ReCl(=C=CH$_2$)(PMe$_3$)$_4$] (3).** Method a: from *trans*-[ReCl(=C=CHSiMe_3)(PMe_3)$_4$] (**2**)**.** To a toluene solution of *trans*-[ReCl(=C=CHSiMe_3)(PMe_3)$_4$] (**2**), excess of MeOH was added. The mixture was stirred at room temperature for 1.5 h. After removal of the solvent *in vacuo*, the dark brown-red oily residue was extracted with THF. The remained insoluble pale purple solid was *trans*-[ReCl(≡C-CH_3)(PMe_3)$_4$]Cl (**4**). The THF extract was dried *in vacuo* and extracted with ether. Further evaporation of the ether fraction *in vacuo* gave the title product. Yield: 40% *trans*-[ReCl(=C=CH_2)(PMe_3)$_4$] (**3**), 10% *trans*-[ReCl(≡C-CH_3)(PMe_3)$_4$]Cl (**4**), based on *trans*-[ReCl(=C=CHSiMe_3)(PMe_3)$_4$] (**2**).

Method b: from *trans*-[ReCl(≡C-CH_3)(PMe_3)$_4$]Cl (**4**)**.** To a THF solution of *trans*-[ReCl(≡C-CH_3)(PMe_3)$_4$]Cl (**4**) (7.6 mg, 0.010 mmol), KO*t*Bu (1.8 mg, 0.016 mmol) was added. After 30 min the solvent was removed, and the residue was extracted with ether and filtered through celite. Removal of solvent *in vacuo* and subsequent washing with -30 °C cold pentane (2 × 1 mL) gave the pure product.Yield: 6 mg, (0.0098 mmol, 98%, based on-[ReCl(≡C-CH_3)(PMe_3)$_4$]Cl (**4**)). The fine brown red crystals of *trans*-[ReCl(=C=CH_2)(PMe_3)$_4$] (**3**), suitable for single crystal X-ray diffraction studies, were obtained from a saturated solution of pentan cooled at -30 °C for 1 d. Anal. Calcd for $C_{14}H_{38}ClP_4Re$ (552.01 g/mol): C, 30.46; H, 6.94. Found: C 30.70; H, 7.08. MS (ESI): *m/z* (100%): 553.1 [M+H]. IR (ATR, cm^{-1})**:** ν = 1550 (C=C), 923 (C-P). ^{1}H NMR (C_6D_6, 200 MHz, 22 °C): δ = 1.46 (m, 36H, PMe_3), 1.22 (quint, $^4J_{PH}$ = 4.4 Hz, 2H, CH_2); ^{13}C (C_6D_6, 125.8 MHz, 22 °C): δ = 291.4 (quint, $^2J_{PC}$ = 10.8 Hz, C_α), 80.8 (quint, $^3J_{PC}$ = 2.2 Hz, C_β), 20.4 (s, PMe_3); ^{31}P NMR (C_6D_6, 81 MHz, 22 °C): δ = -34.4 (s, PMe_3).

***trans*-[ReCl(≡C-CH$_3$))(PMe$_3$)$_4$]Cl (4).** *Trans*-[$ReClN_2$(PMe_3)$_4$] (**1**) (0.079 g, 0.143 mmol), HC≡C$SiMe_3$ (0.123 mL, 0.856 mmol) and toluene (5 mL) was mixed in glove box, then N_2 was removed by freeze-pump-thaw cycles. The mixture was irradiated with sunlight until no further

color change was observed. Addition of 1 M HCl in ether (0.22 mL, 0.22 mmol) resulted in a pale yellow precipitate immediately. The reaction mixture was stirred at room temperature for 30 min. After removal of solvent *in vacuo*, the residue was extracted with CH_2Cl_2 and filtered. Concentration of the solution was followed by addition of diethyl ether to precipitate the product. The precipitate was collected, washed with diethyl ether until the washing while colorless, and dried *in vacuo*. Yield: 89 mg (0.159 mmol, 80% based on *trans*-[$ReClN_2(PMe_3)_4$] (**1**)). Anal. Calcd for $C_{14}H_{39}Cl_2P_4Re$ (588.47 g/mol): C, 28.57; H, 6.68. Found: C, 28.69; H, 6.74. IR (ATR, cm^{-1}): ν = 940 (C-P). MS (ESI): *m/z* (100%): 553 [M]. ^{1}H NMR (CD_2Cl_2, 200 MHz, 22 °C): δ = 1.76 (s, 36H, PMe_3), 1.50 (quint, $^4J_{PH}$ = 4.0Hz, 3H, CH_3); ^{13}C (CD_2Cl_2, 50 MHz, 10°C): δ = 260.0 (s, C_α), 37.4 (s, C_β), 20.3 (m, $P(CH_3)_3$); ^{31}P NMR (CD_2Cl_2, 81 MHz, 22°C): δ = -34.8 (s, PMe_3).

***trans*-[ReCl(≡C-CH$_3$))(PMe$_3$)$_4$][PF$_6$] (5).** A mixture of *trans*-[ReCl(≡C-CH_3))(PMe_3)$_4$]Cl (**4**) (10.2 mg, 0.017 mmol) and $NaPF_6$ (3.0 mg, 0.017 mmol) in THF was stirred at room temperature for 1h. After removal of the solvent *in vacuo*, the residue was extracted with CH_2Cl_2 followed by filtration through celite. Evaporation of the solvent until dryness gave the title compound. Yield: 13.0 mg (0.017 mmol, 99% based on *trans*-[ReCl(≡C-CH_3))(PMe_3)$_4$]Cl(**4**)). Anal. Calcd for $C_{14}H_{39}ClF_6P_5Re$ (697.96 g/mol): C, 24.09; H, 5.63. Found: C, 24.31; H, 5.51. IR (ATR, cm^{-1}): ν = 939 (C-P). MS (ESI): *m/z* (100%): 553.0 [M]. ^{1}H NMR (CD_2Cl_2, 200 MHz, 22 °C): δ = 1.75 (tri, 36H, PMe_3), 1.40 (quint, $^4J_{PH}$ = 4.1 Hz, 3H, CH_3); ^{13}C (CD_2Cl_2, 75 MHz, 22 °C): δ = 272.6 (s, C_α), 36.4 (s, C_β), 19.8 (m, $P(CH_3)_3$); ^{31}P NMR (CD_2Cl_2, 81 MHz, 22 °C): δ = -35.0 (s, PMe_3), -144.0 (sept, *J* = 710 Hz, PF_6); ^{19}F NMR (CD_2Cl_2, 188 MHz, 22 °C): δ = -74.5 (d, *J* = 711 Hz, PF_6).

***trans*-[Re(≡C-CH$_3$)(C≡CSiMe$_3$)(PMe$_3$)$_4$][PF$_6$] (6).** A mixture of *trans*-[$ReClN_2(PMe_3)_4$] (**1**) (61.5 mg, 0.111 mmol), $TlPF_6$ (77.6 mg, 0.222 mmol), $HC{\equiv}CSiMe_3$ (56 μL, 0.389 mmol), DIPEA (5 mL), and 5 mL of THF in a Young schlenk was heated at 95 °C for 24 h. After cooling down to the room temperature and keeping at this temperature for 12 h, the solvent was removed *in vacuo*, the residue was extracted with CH_2Cl_2 and filtered through celite. Evaporation of the solution to dryness *in vacuo*, the pure product was obtained by recrystallization from THF/ether and washed with ether (3 × 2 mL). Yield: 81.1 mg (0.107 mmol, 90%, based on *trans*-[$ReClN_2(PMe_3)_4$] (**1**)). Anal. Calcd for $C_{19}H_{48}F_6P_5ReSi$ (759.72 g/mol): C, 30.04; H, 6.37.

Found: C, 29.99; H, 6.30. IR (ATR, cm^{-1}): ν = 2029 (C≡C), 939 (C-P), 827 (P-F). MS (ESI): *m/z* (100%): 615.1 [M]. ^{1}H NMR (CD_2Cl_2, 200 MHz, 22 °C): δ = 1.78 (m, 48H, PMe_3), 1.27 (quint, $^4J_{PH}$ = 4.0 Hz, 3H, CH_3), 0.02 (m, 12H, $SiMe_3$); ^{13}C NMR (CD_2Cl_2, 125.8 MHz, 10 °C): δ = 284.5 (quint, $^2J_{PC}$ = 13.6 Hz, C_α), 134.7 (quint, $^2J_{PC}$ = 18.9 Hz, C_α'), 125.7 (s, C_β'), 38.4 (s, C_β), 21.8 (m, $P(CH_3)_3$), 0.4 (s, $Si(CH_3)$); ^{31}P NMR (CD_2Cl_2, 81 MHz, 22 °C): δ = -41.6 (s, PMe_3), -144.0 (sept, *J* = 710 Hz, PF_6); ^{19}F NMR (CD_2Cl_2, 188 MHz, 22°C): δ = -74.8 (d, *J* = 711 Hz, PF_6); ^{29}Si NMR (CD_2Cl_2, 99.4 MHz, 10 °C): δ = 24.8 (quint, $^4J_{PSi}$ = 2.3 Hz, $SiMe_3$).

***trans*-[Re(=C=CH$_2$)(C≡CSiMe$_3$)(PMe$_3$)$_4$] (7).** To a THF solution of *trans*-[Re(≡C-CH_3)(C≡C$SiMe_3$)(PMe_3)$_4$][PF_6] (**6**) (7.6 mg, 0.010 mmol), KO*t*Bu (1.8 mg, 0.016 mmol) was added. After 10 min the solvent was removed *in vacuo*, the residue was extracted with pentane and filtered through celite. Removal of the solvent *in vacuo*, gave the pure product.Yield: 6mg, (0.0098 mmol, 98%, based on *trans*-[Re(≡C-CH_3)(C≡C$SiMe_3$)(PMe_3)$_4$][PF_6] (**6**)). Anal. Calcd for $C_{19}H_{48}F_6P_5ReSi$ (613.76 g/mol): C, 37.78; H, 7.72. Found: C, 37.30; H, 7.59. IR (ATR, cm^{-1}): ν = 1982 (C≡C), 1558 (C=C), 930 (C-P). MS (ESI): *m/z* (100%): 615.2 [M+H]. ^{1}H NMR (C_6D_6, 200 MHz, 22 °C): δ = 1.53 (s, 48H, PMe_3); 1.35 (quint, $^4J_{PH}$ = 3.5 Hz, 2H, CH_2), 0.31 (s, 12H, $SiMe_3$); ^{13}C NMR (C_6D_6, 125.8 MHz, 10 °C): δ = 301.6 (quint, $^2J_{PC}$ = 11.9 Hz, C_α), 150.1 (s, C_α'), 87.8 (m, C_β), 67.8 (s, C_β'), 21.3 (m, $P(CH_3)_3$), 1.9 (s, $Si(CH_3)$); ^{31}P NMR (C_6D_6, 81 MHz, 22 °C): δ = -41.4 (s, PMe_3);. ^{29}Si NMR (C_6D_6, 99.4 MHz, 10 °C): δ = -30.6 (quint, $^4J_{PSi}$ = 1.9 Hz, $SiMe_3$).

***trans*-[Re(≡C-CH$_3$)(C≡CSiMe$_3$)(PMe$_3$)$_4$]Cl (8).** To *trans*-[Re(=C=CH_2)(C≡C$SiMe_3$)(PMe_3)$_4$] (**7**) (26.4 mg, 0.043 mmol) in 1:3 THF/ether (3 mL), 1 M HCl ether solution (0.065 mL, 0.065 mmol) was added resulting in the formation of a pale orange precipitate immediately. The resulting suspension was stirred at room temperature for 30 min. The solvent was removed *in vacuo* and the pure product was obtained by recrystallization from THF/ether (1:2) and washed with ether (3 × 2 mL). Yield: 23.5 mg, (0.036 mmol, 84%, based on *trans*-[Re(=C=CH_2)(C≡C$SiMe_3$)(PMe_3)$_4$] (**7**)). Anal. Calcd for $C_{19}H_{48}ClP_4ReSi$ (650.23 g/mol): C, 35.10; H, 7.44. Found: C, 35.01; H, 7.26. IR (ATR, cm^{-1}): ν = 2025 (C≡C), 941 (C-P). MS (ESI): *m/z* (100%): 615.2 [M]. ^{1}H NMR (CD_2Cl_2, 200 MHz, 22 °C): δ = 1.78 (m, 48H, PMe_3), 1.31 (quint, $^4J_{PH}$ = 4.0 Hz, 3H, CH_3), 0.01 (m, 12H, $SiMe_3$); ^{13}C NMR (CD_2Cl_2, 125.8 MHz, 10 °C): δ = 284.9 (m, C_α), 135.0 (s, C_α'), 125.8 (s, C_β'), 38.7 (s, C_β), 21.9 (m, $P(CH_3)_3$), 0.4 (s, $Si(CH_3)$);

^{31}P NMR (CD_2Cl_2, 81 MHz, 22 °C): δ = -41.5 (s, PMe_3); ^{29}Si NMR (CD_2Cl_2, 99.4 MHz, 10 °C): δ = -24.8 (quint, $^4J_{PSi}$ = 2.3 Hz, $SiMe_3$).

***trans*-[Cl(PMe$_3$)$_4$Re≡C-CH$_2$-CH$_2$-C≡Re(PMe$_3$)$_4$Cl][PF$_6$]$_2$ (9).** To a 1:3 CH_3CN/THF (4 mL) solution of [Cp_2Fe][PF_6] (96.4 mg, 0.291 mmol) at -78 °C, *trans*-[ReCl(=C=CH_2)(PMe_3)$_4$] (**3**) (134 mg, 0.243 mmol) in THF (14 mL) was added. The reaction mixture was stirred at this temperature for 1.5 h. It was gradually warmed up to room temperature and stirred overnight. The resulting yellowish green suspension was evaporated until dryness. The residue was extracted with CH_3CN followed by filtration through celite. The solution was concentrated and ether was added to precipitate. The pale yellow solid was collected, recrystallized from CH_3CN/ ether again, This was further washed with ether (3 × 5 mL), and dried to give the pure product *trans*-[ReCl(≡CCH_2)(PMe_3)$_4$]$_2$[PF_6]$_2$ (**9**). Yield: 152 mg, (0.109 mmol, 90%, based on *trans*-[ReCl(=C=CH_2)(PMe_3)$_4$] (**3**)). Single crystals suitable for X-Ray diffraction studies were grown by layering diethyl ether over an acetonitrile solution of the title compound. Anal. Calcd For $C_{28}H_{76}Cl_2F_{12}P_{10}Re_2$ (1393.95 g /mol): C, 24.13; H, 5.50. Found: C, 24.44; H, 5.31. IR (ATR, cm^{-1}): ν = 937 (C-P). MS (ESI): *m/z* (100%): 1247 [M$^+$-2H]. ^{1}H NMR (CD_2Cl_2, 200 MHz, 22 °C) δ = 1.75 (s, 38H, P(CH_3)$_3$+CH_2); ^{13}C NMR (CD_2Cl_2, 125.8 MHz, 10 °C): δ = 267.3 (quint, $^2J_{PC}$ = 13.0 Hz, C_α), 44.8 (s, C_β), 20.6 (m, P(CH_3)$_3$); ^{31}P NMR (CD_2Cl_2, 81 MHz, 22 °C) δ = -35.8 (s, P(CH_3)$_3$), -143.9 (sept, *J* = 711 Hz, PF_6); ^{19}F NMR (CD_2Cl_2, 188 MHz, 22 °C) δ = -73.3 (d, *J* = 711 Hz, PF_6).

***trans*-[(Me$_3$SiC≡C)(PMe$_3$)$_4$Re≡C-CH$_2$-CH$_2$-C≡Re(PMe$_3$)$_4$(C≡CSiMe$_3$)][PF$_6$]$_2$ (10).** To a 1:3 CH_3CN/THF (2 mL) solution of [Cp_2Fe][PF_6] (18.6 mg, 0.056 mmol) at -78 °C, *trans*-[Re(C≡C$SiMe_3$)(=C=CH_2)(PMe_3)$_4$] (**7**) (28.8 mg, 0.047 mmol) in THF (2mL) was added. The reaction mixture was stirred at this temperature for 1.5 h. It was gradually warmed up to room temperature and stirred overnight. The residue was extracted with CH_3CN followed by filtration through celite. The solution was concentrated and diethyl ether was added to precipitate. The pale yellow solid was collected, recrystallized from CH_3CN/ether again. Further it was washed with diethyl ether (3 × 2 mL), and dried to give the pure product *trans*-[Re(C≡C$SiMe_3$)(≡CCH_2)(PMe_3)$_4$]$_2$[PF_6]$_2$ (**10**). Yield: 32.8 mg, (0.022 mmol, 92%, based on *trans*-[Re(C≡C$SiMe_3$)(=C=CH_2)(PMe_3)$_4$] (**7**)). Single crystals suitable for X-Ray diffraction studies were grown by layering diethyl ether over an acetonitrile solution of the title compound.

Anal. Calcd For $C_{38}H_{94}F_{12}P_{10}Re_2Si_2$ (1517.46 g/mol): C, 30.08; H, 6.24. Found: C, 29.93; H, 6.16. IR (ATR, cm^{-1}): ν = 2027 (C≡C), 940 (C-P). MS (ESI): *m/z* (%): 1373 [M^+]. ^{1}H NMR (CD_2Cl_2, 200 MHz, 22 °C) δ = 1.75 (s, $P(CH_3)_3$), 1.56 (s, CH_2), 0.05 (s, $Si(CH_3)_3$); ^{13}C NMR (CD_2Cl_2, 125.8 MHz, 10 °C) δ = 279.9 (tri, $^2J_{PC}$ = 13.8 Hz, C_α), 134.0 (tri, $^2J_{PC}$ = 19.4 Hz, C_α'), 126.6 (s, C_β'), 46.4 (s, C_β), 22.4 (m, $P(CH_3)_3$), 0.3 (s, $Si(CH_3)_3$); ^{31}P NMR (CD_2Cl_2, 81 MHz, 22 °C) δ = -42.2 (s, $P(CH_3)_3$), -146.6 (sept, *J* = 711 Hz, PF_6); ^{19}F NMR (CD_2Cl_2, 188 MHz, 22 °C) δ = -76.2 (d, *J* = 711 Hz, PF_6). ^{29}Si NMR (CD_2Cl_2, 99 MHz, 10 °C): δ = -23.2 (s, $SiMe_3$)

2.5 References

(1) Heath, J. R. *Annu. Rev. Mater. Res.* **2009**, *39*, 1-23.

(2) Carroll, R. L.; Gorman, C. B. *Angew. Chem. Int. Ed.* **2002**, *41*, 4379-4400.

(3) Chen, F.; Hihath, J.; Huang, Z. F.; Li, X. L.; Tao, N. J. *Annu. Rev. Phys. Chem.* **2007**, *58*, 535-564.

(4) Tao, N. J. *Nat. Nanotechnol.* **2006**, *1*, 173-181.

(5) Zhirnov, V. V.; Cavin, R. K. *Nat. Mater.* **2006**, *5*, 11-12.

(6) Tuccitto, N.; Ferri, V.; Cavazzini, M.; Quici, S.; Zhavnerko, G.; Licciardello, A.; Rampi, M. A. *Nat. Mater.* **2009**, *8*, 41-46.

(7) Kurita, T.; Nishimori, Y.; Toshimitsu, F.; Muratsugu, S.; Kume, S.; Nishihara, H. *J. Am. Chem. Soc.* **2010**, *132*, 4524-4525.

(8) Szesni, N.; Drexler, M.; Maurer, J.; Winter, R. F.; de Montigny, F.; Lapinte, C.; Steffens, S.; Heck, J.; Weibert, B.; Fischer, H. *Organometallics.* **2006**, *25*, 5774-5787.

(9) Kaim, W.; Lahiri, G. K. *Angew. Chem. Int. Ed.* **2007**, *46*, 1778-1796.

(10) Kowalski, K.; Linseis, M.; Winter, R. F.; Zabel, M.; Zalis, S.; Kelm, H.; Kruger, H. J.; Sarkar, B.; Kaim, W. *Organometallics.* **2009**, *28*, 4196-4209.

(11) Paul, F.; Lapinte, C. *Coord. Chem. Rev.* **1998**, *180*, 431-509.

(12) Balzani, V.; Juris, A.; Venturi, M.; Campagna, S.; Serroni, S. *Chem. Rev.* **1996**, *96*, 759-833.

(13) Schwab, P. F. H.; Levin, M. D.; Michl, J. *Chem. Rev.* **1999**, *99*, 1863-1933.

(14) Belser, P.; Bernhard, S.; Blum, C.; Beyeler, A.; De Cola, L.; Balzani, V. *Coord. Chem. Rev.* **1999**, *192*, 155-169.

(15) Dembinski, R.; Bartik, T.; Bartik, B.; Jaeger, M.; Gladysz, J. A. *J. Am. Chem. Soc.* **2000**, *122*, 810-822.

(16) Jiao, H. J.; Costuas, K.; Gladysz, J. A.; Halet, J. F.; Guillemot, M.; Toupet, L.; Paul, F.; Lapinte, C. *J. Am. Chem. Soc.* **2003**, *125*, 9511-9522.

(17) Robin, M. B.; Day, P. *Adv. Inorg. Chem. Radiochem.* **1967**, *10*, 247 – 422.

(18) Kheradmandan, S.; Heinze, K.; Schmalle, H. W.; Berke, H. *Angew. Chem. Int. Ed.* **1999**, *38*, 2270-2273.

(19) Venkatesan, K.; Fox, T.; Schmalle, H. W.; Berke, H. *Organometallics.* **2005**, *24*, 2834-2847.

(20) Venkatesan, K.; Fernandez, F. J.; Blacque, O.; Fox, T.; Alfonso, M.; Schmalle, H. W.; Berke, H. *Chem. Commun.* **2003**, 2006-2008.

(21) Lenarvor, N.; Toupet, L.; Lapinte, C. *J. Am. Chem. Soc.* **1995**, *117*, 7129-7138.

(22) Brady, M.; Weng, W. Q.; Zhou, Y. L.; Seyler, J. W.; Amoroso, A. J.; Arif, A. M.; Bohme, M.; Frenking, G.; Gladysz, J. A. *J. Am. Chem. Soc.* **1997**, *119*, 775-788.

(23) Zhou, Y. L.; Seyler, J. W.; Weng, W. Q.; Arif, A. M.; Gladysz, J. A. *J. Am. Chem. Soc.* **1993**, *115*, 8509-8510.

(24) Yam, V. W. W.; Lau, V. C. Y.; Cheung, K. K. *Organometallics.* **1996**, *15*, 1740-1744.

(25) Paul, F.; Meyer, W. E.; Toupet, L.; Jiao, H. J.; Gladysz, J. A.; Lapinte, C. *J. Am. Chem. Soc.* **2000**, *122*, 9405-9414.

(26) Bruce, M. I.; Low, P. J.; Costuas, K.; Halet, J. F.; Best, S. P.; Heath, G. A. *J. Am. Chem. Soc.* **2000**, *122*, 1949-1962.

(27) Onitsuka, K.; Ose, N.; Ozawa, F.; Takahashi, S. *J. Organomet. Chem.* **1999**, *578*, 169-177.

(28) Woodworth, B. E.; White, P. S.; Templeton, J. L. *J. Am. Chem. Soc.* **1997**, *119*, 828-829.

(29) Roberts, R. L.; Puschmann, H.; Howard, J. A. K.; Yamamoto, J. H.; Carty, A. J.; Low, P. J. *Dalton. Trans.* **2003**, 1099-1105.

(30) Semenov, S. N.; Blacque, O.; Fox, T.; Venkatesan, K.; Berke, H. *J. Am. Chem. Soc.* **2010**, *132*, 3115-3127.

(31) Novikova, L. N.; Peterleitner, M. G.; Sevumyan, K. A.; Semeikin, O. V.; Valyaev, D. A.; Ustynyuk, N. A. *Appl. Organomet. Chem.* **2002**, *16*, 530-536.

(32) Ustynyuk, N. A.; Gusev, O. V.; Novikova, L. N.; Peterleitner, M. G.; Denisovich, L. I.; Peganova, T. A.; Semeikin, O. V.; Valyaev, D. A. *J. Solid State Electrochem.* **2007**, *11*, 1621-1634.

(33) Unseld, D.; Krivykh, V. V.; Heinze, K.; Wild, F.; Artus, G.; Schmalle, H.; Berke, H. *Organometallics.* **1999**, *18*, 1525-1541.

(34) Venkatesan, K.; Blacque, O.; Fox, T.; Alfonso, M.; Schmalle, H. W.; Berke, H. *Organometallics.* **2004**, *23*, 1183-1186.

(35) Venkatesan, K.; Blacque, O.; Fox, T.; Alfonso, M.; Schmalle, H. W.; Kheradmandan, S.; Berke, H. *Organometallics.* **2005**, *24*, 920-932.

(36) Venkatesan, K.; Blacque, O.; Berke, H. *Organometallics.* **2006**, *25*, 5190-5200.

(37) Fernandez, F. J.; Venkatesan, K.; Blacque, O.; Alfonso, M.; Schmalle, H. W.; Berke, H. *Chem. Eur. J.* **2003**, *9*, 6192-6206.

(38) Fernandez, F. J.; Alfonso, M.; Schmalle, H. W.; Berke, H. *Organometallics.* **2001**, *20*, 3122-3131.

(39) Antinolo, A.; Otero, A.; Fajardo, M.; GarciaYebra, C.; LopezMardomingo, C.; Martin, A.; GomezSal, P. *Organometallics.* **1997**, *16*, 2601-2611.

(40) Beddoes, R. L.; Bitcon, C.; Grime, R. W.; Ricalton, A.; Whiteley, M. W. *J. Chem. Soc., Dalton. Trans.* **1995**, 2873-2883.

(41) Novikova, L. N.; Peterleitner, M. G.; Sevumyan, K. A.; Semeikin, O. V.; Valyaev, D. A.; Ustynyuk, N. A.; Khrustalev, V. N.; Kuleshova, L. N.; Antipin, M. Y. *J. Organomet. Chem.* **2001**, *631*, 47-53.

(42) Valyaev, D. A.; Semelkin, O. V.; Peterleitner, M. G.; Borisov, Y. A.; Khrustalev, V. N.; Mazhuga, A. M.; Kremer, E. V.; Ustynyuk, N. A. *J. Organomet. Chem.* **2004**, *689*, 3837-3846.

(43) Iyer, R. S.; Selegue, J. P. *J. Am. Chem. Soc.* **1987**, *109*, 910-911.

(44) Bruce, M. I.; Ellis, B. G.; Low, P. J.; Skelton, B. W.; White, A. H. *Organometallics.* **2003**, *22*, 3184-3198.

(45) Bruce, M. I. *Chem.Rev.* **1991**, *91*, 197-257.

(46) Valyaev, D. A.; Semeikin, O. V.; Ustynyuk, N. A. *Coord. Chem. Rev.* **2004**, *248*, 1679-1692.

(47) Bruneau, C.; Dixneuf, P. *Metal Vinylidenes and Allenylidenes in Catalysis; From Reactivity to Application in Synthesis.*; Wiley-VCH Verlag GmbH&Co. KGaA: Weinheim, **2008**.

(48) Werner, H. *Coord. Chem. Rev.* **2004**, *248*, 1693-1702.

(49) Almeida, S. S. P. R.; Pombeiro, A. J. L. *Organometallics.* **1997**, *16*, 4469-4478.

(50) Balzani, V.; Credi, A.; Venturi, M. *Molecular Devices and Machines: Concepts and Perspectives for the Nanoworld*; 2nd ed.; Wiley-VCH Verlag GmbH & Co. KGaA: Weinheim, 2008.

(51) Pombeiro, A. J. L.; Fatima, M.; da Silva, C. G. *J. Organomet. Chem.* **2001**, *617*, 65-69.

(52) Ilg, K.; Paneque, M.; Poveda, M. L.; Rendon, N.; Santos, L. L.; Carmona, E.; Mereiter, K. *Organometallics.* **2006**, *25*, 2230-2236.

(53) Pombeiro, A. J. L.; Hills, A.; Hughes, D. L.; Richards, R. L. *J. Organomet. Chem.* **1988**, *352*, C5-C7 and references therein.

(54) Chatt, J.; Dilworth, J. R.; Leigh, G. J.; Gupta, V. D. *J. Chem. Soc. (A).* **1971**, 2631-2639.

(55) Chatt, J.; Dilworth, J. R.; Leigh, G. J. *J. Chem. Soc., Dalton. Trans.* **1973**, 612-618.

(56) Chatt, J.; Hussain, W.; Leigh, G. J.; Ali, H. M.; Pickett, C. J.; Rankin, D. A. *J. Chem. Soc., Dalton. Trans.* **1985**, 1131-1136.

(57) Version 2.87 5/1998 ed.; STOE & Cie: Darmstadt, Germany, **1998**.

(58) Version 1.171.32.5 ed.; Oxford Diffraction Ltd: Abingdon, Oxfordshire, England.

(59) Sheldrick, G. M. *Acta Cryst.* **2008**, *A64*, 112-122.

(60) Spek, A. L. *J. Appl. Cryst.* **2003**, *36*, 7-13.

3. Electronic Communication in C_4H_2-bridged Dinuclear Rhenium Complexes

ABSTRACT. The reactions of the dinuclear rhenium biscarbyne complexes *trans*-[X(PMe$_3$)$_4$Re≡C-CH$_2$-CH$_2$-C≡Re(PMe$_3$)$_4$X][PF$_6$] (X = Cl, **9**; C≡CSiMe$_3$, **10**) with an excess of KO*t*Bu in THF produced the diamagnetic neutral bisvinylidene complexes *trans*-[X(PMe$_3$)$_4$Re=C=CH-CH=C=Re(PMe$_3$)$_4$X] (X = Cl, **11**; C≡CSiMe$_3$, **12**) in good yields. The oxidation of **11** and **12** with two equiv. of [Cp$_2$Fe][PF$_6$] resulted in the diamagnetic dicationic ethylenylidene biscarbyne complexes *trans*-[X(PMe$_3$)$_4$Re≡C-CH=CH-C≡Re(PMe$_3$)$_4$X][PF$_6$]$_2$ (X = Cl, **11[PF$_6$]$_2$**; C≡CSiMe$_3$, **12[PF$_6$]$_2$**). The cyclic voltammetry (CV) studies on **11[PF$_6$]$_2$** and **12[PF$_6$]$_2$** displayed two fully reversible redox processes. The corresponding potential differences ($\Delta E_{1/2}$) 0.597 V and 0.457 V established large comproportionation constants K_c of 1.8×10^{10} and 7.1×10^7, respectively, revealing a high thermodynamic stability of the mixed-valence (MV) complexes under CV condition. The paramagnetic MV complexes **11[PF$_6$]** and **12[PF$_6$]** were obtained by the comproportionation reactions of the corresponding neutral complexes (**11** or **12**) with the dicationic complexes (**11[PF$_6$]$_2$** or **12PF$_6$]$_2$**) or by the oxidation of **11** and **12** with one equiv. of [Cp$_2$Fe][PF$_6$]. All the dinuclear rhenium complexes have been characterized by NMR, IR, Raman, elemental analysis and single crystal X-ray diffraction studies. UV-vis spectroscopy for all dinuclear rhenium complexes, EPR spectroscopy and variable-temperature magnetization measurements for the MV complexes **11[PF$_6$]** and **12[PF$_6$]** have also been investigated. The overlapping IVCT bands of **11[PF$_6$]** and **12[PF$_6$]** were deconvoluted into three Gaussian-shape bands with a feature pertaining to class III species (Robin & Day classification). **11[PF$_6$]** and **12[PF$_6$]** were EPR-silent at 300-30K, broad signals with reasonable intensities only observed below 13 K without hyperfine coupling. Variable-temperature magnetic susceptibility measurements for **11[PF$_6$]** and **12[PF$_6$]** displayed a typical paramagnetic behavior.

KEYWORDS. Carbyne, Dinuclear rhenium complexes, Electron transfer, Mixed-valence complexes, Molecular electronics, Vinylidene.

3.1 Introduction

In recent years, there has been great interest in the study of organometallic dinuclear metal complexes linked by a "conducting" π-conjugated bridging ligand due to their potential

applications in the field of molecular electronics.[1-14] The through-bridge electronic interaction of the metal centers exerts significant influence on the chemical and physical properties of these complexes, which greatly depend on the metal centers, the ancillary ligands and the bridging ligands.[12,15-19] The study on the influence of different bridging ligands on the through-bridge electronic communication will give us new insight into the electronic properties of these complexes.

Based on the nature of the unsaturated hydrocarbon bridge these complexes can be divided into two general groups (a) unsaturated carbon chains containing sp- and/or sp^2 bridges, where the metal is σ-bonded to the C atom, and (b) aromatic rings linked directly (fulvalene), separated by hydrocarbon chains or fused aromatic bridges; having π-coordinated metal centers.[19] Intensive investigations have been carried out on the complexes of the first group especially of the type $[L_nMC_4ML_n]$ with different transition metal centres, such as Mn,[20-22] Fe,[18,23] Re,[24-26] Ru,[27-28] Pt,[29] W and Mo.[30-32] Although the dinuclear bisvinylidene complexes containing different transition metals, such as Nb,[33] W,[30] Mo,[30,34] Fe,[23,35] Ru,[36] Mn[21,37-42] and Re[43], have been reported, it is surprising that the investigation of their physical properties on these type complexes are rare. Our previous work concerning the CV studies on the dicationic species of the dinuclear manganese ethylenylidene biscarbyne complexes $[(MeC_5H_4)(L)Mn{\equiv}C\text{-}CR{=}CR\text{-}C{\equiv}Mn(L)(C_5H_4Me)]^{2+}$ (L = dmpe, depe; R = Ph, H) revealed the thermodynamic stability of the corresponding MV complexes as evident from the comproportionation constants K_c of 8×10^3 and 6.6×10^9, respectively.[39,44] However, there still remains a lack of investigation on this type of MV complexes. It is worth mentioning that all the reported bisvinylidene compounds are stopper-type complexes, which prevents further functionalization for fixation of the electrode "anchor" groups and extension of these systems to form oligonuclears.

Herein, we describe the access to a family of sp^2 C_4H_2-bridged dinuclear rhenium complexes with a replaceable π-donor Cl^- ligand and a more π-accepting $Me_3SiC{\equiv}C^-$ ligand by the deprotonation of the complexes *trans*-$[X(PMe_3)_4Re{\equiv}C\text{-}CH_2\text{-}CH_2\text{-}C{\equiv}Re(PMe_3)_4X][PF_6]_2$ (X = Cl, **9**; $C{\equiv}CSiMe_3$, **10**) and the oxidation of the deprotonated products. A thorough physical study of these complexes was sought to unravel their potential as a precursor for the build-up of a "molecular wire".

3.2 Syntheses and characterization of the dinuclear rhenium complexes 11, 11[PF_6], 11[PF_6]$_2$, 12, 12[PF_6] and 12[PF_6]$_2$

3.2.1 Syntheses of the sp^2 C_4H_2-bridged dinuclear rhenium complexes **11, 11[PF_6], 11[PF_6]$_2$, 12, 12[PF_6]**, and **12[PF_6]$_2$**

According to Scheme 1 the deprotonation of the biscarbyne complex *trans*-[Cl(PMe_3)$_4$Re≡C-CH_2-CH_2-C≡Re(PMe_3)$_4$Cl][PF_6]$_2$ (**9**) with an excess of KO*t*Bu in THF at 65 °C for 1 h resulted in a brownish green, diamagnetic neutral bisvinylidene complex *trans*-[Cl(PMe_3)$_4$R=C=CH-CH=C=Re(PMe_3)$_4$Cl] (**11**) in 85% yield. At room temperature, **11** was stable towards base such as MeLi, but decomposed in the presence of *n*-BuLi and *t*-BuLi. Another brownish green, diamagnetic neutral bisvinylidene complex *trans*-[(Me_3SiC≡C)(PMe_3)$_4$Re=C=CH-CH=C=Re(PMe_3)$_4$(C≡CSiMe_3)] (**12**) was obtained in 83% yield by the deprotonation of t*rans*-[(Me_3SiC≡C)(PMe_3)$_4$Re≡C-CH_2-CH_2-C≡Re(PMe_3)$_4$(C≡CSiMe_3)][PF_6]$_2$ (**10**) with an excess of KO*t*Bu in THF at room temperature. **10** could be deprotonated by using a stronger base such as LDA, while **9** decomposed upon treatment with LDA. The possible reason for this difference in the reactivity can be attributed to the relatively harder acid Li^+ compared to K^+ that more easily abstracts the Cl^- to form the insoluble LiCl and causes the decomposition. **10** with the π-acceptor acetylide end group shows increased reactivity towards KO*t*Bu than **9** bearing the π-donor chloride end group, which clearly demonstrates an influence of the end groups with different properties on their subsequent reactivity. Such influence is also evident from the down-field shift of the resonances of H, C_α, and C_β and the increase of the Re-C1 bond distances from Cl^- to $Me_3SiC{\equiv}C^-$.

As shown in Scheme 2, the diamagnetic neutral bisvinylidene complexes **11** and **12** were readily oxidized with two equiv. of [Cp_2Fe][PF_6] to the diamagnetic dicationic complexes **11[PF_6]$_2$** and **12[PF_6]$_2$**. **11[PF_6]$_2$** and **12[PF_6]$_2$** showed good solubilities and stabilities in polar solvents, such as CH_2Cl_2 and CH_3CN, while **11** and **12** quickly decomposed in CH_2Cl_2 and gradually in CH_3CN. **11** and **12** undergo facile oxidation in the solid state and in solution. Therefore exclusion of O_2, CH_2Cl_2 and CH_3CN is necessary during the handling of these neutral complexes and the separated products should be stored in solid state at low temperature (**11** and **12** is stable in the solid state for several months under an inert atmosphere at -30 ºC). The

reduction of **12[PF$_6$]$_2$** with an excess of Na/Na(PhCOPh) regenerated **12**. **11[PF$_6$]$_2$** could be reduced by Na/Na(PhCOPh) as well, but the resulting neutral product was obtained along with other unidentifiable side products. The reason for the appearance of the side products is probably due to the ability of Na^+ to abstract the Cl^- from **11[PF$_6$]$_2$** and resulting in decomposition. The comproportionation reaction of **11** with **11[PF$_6$]$_2$** (Scheme 3) or the oxidation of **11** with one equiv. of $[Cp_2Fe][PF_6]$ produced the bluish green paramagnetic MV complex **11[PF$_6$]**. **12** exhibited a similar behaviour and gave the corresponding yellowish green paramagnetic MV complex **12[PF$_6$]**. **11[PF$_6$]** is insoluble in most organic solvents such as pentane, diethyl ether, benzene and THF, and sparingly dissolves in CH_3CN, but decomposes immediately in CH_2Cl_2. **12[PF$_6$]** quickly decomposes in CH_2Cl_2 as well, but shows better solubility in THF and CH_3CN than **11[PF$_6$]**. A similar slow decomposition of the MV complex $[(\eta^5\text{-}C_5Me_5)Re(NO)(P(C_6H_4CH_3)_3)(C{\equiv}CC{\equiv}C)(H_3CC_6H_4)_3(ON)Re(\eta^5\text{-}C_5Me_5)]^+$ in CH_2Cl_2 was reported by Gladysz and co-workers.[45]

Scheme 1

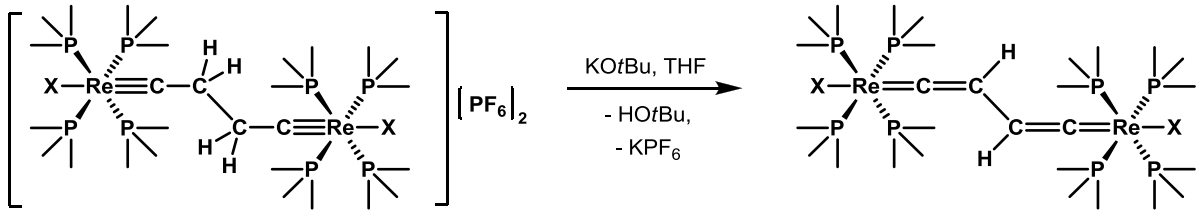

(X = Cl **9**, C≡CSiMe$_3$ **10**)

(X = Cl **11** 85%, C≡CSiMe$_3$ **12** 83%)

Scheme 2

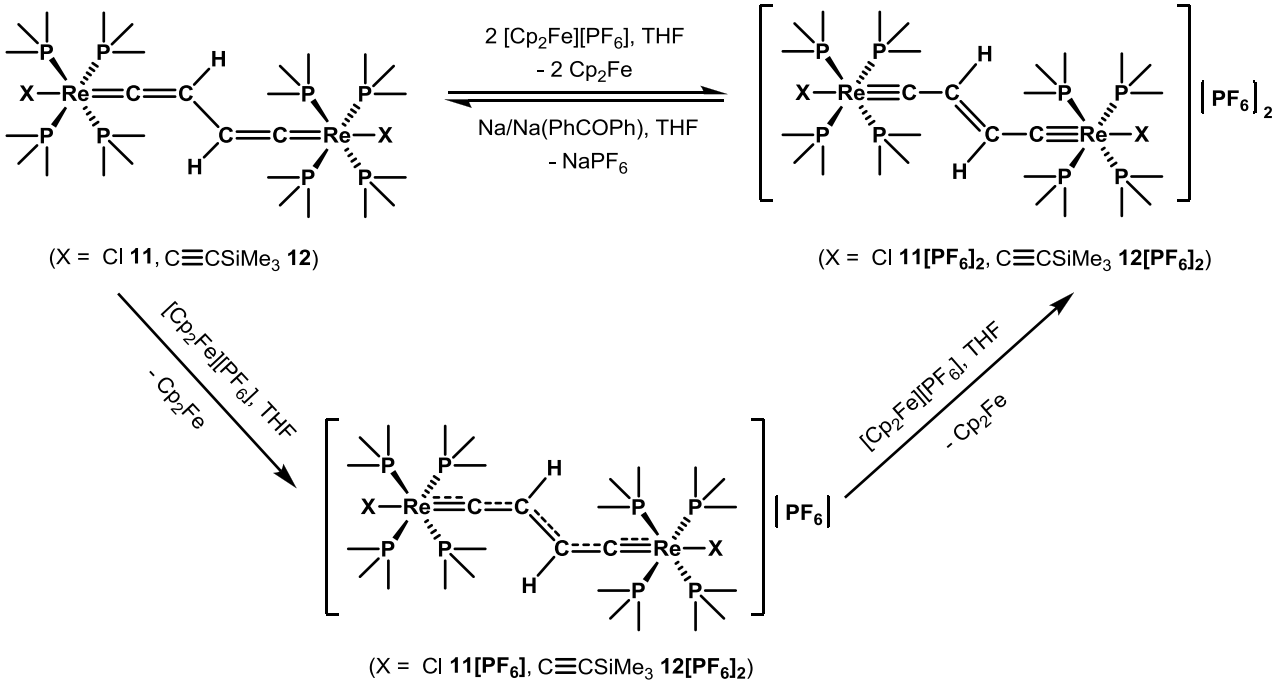

Scheme 3

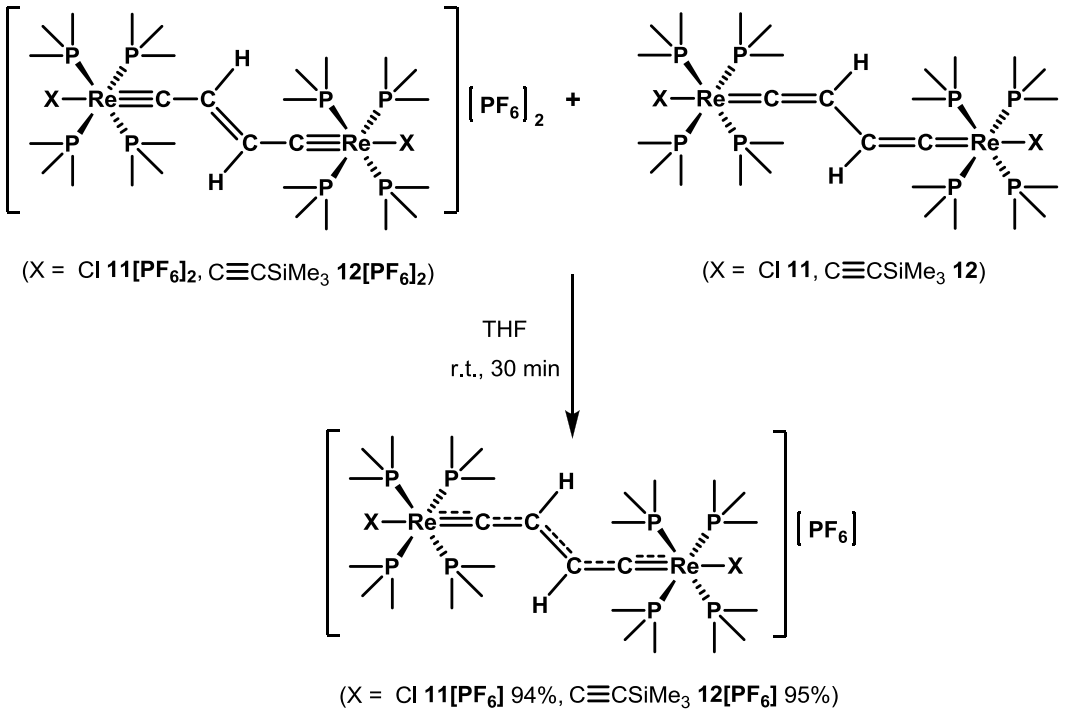

3.2.2 Characterization of the dinuclear rhenium complexes **11, 11[PF$_6$], 11[PF$_6$]$_2$, 12, 12[PF$_6$]**, and **12[PF$_6$]$_2$**

The dinuclear rhenium complexes **11**, **11[PF$_6$]**, **11[PF$_6$]$_2$**, **12**, **12[PF$_6$]** and **12[PF$_6$]$_2$** were characterized by NMR, IR, Raman and elemental analysis. Selected ^{1}H NMR, ^{13}C NMR and ^{31}P NMR data for the neutral complexes **11** and **12** and for the dicationic complexes **9**, **10**, **11[PF6]$_2$** and **12[PF$_6$]$_2$** are listed in Table 3-1 for comparison.

Table 3-1. Selected ^{1}H NMR and ^{31}P NMR data for the neutral complexes **11** and **12** in C_6D_6, and the dicationic complexes **9**, **10**, **11[PF$_6$]$_2$** and **12[PF$_6$]$_2$** in CD_2Cl_2

Complexes	^{13}C NMR (δ, ppm)		^{1}H NMR (δ, ppm)	^{31}P NMR (δ, ppm)
	C_α	C_β	H_β	PMe_3
$[Cl(PMe_3)_4Re{=}C{=}CH]_2$ (**11**)	298.5	90.5	2.00	-34.0
$[(Me_3SiC{\equiv}C)(PMe_3)_4Re{=}C{=}CH]_2$ (**12**)	309.4	96.7	2.51	-40.5
$[Cl(PMe_3)_4Re{\equiv}C\text{-}CH_2]_2[PF_6]_2$ (**9**)	267.3	44.8	1.75	-35.8
$[(Me_3SiC{\equiv}C)(PMe_3)_4Re{\equiv}C\text{-}CH_2]_2[PF_6]_2$ (**10**)	279.9	46.4	1.56	-42.2
$[Cl(PMe_3)_4Re{\equiv}C\text{-}CH]_2[PF_6]_2$ (**11[PF$_6$]$_2$**)	255.5	144.0	5.76	-37.3
$[(Me_3SiC{\equiv}C)(PMe_3)_4Re{\equiv}C\text{-}CH]_2[PF_6]_2$ (**12[PF$_6$]$_2$**)	265.3	145.8	5.82	-43.8

The ^{1}H NMR spectra of the neutral complexes *trans*-[X(PMe$_3$)$_4$Re=C=CH-CH=C=Re(PMe$_3$)$_4$X] (X = Cl, **11**; C≡CSiMe$_3$, **12**) showed doublet resonances for the vinylidene protons at 2.00 ppm and 2.51 ppm, respectively. The ^{13}C{^{1}H} NMR spectra revealed two characteristic signals for the vinylidene C_α and C_β atoms of **11** at 298.5 ppm ($^2J_{PC}$ = 11.3 Hz) and 90.5 ppm, and those of **12** at 309.4 ppm ($^2J_{PC}$ = 12.8 Hz) and 96.7 ppm. In comparison to the resonances of the vinylidene C_α and C_β atoms for the mononuclear rhenium vinylidene complexes *trans*-[ReCl(=C=CH$_2$)(PMe$_3$)$_4$] (**3**, 291.4 ppm and 80.8 ppm) and *trans*-[Re(=C=CH$_2$)(C≡CSiMe$_3$)(PMe$_3$)$_4$] (**7**, 301.6 ppm and 87.8 ppm), the resonances for the corresponding dinuclear bisvinylene complexes displayed a slightly down-field shift. In the

mononuclear rhenium vinylidene complexes, the electron-rich nature of the C_β atom makes it susceptible to electrophilic attack in CH_2Cl_2. Perhaps a similar reason can be attributed to the observed decomposition of the neutral bisvinylidene complexes in polar solvents such as CH_2Cl_2 and CH_3CN. Two additional resonances of **12** at 152.8 ppm ($^2J_{PC}$ = 16.0 Hz) and 127.8 ppm were assigned to the C_α' and C_β' atoms of acetylide group. As shown in Table 3-1 and in view of the electronic influence of the different end groups *trans* to the bisvinylidene ligand, the resonances in **12** displayed a down-field shift in contrast to those in **11**. In the IR and Raman spectra, strong ν(C=C-C=C) vibrations were observed for **11** at 1552 cm^{-1} (IR) and 1588 cm^{-1} (Raman). The spectra of **12** showed a strong ν(C≡C) band at 1975 cm^{-1} (IR) and 1973 cm^{-1} (Raman) and the ν(C=C-C=C) band at 1543 cm^{-1}(IR) and 1581 cm^{-1} (Raman). The observed ν(C=C-C=C) bands were assigned to asymmetric stretches in the IR spectra, while in the Raman spectra they were attributed to the symmetric stretches. For conjugated dienes with a center of symmetry, the symmetric stretches are IR-inactive, whereas the asymmetric stretches are Raman-inactive.

The ^1H NMR spectra of the dicationic ethylenylidene biscarbyne complexes *trans*-$[X(PMe_3)_4Re{\equiv}C\text{-}CH{=}CH\text{-}C{\equiv}Re(PMe_3)_4X][PF_6]_2$ (X = Cl, **11[PF$_6$]$_2$**; C≡CSiMe$_3$, **12[PF$_6$]$_2$**) showed the resonances of the vinylidene protons as a singlet at 5.76 ppm and 5.82 ppm, respectively. The $^{13}C\{^1H\}$ NMR spectra of **11[PF$_6$]$_2$** and **12[PF$_6$]$_2$** revealed characteristic resonances for the C_α and C_β at 255.5 ppm and 144.0 ppm, and 265.3 ppm and 145.8 ppm, respectively. The $^{13}C\{^1H\}$ NMR spectra showed signals of low intensities for these complexes which did not allow to extract the J_{PC} values. The additional resonances at 135.5 ppm and 130.9 ppm in **12[PF$_6$]$_2$** were attributed to the acetylide group. In the ^{31}P NMR spectra, the resonances at -37.3 ppm and -43.8 ppm were ascribed to the $P(CH_3)_3$ ligand in **11[PF$_6$]$_2$** and **12[PF$_6$]$_2$**. The PF_6^- characteristic signals appeared as a septet at -143.9 ppm. As depicted in Table 3-1, the oxidations of the neutral complexes to the dicationic complexes led to considerable changes in the NMR spectra. On oxidation of **11** and **12** to **11[PF$_6$]$_2$** and **12[PF$_6$]$_2$**, the resonances of C_α showed an up-field shift, while those of C_β and H moved to down-field revealing the transformation of the valence structure from a bisvinylidene (=C=CH-CH=C=) form to an ethylenylidene biscarbyne (≡C-CH=CH-C≡) form. Only broad signals were observed in the ^1H NMR spectra for the MV complexes **11[PF$_6$]** and **12[PF$_6$]** indicating paramagnetic behavior of these complexes. In the IR and Raman spectra, no ν(C=C) vibrations were observed for the MV

complexes and the dicationic complexes. This was interpreted in terms of a rapid electron exchange between both ends on the IR time scale (10^{-13} s) leading to coalescence of the IR bands of the bridge. Similar observations are described in the literature. For the complexes with acetylide end group (**12[PF$_6$]** and **12[PF$_6$]$_2$**), the IR spectra showed weak ν(C≡C) vibrations at 2022 cm^{-1} and 1987 cm^{-1}, which had also low intensities in the Raman spectra at 2017 cm^{-1} and 2001 cm^{-1}, respectively.

X-ray diffraction analyses (Fig 3-1) were carried out on the neutral complexes **11** and **12**, the MV complexes **11[PF$_6$]** and **12[PF$_6$]**, and the dicationic complexes **11[PF$_6$]$_2$** and **12[PF$_6$]$_2$**. Selected bond distances and bond angles are summarized in Table 3-2 for all the dinuclear rhenium complexes.

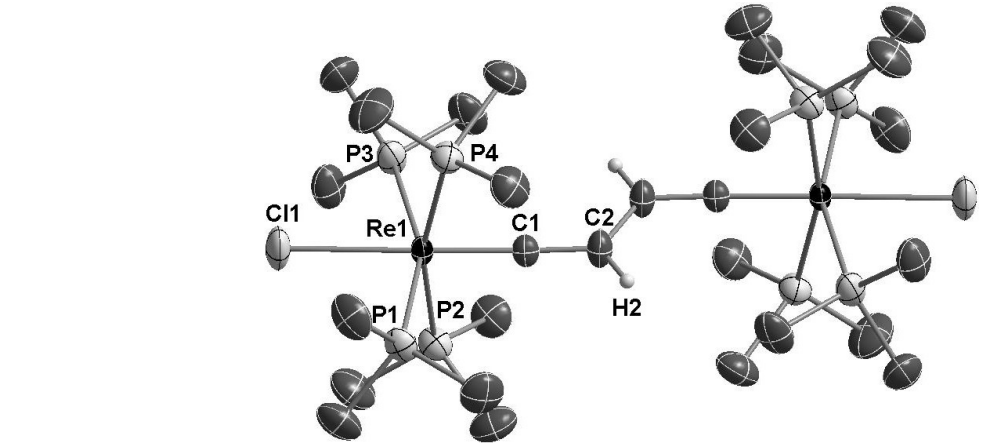

(a)

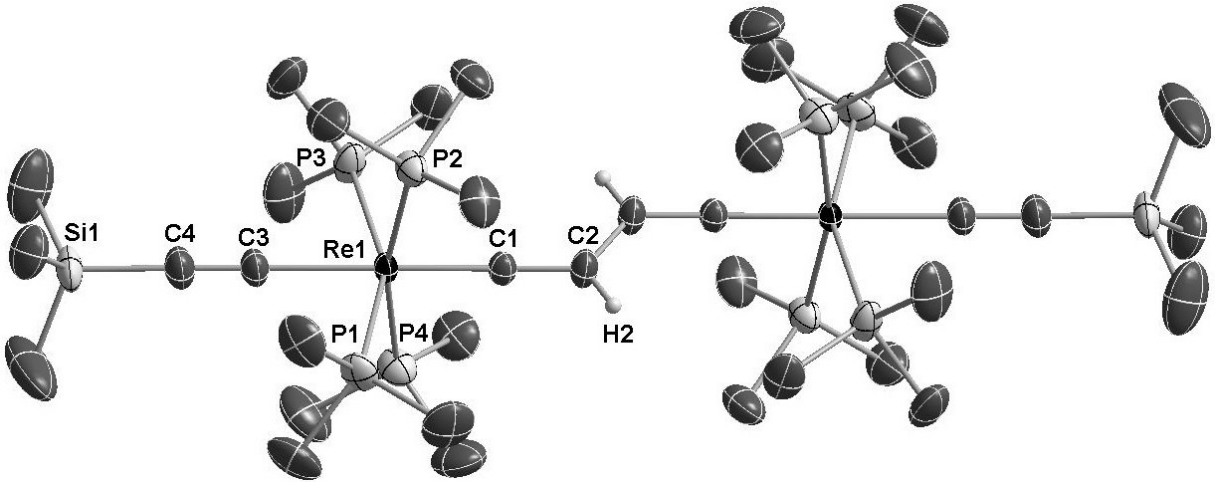

(b)

Fig 3-1. ORTEP like drawing of (a) *trans*-[Cl(PMe_3)$_4$Re=C=CH-CH=C=Re(PMe_3)$_4$Cl] (**11**) and of (b) *trans*-[($Me_3SiC{\equiv}C$)(PMe_3)$_4$Re=C=CH-CH=C=Re(PMe_3)$_4$($C{\equiv}CSiMe_3$)] (**12**) (50% probability level of thermal ellipsoids, solvent molecules and selected hydrogen atoms are omitted for clarity.)

Table 3-2. Selected bond lengths [Å] and angles [°] for **11**, **11[PF$_6$]**, **11[PF$_6$]$_2$**, **12**, **12[PF$_6$]** and **12[PF$_6$]$_2$**, assignment of the bond lengths in the C_4 bridge according to the following notation: [Re]C1C2C2'C1'[Re']

Complexes	**11**	**11[PF$_6$]**	**11[PF$_6$]$_2$**	**12**	**12[PF$_6$]**	**12[PF$_6$]$_2$**
C2-C2'	1.475(6)	1.424(13)	1.317(8)	1.469(4)	1.388(10)	1.331(10)
C1-C2	1.329(4)	1.381(9)	1.439(5)	1.337(3)	1.375(8)	1.414(7)
C1-Re1	1.859(3)	1.802(7)	1.766(3)	1.904(2)	1.851(6)	1.805(5)
Cl1-Re1	2.5844(8)	2.5510(16)	2.5075(8)	/	/	/
C3-Re1	/	/	/	2.142(2)	2.167(6)	2.179(4)
C3-C4	/	/	/	1.220(3)	1.218(9)	1.172(6)
C4-Si1	/	/	/	1.800(3)	1.813(6)	1.836(5)
Re···Re	7.306	7.292	7.268	7.416	7.371	7.282
C1-C2-C2'	125.2(4)	123.9(9)	124.7(5)	125.2(3)	125.2(7)	125.5(7)
C2-C1-Re1	178.0(3)	175.9(6)	176.8(3)	178.88(19)	177.2(5)	177.1(4)
C1-Re1-Cl1	179.13(9)	177.4(2)	177.90(13)	/	/	/
C1-Re1-C3	/	/	/	178.62(10)	177.5(2)	171.2(2)
Re1-C3-C4	/	/	/	179.4(3)	178.1(6)	178.7(4)
C3-C4-Si1	/	/	/	177.4(3)	171.0(6)	177.8(4)

The Re1-C1 bond distances for the neutral complexes **11** and **12** are 1.859(3) Å and 1.904(2) Å, and for the MV complexes **11[PF$_6$]** and **12[PF$_6$]** are 1.802(7) Å and 1.851(6) Å, and for the dicationic complexes **11[PF$_6$]$_2$** and **12[PF$_6$]$_2$** are 1.766(3) Å and 1.805(5) Å, respectively. The Re1-C1 (Re=C, sp^2) bond length for **11** is shorter than the reported Re=C distances 2.046(8) Å for the vinylidene complex *trans*-[ReCl(=C=CHPh)(dppe)$_2$][46] and 1.909(7)/1.916(7) Å for the

cumulenic complex $[(C_5Me_5)(NO)(PPh_3)Re=C=C=C=C=Re(PPh3)(NO)(C_5Me_5)][PF_6]_2$,[24] but close to that of the mononuclear rhenium vinylidene complexes *trans*-$[ReCl(=C=CHSiMe_3)(PMe_3)_4]$ (**2**) [1.854(3) Å] and *trans*-$[ReCl(=C=CH_2)(PMe_3)_4]$ (**3**) [1.861(9) Å]. The Re1-C1 bond length of **11[PF$_6$]$_2$** is slightly longer than the expected distance range (1.75-1.72 Å) of the Re≡C (sp) triple-bonded covalent radii. The higher *trans* influence of $Me_3SiC{\equiv}C^-$ weakens the Re1-C1 bond, which is reflected in the lengthening of the Re1-C1 distances observed in the complexes on going from Cl^- to $Me_3SiC{\equiv}C^-$. The C1-C2 bond lengths of **11** and **12** are 1.329(4) Å and 1.337(3) Å, close to the lower limit of the C=C bond (1.33-1.38 Å), whereas the C2–C2' distances 1.475(6) Å and 1.469(4) Å are close to the lower limit of the C-C bond (1.47-1.54 Å). The C1-C2 bond lengths in **11[PF$_6$]$_2$** and **12[PF$_6$]$_2$** are 1.439(5) Å and 1.414(7) Å respectively, somewhat shorter than the lower limit of the C-C bond (1.47-1.54 Å). The C2–C2' distances 1.317(8) Å and 1.331(10) Å are close to a C=C double bond (1.33-1.38 Å). The C1–C2 and C2–C2' distances of the MV complexes **11[PF$_6$]** [1.424(13) Å and 1.381(9) Å] and **12[PF$_6$]** [1.375(8) Å and 1.388(10) Å], which are in the range between a single bond and a double bond, are very close to the average of the corresponding bond distances of the neutral and dicationic complexes. On oxidation of the neutral complexes to the MV complexes, these two distances get gradually close to each other, especially for **12[PF$_6$]**. In conclusion, according to Table 3-3 and on oxidation of the neutral complexes to the dicationic complexes, the Re1-C1 distances gradually shorten coinciding with a change in bond distances from Re=C to Re≡C bond. The C1-C2 distances gradually lengthen from C=C to C-C bond while C2–C2' distances shorten from a C-C single bond to a C=C double bond. The Re···Re distances gradually decrease from the neutral complexes **11** and **12** to the corresponding dicationic complexes **11[PF$_6$]$_2$** and **12[PF$_6$]$_2$**. All these observations clearly indicate that the oxidations of **11** and **12** cause a structural change of the sp^2 C_4H_2 linkage gradually transform from a bisvinylidene (=C=CH-CH=C=) form to an ethylenylidene biscarbyne (≡C-CH=CH-C≡) form (Scheme 4). From Table 3-2, one could derive that the Re1-Cl1 distance shortens on oxidation of **11** to **11[PF$_6$]$_2$**, while the Re1-C3 distance increase from **12** to **12[PF$_6$]$_2$**. The bond distance differences result from the different properties of the Cl^- group and the $Me_3SiC{\equiv}C^-$ group. It seems that removal of the electron from the metal centers favors the bonding with the π-donor Cl^- ligand, while weakens the bonding with π-acceptor $Me_3SiC{\equiv}C^-$ ligand. As shown in Figure 3-1 and Table 3-2 the C1-

C2-C2' bond angles are nearly 125° in all compounds. The Re-C-C and Cl-Re-C bond angles in the compounds with chloride end group are close to 180°. The atoms Si1, C4, C3, Re1, C1 and C2 are almost linear in the compounds bearing acetylide end group.

Scheme 4

Electronic structures using canonical representations of sp^2 C_4H_2-bridged system

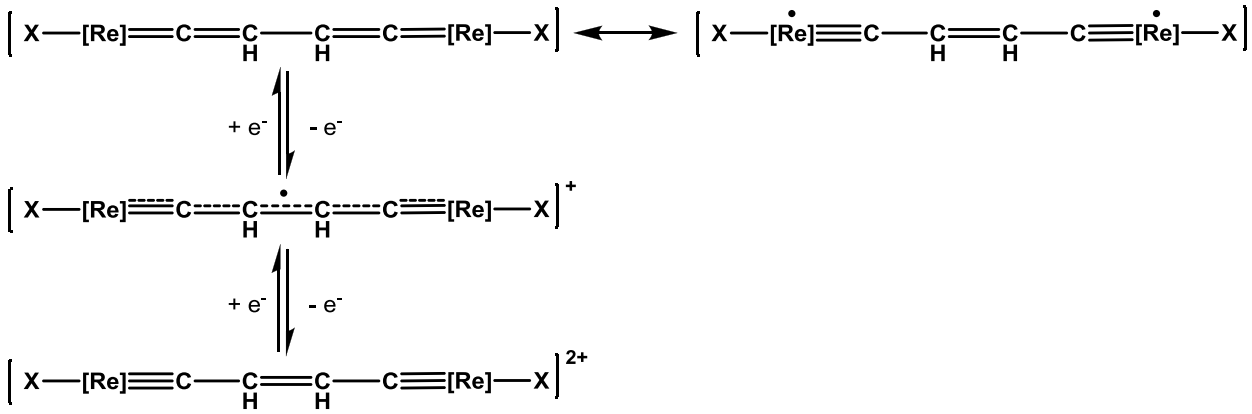

3.3 Spectroscopic Studies

3.3.1 Cyclic voltammetry (CV) studies of the dinuclear rhenium complexes

Cyclic voltammetry (CV) is the easiest way to evaluate the thermodynamic stability of MV compounds (under CV condition). For a totally delocalized class III species containing two equal redox-active metal centres, the equilibrium 1 of Scheme 5 can be used to represent the comproportionation reaction of the formation of MV compound.

Scheme 5

$$[M_1]^n\text{-L-}[M_2]^n + [M_1]^{n+1}\text{-L-}[M_2]^{n+1} \underset{}{\overset{K_c}{\rightleftharpoons}} 2[M_1]^{(n+1)/2}\text{-L-}[M_2]^{(n+1)/2} \qquad (16)$$

$$K_c = ([M_1]^{(n+1)/2}\text{-L-}[M_2]^{(n+1)/2})^2/([M_1]^n\text{-L-}[M_2]^n)([M_1]^{n+1}\text{-L-}[M_2]^{n+1}) \qquad (17)$$

The comproportionation constant K_c given in eq. 17 is proportional to the potential difference (ΔE) between two reversible redox couples observed in the CV spectrum. Using the Nernst equation, K_c is equal to $\exp(F\Delta E_{1/2}/RT)$, where the F is the Faraday constant 96485.33 C/mol, R is the universal gas constant 8.314 $J\cdot mol^{-1}\cdot K^{-1}$, and T is temperature (K). In general, a large ΔE

value (or K_c value) indicates the equilibrium to be on the mixed valence side, concomitant with a high possibility to isolate the MV compound.

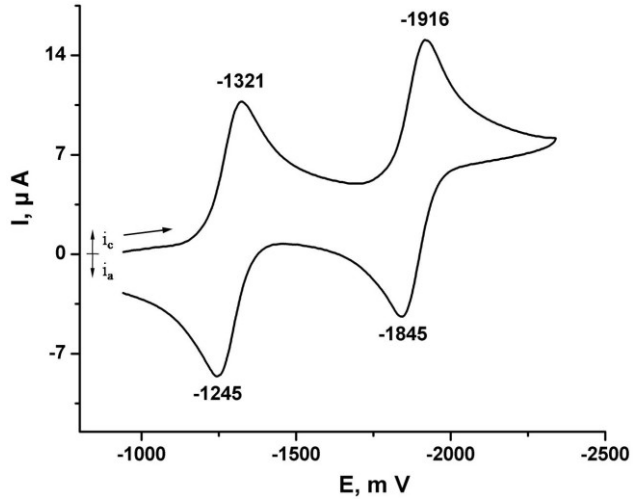

Fig 3-2. CV of **11[PF$_6$]$_2$** in 0.1 M CH_3CN solution of [*n*-Bu_4N][PF_6]; Au electrode; E vs $Fc^{0/+}$; scan rate = 100 mV·s^{-1}; 20 °C

The CV spectrum of **11[PF$_6$]$_2$** (Figure 3-2) in CH_3CN displayed two fully reversible waves at $E_{1/2}$ = -1.283 V and $E_{1/2}$ = -1.880 V corresponding to the Re(III)-Re(III)/Re(III)-Re(II)/Re(I)-Re(I) redox couples, respectively. According to Scheme 4, there could be two alternative electronic structures for the neutral complexes: the bisvinylidene complex with Re(I)-Re(I) oxidation states for the two rhenium centers and its isomer-biscarbyne vinylidene-bridged complex with Re(II)-Re(II) oxidation states. The sharp, well-defined resonances found in the ^1H NMR, ^{13}C NMR and ^{31}P NMR spectra of the isolated complexes **11** and **12** suggest that the neutral complexes are diamagnetic or have strongly antiferro-magnetically coupled rhenium centers. The determined structural data (Table 3-2) imply the canonical form of a bisvinylidene bridge (=C=CH-CH=C=). Therefore we assume two Re(I) sites and there is no evidence for an uncoupled triplet excited state (**·**Re≡C-CH=CH-C≡Re**·**). The potential difference $\Delta E_{1/2}$ of these two values is 0.597 V establishing a large K_c value of 1.8×10^{10}.

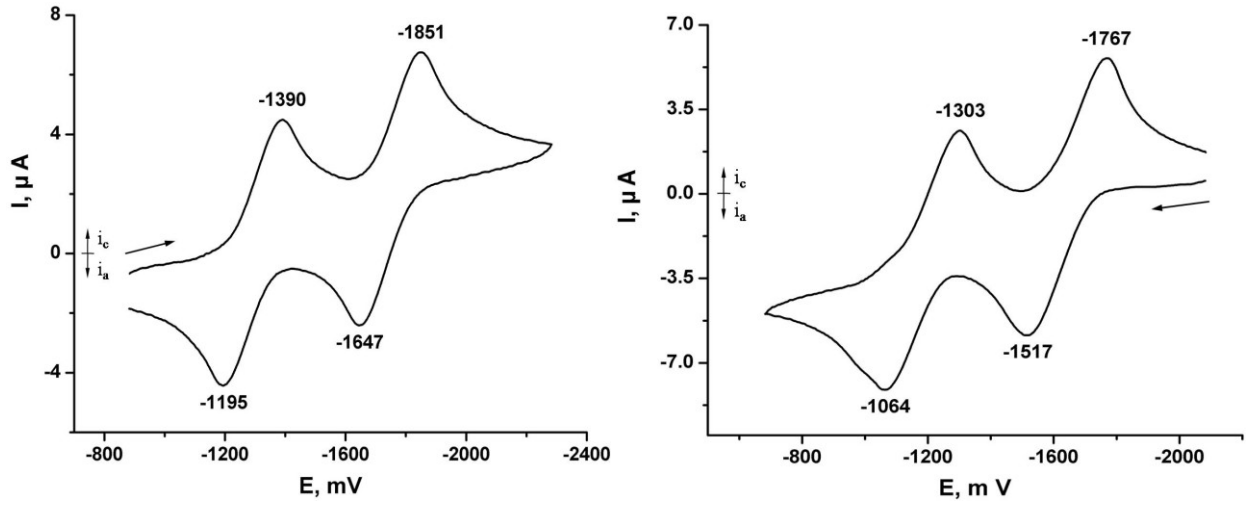

(a) (b)

Fig 3-3. CV of (a) **12[PF$_6$]$_2$** in 0.1M THF solution of [*n*-Bu$_4$N][PF$_6$]; (b) **12** in 0.1M THF solution of [*n*-Bu$_4$N][PF$_6$]; Au electrode; E vs $Fc^{0/+}$; scan rate = 100 mV·s^{-1}; 20 °C

The CV spectrum of **12[PF$_6$]$_2$** (Figure 3-3a) recorded in THF displayed two reversible waves of $E_{1/2}$ = -1.292 V and $E_{1/2}$ = -1.749 V, corresponding to the Re(III)-Re(III)/Re(III)-Re(II)/Re(I)-Re(I) redox couples. The potential difference $\Delta E_{1/2}$ between these two redox peaks is 0.457 V resulting in a K_c value of 7.1×10^7. The CV spectrum of **12** (Figure 3-3b) in THF displayed two reversible waves $E_{1/2}$ = -1.184 V and $E_{1/2}$ = -1.642 V corresponding to the Re(III)-Re(III)/Re(III)-Re(II)/Re(I)-Re(I) redox couples and the $\Delta E_{1/2}$ value is 0.458 V. In comparison with the electrochemical data for **12[PF$_6$]$_2$** and **12** (Table 3-3), the presence of PF_6^- decreases the $E_{1/2}$ value by about 90 mV in **12[PF$_6$]$_2$** as a consequence of ion-pairing effect. In other words, the formation of ion-pairs in the solution makes complex **12[PF$_6$]$_2$** thermodynamically more difficult to reduce but easier to oxidize than complex **12**.

Table 3-3. Electrochemical data for **11[PF$_6$]$_2$**, **12**, and **12[PF$_6$]$_2$** and for some dinuclear manganese in leterature, E vs $Fc^{0/+}$

Complexes	Couple 1 $E_{1/2}$ (V)	Couple 2 $E_{1/2}$ (V)	ΔE (V)	K_c	Ref.
$[(MeC_5H_4)(dmpe)Mn\text{-}C]_2[PF_6]_2$ (CH_3CN/THF)	-0.847	-1.835	0.988	8.6×10^{16}	[44]
$[(MeC_5H_4)(dmpe)Mn{=}C{=}CPh]_2$ (CH_2Cl_2)	-0.445	-0.656	0.211	8.0×10^{3}	[39]
$[(MeC_5H_4)(depe)Mn{\equiv}C\text{-}CH]_2[PF_6]_2$ (CH_3CN)	-0.820	-1.386	0.576	6.6×10^{9}	[44]
$[Cl(PMe_3)_4Re{\equiv}C\text{-}CH]_2[PF_6]_2$ (**11[PF$_6$]$_2$**, CH_3CN)	-1.283	-1.880	0.597	1.8×10^{10}	Present work
$[(Me_3SiC{\equiv}C)(PMe_3)_4Re{=}C{=}CH]_2$ (**12**, THF)	-1.184	-1.642	0.458	7.1×10^{7}	Present work
$[(Me_3SiC{\equiv}C)(PMe_3)_4Re{\equiv}C\text{-}CH]_2[PF_6]_2$ (**12[PF$_6$]$_2$**, THF)	-1.292	-1.749	0.457	7.1×10^{7}	Present work

As shown in Table 3-3, the end group has a significant influence on the $\Delta E_{1/2}$ value. The complex **11[PF$_6$]$_2$** with chloride end groups shows larger K_c value than the complex **12[PF$_6$]$_2$** with acetylide end groups and this trend is observed in the Mn system as well,[44] which is related to the different π-donating properties of the Cl^- ligand and the $Me_3SiC{\equiv}C^-$ ligand. The halide as a π-donor would make the metal centers more electron-rich than those in the complexes with acetylide ligand of lower π-donicity and accordingly are expected to lead to thermodynamically more favorable oxidations and $E_{1/2}$ values. By the same token the halide substituted rhenium fragment is greater difficulty to accept the second electron than that with acetylide ligand. As a result, the potential differences $\Delta E_{1/2}$ was enlarged and resulted in a larger K_c value. The values of the second redox couples based on **11[PF$_6$]$_2$** and **12[PF$_6$]$_2$** are very negative and such negative potentials have been observed in the C_2-bridged complex $[(MeC_5H_4)(dmpe)Mn\text{-}C{\equiv}C\text{-}Mn(dmpe)(MeC_5H_4)][PF_6]_2$ with very strong through-bridge interactions (Table 3-3). In accordance with the CV studies, the neutral bisvinylidene complexes **11** and **12** are very easy to

oxidize. The evidence that **11** and **12** is a good reducing agent is evident from the reaction of **11** with Tl(OTf) in THF (Scheme 5). The emerald colored dicationic complex *trans*-$[Cl(PMe_3)_4Re{\equiv}C\text{-}CH{=}CH\text{-}C{\equiv}Re(PMe_3)_4Cl][OTf]_2$ **13** precipitated immediately and was isolated in 86% yield. **13** has been characterized by NMR, elemental analysis and mass spectroscopy. **11** even reacted with Li(OTf) in THF at room temperature with the formation of the bluish green MV complex *trans*-$[Cl(PMe_3)_4Re{\equiv}C\text{-}CH{=}CH\text{-}C{\equiv}Re(PMe_3)_4Cl][OTf]$ that was confirmed by NMR and mass spectroscopy.

Scheme 5

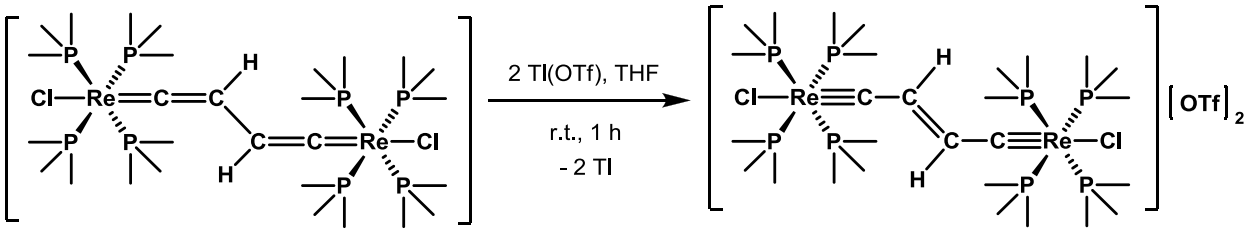

11 **13** 86%

3.3.2 NIR evidence for through-bridge electronic interaction

UV-vis/NIR spectroscopy can provide decisive information on the extent of the electronic communication of two redox-active metal centers. From the IVCT bands observed in the UV-vis/NIR spectrum, two most important electron transfer parameters, the reorganization energy λ and the electronic coupling energy H_{ab} (cm^{-1}), can be obtained. A class I complex with zero or very weak electronic coupling has a completely localized charge ($H_{ab} \approx 0$) and no IVCT band is observed. The free energy of activation for interconversion of two sites ΔG^* is equal to $\lambda/4$. A valence-trapped or charge localized Class II species with a moderate strength electronic interaction, H_{ab} value ($0 < H_{ab} < \lambda/2$) is large enough to result in an observable IVCT band and ΔG^* is given by $(\lambda\text{-}2H_{ab})^2/4\lambda$. In a symmetric homobimetallic MV system, the H_{ab} value can be extracted from the IVCT band by using the Mulliken-Hush expression for a class II compound:[19,47-48]

$$H_{ab}\,(cm^{-1}) = (0.0206/d)(\lambda \Delta \nu_{1/2} \varepsilon_{max})^{1/2} \qquad (11)$$

Where the reorganization energy λ is equal to the energy of the band maximum ν_{max} (cm^{-1}), $\Delta\nu_{1/2}$ is the bandwidth at half height for a Gaussian-shaped IVCT band (cm^{-1}), ε_{max} is the absorption coefficient at band maximum ($M^{-1}cm^{-1}$), and d is the electron transfer distance in Å. In a class III system with strong electronic interaction ($H_{ab} \geq \lambda/2$ and $\Delta G^* = 0$), the odd electron

is completely delocalized between two metal centers. Then the electronic coupling energy H_{ab} (cm^{-1}) is simply related to the energy of IVCT band.

$$H_{ab}\,(cm^{-1}) = \nu_{max}/2 \qquad (12)$$

The bandwidth at half height predicted by Hush theory is given by equation 13, which is derived from class II species in the Robin and Day classification of the MV systems:

$$\Delta\nu_{1/2}(cm^{-1}) = (16RT\ln 2\lambda)^{1/2} \qquad (13)$$

At room temperature, this equation 13 reduces to equation 14:

$$\Delta\nu_{1/2}(cm^{-1}) = (2310\nu_{max})^{1/2} \qquad (14)$$

Comparison between the calculated and observed $\Delta\nu_{1/2}$ is a useful method to distinguish class II and class III species, as class III species typically exhibit IVCT bands with bandwidths at half height narrower than the Hush limits calculated from equation 13 or 14, while the bands of class II species are typically broader than the theoretical limit. The delocalization parameter Γ (eq. 15) is also a useful tool to evaluate the coupling of a complex. Weakly coupled class II systems display values of $0 < \Gamma < 0.1$, moderately coupled class II, $0 < \Gamma < 0.5$; borderline class II/III, $\Gamma \approx 0.5$; and class III $\Gamma >> 0.5$.[19,49]

$$\Gamma = 1\text{-}\Delta\nu_{1/2}/(2310\nu_{max})^{1/2} \qquad (15)$$

The sensitivity of IVCT bands to solvent variation is often employed as a criterion for the class of a MV species. For a valence-trapped class II system the absorption band maximum is predicted to show the full solvent dependence regardless of the value of H_{ab}. While the optical transition in a symmetric class III system, although intense, no longer involves charge transfer and is therefore not accompanied by a net dipole-moment change and should show no solvent dependence. [49-50]

To further assess the extent of the electronic interaction between the two redox-active rhenium centers, the UV-vis spectra for **11**, **11[PF$_6$]**, **11[PF$_6$]$_2$**, **12**, **12[PF$_6$]**, and **12[PF$_6$]$_2$** (Figure 3-3) were examined. Due to the limitation of the solubility and stability, the neutral complexes were measured in THF and the examination of the solvent effect of the MV complexes could not be performed. The UV-vis spectral data and IVCT absorption data for the MV complexes are listed in Table 3-5 and Table 3-6.

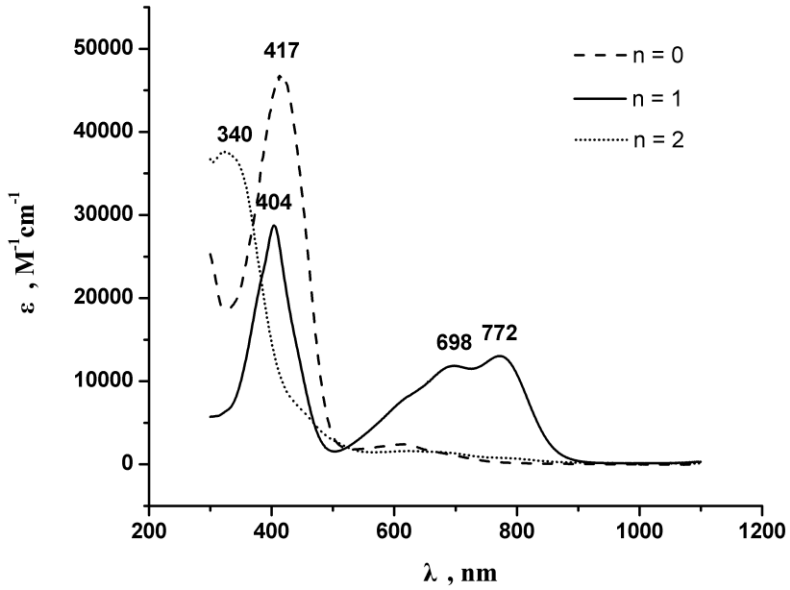

(a)

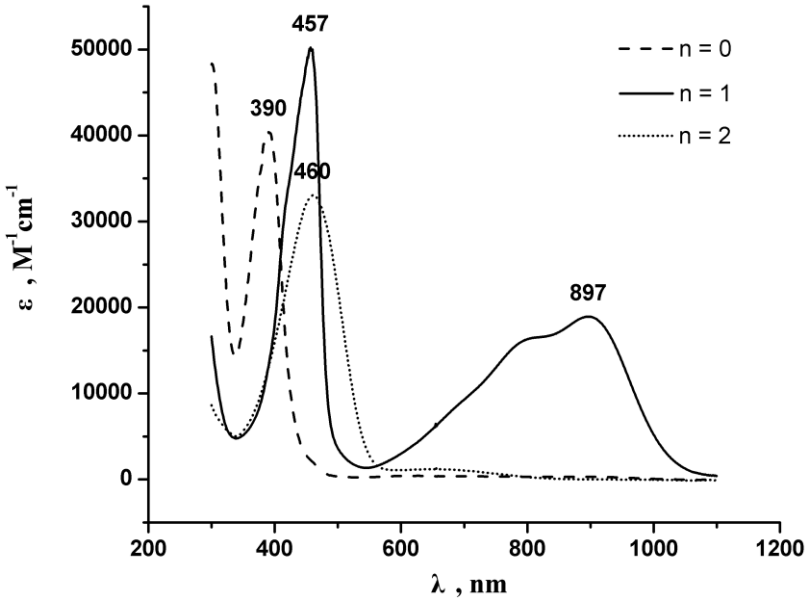

(b)

Fig 3-3. UV-vis spectra of (a) $\mathbf{11}^{n+}$; (b) $\mathbf{12}^{n+}$ (n = 0 in THF; n = 1 and n = 2 in CH_3CN, ambient temperature, 5×10^{-5} M)

Table 3-4. UV-vis spectral data for complexes **11**, **11[PF$_6$]**, **11[PF$_6$]$_2$**, **12**, **12[PF$_6$]**, and **12[PF$_6$]$_2$**

Complex	λ_{max} (nm)	ν_{max} (cm^{-1})	ε_{max} ($M^{-1}cm^{-1}$)
11	417	23 981	47 018
11[PF$_6$]	404	24 752	28 706
11[PF$_6$]$_2$	340	29 412	36 892
12	390	25 641	40 374
12[PF$_6$]	457	21 882	50 177
12[PF$_6$]$_2$	460	21 739	33 015

The UV-vis spectra of all complexes **11**, **11[PF$_6$]**, **11[PF$_6$]$_2$**, **12**, **12[PF$_6$]**, and **12[PF$_6$]$_2$** show intense absorption bands in the visible and ultraviolet region (Figure 3-3 and Table 3-4), which can be attributed to the metal-to-ligand charge transfer (MLCT) transition. In the visible and near-infrared region additional absorption band is observed at approximately 772 nm (ε is about 1.3×10^4 M^{-1} cm^{-1}) with a notable shoulder at ~ 700 nm for **11[PF$_6$]** and at 897 nm (ε is about 1.9×10^4 M^{-1} cm^{-1}) with a remarkable shoulder at ~ 800 nm for **12[PF$_6$]**. There are no counterparts in the spectra of the corresponding neutral and dicationic complexes. The observations of multiple IVCT bands have been reported previously for the MV complexes {[(MeC_5H_4)(dmpe)Mn]$_2$(≡C-CPh=CPh-C≡)}$^+$ [39], {[(η^5-C_5Me_5)(NO)(PPh_3)Re]$_2$(μ-C≡C-C≡C)}$^+$ [24], {[Cp*(dppm)Ru]$_2$(μ-C≡C-C≡C)}$^+$ [36] and {[Cp*(dppm)Fe]$_2$(μ-C≡C-X-C≡C)}$^+$ (X = 2,5-C_4H_2S, -C_4-)[51]. One explanation considered is spin-orbital coupling, which is more pronounced in third-row transition metals but cannot be completely ruled out for first-row transition metals.[50,52] The other reason could be that one absorption might be a LMCT transition, and the other a MLCT transition.[24,36,39,51,53] To calculate the electronic coupling energy H_{ab} of the MV species with multiple NIR absorptions, the Gaussian analysis of IVCT absorption band of MV complex is adopted.[51,53] The spectra of both mixed valence complexes **11[PF$_6$]** and **12[PF$_6$]** are deconvoluted into three Gaussian bands (A, B, and C shown in Figure 3-4, where band B is major component) and with a tail of MLCT

band observed in the visible and ultraviolet region. Table 3-5 summarizes spectral data extracted from the IVCT band shape analyses. The observed bandwidths of the three bands at half height ($\Delta\nu_{1/2}$) are narrower than the predicted widths from the equation 5, which are in agreement with the class III character for the MV complexes. In addition, the delocalization parameters Γ for all bands of **11[PF_6]** and **12[PF_6]** calculated form equation 6 are more than 0.5 indicating a class III species as well. Based on the CV and NIR spectroscopic data, the MV complexes **11[PF_6]** and **12[PF_6]** can be described as a class III MV compound with the odd electron fully delocalized. Therefore, the electronic coupling energies H_{ab}^{III} for band A, band B, and band C of **11[PF_6]** and **12[PF_6]**derived from equation 4 are 6350 cm^{-1} and 5434 cm^{-1}, 7068 cm^{-1} and 6100 cm^{-1}, and 8176 cm^{-1} and 7238 cm^{-1}, respectively. The H_{ab}^{II} values calculated from equation 3 for a class II MV compound are also listed in the Table 3-5 for comparison.

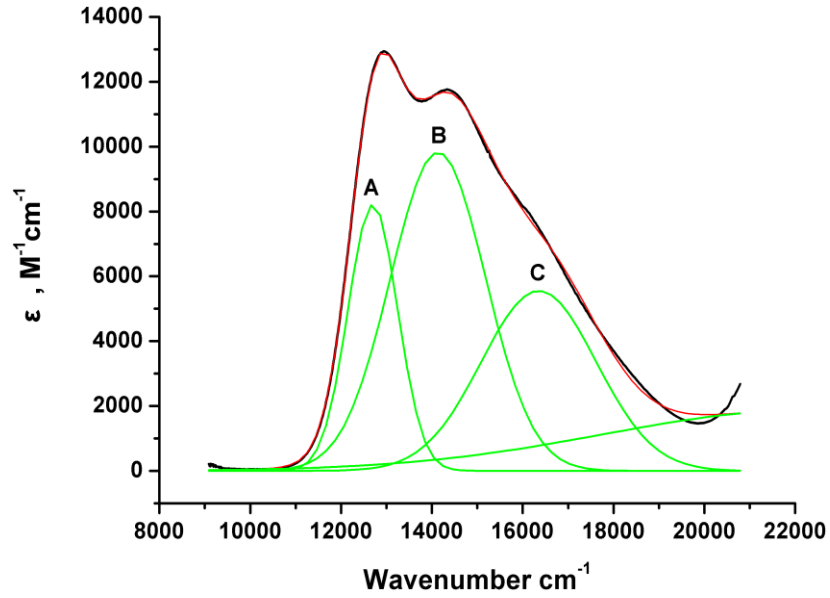

(a)

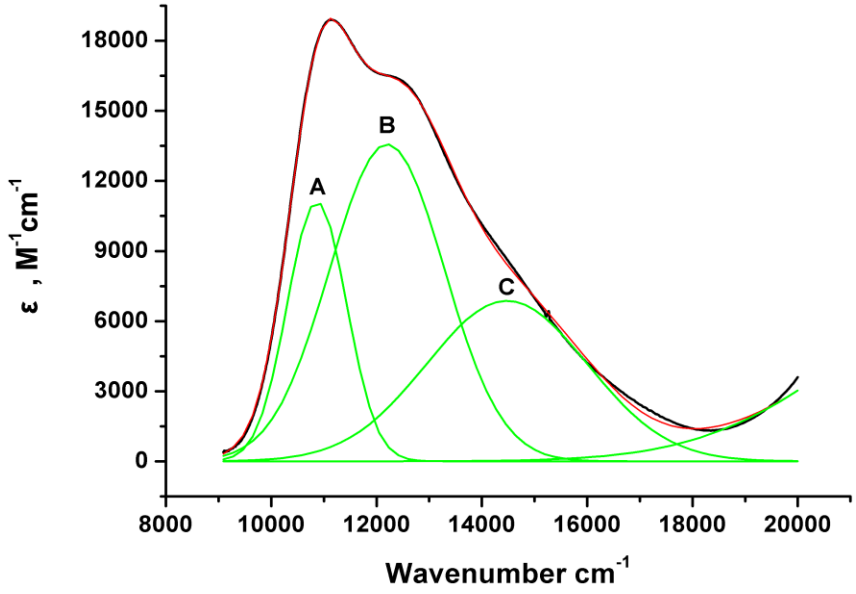

(b)

Fig 3-4. Comparison of the observed (black line) and the simulated (red line) IVCT band of (a) **11[PF_6]** (b) **12[PF_6]** as obtained by spectral deconvolution into the four individual Gaussian bands shown in green

Table 3-5. Summary of the spectral data of the Gaussian analyses of the IVCT band absorptions of the MV complexes **11[PF_6]** and **12[PF_6]**

Complexes		λ_{max} (nm)	ν_{max} (cm^{-1})	ε_{max} ($M^{-1}cm^{-1}$)	$\Delta\nu_{1/2}$ (obsd, cm^{-1})	$\Delta\nu_{1/2}$ (calcd, cm^{-1})
11[PF_6]	A	787	12700	8219	1093	5416
	B	707	14135	9826	2093	5714
	C	612	16353	5552	2531	6146
12[PF_6]	A	920	10867	11117	1126	5010
	B	820	12200	13575	2176	5309
	C	691	14476	6869	3051	5783

Complexes		$d_{Re\text{-}Re}$ (Å)	H_{ab}^{II} (cm^{-1})	$H_{ab}^{III} = \nu_{max}/2$ (cm^{-1})	Γ
11[PF_6]	A	7.292	954	6350	0.80
	B		1523	7068	0.63
	C		1354	8176	0.59
12[PF_6]	A	7.371	1030	5434	0.78
	B		1678	6100	0.59
	C		1539	7238	0.47

3.3.3 EPR studies and magnetic measurements

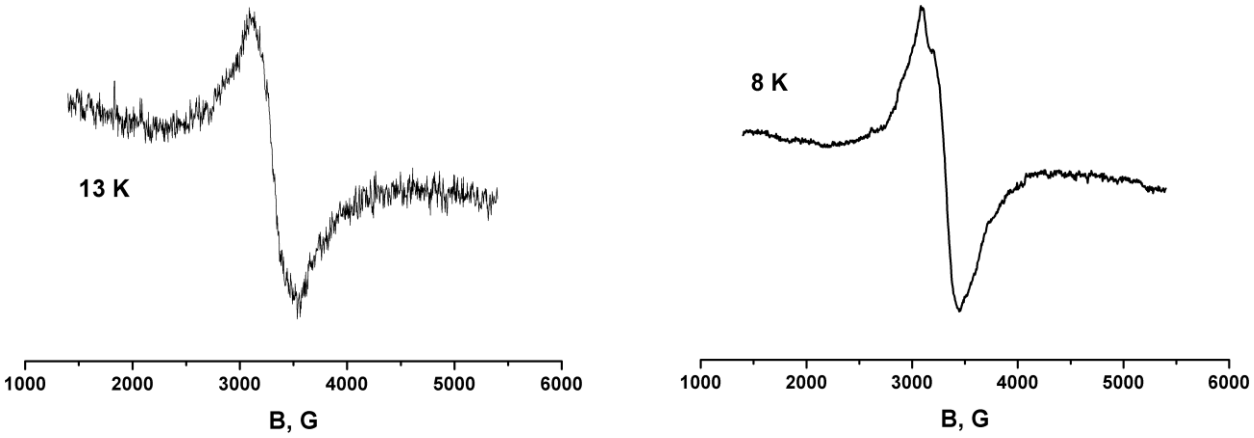

(a) (b)

Fig 3-5. EPR spectra of (a) **11[PF$_6$]** at 13 K in CH_3CN glass; (b) **12[PF$_6$]** at 8 K in CH_3CN glass

Electron paramagnetic resonance (EPR) is a major technique allowing distinguishing between ligand centered radicals, metal centered radicals and radicals with a mixed metal-ligand characters. It is also an attractive technique to obtain important information about the extent of electronic and nuclear interactions.[54] The ideal situation for EPR studies could be achieved when the paramagnetic species have non-degenerate ground-states and hyperfine coupling can be observed.[19] The EPR measurements were carried out on the paramagnetic MV complexes **11[PF$_6$]** and **12[PF$_6$]** (Figure 3-4 and Figure 3-5). **11[PF$_6$]** and **12[PF$_6$]** are EPR-silent at room temperature. For **11[PF$_6$]**, a broad signal of reasonable intensity with *g* factor of 1.89 is observed only below 13 K without hyperfine coupling and **12[PF$_6$]** shows similar behavior with g value of 1.89 at 8 K. The observed g values deviate from the free electron value *g* of 2.0023 confirming electron delocalization over both rhenium fragments [*trans*-ReX(PMe_3)$_4$] or a rapid electron transfer (time scale of the EPR method: 10^{-8} s^{-1}). The broad signals without hyperfine coupling can be interpreted in terms of electronic dynamics with intramolecular transfer between the remote metal ends or with a strong spin-orbital coupling.[32,54] The variable-temperature magnetic susceptibility measurements for **11[PF$_6$]** and **12[PF$_6$]** were carried out in the temperature range from 5 K to 300 K. The magnetic properties in the form of χ_m and $\chi_m T$ vs T plots are presented in Figure 3-6. The MV complexes **11[PF$_6$]** and **12[PF$_6$]** showed typical paramagnetic behavior with the magnetic susceptibility χ_m dropping abruptly from the temperature 5 K to 50 K then gradually

to be constant and the $\chi_m T$ value decreasing from 5 K to 300 K. This is a manifestation of paramagnetism expected from the odd electron in these molecules.[55]

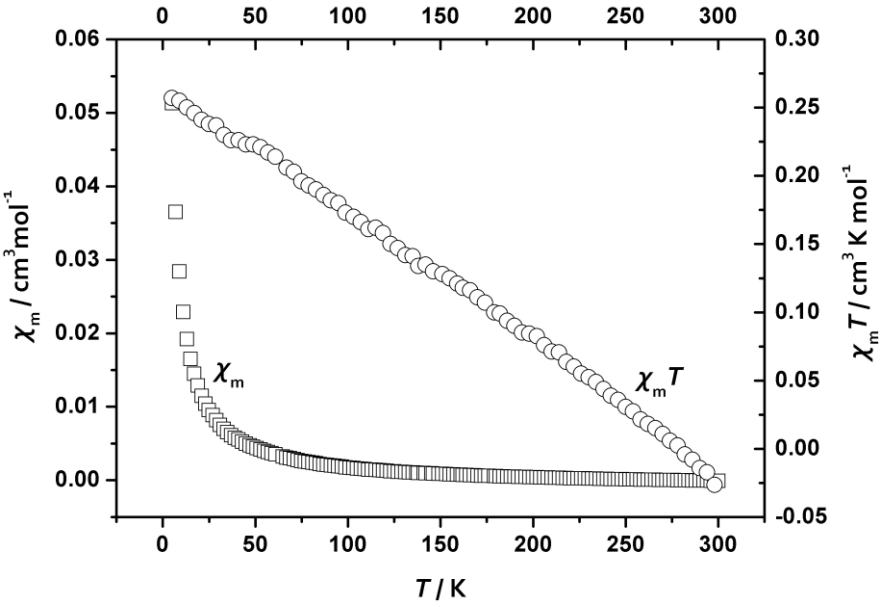

(a)

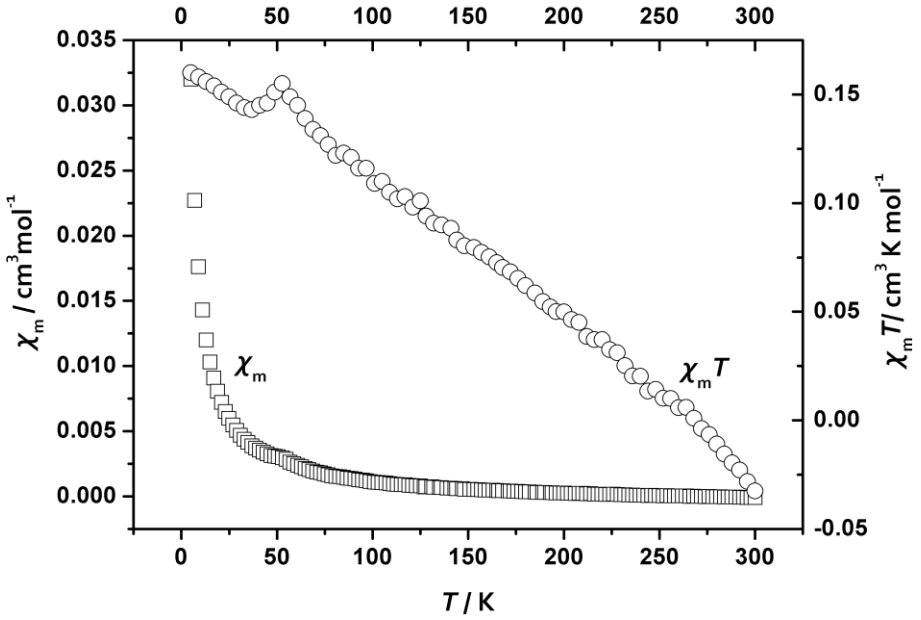

(b)

Fig 3-6. Plots of χ_m and $\chi_m T$ vs T for (a) **11[PF$_6$]** (b) **12[PF$_6$]**

3.4 Conclusion

A family of sp^2 C_4H_2-bridged dinuclear rhenium complexes was synthesized. The neutral complexes *trans*-[X(PMe$_3$)$_4$Re=C=CH-CH=C=Re(PMe$_3$)$_4$X] (X = Cl, **11**; C≡CSiMe$_3$, **12**) were obtained by the deprotonation of the biscarbyne complexes *trans*-[X(PMe$_3$)$_4$Re≡C-CH$_2$-CH$_2$-C≡Re(PMe$_3$)$_4$X][PF$_6$] (X = Cl, **9**; C≡CSiMe$_3$, **10**). The stepwise oxidation of the neutral complexes with [Cp$_2$Fe][PF$_6$] gave the MV complexes **11[PF$_6$]** and **12[PF$_6$]** and the dicationic complexes **11[PF$_6$]$_2$** and **12[PF$_6$]$_2$**. The oxidations of **11** and **12** to **11[PF$_6$]$_2$** and **12[PF$_6$]$_2$** resulted in the transformation of the valence structure of the sp^2 C_4H_2 bridge from a bisvinylidene (=C=CH-CH=C=) form to an ethylenylidene biscarbyne (≡C-CH=CH-C≡) form. These transformations were verified by NMR, IR and Raman, and X-ray diffraction analyses. The CV spectra of the dicationic species **11[PF$_6$]$_2$** and **12[PF$_6$]$_2$** indicate that the neutral complexes **11** and **12** are good reducing agents and give large K_c of 1.8×10^{10} and 7.1×10^7, respectively. The large K_c values reveal the high thermodynamic stabilities of the MV compounds. The electronic coupling energy H_{ab} and the delocalization parameters Γ for the MV complexes **11[PF$_6$]** and **12[PF$_6$]** are 7068 cm^{-1} and 6100 cm^{-1}, and 0.63 and 0.59, respectively. Base on the CV and NIR spectroscopic data, **11[PF$_6$]$_2$** and **12[PF$_6$]$_2$** can be safely described as a class III MV compound.

3.5 Experimental section

General procedures: All the manipulations were carried out under a nitrogen atmosphere using Schlenk techniques or a glove box (M. Braun150B-G-II). Reagent grade benzene, toluene, hexane, pentane, diethyl ether and tetrahydrofuran were dried and distilled from sodium benzophenone ketyl prior to use. Dichloromethane and acetonitrile were distilled from CaH_2. All other chemicals were directly used as obtained from commercial suppliers. CHN elemental analyses were performed with a LECO CHN-932 microanalyzer. IR spectra were obtained on a Bio-Rad FTS-45 instrument. Raman spectra were recorded on a Renishaw Ramanscope spectrometer (633 nm). NMR spectra were measured on a Varian Mercury spectrometer at 200 MHz for ^{1}H NMR, 81 MHz for ^{31}P NMR, 188 MHz for ^{19}F NMR, Varian Gemini-2000 spectrometer at 300 MHz for ^{1}H and 75 MHz for ^{13}C NMR, and on a Bruker-DRX-500 spectrometer at 500 MHz for ^{1}H NMR, 125.8 MHz for ^{13}C NMR, 202.5 MHz for ^{31}P NMR, and 99.4 MHz for ^{29}Si NMR. Chemical shift for ^{1}H NMR, ^{31}P NMR, ^{13}C NMR, and ^{29}Si NMR is given in ppm relative to TMS and that for ^{31}P relative to phosphoric acid. Cyclic voltammograms

were obtained with BAS 100W voltammetric analyzer equipped with an Au working and a Pt counter electrode, and a non-aqueous reference electrode. All sample solutions were approximately 5×10^{-3} M in substrate and in 0.1 M THF or CH_3CN solution of $[nBu_4N][PF_6]$ and prepared under nitrogen. Ferrocene was subsequently added and the calibration of voltammograms recorded. BAS 100W program was employed for data analysis. X-band EPR spectra were obtained using Bruker EMX Electron Spin Resonance system. Magnetization measurements were carried out on a Quantum Design SQUID magnetometer, molar magnetic susceptibility was calculated according to the equation $\chi = (M \cdot M_w)/(m \cdot H)$, where M – experimental magnetization, M_w – molecular weight, m – sample weight, H – magnetic field.

X-ray diffraction studies on 11, 11[PF$_6$], 11[PF$_6$]$_2$, 12, 12[PF$_6$] and 12[PF$_6$]$_2$: Data collection for all crystals were carried out on Stoe IPDS diffractometer (Imaging Plate Detector System with graphite-monochromated MoK radiation, $\lambda = 0.71073$ Å)[56] and for others on Oxford Diffraction Xcalibur R diffractometer (4-circle kappa platform, Ruby CCD detector and a single wavelength Enhance X-ray source with MoK radiation, $\lambda = 0.71073$ Å) at 183(2) K using a cold N_2-gas stream from an Oxford Cryogenic System. Pre-experiment, data collection and data reduction (unit cell determination, intensity data integration and empirical absorption correction) were carried out with the Oxford *CrysAlisPro* software.[57] The structures were solved with the unique data sets using the Patterson method of the program SHELXS-97. The structure refinement was performed with the program SHELXL-97.[58] Non-hydrogen atoms were refined anisotropically by full-matrix least-squares techniques based on F^2. The hydrogen atoms of the organic groups were placed in calculated positions and refined with a riding model with a fixed temperature factor. The program PLATON[59] was used to check the result of the X-ray analysis.

***trans*-[Cl(PMe$_3$)$_4$Re=C=CH-CH=C=Re(PMe$_3$)$_4$Cl] (11).** *Trans*-[ReCl(≡C-CH_2)(PMe$_3$)$_4$]$_2$[PF$_6$]$_2$ (**9**) (28.0 mg, 0.020 mmol) and KO*t*Bu (12.0 mg, 0.106 mmol) were mixed with THF (2 mL) in a Young-schlenk flask. The yellowish green suspension was heated at 65 °C for 1 h resulting in a brown solution. After filtration, the solution was dried *in vacuo*. The residue was extracted with benzene followed by filtration. Evaporation of the solution to dryness gave the crude neutral complex *trans*-[Cl(PMe$_3$)$_4$Re=C=CH-CH=C=Re(PMe$_3$)$_4$Cl] (**11**), which was washed with -30 °C pentane (3 × 1 mL), and dried *in vacuo*. Yield: 18.5 mg (0.017 mmol, 85% based on *trans*-[ReCl(≡C-CH_2)(PMe$_3$)$_4$]$_2$[PF$_6$] (**9**)). Single crystals suitable for X-ray diffraction

were grown by layering pentane over a THF solution of the title compound. Anal. Calcd For $C_{28}H_{74}Cl_2P_8Re_2$ (1102.00 g/mol): C 30.52; H 6.77. Found: C 30.43; H 6.70. IR (ATR, cm^{-1}): ν = 1552 (C=C), 926 (C-P). ^{1}H NMR (THF-d_8, 200 MHz, 22 °C): δ = 1.54 (s, $P(CH_3)_3$), 2.00 (d, CH); ^{13}C NMR (THF-d_8, 125.8 MHz, 10 °C): δ = 298.5 (quint, $^2J_{PC}$ = 11.3 Hz, Re-C_α), 90.5 (s, C_β), 25.7 (s, $P(CH_3)_3$); ^{31}P NMR (THF-d_8, 81 MHz, 22 °C:) δ = -34.0 (s, $P(CH_3)_3$).

***trans*-[Cl(PMe$_3$)$_4$Re≡C-CH=CH-C≡Re(PMe$_3$)$_4$Cl][PF$_6$] (11[PF$_6$]).** Method a: To a mixture of the neutral complex *trans*-[Cl(PMe$_3$)$_4$Re=C=CH-CH=C=Re(PMe$_3$)$_4$Cl] (**11**) (6.6 mg, 0.006 mmol) and the dicationic complex *trans*-[Cl(PMe$_3$)$_4$Re≡C-CH=CH-C≡Re(PMe$_3$)$_4$Cl][PF$_6$]$_2$ (**11[PF$_6$]$_2$**) (8.3 mg, 0.006 mmol), CH_3CN was added. The resulting dark bluish green suspension was stirred at room temperature for 30 min. After removal of the solvent, the solid was washed with THF, and dried *in vacuo*. Yield: 14 mg (0.011 mmol, 94%, based on *trans*-[Cl(PMe$_3$)$_4$Re=C=CH-CH=C=Re(PMe$_3$)$_4$Cl] (**11**)).

Method b: To a mixture of the neutral complex *trans*-[Cl(PMe$_3$)$_4$Re=C=CH-CH=C=Re(PMe$_3$)$_4$Cl] (**11**) (11.6 mg, 0.010 mmol) and [Cp_2Fe][PF_6] (3.3 mg, 0.010 mmol), CH_3CN was added. The resulting dark bluish green suspension was stirred at room temperature for 30 min. After filtration through celite, the solvent was removed *in vacuo*. The pure product was obtained after washing with THF and drying *in vacuo*. Yield: 12.0 mg (0.011 mmol, 96% based on *trans*-[Cl(PMe$_3$)$_4$Re=C=CH-CH=C=Re(PMe$_3$)$_4$Cl] (**11**)).

Single crystals suitable for X-ray diffraction were grown by layering ether over an acetonitrile solution of the title compound. Anal. Calcd For $C_{28}H_{74}Cl_2F_6P_9Re_2$ (1246.96 g /mol): C 26.97; H 5.98. Found: C 27.12; H 5.86. IR (ATR, cm^{-1}): ν = 931 (C-P). ^{1}H NMR (CD_3CN, 200 MHz, 22 °C): δ = -0.88 (s, C_βH), 0.29 (br, $P(CH_3)_3$).

***trans*-[Cl(PMe$_3$)$_4$Re≡C-CH=CH-C≡Re(PMe$_3$)$_4$Cl][PF$_6$]$_2$ (11[PF$_6$]$_2$).** To a mixture of the neutral complex *trans*-[Cl(PMe$_3$)$_4$Re=C=CH-CH=C=Re(PMe$_3$)$_4$Cl] (**11**) (45.6 mg, 0.041 mmol) and [Cp_2Fe][PF_6] (27.4 mg, 0.083 mmol), CH_3CN was added. The reaction mixture was stirred at room temperature for 30 min resulting in a dark yellowish green solution. After filtration through celite, the solution was concentrated and precipitation was effected by the addition of diethyl ether. The yellowish green solid was collected, washed with ether (3 × 2 mL), and dried *in vacuo*. Yield: 55.8 mg (0.040 mmol, 97% based on *trans*-[Cl(PMe$_3$)$_4$Re=C=CH-CH=C=Re(PMe$_3$)$_4$Cl] (**11**)). Single crystals suitable for X-ray diffraction were grown by layering

diethyl ether over an acetonitrile solution of the title compound. Anal. Calcd For $C_{28}H_{74}Cl_2F_{12}P_{10}Re_2$ (1391.93 g/mol): C 24.16; H 5.35. Found: C 24.31; H 5.44. IR (ATR, cm^{-1}): ν = 938 (C-P). MS(ESI): *m/z* (100%):1245 [M^+-2H]. ^{1}H NMR (CD_2Cl_2, 200 MHz, 22 °C): δ = 5.76 (s, $C_\beta H$), 1.76 (s, $P(CH_3)_3$); ^{13}C NMR (CD_2Cl_2, 125.8 MHz, 10 °C): δ = 255.5 (quint, $Re{\equiv}C_\alpha$), 144.0 (s, $C_\beta H$), 20.6 (s, $P(CH_3)_3$); ^{31}P NMR (CD_2Cl_2, 81 MHz, 22 °C): δ = -37.3 (s, $P(CH_3)_3$), -143.9 (sept, *J* = 710 Hz, 1P, PF_6); ^{19}F NMR (CD_2Cl_2, 188 MHz, 22 °C): δ = -73.5 (d, *J* = 713 Hz, PF_6).

***trans*-[(Me$_3$SiC≡C)(PMe$_3$)$_4$Re=C=CH-CH=C=Re(PMe$_3$)$_4$(C≡CSiMe$_3$)] (12).** Method a: Deprotonation of the dinuclear rhenium biscarbyne complex *trans*-[($Me_3SiC{\equiv}C$)(PMe_3)$_4$Re≡C-CH_2-CH_2-C≡Re(PMe_3)$_4$(C≡CSiMe$_3$)][PF_6]$_2$ (**10**) with KO*t*Bu. To a THF (1 mL) solution of tr*ans*-[Re(C≡CSiMe$_3$)(≡C-CH_2)(PMe_3)$_4$]$_2$[PF_6]$_2$ (**10**) (22.8 mg, 0.015 mmol), KO*t*Bu (6.2 mg, 0.055 mmol) was added in two equal portions. The interval of the addition of KO*t*Bu was 30 min. The resulting brownish green solution was dried *in vacuo*. The residue was extracted with pentane followed by filtration. Evaporation of the solution to dryness gave the crude neutral complex *trans*-[(C≡CSiMe$_3$)(PMe_3)$_4$Re=C=CH-CH=C=Re(PMe_3)$_4$(C≡CSiMe$_3$)] (**12**), which was washed with pentane (3 × 1 mL, -30 °C), and dried *in vacuo*. Yield: 16.0 mg (0.013 mmol, 87% based on *trans*-[Re(C≡CSiMe$_3$)(≡C-CH_2)(PMe_3)$_4$]$_2$[PF_6]$_2$ (**10**)).

Method b: Deprotonation of the dinuclear rhenium biscarbyne complex *trans*-[($Me_3SiC{\equiv}C$)(PMe_3)$_4$Re≡C-CH_2-CH_2-C≡Re(PMe_3)$_4$(C≡CSiMe$_3$)][PF_6]$_2$ (**10**) with LDA. To a THF (1 mL) solution of tr*ans*-[Re(C≡CSiMe$_3$)(≡C-CH_2)(PMe_3)$_4$]$_2$[PF_6]$_2$ (**10**) (15.0 mg, 0.010 mmol), LDA (3.8 mg, 0.035 mmol) was added in two equal portions. The addition of LDA was done during 30 min. The resulting brownish green solution was dried *in vacuo*. The residue was extracted with pentane followed by filtration. Evaporation of the solution to dryness gave the crude neutral complex **12**, which was washed with -30 °C pentane (3 × 1 mL), and dried *in vacuo*. Yield: 10.5 mg (0.008 mmol, 83% based on *trans*-[Re(C≡CSiMe$_3$)(≡C-CH_2)(PMe_3)$_4$]$_2$[PF_6]$_2$ (**10**)).

Method c: Reduction of the dinuclear rhenium biscarbyne vinylidene-bridged complex *trans*-[($Me_3SiC{\equiv}C$)(PMe_3)$_4$Re≡C-CH=CH-C≡Re(PMe_3)$_4$(C≡CSiMe$_3$)][PF_6]$_2$ (**12[PF$_6$]$_2$**) with LDA. To a THF solution of tr*ans*-[Re(C≡CSiMe$_3$)(≡C-CH)(PMe_3)$_4$]$_2$[PF_6]$_2$ (**12[PF$_6$]$_2$**) (13.6 mg, 0.009 mmol), LDA (2.0 mg, 0.019 mmol) was added. The resulting yellowish green solution was

stirred at room temperature for 30 min and further the same amount of LDA was added. The color of the solution changed to dark blue, finally resulting in a brownish green solution. After removal of the solvent *in vacuo*, the residue was extracted with pentane followed by filtration. Evaporation of the pentane solution to dryness gave the crude neutral complex, which was washed with pentane (3 × 1 mL, -30 °C), and dried *in vacuo*. Yield: 10.5 mg (0.008 mmol, 83% based on *trans*-[Re(C≡CSiMe$_3$)(≡C-CH)(PMe$_3$)$_4$]$_2$[PF$_6$]$_2$ (**12[PF$_6$]$_2$**)).

Single crystals suitable for X-ray diffraction were grown by evaporation of a pentane solution of the title compound in glove box. Anal. Calcd For $C_{38}H_{92}P_8Re_2Si_2$ (1225.51 g/mol): C 37.24; H 7.57. Found: C 37.11; H 7.46. IR (ATR, cm^{-1}): ν = 1975 (C≡C), 1543 (C=C), 933 (C-P). ^{1}H NMR (THF-d$_8$, 200 MHz, 22 °C): δ = 1.59 (s, P(CH$_3$)$_3$), 2.51(d, CH), -0.03 (s, Si(CH$_3$)$_3$); ^{13}C NMR (THF-d$_8$, 125.8 MHz, 10°C): δ = 309.4 (quint, $^2J_{PC}$ = 12.8 Hz, Re≡C$_\alpha$), 152.8 (quint, $^2J_{PC}$ = 16.0 Hz, Re-C$_\alpha$,≡), 127.8 (s, ≡C$_\beta$,-Si), 96.7 (s, C$_\beta$), 24.0 (s, P(CH$_3$)$_3$); 2.2 (s, Si(CH$_3$)$_3$). ^{31}P NMR (THF-d$_8$, 81MHz, 22 °C): δ = -40.5 (s, P(CH$_3$)$_3$). ^{29}Si NMR (THF-d$_8$, 99.4 MHz, 10 °C): δ = -31.8 (s, SiMe$_3$).

***trans*-[(Me$_3$SiC≡C)(PMe$_3$)$_4$Re≡C-CH=CH-C≡Re(PMe$_3$)$_4$(C≡CSiMe$_3$)][PF$_6$] (12[PF$_6$]).** Method a: To the THF solution of the dicationic complex *trans*-[(Me$_3$SiC≡C)(PMe$_3$)$_4$Re≡C-CH=CH-C≡Re(PMe$_3$)$_4$(C≡CSiMe$_3$)][PF$_6$]$_2$ (**12[PF$_6$]$_2$**) (12.5 mg, 0.008 mmol) was added a THF solution of neutral complex *trans*-[(Me$_3$SiC≡C)(PMe$_3$)$_4$Re≡C-CH=CH-C≡Re(PMe$_3$)$_4$(C≡CSiMe$_3$)] (**12**) (11.0 mg, 0.008 mmol). The resulting yellowish green solution was stirred at room temperature for 30 min. After removal of solvent, the solid was washed with ether (3 × 1 mL) and dried *in vacuo*. Yield: 19.6 mg (0.014 mmol, 87%, based on *trans*-[Cl(PMe$_3$)$_4$Re=C=CH-CH=C=Re(PMe$_3$)$_4$Cl] (**12**)).

Method b: To the mixture of neutral complex *trans*-[Cl(PMe$_3$)$_4$Re=C=CH-CH=C=Re(PMe$_3$)$_4$Cl] (**12**) (21.0 mg, 0.017 mmol) and [Cp$_2$Fe][PF$_6$] (5.7 mg, 0.017 mmol) was added CH$_3$CN. The resulting yellowish green suspension was stirred at room temperature for 30 min. After filtration through celite, the solvent was removed *in vacuo*. The pure product was obtained by washing with THF, recrystallized from CH$_3$CN/ether. Yield: 19.0 mg (0.014 mmol, 82%, based on *trans*-[Cl(PMe$_3$)$_4$Re=C=CH-CH=C=Re(PMe$_3$)$_4$Cl] (**12**)).

Single crystals suitable for X-ray diffraction were grown by layering ether on the top of a THF solution of the title compound. Anal. Calcd For $C_{38}H_{92}F_6P_9Re_2Si_2$ (1370.48 g/mol): C 33.30; H

6.77. Found: C 33.08; H 6.69. IR (ATR, cm^{-1}): ν = 1987 (C≡C), 937 (C-P). ^1H NMR (THF-d_8, 200 MHz, 22 °C): δ = 0.89 (s, $C_\beta H$), 0.10 (s, $Si(CH_3)_3$).-0.05 (br, $P(CH_3)_3$).

***trans*-[(Me$_3$SiC≡C)(PMe$_3$)$_4$Re≡C-CH=CH-C≡Re(PMe$_3$)$_4$(C≡CSiMe$_3$)][PF$_6$]$_2$ (12[PF$_6$]$_2$).** To a THF solution of *trans*-[Re(C≡CSiMe$_3$)(≡C-CH$_2$)(PMe$_3$)$_4$]$_2$[PF$_6$] (**10**) (32.8 mg, 0.022 mmol), LDA (6.7 mg, 0.062 mmol) was added. The resulting dark brownish green solution was kept stirring at room temperature for 30 min. Then [Cp$_2$Fe][PF$_6$] (14.3 mg, 0.043 mmol) was added in one portion. The reaction mixture was stirred at room temperature for 1.5 h. After removal of solvent *in vacuo*, the residue was extracted with CH_3CN followed by filtration through celite. After concentration diethyl ether was added to precipitate. The brown red solid was collected, washed with ether (3 × 2 mL), and dried *in vacuo*. Yield: 28 mg (0.018 mmol, 86% based on [Re(C≡CSiMe$_3$)(≡C-CH$_2$)(PMe$_3$)$_4$]$_2$[PF$_6$] (**10**)). Single crystals suitable for X-ray diffraction were grown by layering pentane over a dichloromethane solution of the title compound. Anal. Calcd For $C_{38}H_{92}F_{12}P_{10}Re_2Si_2$ (1515.45 g/mol): C 30.12; H 6.12. Found: C, 29.91; H, 6.04. IR (ATR, cm^{-1}): ν = 2022 (C≡C), 942 (C-P). MS(ESI): *m/z* (100%):1368 [M^+-2H]. ^1H NMR (CD_2Cl_2, 200 MHz, 22 °C): δ = 5.82 (s, $C_\beta H$), 1.78 (s, $P(CH_3)_3$), 0.03 (s, $Si(CH_3)_3$); ^{13}C NMR (CD_2Cl_2, 125.8 MHz, 10 °C): δ = 265.3 (t, Re≡C_α), 145.8 (s, $C_\beta H$), 135.5 (s, Re-C_α≡), 130.9 (s, ≡$C_{\beta'}$-Si), 22.3 (s, $P(CH_3)_3$), 0.2 (s, $Si(CH_3)_3$); ^{31}P NMR (CD_2Cl_2, 81 MHz, 22 °C): δ = -43.8 (s, $P(CH_3)_3$), -143.9 (sept, *J* = 710 Hz, 1P, PF_6); ^{19}F NMR (CD_2Cl_2, 188 MHz, 22 °C): δ = -73.9 (d, *J* = 711 Hz, PF_6). ^{29}Si NMR (CD_2Cl_2, 99.4 MHz, 10 °C): δ = -23.9 (s, $SiMe_3$).

***trans*-[Cl(PMe$_3$)$_4$Re≡C-CH=CH-C≡Re(PMe$_3$)$_4$Cl][OTf]$_2$ (13).** To a THF solution of neutral complex *trans*-[Cl(PMe$_3$)$_4$Re=C=CH-CH=C=Re(PMe$_3$)$_4$Cl] (**11**) (11.3 mg, 0.01 mmol), Tl(OTf) (35.3 mg, 0.1 mmol) was added. The brownish green solution turned into dark yellowish green immediately, which was stirred at room temperature for 1 h. After removal of the solvent *in vacuo*, the residue was extracted with CH_2Cl_2 followed by filtration through celite. After concentration diethyl ether was added to effect precipitation. The grey green solid was collected, washed with ether (3 × 2 mL), and dried *in vacuo*. Yield: 12.0 mg (0.086 mmol, 86% based on *trans*-[ReCl(=C=CH)(PMe$_3$)$_4$]$_2$ (**11**)). Anal. Calcd For $C_{30}H_{74}Cl_2F_6O_6P_8Re_2S_2$ (1400.14 g/mol): C 25.73; H 5.33. Found: C 25.99; H 5.25. MS(ESI): *m/z* (100%):1249 [M^+]. ^1H NMR (CD_3CN, 200 MHz, 22 °C): δ = 5.71 (s, $C_\beta H$), 1.71 (s, $P(CH_3)_3$); ^{31}P NMR (CD_2Cl_2, 81 MHz, 22 °C): δ = -36.2 (s, $P(CH_3)_3$; ^{19}F NMR (CD_2Cl_2, 188 MHz, 22 °C): δ = -79.9 (s, CF_3).

3.6 References

(1) Heath, J. R. *Annu. Rev. Mater. Res.* **2009**, *39*, 1-23.

(2) Carroll, R. L.; Gorman, C. B. *Angew. Chem. Int. Ed.* **2002**, *41*, 4379-4400.

(3) Chen, F.; Hihath, J.; Huang, Z. F.; Li, X. L.; Tao, N. J. *Annu. Rev. Phys. Chem.* **2007**, *58*, 535-564.

(4) Tao, N. J. *Nat. Nanotechnol.* **2006**, *1*, 173-181.

(5) Zhirnov, V. V.; Cavin, R. K. *Nat. Mater.* **2006**, *5*, 11-12.

(6) Tuccitto, N.; Ferri, V.; Cavazzini, M.; Quici, S.; Zhavnerko, G.; Licciardello, A.; Rampi, M. A. *Nat. Mater.* **2009**, *8*, 41-46.

(7) Kurita, T.; Nishimori, Y.; Toshimitsu, F.; Muratsugu, S.; Kume, S.; Nishihara, H. *J. Am. Chem. Soc.* **2010**, *132*, 4524-4525.

(8) Szesni, N.; Drexler, M.; Maurer, J.; Winter, R. F.; de Montigny, F.; Lapinte, C.; Steffens, S.; Heck, J.; Weibert, B.; Fischer, H. *Organometallics.* **2006**, *25*, 5774-5787.

(9) Kaim, W.; Lahiri, G. K. *Angew. Chem. Int. Ed.* **2007**, *46*, 1778-1796.

(10) Kowalski, K.; Linseis, M.; Winter, R. F.; Zabel, M.; Zalis, S.; Kelm, H.; Kruger, H. J.; Sarkar, B.; Kaim, W. *Organometallics.* **2009**, *28*, 4196-4209.

(11) Paul, F.; Lapinte, C. *Coord. Chem. Rev.* **1998**, *180*, 431-509.

(12) Balzani, V.; Juris, A.; Venturi, M.; Campagna, S.; Serroni, S. *Chem. Rev.* **1996**, *96*, 759-833.

(13) Schwab, P. F. H.; Levin, M. D.; Michl, J. *Chem. Rev.* **1999**, *99*, 1863-1933.

(14) Belser, P.; Bernhard, S.; Blum, C.; Beyeler, A.; De Cola, L.; Balzani, V. *Coord. Chem. Rev.* **1999**, *192*, 155-169.

(15) Adams, H.; Costa, P. J.; Newell, M.; Vickers, S. J.; Ward, M. D.; Felix, V.; Thomas, J. A. *Inorg. Chem.* **2008**, *47*, 11633-11643.

(16) Ceccon, A.; Santi, S.; Orian, L.; Bisello, A. *Coord. Chem. Rev.* **2004**, *248*, 683-724.

(17) Dembinski, R.; Bartik, T.; Bartik, B.; Jaeger, M.; Gladysz, J. A. *J. Am. Chem. Soc.* **2000**, *122*, 810-822.

(18) Jiao, H. J.; Costuas, K.; Gladysz, J. A.; Halet, J. F.; Guillemot, M.; Toupet, L.; Paul, F.; Lapinte, C. *J. Am. Chem. Soc.* **2003**, *125*, 9511-9522.

(19) Aguirre-Etcheverry, P.; O'Hare, D. *Chem. Rev.* **2010**, *110*, 4839-4864.

(20) Kheradmandan, S.; Heinze, K.; Schmalle, H. W.; Berke, H. *Angew. Chem. Int. Ed.* **1999**, *38*, 2270-2273.

(21) Venkatesan, K.; Fox, T.; Schmalle, H. W.; Berke, H. *Organometallics.* **2005**, *24*, 2834-2847.

(22) Venkatesan, K.; Fernandez, F. J.; Blacque, O.; Fox, T.; Alfonso, M.; Schmalle, H. W.; Berke, H. *Chem. Commun.* **2003**, 2006-2008.

(23) Lenarvor, N.; Toupet, L.; Lapinte, C. *J. Am. Chem. Soc.* **1995**, *117*, 7129-7138.

(24) Brady, M.; Weng, W. Q.; Zhou, Y. L.; Seyler, J. W.; Amoroso, A. J.; Arif, A. M.; Bohme, M.; Frenking, G.; Gladysz, J. A. *J. Am. Chem. Soc.* **1997**, *119*, 775-788.

(25) Zhou, Y. L.; Seyler, J. W.; Weng, W. Q.; Arif, A. M.; Gladysz, J. A. *J. Am. Chem. Soc.* **1993**, *115*, 8509-8510.

(26) Yam, V. W. W.; Lau, V. C. Y.; Cheung, K. K. *Organometallics.* **1996**, *15*, 1740-1744.

(27) Paul, F.; Meyer, W. E.; Toupet, L.; Jiao, H. J.; Gladysz, J. A.; Lapinte, C. *J. Am. Chem. Soc.* **2000**, *122*, 9405-9414.

(28) Bruce, M. I.; Low, P. J.; Costuas, K.; Halet, J. F.; Best, S. P.; Heath, G. A. *J. Am. Chem. Soc.* **2000**, *122*, 1949-1962.

(29) Onitsuka, K.; Ose, N.; Ozawa, F.; Takahashi, S. *J. Organomet. Chem.* **1999**, *578*, 169-177.

(30) Woodworth, B. E.; White, P. S.; Templeton, J. L. *J. Am. Chem. Soc.* **1997**, *119*, 828-829.

(31) Roberts, R. L.; Puschmann, H.; Howard, J. A. K.; Yamamoto, J. H.; Carty, A. J.; Low, P. J. *Dalton. Trans.* **2003**, 1099-1105.

(32) Semenov, S. N.; Blacque, O.; Fox, T.; Venkatesan, K.; Berke, H. *J. Am. Chem. Soc.* **2010**, *132*, 3115-3127.

(33) Antinolo, A.; Otero, A.; Fajardo, M.; GarciaYebra, C.; LopezMardomingo, C.; Martin, A.; GomezSal, P. *Organometallics.* **1997**, *16*, 2601-2611.

(34) Beddoes, R. L.; Bitcon, C.; Grime, R. W.; Ricalton, A.; Whiteley, M. W. *J. Chem. Soc., Dalton. Trans.* **1995**, 2873-2883.

(35) Iyer, R. S.; Selegue, J. P. *J. Am. Chem. Soc.* **1987**, *109*, 910-911.

(36) Bruce, M. I.; Ellis, B. G.; Low, P. J.; Skelton, B. W.; White, A. H. *Organometallics.* **2003**, *22*, 3184-3198.

(37) Novikova, L. N.; Peterleitner, M. G.; Sevumyan, K. A.; Semeikin, O. V.; Valyaev, D. A.; Ustynyuk, N. A.; Khrustalev, V. N.; Kuleshova, L. N.; Antipin, M. Y. *J. Organomet. Chem.* **2001**, *631*, 47-53.

(38) Novikova, L. N.; Peterleitner, M. G.; Sevumyan, K. A.; Semeikin, O. V.; Valyaev, D. A.; Ustynyuk, N. A. *Appl. Organomet. Chem.* **2002**, *16*, 530-536.

(39) Unseld, D.; Krivykh, V. V.; Heinze, K.; Wild, F.; Artus, G.; Schmalle, H.; Berke, H. *Organometallics.* **1999**, *18*, 1525-1541.

(40) Venkatesan, K.; Blacque, O.; Fox, T.; Alfonso, M.; Schmalle, H. W.; Berke, H. *Organometallics.* **2004**, *23*, 1183-1186.

(41) Venkatesan, K.; Blacque, O.; Fox, T.; Alfonso, M.; Schmalle, H. W.; Kheradmandan, S.; Berke, H. *Organometallics.* **2005**, *24*, 920-932.

(42) Venkatesan, K.; Blacque, O.; Berke, H. *Organometallics.* **2006**, *25*, 5190-5200.

(43) Valyaev, D. A.; Semelkin, O. V.; Peterleitner, M. G.; Borisov, Y. A.; Khrustalev, V. N.; Mazhuga, A. M.; Kremer, E. V.; Ustynyuk, N. A. *J. Organomet. Chem.* **2004**, *689*, 3837-3846.

(44) Venkatesan, K.; Blacque, O.; Berke, H. *Dalton. Trans.* **2007**, 1091-1100.

(45) Meyer, W. E.; Amoroso, A. J.; Horn, C. R.; Jaeger, M.; Gladysz, J. A. *Organometallics.* **2001**, *20*, 1115-1127.

(46) Pombeiro, A. J. L.; Hills, A.; Hughes, D. L.; Richards, R. L. *J. Organomet. Chem.* **1988**, *352*, C5-C7 and references therein.

(47) Hush, N. S. *Prog. Inorg. Chem.* **1967**, *8*, 391-444.

(48) Hush, N. S. *Coord. Chem. Rev.* **1985**, *64*, 135-157.

(49) Brunschwig, B. S.; Creutz, C.; Sutin, N. *Chem. Soc. Rev.* **2002**, *31*, 168-184.

(50) D'Alessandro, D. M.; Keene, F. R. *Chem. Soc. Rev.* **2006**, *35*, 424-440.

(51) Le Stang, S.; Paul, F.; Lapinte, C. *Organometallics.* **2000**, *19*, 1035-1043.

(52) Demadis, K. D.; Hartshorn, C. M.; Meyer, T. J. *Chem. Rev.* **2001**, *101*, 2655-2685.

(53) Reimers, J. R.; Hush, N. S. *Inorg. Chem.* **1990**, *29*, 4510-4513.

(54) Astruc, D. *Electron Transfer and Radical Processes in Transition-Metal Chemstry*; VCH Publishers, Inc.: New York, **1995**.

(55) Kheradmandan, S.; Venkatesan, K.; Blacque, O.; Schmalle, H. W.; Berke, H. *Chem. Eur. J.* **2004**, *10*, 4872-4885.

(56) Version 2.87 5/1998 ed.; STOE & Cie: Darmstadt, Germany, **1998**.

(57) Version 1.171.32.5 ed.; Oxford Diffraction Ltd: Abingdon, Oxfordshire, England.

(58) Sheldrick, G. M. *Acta Cryst.* **2008**, *A64*, 112-122.

(59) Spek, A. L. *J. Appl. Cryst.* **2003**, *36*, 7-13.

4. Studies on C_4-bridged Dinuclear Rhenium Complexes

ABSTRACT. The deprotonation of the dicationic dinuclear rhenium ethylenylidene biscarbyne complexes *trans*-$[X(PMe_3)_4Re{\equiv}C\text{-}CH{=}CH\text{-}C{\equiv}Re(PMe_3)_4X][PF_6]_2$ (X = Cl, **11[PF$_6$]$_2$**; C≡CSiMe$_3$, **12[PF$_6$]$_2$**) with an excess of KO*t*Bu resulted in a mixture of the corresponding neutral bisvinylidene complexes *trans*-$[X(PMe_3)_4Re{=}C{=}CH\text{-}CH{=}C{=}Re(PMe_3)_4X]$ (X = Cl, **11**; C≡CSiMe$_3$, **12**) and the neutral cumulenic complexes *trans*-$[X(PMe_3)_4Re{=}C{=}C{=}C{=}C{=}Re(PMe_3)_4X]$ (X = Cl, **14**; C≡CSiMe$_3$, **15**). The subsequent oxidation with $[Cp_2Fe][PF_6]$ in CH_3CN gave a mixture of the corresponding dicationic complexes *trans*-$[X(PMe_3)_4Re{\equiv}C\text{-}CH{=}CH\text{-}C{\equiv}Re(PMe_3)_4X][PF_6]_2$ (X = Cl, **11[PF$_6$]$_2$**; C≡CSiMe$_3$, **12[PF$_6$]$_2$**) and *trans*-$[X(PMe_3)_4Re{\equiv}C\text{-}C{\equiv}C\text{-}C{\equiv}Re(PMe_3)_4X][PF_6]_2$ (X = Cl, **14[PF$_6$]$_2$**; C≡CSiMe$_3$, **15[PF$_6$]$_2$**). The dicationic alkynediyl biscarbyne complex *trans*-$[(Me_3SiC{\equiv}C)(PMe_3)_4Re{\equiv}C\text{-}C{\equiv}C\text{-}C{\equiv}Re(PMe_3)_4(C{\equiv}CSiMe_3)][PF_6]_2$ **15[PF$_6$]$_2$** was obtained by deprotonation of **12[PF$_6$]$_2$** with KO*t*Bu followed by oxidation with $[Cp_2Fe][PF_6]$. However, a similar reaction carried out on **11[PF$_6$]$_2$** gave the dicationic akynediyl biscarbyne complex *trans*-$[Cl(PMe_3)_4Re{\equiv}C\text{-}C{\equiv}C\text{-}C{\equiv}Re(PMe_3)_4Cl][PF_6]_2$ **14[PF$_6$]$_2$** as a product along with 5~10% starting material **11[PF$_6$]$_2$**. The cyclic voltammetry (CV) studies on **14[PF$_6$]$_2$** and **15[PF$_6$]$_2$** displayed four fully reversible redox processes. The corresponding potential differences ($\Delta E_{1/2}$) between the first redox peaks are 0.570 V and 0.504 V established large comproportionation constants K_c of 6.4×10^9 and 4.7×10^8, respectively, revealing the high thermodynamic stability of the mixed-valence (MV) complexes under the CV condition.

KEYWORDS. Dinuclear rhenium complexes, Bisarbyne, Cumulenic complexes, Cyclic voltammetry

4.1 Introduction

Organometallic rigid-rod type dinuclear complexes consisting of a "conducting" π-conjugated organic bridge with redox-active metal end-groups of the type $[L_nMC_xML_n]$ (M = metal; L = ligand, C_x = carbon chain), have received considerable attention due to their potential to function as electrical devices in molecular electronics. The simplest of such devices is the molecular wire providing single-electron-conductance between the remote ends.[1-14] More sophisticated devices are based on molecular wires. According to the synthetic ease, stability and favorable electronic

properties, polyynediyl with a x = 4 carbon chain was thought to be the ideal bridge for electronic communication between the metal centers.[15-16] Therefore many studies have focused on complexes of the type $[L_nMC_4ML_n]$ with various transition metal centres, such as Mn,[17-19] Fe,[16,20] Re,[21-23] Ru,[24-25] Pt,[26] W and Mo[27-29].

Herein, we present the syntheses of the C_4-bridged dinuclear rhenium alkynediyl biscarbyne complexes *trans*-$[X(PMe_3)_4Re{\equiv}C\text{-}C{\equiv}C\text{-}C{\equiv}Re(PMe_3)_4X][PF_6]_2$ (X = Cl, **14[PF$_6$]$_2$**; C≡CSiMe$_3$, **15[PF$_6$]$_2$**) obtained by the deprotonation and subsequent oxidation of the complexes *trans*-$[X(PMe_3)_4Re{\equiv}C\text{-}CH{=}CH\text{-}C{\equiv}Re(PMe_3)_4X][PF_6]_2$ (X = Cl, **11[PF$_6$]$_2$**; C≡CSiMe$_3$, **12[PF$_6$]$_2$**). The dicationic dinuclear rhenium complexes **14[PF$_6$]$_2$** and **15[PF$_6$]$_2$** were characterized by NMR, IR, elemental analysis (only for **15[PF$_6$]$_2$**), mass spectroscopy and single crystal X-ray diffraction studies. The electrochemical properties of **14[PF$_6$]$_2$** and **15[PF$_6$]$_2$** were investigated using cyclic voltammetry (CV).

4.2 Syntheses and characterization of the C_4-bridged dinuclear rhenium complexes 14[PF$_6$]$_2$ and 15[PF$_6$]$_2$

4.2.1 Syntheses of the C_4-bridged dinuclear rhenium complexes 14[PF$_6$]$_2$ and 15[PF$_6$]$_2$

To obtain the neutral cumulenic complexes *trans*-$[X(PMe_3)_4Re{=}C{=}C{=}C{=}Re(PMe_3)_4X]$ (X = Cl, **14**; C≡CSiMe$_3$, **15**) in a straight-forward approach, deprotonation of the dicationic dinuclear rhenium ethylenylidene biscarbyne complexes *trans*-$[X(PMe_3)_4Re{\equiv}C\text{-}CH{=}CH\text{-}C{\equiv}Re(PMe_3)_4X][PF_6]_2$ (X = Cl, **11[PF$_6$]$_2$**; C≡CSiMe$_3$, **12[PF$_6$]$_2$**) with base was pursued as one of the avenues. The NMR experiments showed that the deprotonation of the dicationic complexes **11[PF$_6$]$_2$** and **12[PF$_6$]$_2$** with an excess of KO*t*Bu at room temperature resulted in a mixture containing the corresponding neutral bisvinylidene complexes *trans*-$[X(PMe_3)_4Re{=}C{=}CH\text{-}CH{=}C{=}Re(PMe_3)_4X]$ (X = Cl, **11**; C≡CSiMe$_3$, **12**) and the neutral cumulenic complexes *trans*-$[X(PMe_3)_4Re{=}C{=}C{=}C{=}C{=}Re(PMe_3)_4X]$ (X = Cl, **14**; C≡CSiMe$_3$, **15**) in a ratio of 1:3. The oxidation of this mixture with $[Cp_2Fe][PF_6]$ in CH_3CN gave a mixture of the corresponding dicationic complexes *trans*-$[X(PMe_3)_4Re{\equiv}C\text{-}CH{=}CH\text{-}C{\equiv}Re(PMe_3)_4X][PF_6]_2$ (X = Cl, **11[PF$_6$]$_2$**; C≡CSiMe$_3$, **12[PF$_6$]$_2$**) and *trans*-$[X(PMe_3)_4Re{\equiv}C\text{-}C{\equiv}C\text{-}C{\equiv}Re(PMe_3)_4X][PF_6]_2$ (X = Cl, **14[PF$_6$]$_2$**; C≡CSiMe$_3$, **15[PF$_6$]$_2$**). As depicted in Scheme 1, the formation of neutral bisvinylidene complex *trans*-$[X(PMe_3)_4Re{=}C{=}CH\text{-}CH{=}C{=}Re(PMe_3)_4X]$ (X = Cl, **11**; C≡CSiMe$_3$, **12**) could be attributed to the side reaction occurring simultaneously, where the starting material *trans*-

$[X(PMe_3)_4Re{\equiv}C\text{-}CH{=}CH\text{-}C{\equiv}Re(PMe_3)_4X][PF_6]_2$ (X = Cl, **11[PF$_6$]$_2$**; C≡CSiMe$_3$, **12[PF$_6$]$_2$**) was reduced by the deprotonated product *trans*-$[X(PMe_3)_4Re{=}C{=}C{=}C{=}Re(PMe_3)_4X]$ (X = Cl, **14**; C≡CSiMe$_3$, **15**) to give the neutral bisvinylidene complex **11** (or **12**) and the dicationic complex **14[PF$_6$]$_2$** (or **15[PF$_6$]$_2$**). Half amount of the neutral bisvinylidene complex **11** (or **12**) reacted with the starting cationic complex **11[PF$_6$]$_2$** (or **12[PF$_6$]$_2$**) resulting in the MV complex **11[PF$_6$]** (or **12[PF$_6$]**) and at the same time small amount of the neutral cumulenic complex **14** (or **15**) reacted with the dicationic complex **14[PF$_6$]$_2$** (or **15[PF$_6$]$_2$**) leading to the MV complex **14[PF$_6$]** (or **15[PF$_6$]**). The MV complexes are paramagnetic and undetectable in the NMR spectra. Therefore, in the NMR spectra only the neutral bisvinylidene complex **11** (or **12**) and the neutral cumulenic complex **14** (or **15**) were observed in a ratio of 1:3. As shown in Scheme 2, all the neutral complexes and the MV complexes were oxidized to the corresponding dicationic complexes **11[PF$_6$]$_2$** (or **12[PF$_6$]$_2$**) and **14[PF$_6$]$_2$** (or **15[PF$_6$]$_2$**) after the treatment with $[Cp_2Fe][PF_6]$ in CH_3CN.

Scheme 1

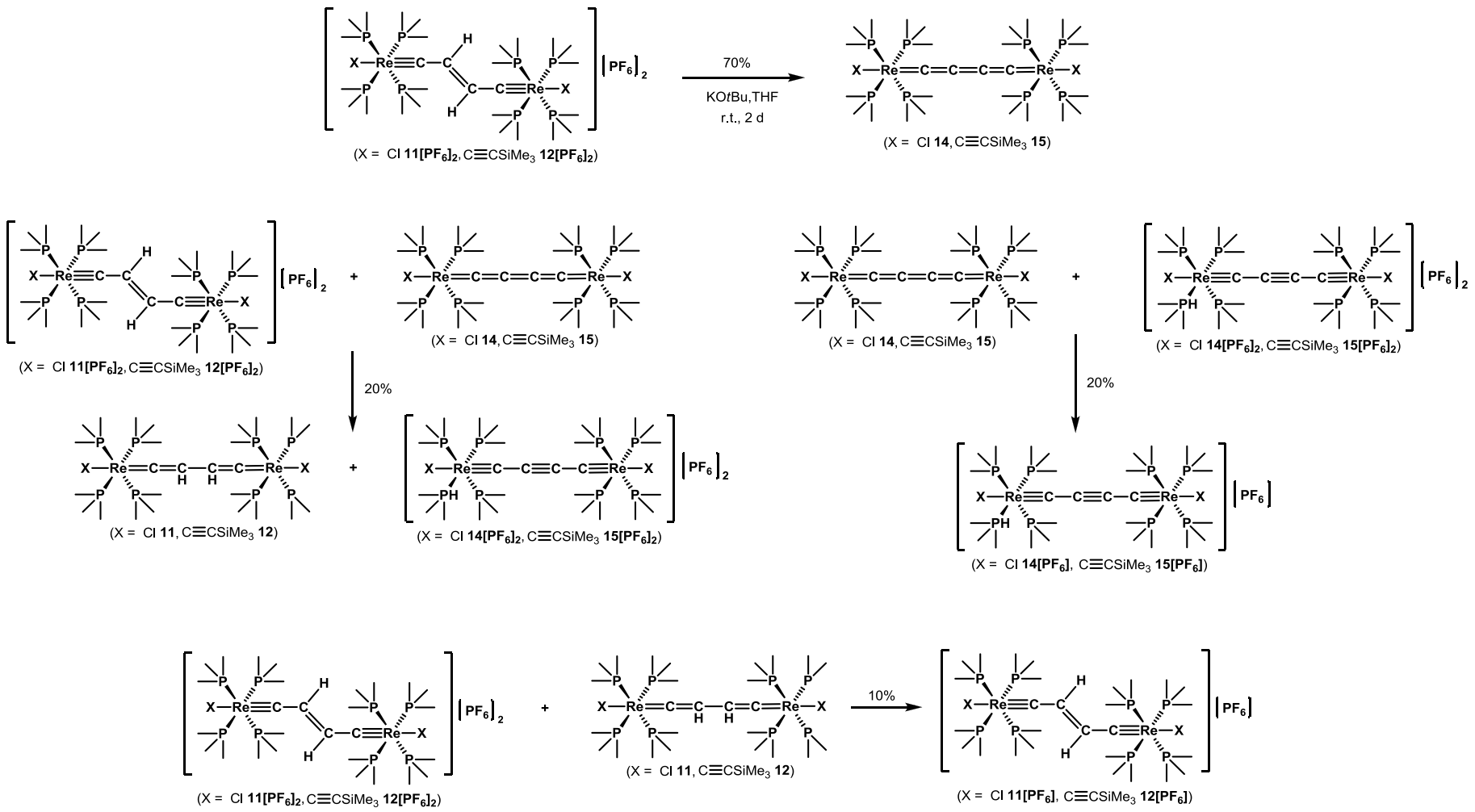

*The percentage in the Scheme is referred to the starting material **11**$[PF_6]_2$ or **12**$[PF_6]_2$

Scheme 2

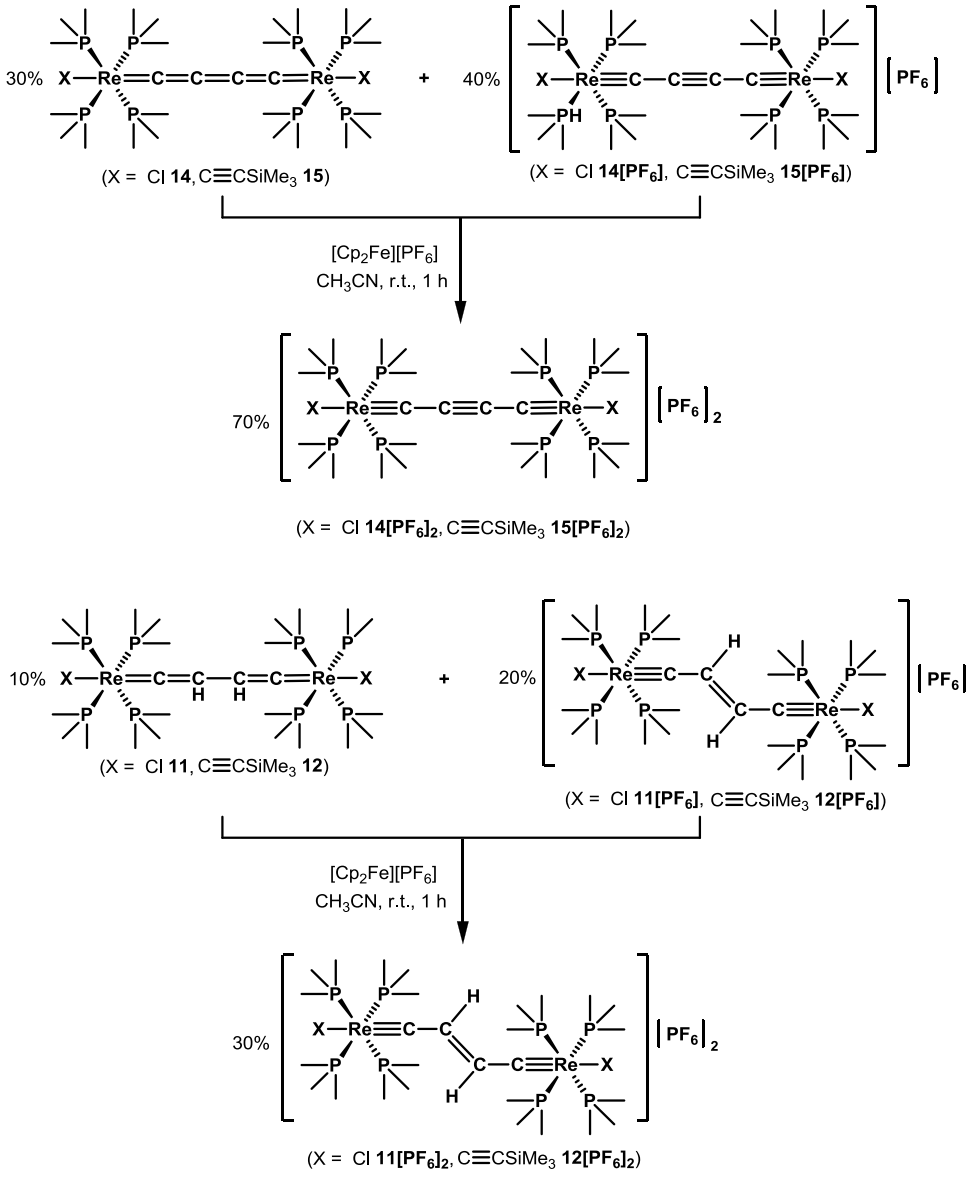

*The percentage in the Scheme is referred to the starting material **11[PF$_6$]$_2$** or **12[PF$_6$]$_2$**

Initially, it was thought that the resulting mixture of complexes **11** and **14** or **12** and **15** was caused by the low basicity of KO*t*Bu and a stronger base LDA was treated with the dicationic complexes **11[PF$_6$]$_2$** and **12[PF$_6$]$_2$**, respectively. However, the dicationic complexes with acetylide end groups *trans*-[(Me$_3$SiC≡C)(PMe$_3$)$_4$Re≡C-CH=CH-C≡Re(PMe$_3$)$_4$(C≡CSiMe$_3$)][PF$_6$]$_2$ (**12[PF$_6$]$_2$**) reacted with LDA and produced the corresponding

neutral complex **12** in 83% yield (Scheme 3), which implied that the LDA might function as a reducing agent rather than a base under the reaction condition. If LDA functions as a reducing agent, the other product tetraisopropylhydrazine *i*-Pr_2NN-*i*-Pr_2 should be detectable in the NMR spectroscopy. However, in the reaction mixture it was the products diisopropylamine and the Schiff base *i*-PrN=C$(CH_3)_2$ were determined, which was in agreement with the work of Ingold and coworkers on the self-reactions of *i*-Pr_2N· radicals. They proposed that the *i*-Pr_2N· radicals were in equilibrium with its dimer, tetraisopropylhydrazine *i*-Pr_2NN-*i*-Pr_2, and reacted to form diisopropylamine and the Schiff base *i*-PrN=C$(CH_3)_2$.[30]

Scheme 3

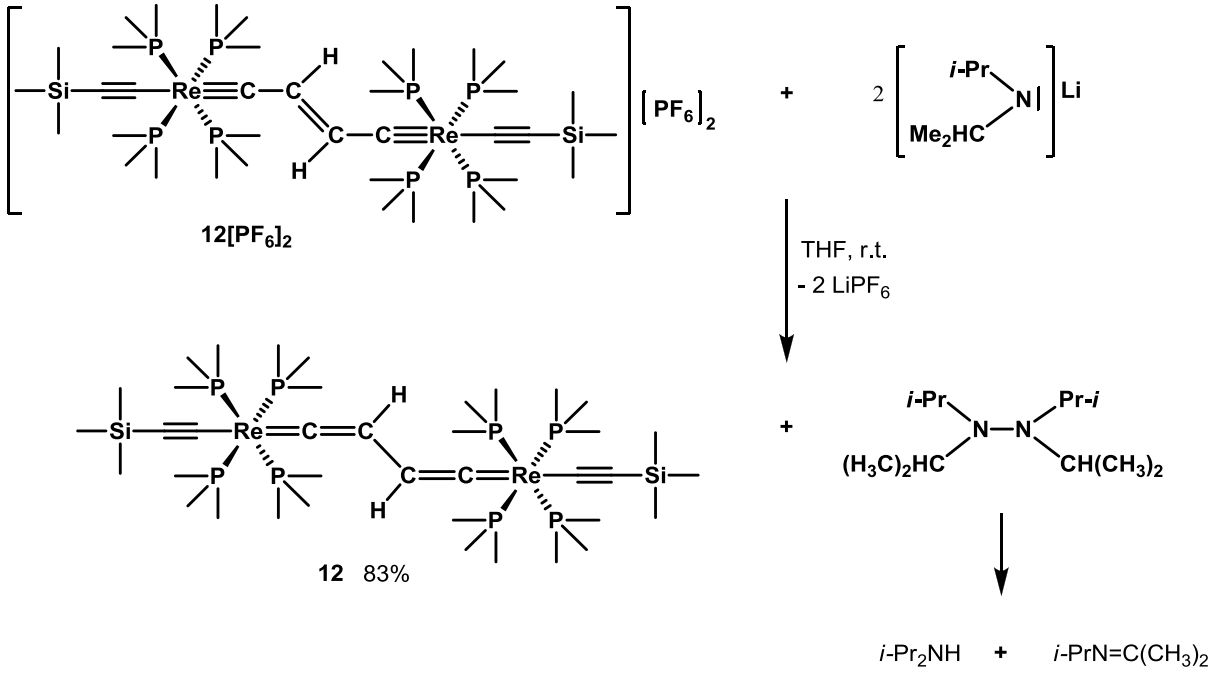

The dicationic complex with chloride end groups *trans*-[Cl$(PMe_3)_4$Re≡C-CH=CH-C≡Re$(PMe_3)_4$Cl][PF_6]$_2$ (**11[PF_6]$_2$**) decomposed after the treatment with LDA and other bases, such as NaN$(SiMe_3)_2$, *n*-BuLi and *t*-BuLi. While its reaction with bases, such as KN$(SiMe_3)_2$ or KH in the presence of 18-crown-6 in THF gave a mixture of the neutral complexes similar to the reaction of the dicationic complex **11[PF_6]$_2$** or **12[PF_6]$_2$** with KO*t*Bu in THF. The reason for the observed decomposition could be attributed to the cation Li^+ or Na^+ being harder acids than K^+ that abstracts the Cl^- resulting in the decomposition of the dicationic complex **11[PF_6]$_2$** with chloride end groups. The superbase KO*t*Bu/*n*-BuLi (LICKOR) was also used to deprotonate the

complex **11[PF$_6$]$_2$**. **11[PF$_6$]$_2$** was added into a THF/hexane solution of KO*t*Bu/*n*-BuLi at -78 °C, which was stirred at this temperature for 1 h followed by the removal of the solvent at the same temperature. The neutral complex *trans*-[Cl(PMe$_3$)$_4$Re=C=CH-CH=C=Re(PMe$_3$)$_4$Cl] (**11**) was isolated in 67% yield (Scheme 4).

Scheme 4

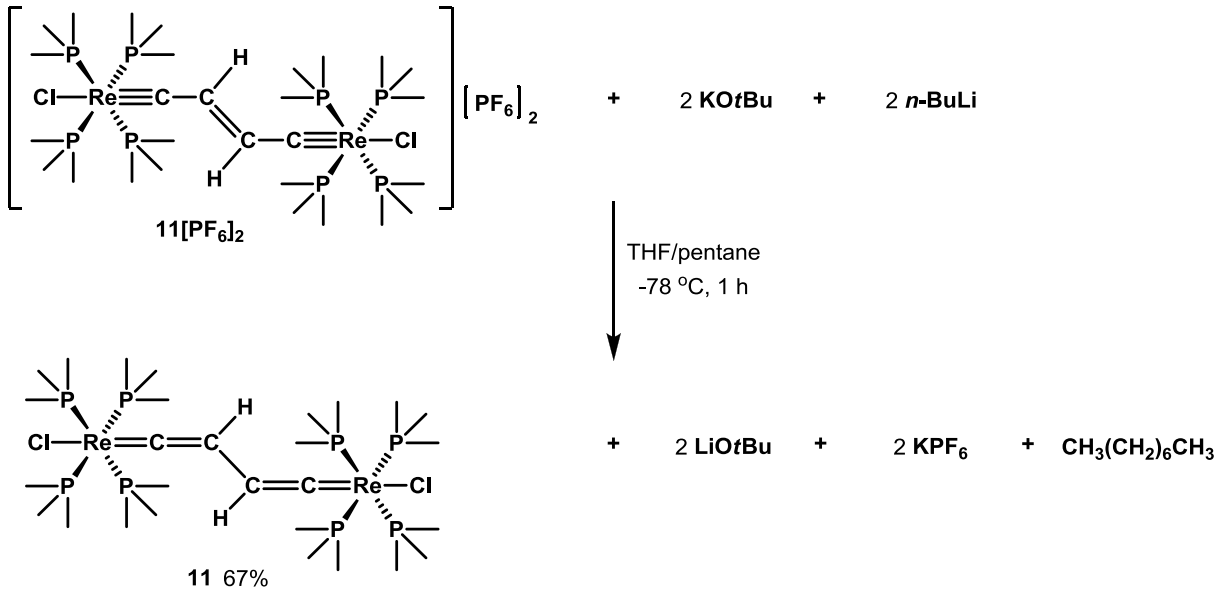

The above mentioned experiments indicated that the bases stronger than KO*t*Bu either reduced the dicationic complexes **11[PF$_6$]$_2$** and **12[PF$_6$]$_2$** to the neutral complexes or decomposition resulted especially in the case of the complex with chloride end groups. Bruce and co-workers observed that the deprotonation of the dicationic dinuclear ruthenium bisvinylidene complex [Cp*(dppm)Ru=C=CH-CH=C=Ru(dppm)Cp*][PF$_6$]$_2$ with DBU gave a single product, while a mixture was obtained when KO*t*Bu was used. However, there is no mention made as to what kind of mixture that they obtained and nor the reason pointed out.[31] Based on their experiments, we infer that perhaps it is because that the ionic base KO*t*Bu partially reduces their dicationic dinuclear ruthenium bisvinylidene complex while the non-ionic base DBU does not. However, in our case, the non-ionic organic bases, such as DBU and TBD, did not react with **11[PF$_6$]$_2$** and **12[PF$_6$]$_2$** at all even at 65 °C for 1 day. Whereas the reaction of the stronger base, such as phosphazene base derivative P$_2$-*t*-Bu, with **11[PF$_6$]$_2$** or **12[PF$_6$]$_2$** gave decomposition products.

Since quinones are often used as a dehydrogenation and oxidizing reagent, chloranil treated with dicationic complex **11[PF_6]$_2$** resulted in a mixture of unidentified products.

The complexes with acetylide end groups (**10** and **12[PF_6]$_2$**) showed more defined reactions towards KO*t*Bu, during the first deprotonations of *trans*-[X(PMe_3)$_4$Re≡C-CH_2-CH_2-C≡Re(PMe_3)$_4$X][PF_6]$_2$ (X = Cl, **9**; C≡C$SiMe_3$, **10**) or in the second deprotonations of *trans*-[X(PMe_3)$_4$Re≡C-CH=CH-C≡Re(PMe_3)$_4$X][PF_6]$_2$ (X = Cl, **11[PF_6]$_2$**; C≡C$SiMe_3$, **12[PF_6]$_2$**), than those with chloride end groups (**9** and **11[PF_6]$_2$**). The reason is that the complexes with chloride end groups (**9** and **11[PF_6]$_2$**) are more electron-rich than those with acetylide end groups (**10** and **12[PF_6]$_2$**) since the chloride ligand is a π donor, while the trimethylsilyl acetylide ligand is more π accepting. Therefore the dicationic complex *trans*-[(Me_3SiC≡C)(PMe_3)$_4$Re≡C-C≡C-C≡Re(PMe_3)$_4$(C≡C$SiMe_3$)][PF_6]$_2$ (**15[PF_6]$_2$**) could be obtained either by method a or by method b shown in Scheme 5 by repetitive sequences of deprotonations and oxidations. Whereas the complex *trans*-[Cl(PMe_3)$_4$Re≡C-C≡C-C≡Re(PMe_3)$_4$Cl][PF_6]$_2$ (**14[PF_6]$_2$**) could not be obtained as a pure product, even after four repetitive cycles of deprotonations and oxidations, the final product still contained 5~10% **11[PF_6]$_2$**.

Scheme 5

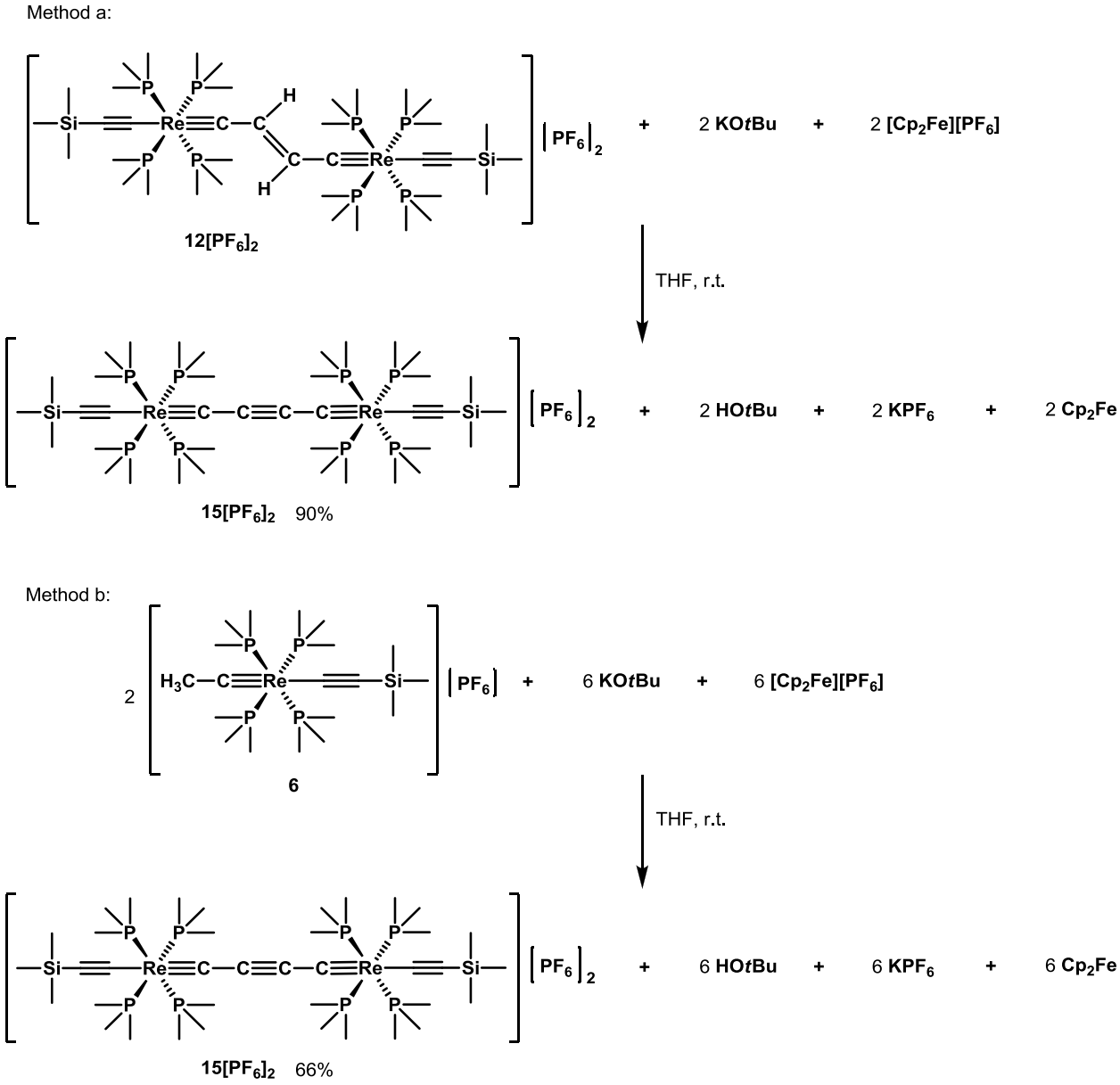

The reduction of the dicationic alkynediyl biscarbyne complex *trans*-[(Me$_3$SiC≡C)(PMe$_3$)$_4$Re≡C-C≡C-C≡Re(PMe$_3$)$_4$(C≡CSiMe$_3$)][PF$_6$]$_2$ (**15[PF$_6$]$_2$**) to the neutral cumulenic complex *trans*-[(Me$_3$SiC≡C)(PMe$_3$)$_4$Re=C=C=C=C=Re(PMe$_3$)$_4$(C≡CSiMe$_3$)] (**15**) was carried out by the treatment of **15[PF$_6$]$_2$** with Na/Hg or Na/Na(PhCOPh). However, these reactions resulted in a mixture of unidentified products. The reaction of **15[PF$_6$]$_2$** with KH in the

presence of 18-crown-6 in THF was also tried (Scheme 6) and the resulting neutral complex **15** was observed in the ^{1}H NMR spectrum of the reaction mixture.

Scheme 6

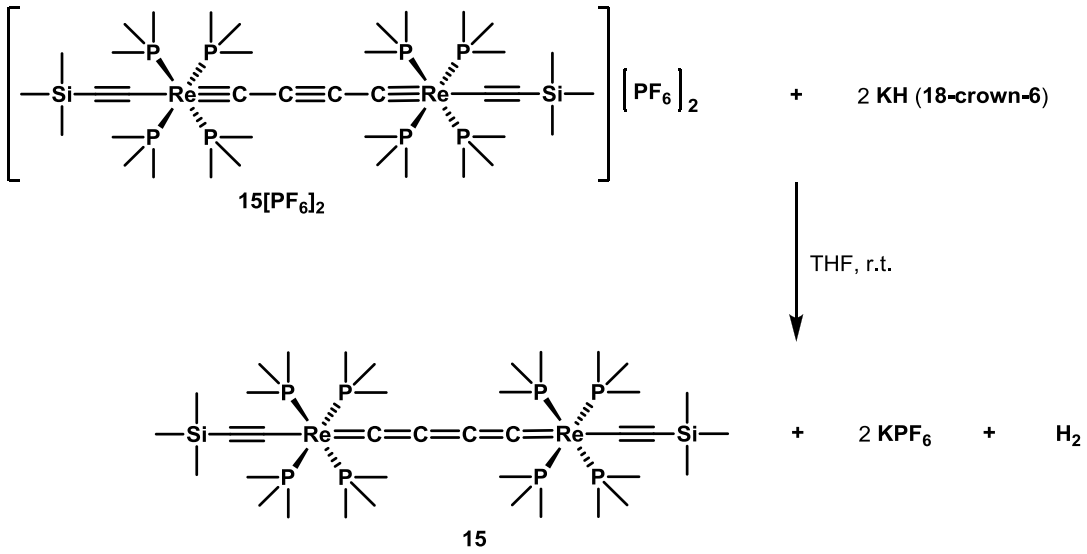

However, the isolation of **15,** after the extraction of the solid residue from the reaction mixture with pentane and benzene, resulted in the gradual regeneration of the bisvinylidene complexes *trans*-[($Me_3SiC{\equiv}C$)(PMe_3)$_4$Re=C=CH-CH=C=Re(PMe_3)$_4$($C{\equiv}CSiMe_3$)] (**12**). During the reaction, it was also found that the neutral complex **15** gradually formed a less-defined brown mixture in solution at room temperature and decomposed immediately upon heating. A similar phenomenon was also observed in the C_2-bridged and C_4-bridged manganese systems. **15** is sensitive to O_2 and decomposed immediately in polar solvents, such as CH_2Cl_2, CH_3CN and acetone. The possible reason of the decomposition might arise from the weak acidity of these solvents. **15** might function as a strong base react with them.

4.2.2 Characterization of the C_4-bridged dinuclear rhenium complexes **14[PF$_6$]$_2$** and **15[PF$_6$]$_2$**

The dicationic dinuclear rhenium complexes **14[PF$_6$]$_2$** and **15[PF$_6$]$_2$** were characterized by NMR, IR, element analysis (only for **15[PF$_6$]$_2$**), mass spectroscopy. Selected ^{1}H NMR, ^{13}C NMR and ^{31}P NMR data for complexes **9, 10**, **11[PF$_6$]$_2$**, **12[PF$_6$]$_2$** **14[PF$_6$]$_2$** and **15[PF$_6$]$_2$** are listed in Table 4-1 for comparison.

Table 4-1. Selected ^{1}H NMR and ^{31}P NMR data for the dicationic complexes **9**, **10**, **11[PF$_6$]$_2$**, **12[PF$_6$]$_2$** **14[PF$_6$]$_2$** and **15[PF$_6$]$_2$** in CD_2Cl_2

Complexes	^{13}C NMR (δ, ppm)		^{1}H NMR (δ, ppm)	^{31}P NMR (δ, ppm)
	C_α	C_β	H_β	PMe_3
$[Cl(PMe_3)_4Re{\equiv}C\text{-}CH_2]_2[PF_6]_2$ (**9**)	267.3	44.8	1.75	-35.8
$[(Me_3SiC{\equiv}C)(PMe_3)_4Re{\equiv}C\text{-}CH_2]_2[PF_6]_2$ (**10**)	279.9	46.4	1.56	-42.2
$[Cl(PMe_3)_4Re{\equiv}C\text{-}CH]_2[PF_6]_2$ (**11[PF$_6$]$_2$**)	255.5	144.0	5.76	-37.3
$[(Me_3SiC{\equiv}C)(PMe_3)_4Re{\equiv}C\text{-}CH]_2[PF_6]_2$ (**12[PF$_6$]$_2$**)	265.3	145.8	5.82	-43.8
$[Cl(PMe_3)_4Re{\equiv}C\text{-}C]_2[PF_6]_2$ (**14[PF$_6$]$_2$**)	226.4	88.1	/	-37.6
$[(Me_3SiC{\equiv}C)(PMe_3)_4Re{\equiv}C\text{-}C]_2[PF_6]_2$ (**15[PF$_6$]$_2$**)	235.0	95.8	/	-43.6

The ^{1}H NMR spectra of the dicationic alkynediyl biscarbyne complexes *trans*-$[X(PMe_3)_4Re{\equiv}C\text{-}C{\equiv}C\text{-}C{\equiv}Re(PMe_3)_4X][PF_6]_2$ (X = Cl, **14[PF$_6$]$_2$**; C≡CSiMe$_3$, **15[PF$_6$]$_2$**) showed the resonances of the $P(CH_3)_3$ ligands at 1.78 ppm and 1.82 ppm, respectively. For **15[PF$_6$]$_2$**, one additional signal at 0.26 ppm was assigned to the protons of the trimethylsilyl groups. The $^{13}C\{^1H\}$ NMR spectra revealed characteristic resonances for the C_α and C_β at 226.4 ppm and 88.1 ppm for **14[PF$_6$]$_2$**, and at 235.0 ppm and 95.8 ppm for **15[PF$_6$]$_2$**, respectively. The $^{13}C\{^1H\}$ NMR spectra showed signals of low intensities for these complexes, which did not allow to extract the J_{PC} values. The additional resonances at 135.5 ppm and 128.4 ppm in **15[PF$_6$]$_2$** were attributed to the acetylide groups. In the ^{31}P NMR spectra, the resonances at -37.6 ppm and -43.6 ppm were ascribed to the $P(CH_3)_3$ ligands in **14[PF$_6$]$_2$** and **15[PF$_6$]$_2$**. The PF_6^- characteristic signals appeared as a septet at -143.9 ppm. As shown in Table 4-1, the removal of the protons from the biscarbyne (≡C-CH_2-CH_2-C≡) bridge of the dicationic complexes **9** and **10** or from the ethylenylidene biscarbyne (≡C-CH=CH-C≡) bridge of the dicationic complexes **11[PF$_6$]$_2$** and

12[PF_6]$_2$ lead to significant change in the $^{13}C\{^1H\}$ NMR spectra. From the complexes **9** and **10** with biscarbyne (≡C-CH_2-CH_2-C≡) bridge to the complexes **11[PF_6]$_2$** and **12[PF_6]$_2$** with ethylenylidene biscarbyne (≡C-CH=CH-C≡) bridge, the resonances of C_α showed an up-field shift while those of C_β moved to down-field. In the transformation of the ethylenylidene biscarbyne (≡C-CH=CH-C≡) bridge to the alkynediyl biscarbyne (≡C-C≡C-C≡) bridge, the resonances of C_α continued moving up-field, whereas those of the C_β shifted up-field. This points to the fact that the carbon frameworks in the alkynediyl biscarbyne complexes **14[PF_6]$_2$** and **15[PF_6]$_2$** are more electron-rich than those in the ethylenylidene biscarbyne complexes **11[PF_6]$_2$** and **12[PF_6]$_2$**. The IR spectra of **14[PF_6]$_2$** and **15[PF_6]$_2$** did not show the ν(C≡C) vibration of the alkynediyl biscarbyne (≡C-C≡C-C≡) bridge. Only a weak band at 2013 cm^{-1} was observed in the IR spectrum of **15[PF_6]$_2$**, which was attributed to the ν(C≡C) vibration of the trimethysilyl acetylide end groups.

The X-ray diffraction analyses (Figure 4-1) were carried out on the dicationic dinuclear rhenium complexes **14[PF$_6$]$_2$** and **15[PF$_6$]$_2$**. Selected bond distances and bond angles for the complexes **11[PF$_6$]$_2$**, **12[PF$_6$]$_2$**, **14[PF$_6$]$_2$** and **14[PF$_6$]$_2$** are summarized in Table 4-2 for comparison.

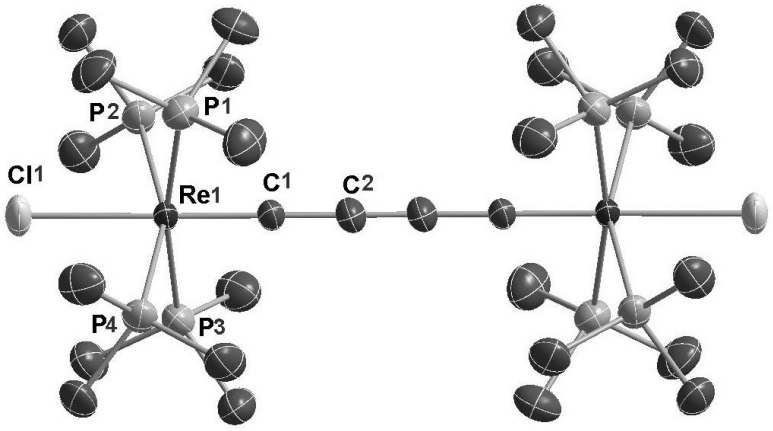

(a)

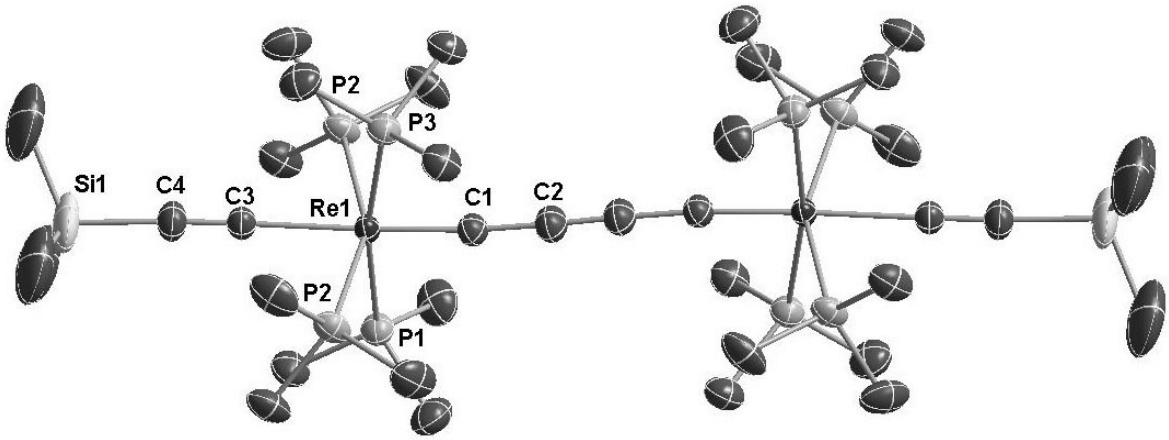

(b)

Fig 4-1. ORTEP like drawing of (a) *trans*-[Cl(PMe$_3$)$_4$Re≡C-C≡C-C≡Re(PMe$_3$)$_4$Cl][PF$_6$]$_2$ **14[PF$_6$]$_2$** and of (b) *trans*-[(Me$_3$SiC≡C)(PMe$_3$)$_4$Re≡C-C≡C-C≡Re(PMe$_3$)$_4$(C≡CSiMe$_3$)][PF$_6$]$_2$ **15[PF$_6$]$_2$** (50% probability level of thermal ellipsoids). Solvent molecules, hydrogen atoms and the counter ion PF_6^- are omitted for clarity.

Table 4-2. Selected bond lengths [Å] and angles [°] for complexes **11[PF$_6$]$_2$**, **12[PF$_6$]$_2$**, **14[PF$_6$]$_2$** and **15[PF$_6$]$_2$**, assignment of the bond lengths in the C_4 bridge according to the following notation: [Re]C1C2C2'C1'[Re]

Complexes	**11[PF$_6$]$_2$**	**14[PF$_6$]$_2$**	**12[PF$_6$]$_2$**	**15[PF$_6$]$_2$**
C2-C2'	1.317(8)	1.229(8)	1.331(10)	1.197(8)
C1-C2	1.439(5)	1.343(8)	1.414(7)	1.363(5)
C1-Re1	1.766(3)	1.783(5)	1.805(5)	1.814(4)
Cl1-Re1	2.5075(8)	2.4882(14)	/	/
C3-Re1	/	/	2.179(4)	2.161(4)
C3-C4	/	/	1.172(6)	1.195(5)
C4-Si1	/	/	1.836(5)	1.824(4)
Re···Re	7.268	7.495	7.282	7.536
C1-C2-C2'	124.7(5)	179.1(7)	125.5(7)	177.8(6)
C2-C1-Re1	176.8(3)	179.6(6)	177.1(4)	173.3(3)
C1-Re1-Cl1	177.90(13)	179.43(17)	/	/
C1-Re1-C3	/	/	171.2(2)	177.08(15)
Re1-C3-C4	/	/	178.7(4)	178.6(4)
C3-C4-Si1	/	/	177.8(4)	176.7(4)

The Re1-C1 bond distances are 1.783(5) Å and 1.814(4) Å for the dicationic complexes **14[PF$_6$]$_2$** and **15[PF$_6$]$_2$**, respectively. These bond lengths are longer than the expected distance range (1.75-1.72 Å) of the triple-bonded covalent radii of the Re≡C(sp) unit. The relatively higher *trans* influence of $Me_3SiC{\equiv}C^-$ than that of Cl^- weakens the Re1-C1 bond, which is reflected in the lengthening of the Re1-C1 distances. According to Table 4-2, the removal of two

protons from the ethylenylidene biscarbyne (≡C-CH=CH-C≡) bridge of the dicationic complexes **11[PF$_6$]$_2$** and **12[PF$_6$]$_2$** to form the alkynediyl biscarbyne (≡C-C≡C-C≡) bridge of the dicationic complexes **14[PF$_6$]$_2$** and **15[PF$_6$]$_2$** result in a slight lengthening of the Re1-C1 bond distances. The C1-C2 bond lengths in **14[PF$_6$]$_2$** and **15[PF$_6$]$_2$** are 1.343(8) Å and 1.363(5) Å, respectively, fall into the C=C double bond range (1.33-1.38 Å). These distances are close to the corresponding C1-C2 bond distance in the tungsten complex [I(dppe)$_2$W≡C-C≡C-C≡W(dppe)$_2$I] where it was assigned to a C-C single bond.[29] The C2–C2' distances 1.229(8) Å and 1.197(8) Å are close to a C≡C triple bond range (1.18-1.20 Å). Therefore the structures of **14[PF$_6$]$_2$** and **15[PF$_6$]$_2$** consist of two symmetrically arranged [*trans*-X(PMe$_3$)$_4$Re] fragments linked by a C_4 system resembling a canonical alkynediyl biscarbynic structure. The Re···Re distances in **14[PF$_6$]$_2$** and **15[PF$_6$]$_2$** are 7.495 Å and 7.536 Å, longer than the metal-metal distances in **11[PF$_6$]$_2$** and **12[PF$_6$]$_2$**. The C-C-C', Re-C-C and Cl-Re-C bond angles in **14[PF$_6$]$_2$** and **15[PF$_6$]$_2$** are close to 180°. The atoms Si1, C4, C3, Re1, C1 and C2 are almost linear in the compounds bearing acetylide end groups.

In contrast to the dicationic dinuclear rhenium complex [(Cp*)(NO)(PPh$_3$)Re=C=C=C=C=Re(PPh$_3$)(NO)(Cp*)][PF$_6$]$_2$ with cumulenic valence structure reported by Gladysz and coworkers, the carbon backbone in the dicationic dinuclear rhenium complexes *trans*-[X(PMe$_3$)$_4$Re≡C-C≡C-C≡Re(PMe$_3$)$_4$X][PF$_6$]$_2$ (X = Cl, **13[PF$_6$]$_2$**; C≡CSiMe$_3$, **14[PF$_6$]$_2$**) is an acetylide-bridged biscarbynic form. These results clearly show the influence of the ancillary ligands on the valence structure of the C_4-bridged dinuclear rhenium complexes. The more electron-rich trimethylphosphine ligand instead of π-accepting nitrosyl ligand would enhance the rhenium basicity and hence should lead to thermodynamically more favorable electron distribution with oxidation of the rhenium centers and stronger Re-C multiple bonding.

4.3 Cyclic voltammetry (CV) studies of the dinuclear rhenium complexes

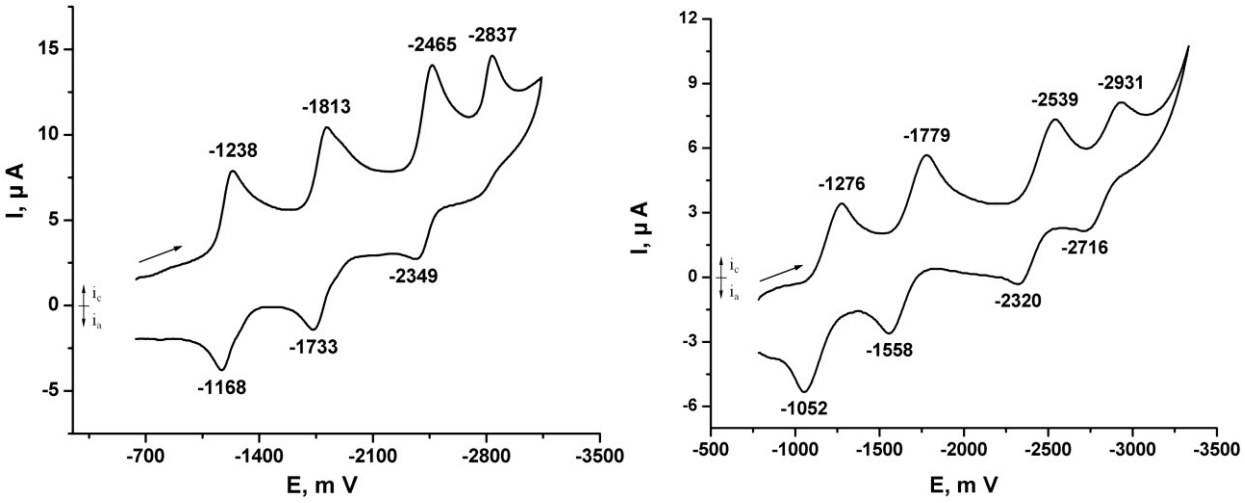

(a) (b)

Fig 4-2. CV of (a) **14[PF$_6$]$_2$** in 0.1 M CH_3CN solution of [*n*-Bu_4N][PF_6]; (b) **15[PF$_6$]$_2$** in 0.1M THF solution of [*n*-Bu_4N][PF_6]; Au electrode; E vs $Fc^{0/+}$; scan rate = 100 mV·s^{-1}; 20 °C

Scheme 7

Electronic structrues using canonical representations of C_4-bridged systems

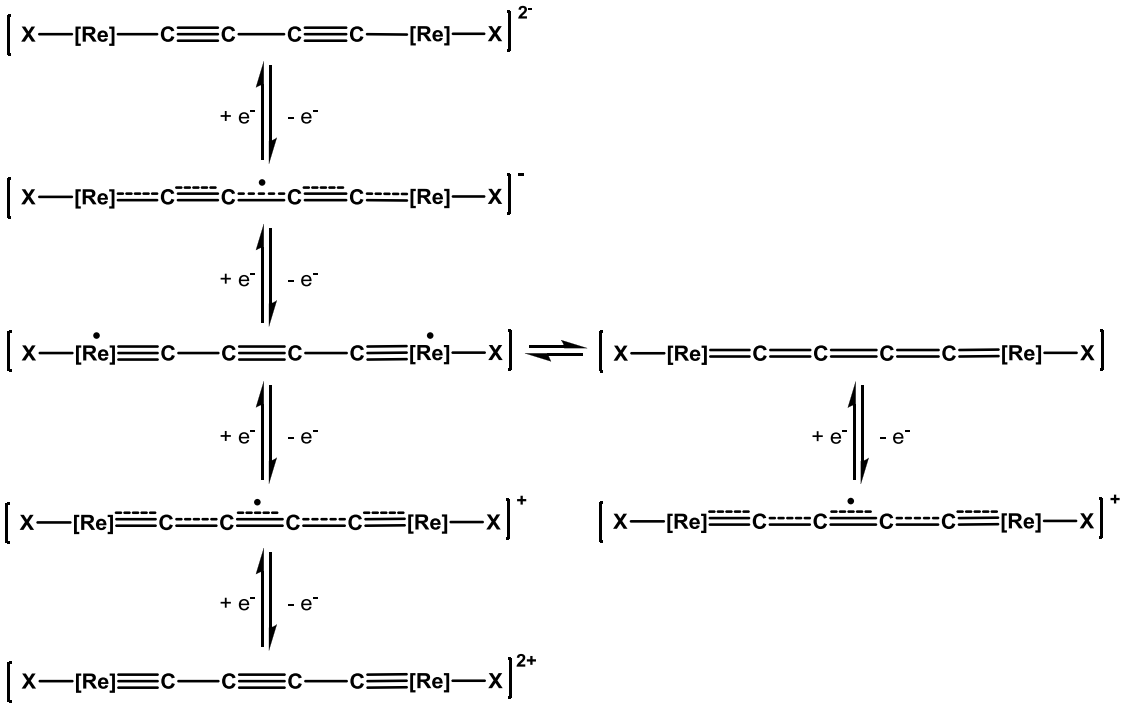

The CV spectra of **14[PF_6]$_2$** in CH_3CN (as shown by the experimental result that 5% of **11[PF_6]$_2$** did not affect the CV result) and **15[PF_6]$_2$** in THF showed four reversible waves (Figure 4-2). According to Scheme 7, there could be two alternative electronic structures for the neutral complexes: the cumulenic form (Re=C=C=C=Re) with Re(I)-Re(I) oxidation state (singlet, S = 0) and its isomeric alkynediyl biscarbynic form (·Re≡C-C≡C-C≡Re·) with antiferromagnetically coupled Re(II)-Re(II) oxidation state (triplet, S = 1). In the ^{1}H NMR spectrum of the reaction mixture of **15[PF_6]$_2$**, KH, 18-crown-6 and THF-d_8**,** two well-defined signals of **15** were observed at 1.10 ppm and 0.53 ppm that could be assigned to the PMe_3 groups and the $SiMe_3$ groups, respectively. However, the ^{13}C NMR and ^{31}P NMR spectra of the reaction mixture did not show any signal for these groups and the ^{29}Si NMR spectrum displayed a broad signal indicating a paramagnetic behavior. This kind of unusual paramagnetic behaviour was also observed in the NMR spectra of the neutral dinuclear manganese complex [(MeC_5H_4)(dmpe)Mn-C≡C-Mn(dmpe)(C_5H_4Me)] reported by Berke and coworkers. In their work, the DFT calculations of the neutral model manganese complex suggested a small energy gap between the singlet and triplet electronic states and a singlet/triplet spin equilibrium is very likely to exist also in this case.[32] Therefore the interpretation for the unusual paramagnetic behavior in the neutral dinuclear rhenium complex **15** might be a singlet/triplet spin equilibrium. The neutral complexes **14** and **15** are also highly reducing and very sensitive towards oxygen and moisture and decompose in solution gradually, very similar to the neutral dinuclear manganese complex [(MeC_5H_4)(dmpe)Mn-C≡C-Mn(dmpe)(C_5H_4Me)]. The singlet/triplet spin equilibrium might be the explanation that the neutral complexes **14** and **15** are thermodynamically less stable than the neutral bisvinylidene complexes **11** and **12**, which prefer the bisvinylidene bridged form (=C=CH-HC=C=) with Re(I)-Re(I) oxidation state (singlet, S = 0). The experiments showed that **15** was more labile towards heat than **12**. **12** still remained after heating at 80 °C for 6 days, while **14** decomposed immediately after heating at 60 °C for several minutes. As mentioned before, unlike the neutral bisvinylidene complexes **11** and **12, 15** gradually formed a less-defined brown mixture of compounds at room temperature. The gradual transformation of the neutral complex **15** to the neutral bisvinylidene complex **12** in solution might be derived from the proton abstraction from the solvent.

The first two waves at $E_{1/2}$ = -1.203 V and $E_{1/2}$ = -1.773 V of the CV spectrum of **14[PF$_6$]$_2$** in CH_3CN might be corresponding to the Re(III)-Re(III)/Re(III)-Re(II)/Re(II)-Re(II) redox couples, respectively. The potential difference $\Delta E_{1/2}$ of these two values is 0.570 V establishing a large K_c value of 6.4×10^9. The CV spectrum of **15[PF$_6$]$_2$** in THF also displayed four reversible waves and the potential difference $\Delta E_{1/2}$ between the first redox waves is 0.504 V ($E_{1/2}$ = -1.164 V and $E_{1/2}$ = -1.668 V) resulting in a K_c value of 4.7×10^8. The third and fourth redox processes have very negative potentials, which make the corresponding redox species difficult to prepare by chemical methods. The complex **14[PF$_6$]$_2$** with chloride end groups shows K_c value slightly larger than that of the complex **15[PF$_6$]$_2$** with acetylide end groups, which is related to the different π-donating properties of the Cl^- ligand and the $Me_3SiC{\equiv}C^-$ ligand as mentioned in chapter 3. As depicted in Table 4-3, if the experimental errors are taken into account, the $\Delta E_{1/2}$ values of the complexes with chloride end groups (0.597 V for **11[PF$_6$]$_2$** and 0.570 V for **14[PF$_6$]$_2$**) are very close to each other, and the $\Delta E_{1/2}$ values of the complexes with acetylide end groups (0.475 V for **12[PF$_6$]$_2$** and 0.504 V for **15[PF$_6$]$_2$**) have the same trend. Due to the only difference in these complexes are the bridges, the electronic communication through the ethylenylidene biscarbyne (≡C-CH=CH-C≡) bridge of the dicationic complexes **11[PF$_6$]$_2$** and **12[PF$_6$]$_2$** and that through the alkynediyl biscarbyne (≡C-C≡C-C≡) bridge of the dicationic complexes **14[PF$_6$]$_2$** and **15[PF$_6$]$_2$** might be the same.

Table 4-3. Electrochemical data for **11[PF$_6$]$_2$**, **12[PF$_6$]$_2$**, **14[PF$_6$]$_2$** and **15[PF$_6$]**, E vs $Fc^{0/+}$

Complexes	Couple 1 $E_{1/2}$ (V)	Couple 2 $E_{1/2}$ (V)	ΔE (V)	K_c	Ref.
$[Cl(PMe_3)_4Re{\equiv}C\text{-}CH]_2[PF_6]_2$ (**11[PF$_6$]$_2$**, CH_3CN)	-1.283	-1.880	0.597	1.8×10^{10}	Present work
$[Cl(PMe_3)_4Re{\equiv}C\text{-}C]_2[PF_6]_2$ (**14[PF$_6$]$_2$**, CH_3CN)	-1.207	-1.773	0.570	6.4×10^9	Present work
$[(Me_3SiC{\equiv}C)(PMe_3)_4Re{\equiv}C\text{-}CH]_2[PF_6]_2$ (**12[PF$_6$]$_2$**, THF)	-1.292	-1.749	0.457	7.1×10^7	Present work
$[(Me_3SiC{\equiv}C)(PMe_3)_4Re{\equiv}C\text{-}C]_2[PF_6]_2$ (**15[PF$_6$]$_2$**, THF)	-1.164	-1.668	0.504	4.7×10^8	Present work

4.4 Conclusion

The deprotonation of the dinuclear rhenium ethylenylidene biscarbyne complexes *trans*-[X(PMe$_3$)$_4$Re≡C-CH=CH-C≡Re(PMe$_3$)$_4$X][PF$_6$]$_2$ (X = Cl, **11[PF$_6$]$_2$**; C≡CSiMe$_3$, **12[PF$_6$]$_2$**) with KO*t*Bu followed by the subsequent oxidation with [Cp$_2$Fe][PF$_6$] led to the dinuclear rhenium alkynediyl bicarbyne complexes *trans*-[X(PMe$_3$)$_4$Re≡C-C≡C-C≡Re(PMe$_3$)$_4$X][PF$_6$]$_2$ (X = Cl, **14[PF$_6$]$_2$**; C≡CSiMe$_3$, **15[PF$_6$]$_2$**). The experimental results showed that the neutral dinuclear rhenium cumulenic complexes *trans*-[X(PMe$_3$)$_4$Re=C=C=C=C=Re(PMe$_3$)$_4$X] (X = Cl, **14**; C≡CSiMe$_3$, **15**) could not be obtained either by deprotonation of the dicationic ethylenylidene biscarbyne complexes **11[PF$_6$]$_2$** and **12[PF$_6$]$_2$** or by the reduction of the alkynediyl bicarbyne complex **15[PF$_6$]$_2$**. The neutral cumulenic complex **15** is apparently thermodynamically less stable than the neutral bisvinylidene complex **12,** probably due to the singlet/triplet spin equilibrium in **15**. The cyclic voltammetry (CV) studies on **14[PF$_6$]$_2$** and **15[PF$_6$]$_2$** displayed large K_c values of 6.4×10^9 and 4.7×10^8, respectively, revealing the high thermodynamic stability of the mixed-valence (MV) species under the CV conditions. The CV investigations also suggest that the electronic properties of the end groups have significant influence on the K_c values and the ability to conduct electrons of the ethylenylidene biscarbyne (≡C-CH=CH-C≡) bridge and of the alkynediyl bisdcarbyne (≡C-C≡C-C≡) bridge might be similar.

4.5 Experimental section

General procedures: All the manipulations were carried out under a nitrogen atmosphere using Schlenk techniques or a glove box (M. Braun150B-G-II). Reagent grade benzene, toluene, hexane, pentane, diethyl ether and tetrahydrofuran were dried and distilled from sodium benzophenone ketyl prior to use. Dichloromethane and acetonitrile were distilled from CaH_2. All other chemicals were directly used as obtained from commercial suppliers. CHN elemental analyses were performed with a LECO CHN-932 microanalyzer. IR spectra were obtained on a Bio-Rad FTS-45 instrument. Raman spectra were recorded on a Renishaw Ramanscope spectrometer (633 nm). NMR spectra were measured on a Varian Mercury spectrometer at 200 MHz for ^{1}H NMR, 81 MHz for ^{31}P NMR, 188 MHz for ^{19}F NMR, Varian Gemini-2000 spectrometer at 300 MHz for ^{1}H NMR and 75 MHz for ^{13}C NMR, and on a Bruker-DRX-500 spectrometer at 500 MHz for ^{1}H NMR, 125.8 MHz for ^{13}C NMR, 202.5 MHz for ^{31}P NMR, and 99.4 MHz for ^{29}Si NMR. Chemical shift for ^{1}H NMR, ^{31}P NMR, ^{13}C NMR, and ^{29}Si NMR is

given in ppm relative to TMS and that for ^{31}P relative to phosphoric acid. Cyclic voltammograms were obtained with BAS 100W voltammetric analyzer equipped with an Au working and a Pt counter electrode, and a non-aqueous reference electrode. All sample solutions were approximately 5×10^{-3} M in substrate and in 0.1 M THF or CH_3CN solution of $[nBu_4N][PF_6]$ and prepared under nitrogen. Ferrocene was subsequently added and the calibration of voltammograms recorded. BAS 100W program was employed for data analysis.

X-ray diffraction studies on complexes 13$[PF_6]_2$ and 14$[PF_6]_2$: Data collection for all crystals were carried out on Stoe IPDS diffractometer (Imaging Plate Detector System with graphite-monochromated MoK_α radiation, $\lambda = 0.71073$ Å)[33] and for others on Oxford Diffraction Xcalibur R diffractometer (4-circle kappa platform, Ruby CCD detector and a single wavelength Enhance X-ray source with MoK_α radiation, $\lambda = 0.71073$ Å) at 183(2) K using a cold N_2-gas stream from an Oxford Cryogenic System. Pre-experiment, data collection and data reduction (unit cell determination, intensity data integration and empirical absorption correction) were carried out with the Oxford *CrysAlisPro* software.[34] The structures were solved with the unique data sets using the Patterson method of the program SHELXS-97. The structure refinement was performed with the program SHELXL-97.[35] Non-hydrogen atoms were refined anisotropically by full-matrix least-squares techniques based on F^2. The hydrogen atoms of the organic groups were placed in calculated positions and refined with a riding model with a fixed temperature factor. The program PLATON[36] was used to check the result of the X-ray analysis.

***trans*-[Cl(PMe$_3$)$_4$Re≡C-C≡C-C≡Re(PMe$_3$)$_4$Cl][PF$_6$]$_2$ (14[PF$_6$]$_2$).** Method a: A mixture of *trans*-[ReCl(≡C-CH)(PMe$_3$)$_4$]$_2$[PF$_6$]$_2$ (**11[PF$_6$]$_2$**) (18.8 mg, 0.014 mmol) and KO*t*Bu (15.2 mg, 0.130 mmol) in THF was stirred at room temperature for 12 h until a dark blue solution resulted. With vigorous stirring $[Cp_2Fe][PF_6]$ (44.5 mg, 0.130 mmol) was added to this reaction mixture in four portions at an interval of 1 h. The solvent was removed *in vacuo* and the residue was extracted with CH_2Cl_2 and filtered through celite. Then ether was added to precipitate the product, which was washed with ether (3 × 2 mL) and dried to give the title product **14[PF$_6$]$_2$** with 5~10% starting material *trans*-[ReCl(≡C-CH)(PMe$_3$)$_4$]$_2$[PF$_6$]$_2$ (**11[PF$_6$]$_2$**). Yield: 13.2 mg (0.010 mmol, 71% based on *trans*-[ReCl(≡C-CH$_2$)(PMe$_3$)$_4$]$_2$[PF$_6$]$_2$ (**11[PF$_6$]$_2$**)).

Method b: *Trans*-[ReCl(≡C-CH$_2$)(PMe$_3$)$_4$]$_2$[PF$_6$]$_2$ (**9**) (13.9 mg, 0.010 mmol), KO*t*Bu (22.4 mg, 0.200 mmol), and THF (5 mL) were mixed in a Young schlenk flask. The yellowish green

suspension was heated at 65 °C for 30 min resulting in a clear brown solution. Subsequently, $[Cp_2Fe][PF_6]$ (6.8 mg, 0.02 mmol) was added. The reaction mixture was kept stirring overnight and the solvent was removed *in vacuo*. The residue was extracted with CH_2Cl_2 and filtered through celite. After concentration to about 0.5 mL, ether was added to precipitate and was placed at -30 °C to effect complete precipitation. The brown red solid was collected, washed with ether (3 × 2 mL), and dried *in vacuo* to give the title product **14[PF$_6$]$_2$** with 5~10% *trans*-$[ReCl(\equiv C\text{-}CH)(PMe_3)_4]_2[PF_6]_2$ (**11[PF$_6$]$_2$**) Yield: 9.8 mg (0.007 mmol, 70% based on *trans*-$[ReCl(\equiv C\text{-}CH_2)(PMe_3)_4]_2[PF_6]$ (**9**)). Single crystals suitable for X-Ray diffraction were grown by layering ether over an acetonitrle solution of **14[PF$_6$]$_2$**. IR (ATR, cm^{-1}): ν = 940 (C-P). MS(ESI): *m/z* (100%):1243 $[M^+\text{-}2H]$. ^1H NMR (CD_2Cl_2, 200 MHz, 22 °C): δ = 1.78 (s, $P(CH_3)_3$); ^{13}C NMR (CD_2Cl_2, 125.8 MHz, 10 °C): δ = 226.4 (t, C_α), 88.1 (s, C_β), 20.5 (s, $P(CH_3)_3$); ^{31}P NMR (CD_2Cl_2, 81 MHz, 22 °C): δ = -37.6 (s, $P(CH_3)_3$), -146.2 (setp, J = 712 Hz, 1P, PF_6); ^{19}F NMR (CD_2Cl_2, 188 MHz, 22 °C): δ = -75.8 (d, J = 713 Hz, PF_6).

***trans*-[(Me$_3$SiC≡C)(PMe$_3$)$_4$Re≡C-C≡C-C≡Re(PMe$_3$)$_4$(C≡CSiMe$_3$)][PF$_6$]$_2$ (15[PF$_6$]$_2$).** Method a: A mixture of *trans*-$[Re(C\equiv CSiMe_3)(\equiv C\text{-}CH)(PMe_3)_4]_2[PF_6]_2$ (**12[PF$_6$]$_2$**) (21.4 mg, 0.014 mmol) and KO*t*Bu (8.0 mg, 0.070 mmol) in THF was stirred at room temperature for 12 h until a dark blue solution was obtained. With vigorous stirring, $[Cp_2Fe][PF_6]$ (24.0 mg, 0.071 mmol) was added to this reaction mixture in two portions with an interval of 1 h. The solvent was removed *in vacuo* and the residue was extracted with CH_2Cl_2 and filtered through celite. The product that was obtained by precipitation with ether and was further washed with ether (3 × 2 mL), and dried to give the pure product **15[PF$_6$]$_2$**. Yield: 20 mg (0.013 mmol, 95% based on *trans*-$[Re(C\equiv CSiMe_3)(\equiv C\text{-}CH)(PMe_3)_4]_2[PF_6]_2$(**12[PF$_6$]$_2$**).

Method b: To a mixture of trans-$[Re(C\equiv CSiMe_3)(\equiv C\text{-}CH_3)(PMe_3)_4][PF_6]$ (**6**) (7.6 mg, 0.010 mmol) and KO*t*Bu (2.2 mg, 0.020 mmol) in THF, $[Cp_2Fe][PF_6]$ (6.6 mg, 0.020 mmol) was added in one portion at -30 °C. The reaction mixture was stirred at room temperature for 1h. The solvent was removed *in vacuo* and the residue was washed with hexane or pentane (3 × 2 mL). The resulting solid was dissolved in THF followed by the addition of KO*t*Bu (1.4 mg, 0.012 mmol). The reaction mixture was stirred at room temperature for 20 min until a dark blue solution was obtained. Then $[Cp_2Fe][PF_6]$ (4.0 mg, 0.012 mmol) was added resulting in a brown suspension and the reaction mixture was allowed to stir at room temperature for further 1h. After the solvent was removed *in vacuo*, the resulting brown solid was extracted with CH_2Cl_2 and the

precipitation was effected with ether. The collected solid was washed with ether (3 × 2 mL), dried and gave pure product **15[PF_6]$_2$**. Yield: 5 mg (0.003 mmol, 66% based on *trans*-[Re(C≡C$SiMe_3$)(≡C-CH_3)(PMe_3)$_4$][PF_6] (**6**)). Single crystals suitable for X-Ray diffraction were grown by layering pentane over a dichloromethane solution of **15[PF_6]$_2$**. Anal. Calcd for $C_{38}H_{90}F_{12}P_{10}Re_2Si_2$: C, 30.16; H, 5.99. Found: C, 30.27; H, 5.91. IR (ATR, cm^{-1}): ν = 2013 (C≡C), 940 (C-P). MS(ESI): *m/z* (100%): 1367 [M^+]. ^{1}H NMR (CD_2Cl_2, 200 MHz, 22 °C): δ = 1.82 (s, P(CH_3)$_3$), 0.26 (s, Si(CH_3)$_3$); ^{13}C NMR (CD_2Cl_2, 125.8 MHz, 10 °C): δ = 235.0 (t, C_α), 135.5 (t, $^2J_{PC}$ = 20.2 Hz, C_α'), 128.4 (s, C_β'), 95.8 (s, C_β), 22.2 (m, P(CH_3)$_3$), 0.4 (s, Si(CH_3)$_3$); ^{31}P NMR (CD_2Cl_2, 81 MHz, 22 °C): δ = -43.6 (s, P(CH_3)$_3$), -143.9 (sept, J = 711 Hz, 1P, PF_6); ^{19}F NMR (CD_2Cl_2, 188 MHz, 22 °C): δ = -74.1 (d, J = 711 Hz, PF_6); ^{29}Si NMR (CD_2Cl_2, 99.4 MHz, 10 °C): δ = -22.1 (s, $SiMe_3$)

4.6 References

(1) Heath, J. R. *Annu. Rev. Mater. Res.* **2009**, *39*, 1-23.

(2) Carroll, R. L.; Gorman, C. B. *Angew. Chem. Int. Ed.* **2002**, *41*, 4379-4400.

(3) Chen, F.; Hihath, J.; Huang, Z. F.; Li, X. L.; Tao, N. J. *Annu. Rev. Phys. Chem.* **2007**, *58*, 535-564.

(4) Tao, N. J. *Nat. Nanotechnol.* **2006**, *1*, 173-181.

(5) Zhirnov, V. V.; Cavin, R. K. *Nat. Mater.* **2006**, *5*, 11-12.

(6) Tuccitto, N.; Ferri, V.; Cavazzini, M.; Quici, S.; Zhavnerko, G.; Licciardello, A.; Rampi, M. A. *Nat. Mater.* **2009**, *8*, 41-46.

(7) Kurita, T.; Nishimori, Y.; Toshimitsu, F.; Muratsugu, S.; Kume, S.; Nishihara, H. *J. Am. Chem. Soc.* **2010**, *132*, 4524-4525.

(8) Szesni, N.; Drexler, M.; Maurer, J.; Winter, R. F.; de Montigny, F.; Lapinte, C.; Steffens, S.; Heck, J.; Weibert, B.; Fischer, H. *Organometallics.* **2006**, *25*, 5774-5787.

(9) Kaim, W.; Lahiri, G. K. *Angew. Chem. Int. Ed.* **2007**, *46*, 1778-1796.

(10) Kowalski, K.; Linseis, M.; Winter, R. F.; Zabel, M.; Zalis, S.; Kelm, H.; Kruger, H. J.; Sarkar, B.; Kaim, W. *Organometallics.* **2009**, *28*, 4196-4209.

(11) Paul, F.; Lapinte, C. *Coord. Chem. Rev.* **1998**, *180*, 431-509.

(12) Balzani, V.; Juris, A.; Venturi, M.; Campagna, S.; Serroni, S. *Chem. Rev.* **1996**, *96*, 759-833.

(13) Schwab, P. F. H.; Levin, M. D.; Michl, J. *Chem. Rev.* **1999**, *99*, 1863-1933.

(14) Belser, P.; Bernhard, S.; Blum, C.; Beyeler, A.; De Cola, L.; Balzani, V. *Coord. Chem. Rev.* **1999**, *192*, 155-169.

(15) Dembinski, R.; Bartik, T.; Bartik, B.; Jaeger, M.; Gladysz, J. A. *J. Am. Chem. Soc.* **2000**, *122*, 810-822.

(16) Jiao, H. J.; Costuas, K.; Gladysz, J. A.; Halet, J. F.; Guillemot, M.; Toupet, L.; Paul, F.; Lapinte, C. *J. Am. Chem. Soc.* **2003**, *125*, 9511-9522.

(17) Kheradmandan, S.; Heinze, K.; Schmalle, H. W.; Berke, H. *Angew. Chem. Int. Ed.* **1999**, *38*, 2270-2273.

(18) Venkatesan, K.; Fox, T.; Schmalle, H. W.; Berke, H. *Organometallics.* **2005**, *24*, 2834-2847.

(19) Venkatesan, K.; Fernandez, F. J.; Blacque, O.; Fox, T.; Alfonso, M.; Schmalle, H. W.; Berke, H. *Chem. Commun.* **2003**, 2006-2008.

(20) Lenarvor, N.; Toupet, L.; Lapinte, C. *J. Am. Chem. Soc.* **1995**, *117*, 7129-7138.

(21) Brady, M.; Weng, W. Q.; Zhou, Y. L.; Seyler, J. W.; Amoroso, A. J.; Arif, A. M.; Bohme, M.; Frenking, G.; Gladysz, J. A. *J. Am. Chem. Soc.* **1997**, *119*, 775-788.

(22) Zhou, Y. L.; Seyler, J. W.; Weng, W. Q.; Arif, A. M.; Gladysz, J. A. *J. Am. Chem. Soc.* **1993**, *115*, 8509-8510.

(23) Yam, V. W. W.; Lau, V. C. Y.; Cheung, K. K. *Organometallics.* **1996**, *15*, 1740-1744.

(24) Paul, F.; Meyer, W. E.; Toupet, L.; Jiao, H. J.; Gladysz, J. A.; Lapinte, C. *J. Am. Chem. Soc.* **2000**, *122*, 9405-9414.

(25) Bruce, M. I.; Low, P. J.; Costuas, K.; Halet, J. F.; Best, S. P.; Heath, G. A. *J. Am. Chem. Soc.* **2000**, *122*, 1949-1962.

(26) Onitsuka, K.; Ose, N.; Ozawa, F.; Takahashi, S. *J. Organomet. Chem.* **1999**, *578*, 169-177.

(27) Woodworth, B. E.; White, P. S.; Templeton, J. L. *J. Am. Chem. Soc.* **1997**, *119*, 828-829.

(28) Roberts, R. L.; Puschmann, H.; Howard, J. A. K.; Yamamoto, J. H.; Carty, A. J.; Low, P. J. *Dalton. Trans.* **2003**, 1099-1105.

(29) Semenov, S. N.; Blacque, O.; Fox, T.; Venkatesan, K.; Berke, H. *J. Am. Chem. Soc.* **2010**, *132*, 3115-3127.

(30) Roberts, J. R.; Ingold, K. U. *J. Am. Chem. Soc.* **1971**, *93*, 6686-&.

(31) Bruce, M. I.; Ellis, B. G.; Low, P. J.; Skelton, B. W.; White, A. H. *Organometallics.* **2003**, *22*, 3184-3198.

(32) Kheradmandan, S.; Venkatesan, K.; Blacque, O.; Schmalle, H. W.; Berke, H. *Chem. Eur. J.* **2004**, *10*, 4872-4885.

(33) Version 2.87 5/1998 ed.; STOE & Cie: Darmstadt, Germany, **1998**.

(34) Version 1.171.32.5 ed.; Oxford Diffraction Ltd: Abingdon, Oxfordshire, England.

(35) Sheldrick, G. M. *Acta Cryst.* **2008**, *A64*, 112-122.

(36) Spek, A. L. *J. Appl. Cryst.* **2003**, *36*, 7-13.

5. Substitution Reactions of a Dinuclear Rhenium Bisvinylidene Complex with Chloride End Groups

ABSTRACT. The neutral bisvinylidene complex *trans*-[I(PMe_3)$_4$Re=C=CH-CH=C=Re(PMe_3)$_4$I] (**16**) with iodide end groups was obtained in 80% yield via a substitution reaction of the neutral dinuclear rhenium bisvinylidene complex *trans*-[Cl(PMe_3)$_4$Re=C=CH-CH=C=Re(PMe_3)$_4$Cl] (**11**) with an excess of NaI in THF at 70 °C for 36 h. The oxidation of the neutral complex *trans*-[I(PMe_3)$_4$Re=C=CH-CH=C=Re(PMe_3)$_4$I] (**16**) with [Cp_2Fe][PF_6] in CH_2Cl_2 resulted in the dicationic dinuclear rhenium ethylenylidene biscarbyne complex *trans*-[I(PMe_3)$_4$Re≡C-CH=CH-C≡Re(PMe_3)$_4$I][PF_6]$_2$ (**16[PF_6]$_2$**) in 90% yield. The neutral dinuclear rhenium bisvinylidene complex **16** was studied by NMR spectroscopy and the dicationic dinuclear rhenium ethylenylidene biscarbyne **16[PF_6]$_2$** was characterized by NMR, IR, mass spectroscopy, elemental analysis and single crystal X-ray diffraction study.

KEYWORDS. Dinuclear rhenium complexes, Substitution reaction

5.1 Introduction

Understanding electronic transport through a single molecule is an interesting scientific challenge.[1-4] To determine the conductance of a molecule, one must bring it into reliable contact with two electrodes. Since most common electrode material is gold and the high affinity of sulfur to gold, our molecules can be equipped with appropriate anchor groups containing sulfur to guarantee strong contact to the gold surface. Thiol group and its protected form, the thioacetyl group are frequently used as anchor group in organic systems. These groups are advantageous owing to the possibility of a comparison with the organic species, such as oligo(2,5-thiophene ethynylene)s (OTEs), oligo(1,4-phenylene ethylene)s (OPEs) systems. The thioacetyl group is especially interesting due to its relative low reactivity and its easy conversion to thiol group by *in-situ* deprotection. Therefore, substitution of the end groups of the synthesized compounds with the thioacetyl end groups for the measurement of single-molecule conductance is one of our targets.

The substitution reaction was mainly carried out on the neutral dinuclear rhenium bisvinylidene complex *trans*-[Cl(PMe_3)$_4$Re=C=CH-CH=C=Re(PMe_3)$_4$Cl] (**11**) with replaceable

chloride end groups. Since the iodide ligand tends to show higher reactivity than the chloride ligand in substitution reactions, the preparation of the neutral dinuclear rhenium bisvinylidene complex with iodide ligands was sought by the substitution of the chloride ligands in the neutral dinuclear rhenium bisvinylidene complex *trans*-[Cl(PMe_3)$_4$Re=C=CH-CH=C=Re(PMe_3)$_4$Cl] (**11**) with NaI in THF. The preparation of the ligands with "anchor groups" thioacetyl groups, such as 1-(S-trimethylacetylthio)-4-iodobenzene and 1-[4-(S-trimethylacetylthio)phenyl]acetylene are also described in the experimental part of this chapter.

5.2 Syntheses and characterization of complexes with iodide end groups

5.2.1 Syntheses of the dinuclear rhenium complexes **16** and **16[PF_6]$_2$**

As depicted in Scheme 1, the iodide substituted complex *trans*-[I(PMe_3)$_4$Re=C=CH-CH=C=Re(PMe_3)$_4$I] (**16**) was obtained by the reaction of the neutral dinuclear rhenium bisvinylidene complex *trans*-[Cl(PMe_3)$_4$Re=C=CH-CH=C=Re(PMe_3)$_4$Cl] (**11**) with an excess of NaI in THF at 70 °C for 36 h. The transformation of **11** to **16** upon treatment with KI was much slower than that with NaI. Applying the same reaction condition, after heating at 70 °C for 8 days, the reaction mixture was still in the 1:1 ratio of **11** and **16**. The oxidation of the complex **16** with [Cp_2Fe][PF_6] in CH_2Cl_2 resulted in dicationic dinuclear rhenium ethylenylidene biscarbyne complex *trans*-[I(PMe_3)$_4$Re≡C-CH=CH-C≡Re(PMe_3)$_4$I][PF_6]$_2$ (**16[PF_6]$_2$**). To avoid the decomposition of **16** in CH_2Cl_2, [Cp_2Fe][PF_6] was mixed with the starting material **11** before the addition of the solvent CH_2Cl_2. Due to the limitation of time, the comproportion reaction of the corresponding neutral complex **16** with the dicationic complex**16[PF_6]$_2$** or the oxidation reaction of **16** with one equiv. of [Cp_2Fe][PF_6] to get the MV complex **16[PF_6]** has not been carried out yet, which will be completed in the future.

Scheme 1

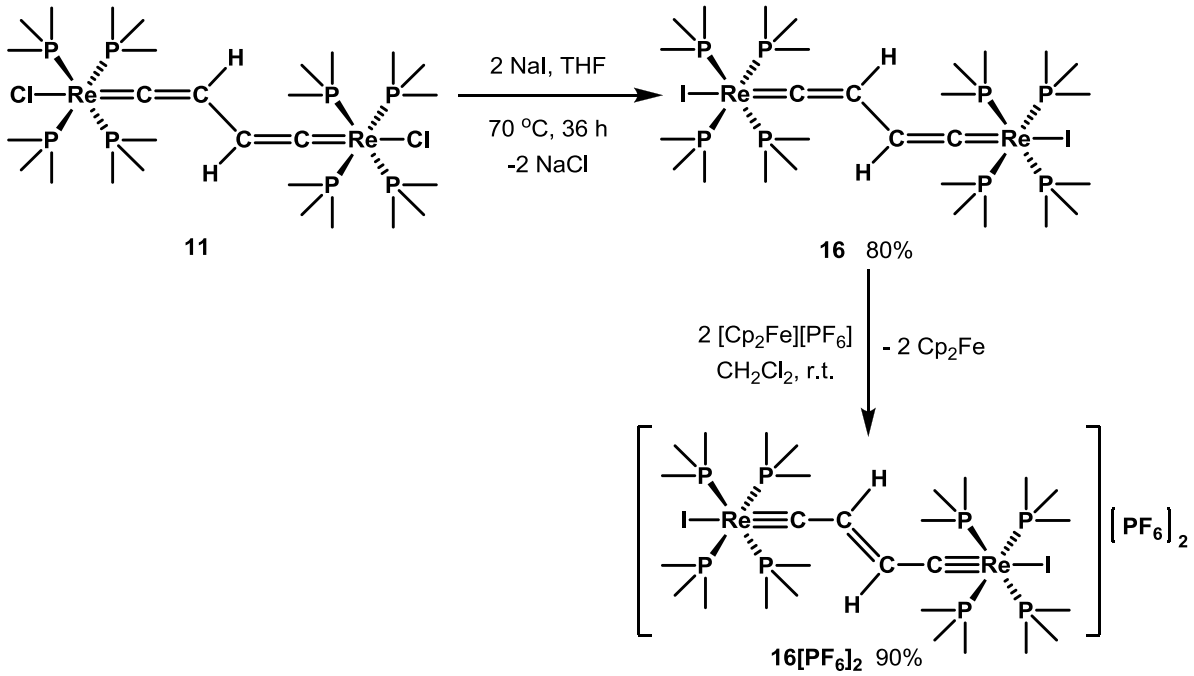

5.2.2 Characterization of the dinuclear rhenium complexes **16** and **16[PF$_6$]$_2$**

The neutral dinuclear rhenium bisvinylidene complex **16** was studied by NMR spectroscopy and the dicationic dinuclear rhenium ethylenylidene biscarbyne **16[PF$_6$]$_2$** was characterized by NMR, IR, mass spectroscopy, elemental analysis and single crystal X-ray diffraction study. Selected ^{1}H NMR, ^{13}C NMR and ^{31}P NMR data for the neutral complex **16** and for the dicationic complex **16[PF$_6$]$_2$** are listed along with selected data for **11[PF$_6$]$_2$** in Table 5-1 for comparison.

Table 5-1. Selected ^{1}H NMR and ^{31}P NMR data for the neutral complex **16** in THF-d$_8$, and the dicationic complexes **11[PF$_6$]$_2$** and **12[PF$_6$]$_2$** in CD_2Cl_2

Complexes	^{13}C NMR (δ, ppm)		^{1}H NMR (δ, ppm)	^{31}P NMR (δ, ppm)
	C_α	C_β	H_β	PMe_3
[I(PMe$_3$)$_4$Re=C=CH] (**16**)	/	/	2.00	-46.6
[Cl(PMe$_3$)$_4$Re≡C-CH]$_2$[PF$_6$]$_2$ (**11[PF$_6$]$_2$**)	255.5	144.0	5.76	-37.3
[I(PMe$_3$)$_4$Re≡C-CH]$_2$[PF$_6$]$_2$ (**16[PF$_6$]$_2$**)	247.4	142.5	5.98	-53.5

The ^{1}H NMR spectrum of the neutral complexes *trans*-[I(PMe$_3$)$_4$Re=C=CH-CH=C=Re(PMe$_3$)$_4$I] (**16**) showed a doublet resonance for the vinylidene protons at 2.00 ppm. The measurement of the $^{13}C\{^{1}H\}$ NMR spectrum was unsuccessful due to the very air-sensitive nature of the compound. During the measurement, the neutral complex gradually transform into a paramagnetic mixture, which prevented detection by the $^{13}C\{^{1}H\}$ NMR. In the ^{31}P NMR spectrum, the resonance at -46.6 ppm was ascribed to the P(CH$_3$)$_3$ ligands. The ^{1}H NMR spectrum of the dicationic ethylenylidene biscarbyne complexes *trans*-[I(PMe$_3$)$_4$Re≡C-CH=CH-C≡Re(PMe$_3$)$_4$I][PF$_6$]$_2$ (**16[PF$_6$]$_2$**) showed resonance of the vinylidene protons appraring as a singlet at 5.98 ppm, which underwent a down-field shift compared to the signal of **11[PF$_6$]$_2$** . The $^{13}C\{^{1}H\}$ NMR spectrum of **16[PF$_6$]$_2$** revealed characteristic resonances for the C_α and C_β nuclei at 247.4 ppm ($^{2}J_{PC}$ = 13.6 Hz) and 142.5 ppm. According to Table 5-1, the resonances of C_α and C_β showed an up-field shift, compared to those of **11[PF$_6$]$_2$**, revealing the carbon backbone in the complex **16[PF$_6$]$_2$** with iodide ligands is slightly more electron-rich than the complex **11[PF$_6$]$_2$** with chloride end groups. In the ^{31}P NMR spectra, the resonances at -53.5 ppm was asigned to the P(CH$_3$)$_3$ ligand. The PF_6^- characteristic signal appeared as a septet at -143.9 ppm.

X-ray diffraction analysis (Fig 5-1) was carried out on the dicationic complex **16[PF$_6$]$_2$**. Selected bond distances and bond angles are summarized in Table 5-2.

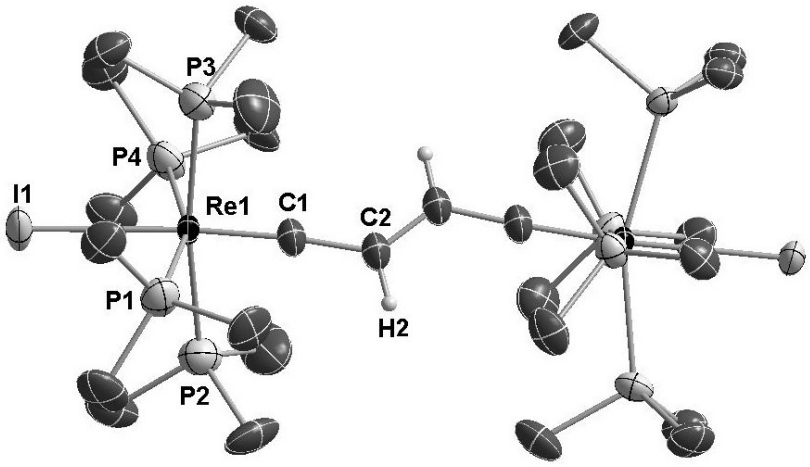

Fig 5-1. ORTEP like drawing of *trans*-[I(PMe$_3$)$_4$Re=C=CH-CH=C=Re(PMe$_3$)$_4$I][PF$_6$]$_2$ (**16[PF$_6$]$_2$**) (50% probability level of thermal ellipsoids, solvent molecules, PF_6^- counterions and selected hydrogen atoms are omitted for clarity.)

Table 5-1. Selected bond lengths [Å] for **16[PF$_6$]$_2$**, assignment of the bond lengths in the C_4 bridge according to the following notation: I[Re]C1C2C2'C1'[Re']I'

Selected bond lengths [Å]						
C2-C2'	C1-C2	C1-Re1	I1-Re1	C2'-C1'	C1'-Re1'	I1'-Re1'
1.30(2)	1.44(3)	1.75(3)	2.8472(6)	1.40(3)	1.78(3)	2.8538(6)

Table 5-2. Selected bond angles [º] for **16[PF$_6$]$_2$**, assignment of the bond angles in the C_4 bridge according to the following notation: I[Re]C1C2C2'C1'[Re']I'

Selected angles [º]		
C2-C1-Re1	C2'-C2-C1	C2'-C1'-Re1'
175(2)	132.6(19)	176.0(19)
C1-Re1-I1	C2- C2'-C1'	C1'-Re1'-I1'
174.3(7)	129.7(19)	175.7(7)

The average Re-I bond distance for the dicationic complexes **16[PF$_6$]$_2$** is 2.8505(6) Å. The average Re-C bond length is 1.76(8) Å, which is slightly longer than the expected distance range (1.75-1.72 Å) of the Re≡C (sp) triple-bonded covalent radii. The average C1-C2 bond lengths is 1.42(3) Å is longer than the C=C double bond range (1.33-1.38 Å), but shorter than the C-C single bond range (1.47-1.54 Å). The C2–C2' distance 1.30(2) is shorter than the C=C double bond range (1.33-1.38 Å). The C1-C2-C2' bond angle and the C2-C2'-C1 bond angle are 132.6(12)° and 129.7(19)°, respectively. The Re-C-C and I-Re-C bond angles are slightly less than 180°.

5.3 Experimental section

General procedures: All the manipulations were carried out under a nitrogen atmosphere using Schlenk techniques or a glove box (M. Braun150B-G-II). Reagent grade benzene, toluene,

hexane, pentane, diethyl ether and tetrahydrofuran were dried and distilled from sodium benzophenone ketyl prior to use. Dichloromethane and acetonitrile were distilled from CaH_2. All other chemicals were directly used as obtained from commercial suppliers. CHN elemental analyses were performed with a LECO CHN-932 microanalyzer. IR spectra were obtained on a Bio-Rad FTS-45 instrument. NMR spectra were measured on a Varian Mercury spectrometer at 200 MHz for ^{1}H NMR, 81 MHz for ^{31}P NMR, 188 MHz for ^{19}F NMR, Varian Gemini-2000 spectrometer at 300 MHz for ^{1}H NMR and 75 MHz for ^{13}C NMR, and on a Bruker-DRX-500 spectrometer at 500 MHz for ^{1}H NMR, 125.8 MHz for ^{13}C NMR, 202.5 MHz for ^{31}P NMR, and 99.4 MHz for ^{29}Si NMR. Chemical shifts for ^{1}H NMR, ^{31}P NMR, ^{13}C NMR, and ^{29}Si NMR are given in ppm relative to TMS and those for ^{31}P are relative to phosphoric acid.

X-ray diffraction study on 16[PF_6]$_2$: Data collection for all crystals were carried out on Stoe IPDS diffractometer (Imaging Plate Detector System with graphite-monochromated MoK_α radiation, λ = 0.71073 Å)[5] and for others on Oxford Diffraction Xcalibur R diffractometer (4-circle kappa platform, Ruby CCD detector and a single wavelength Enhance X-ray source with MoK_α radiation, λ = 0.71073 Å) at 183(2) K using a cold N_2-gas stream from an Oxford Cryogenic System. Pre-experiment, data collection and data reduction (unit cell determination, intensity data integration and empirical absorption correction) were carried out with the Oxford *CrysAlisPro* software.[6] The structures were solved with the unique data sets using the Patterson method of the program SHELXS-97. The structure refinement was performed with the program SHELXL-97.[7] Non-hydrogen atoms were refined anisotropically by full-matrix least-squares techniques based on F^2. The hydrogen atoms of the organic groups were placed in calculated positions and refined with a riding model with a fixed temperature factor. The program PLATON[8] was used to check the result of the X-ray analysis.

***trans*-[I(PMe$_3$)$_4$Re=C=CH-CH=C=Re(PMe$_3$)$_4$I] (16).** *Trans*-[ReCl(≡C-CH)(PMe$_3$)$_4$]$_2$ (**11**) (26.8 mg, 0.024 mmol), NaI (14.2 mg, 0.24 mmol) and THF (5 mL) were mixed in a Young-schlenk flask. The reaction mixture was heated at 70 °C for 36 h. After filtration, the solution was dried *in vacuo* and the residue was extracted with benzene followed by filtration. Evaporation of the solution to dryness gave the compound *trans*-[I(PMe$_3$)$_4$Re=C=CH-CH=C=Re(PMe$_3$)$_4$I]. Yield: 25.0 mg (0.019 mmol, 80% based on *trans*-[ReCl(≡C-

CH)(PMe_3)$_4$]$_2$). ^{1}H NMR (THF-d_8, 200 MHz, 22 °C): δ = 1.68 (s, P(CH_3)$_3$), 2.00 (d, CH); ^{31}P NMR (THF-d_8, 81 MHz, 22 °C:) δ = -46.6 (s, P(CH_3)$_3$).

***trans*-[I(PMe_3)$_4$Re≡C-CH=CH-C≡Re(PMe_3)$_4$I][PF_6]$_2$ (16[PF_6]$_2$).** *Trans*-[ReCl(≡C-CH)(PMe_3)$_4$]$_2$ (**11**) (11.0 mg, 0.01 mmol), NaI (6.0 mg, 0.10 mmol) and THF (2 mL) were mixed in a Young-schlenk flask. The reaction mixture was heated at 70 °C for 36 h. After evaporation of solvent to dryness *in vacuo*, the residue was mixed with [Cp_2Fe][PF_6] (6.4 mg, 0.02 mmol) and CH_2Cl_2 was added. The reaction mixture was stirred at room temperature for 30 min resulting in an orange-red solution. After filtration through celite, the solution was concentrated and precipitation was effected by the addition of diethyl ether. The product **16[PF_6]$_2$** was collected, washed with ether (3 × 2 mL), and dried *in vacuo*. Yield: 14.2 mg (0.009 mmol, 90% based on *trans*-[ReCl(≡C-CH)(PMe_3)$_4$]$_2$ (**11**)). Single crystals suitable for X-ray diffraction were grown by layering diethyl ether over an acetonitrile solution of **16[PF_6]$_2$**. Anal. Calcd For $C_{28}H_{74}F_{12}I_2P_{10}Re_2$ (1574.83 g/mol): C 21.35; H 4.74. Found: C 21.58; H 4.80. IR (ATR, cm^{-1}): ν = 938 (C-P). MS(ESI): *m/z* (100%):1429 [M^+-2H]. ^{1}H NMR (CD_2Cl_2, 200 MHz, 22 °C): δ = 5.98 (s, C_βH), 1.93 (s, P(CH_3)$_3$); ^{13}C NMR (CD_2Cl_2, 125.8 MHz, 10 °C): δ = 247.4 (quint, $^2J_{PC}$ = 13.6 Hz, Re≡C_α), 142.5 (s, C_βH), 22.9 (s, P(CH_3)$_3$); ^{31}P NMR (CD_2Cl_2, 81 MHz, 22 °C): δ = -53.5 (s, P(CH_3)$_3$), -143.9 (sept, J = 710 Hz, 1P, PF_6); ^{19}F NMR (CD_2Cl_2, 188 MHz, 22 °C): δ = -73.3 (d, J = 713 Hz, PF_6).

1-(S-trimethylacetylthio)-4-iodobenzene. Method a: A solution of pipsyl chloride (3.1 g, 10.2 mmol) and dimethylacetamide (2.9 mL, 30.7 mmol) in 1,2-dichloroethane (50 mL) was added dropwise into a stirring suspension of zinc powder (2.4 g, 35.9 mmol) and dichloromethylsilane (4.4 mL, 35.9 mmol) in 1,2-dichloroethane (50 mL) during 30 min. The reaction mixture was stirred at 75 °C for 1.5 h followed by the addition of K_2CO_3 powder (0.9 g, 5.6 mmol). When the zinc powder almost disappeared, the mixture was kept stirring for further 30 min at the same temperature. Then the mixture was cooled to 60 °C and the trimethylacetyl chloride (5.1 mL, 41.0 mmol) was added in one portion. The resulting mixture was stirred at 60 °C for 3 h and subsequently warmed up to room temperature and kept stirring overnight. The filtrate was washed with brine and then extracted with methylene chloride (3 × 50 mL). The combined organic fractions were dried over magnesium sulfate. After filtration, the solvent was

evaporated and the residue was purified by silica gel flash chromatography using 1:1 hexane/CH_2Cl_2 elution (3.0 g, 90%).

Method b: To a solution of 1, 4-diiodobenzene (5.0 g, 15.0 mmol) in diethyl ether (50 mL), tert-butyllithium (8.3 mL , 15.0 mmol, 1.8 M in heptane) was added dropwise at -78 °C. The reaction mixture was stirred at -78 °C for 5 min. Sulfur powder (0.08 g, 15.0 mmol) in THF (75 mL) was added at 0 °C and the mixture was warmed up to 0 °C for 30 min. Afterwards, it was cooled to -78 °C again, subsequently trimethylacetyl chloride (1.9 mL, 15.0 mmol) was added in one portion. The mixture was allowed to warm up to room temperature and kept stirring overnight. The mixture was extracted with dichloromethane and dried over magnesium sulfate. After removal of the solvent, the residue was purified by silica gel flash chromatography using 25:1 hexane/diethyl ether elution (2.5 g, 56%). IR (ATR, cm^{-1})**:** ν(C-H) 2974, 29301, 2902, 2866; ν(CO) 1691, 1468; $\nu(C{=}C)_{Ar}$ 1564; ν(C-S) 920, 619. ^{1}H NMR ($CDCl_3$, 300 MHz, 22 °C)**:** δ = 7.7 (2H, Ar-H), 7.1(2H, Ar-H), 1.3 (9H, $-CH_3$). ^{13}C NMR ($CDCl_3$, 75 MHz, 22 °C)**:** δ = 204.0 (CO), 138.3 ($C_{Ar\text{-}H}$), 136.6 ($C_{Ar\text{-}H}$), 128.2 ($C_{Ar\text{-}S}$), 95.7 ($C_{Ar\text{-}I}$), 47.2 (*t*-C), 27.5 ($-CH_3$).

1-[4-(S-trimethylacetylthio)phenyl)]-2-(trimethylsilyl)acetylene. To a solution of 1-(S-trimethylacetylthio)-4-iodobenzene (0.64 g, 2.0 mmol) in THF (5 mL) was added $Pd(PPh_3)_2Cl_2$ (0.07 g, 0.1 mmol), CuI (0.02 g, 0.1 mmol), DIPEA(5 mL) and trimethylsilylacetylene (0.3 mL, 2.0 mmol), then the mixture was stirred at 85 °C for 10 h. After filtration, the solvent was removed, and the residue was purified by silica gel flash chromatography using 4:1 hexane/CH_2Cl_2 elution (0.5 g, 86%). IR (ATR, cm^{-1})**:** ν(C-H) 2970; ν(C≡C) 2158; ν(CO) 1689, 1483, ν(C-S) 926, 622. ^{1}H NMR ($CDCl_3$, 300MHz, 22 °C)**:** δ = 7.47 (2H, Ar-H), 7.34 (2H, Ar-H), 1.32 (9H, $-CH_3$), 0.26 (9H, Si-CH_3). ^{13}C NMR ($CDCl_3$, 75 MHz, 22 °C)**:** δ = 204.0 (CO), 134.7 ($C_{Ar\text{-}H}$), 132.5 ($C_{Ar\text{-}H}$), 128.7 ($C_{Ar\text{-}S}$), 124.1 ($C_{Ar\text{-}C}$), 104.4 (≡C-Ph), 96.0 (≡C-Si), 47.2 (*t*-C), 27.5 ($-CH_3$), 0.1 (Si-CH_3).

1-[4-(S-trimethylacetylthio)phenyl]acetylene. To a solution of 1-[4-(S-trimethylacetylthio)phenyl]-2-(trimethylsilyl)acetylene (1.0 g, 3.4 mmol) in CH_2Cl_2 (50 mL), *n*-Bu_4NF (3.4 mL, 1.0 M in THF) was added dropwise during 5 min. The reaction mixture was stirred at 0 °C for another 10 min and then purified via silica gel flash chromatography (1:7 CH_2Cl_2/hexane) to provide 0.64 g (85%) of the desired product as a pale yellow-orange solid. IR (ATR, cm^{-1})**:** ν(C-H) 3261, 2973; ν(C≡C) 2111; ν(CO) 1678, 1475; ν(C-S) 931, 625. ^{1}H NMR

($CDCl_3$, 300MHz, 22 °C)**:** δ = 7.51 (2H, Ar-H), 7.37 (2H, Ar-H), 3.15(1H, C≡C-H), 1.33 (9H, -CH_3). ^{13}C NMR ($CDCl_3$, 75 MHz, 22 °C)**:** δ = 204.0 (CO), 134.8 (C_{Ar-H}), 132.7 (C_{Ar-H}), 129.2 (C_{Ar-S}), 123.1 (C_{Ar-C}), 83.1 (≡C-H), 78.7 (≡C-Ph), 47.2 (*t*-C), 27.5 (-CH_3).

5.4 References

(1) Aviram, A.; Ratner, M. A. *Chem. Phys. Lett.* **1974**, *29*, 277-283.

(2) Joachim, C.; Gimzewski, J. K.; Aviram, A. *Nature.* **2000**, *408*, 541-548.

(3) Nitzan, A.; Ratner, M. A. *Science.* **2003**, *300*, 1384-1389.

(4) Mayor, M.; Weber, H. B.; Reichert, J.; Elbing, M.; von Hanisch, C.; Beckmann, D.; Fischer, M. *Angew. Chem. Int. Ed.* **2003**, *42*, 5834-5838.

(5) Version 2.87 5/1998 ed.; STOE & Cie: Darmstadt, Germany, **1998**.

(6) Version 1.171.32.5 ed.; Oxford Diffraction Ltd: Abingdon, Oxfordshire, England.

(7) Sheldrick, G. M. *Acta Cryst.* **2008**, *A64*, 112-122.

(8) Spek, A. L. *J. Appl. Cryst.* **2003**, *36*, 7-13.

6. Summary

During the recent years, in the pursuit of a miniaturization of electronic components, the field of molecular electronics has greatly expanded in chemistry, physics, and material science. Molecular wire is one of the basic components of a molecular-level electrical circuitry. Many sophisticated devices are based on molecular wires.

Organometallic molecular wires obtained by the incorporation of redox-active metal centers into rigid-rod π-conjugated organic backbones are one of the promising species for long-ditance and highly "conductive" molecular wires. The through-bridge electronic interaction of the metal centers exerts significant influence on the chemical and physical properties, which greatly depend on the metal centers, the ancillary ligands and the bridging ligands. The reported C_4-bridged dinuclear rhenium complexes indicated strong electronic communication between the metal centers. However, these complexes are stopper-type, since further functionalization for fixation of the electrode "anchor" groups and extension to oligonuclears is prevented.

Scheme 1

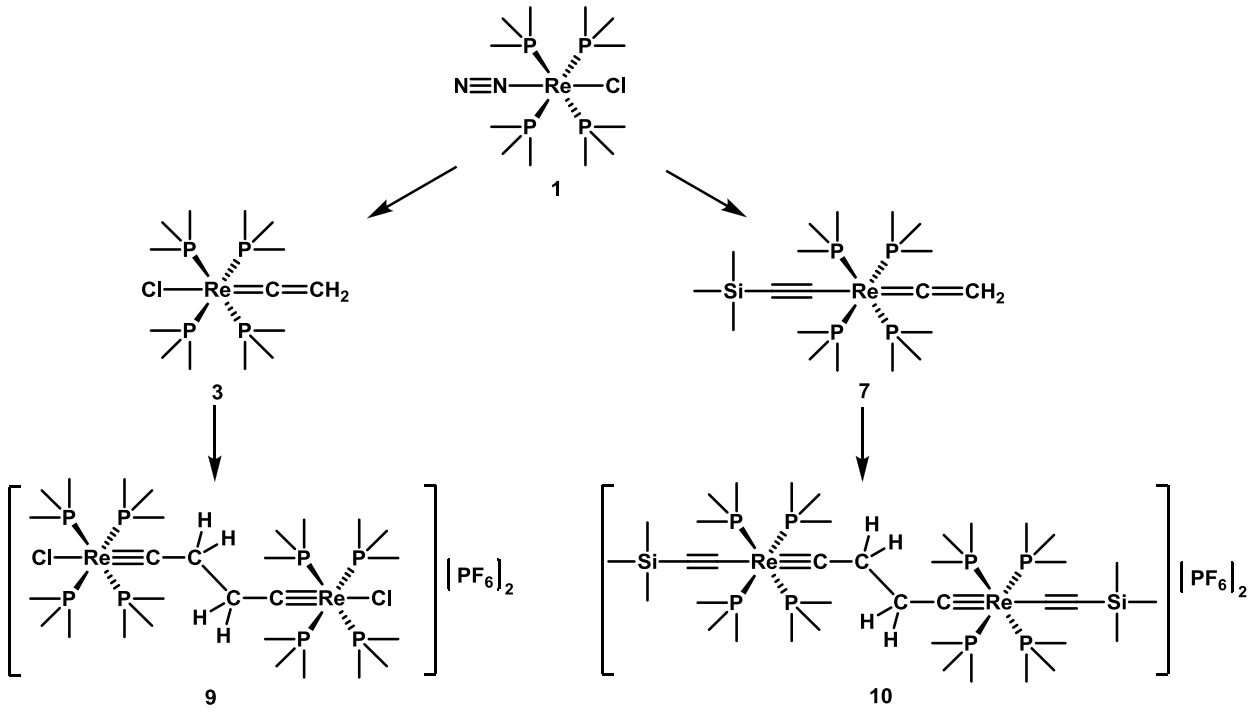

As shown in Scheme 1, to obtain C_4-bridged dinuclear rhenium complexes with replaceable substituents, the dinitrogen rhenium complex *trans*-[$ReCl(N_2)(PMe_3)_4$] (**1**) was chosen as a

suitable starting material due to the oxidative coupling of metal alkynyls or oxidative dehydro-dimerization of metal vinylidenes was sought as an effective method to access dinuclear bis(acetylide) or bis(vinylidene) complexes. Two kinds of mononuclear rhenium vinylidene complexes *trans*-[XRe(=C=CH_2)(PMe_3)$_4$] (X = Cl, **3**; C≡$CSiMe_3$, **7**) were prepared in excellent yields starting from the dinitrogen complex **1** and the oxidative coupling reaction of the vinylidene complexes **3** and **7** were explored. Factors, such as temperature, solvent and the order of reagent addition significantly affected the formation of the final product, from a mixture to the exclusive formation of the C_β-C_β' coupled products *trans*-[X(PMe_3)$_4$Re≡C-CH_2-CH_2-C≡Re(PMe_3)$_4$X][PF_6] (X = Cl, **9**; C≡$CSiMe_3$, **10**) in excellent yields. The reduction of **10** with sodium benzophenone ketyl in THF resulted in the corresponding neutral bisvinylidene complex.

Scheme 2

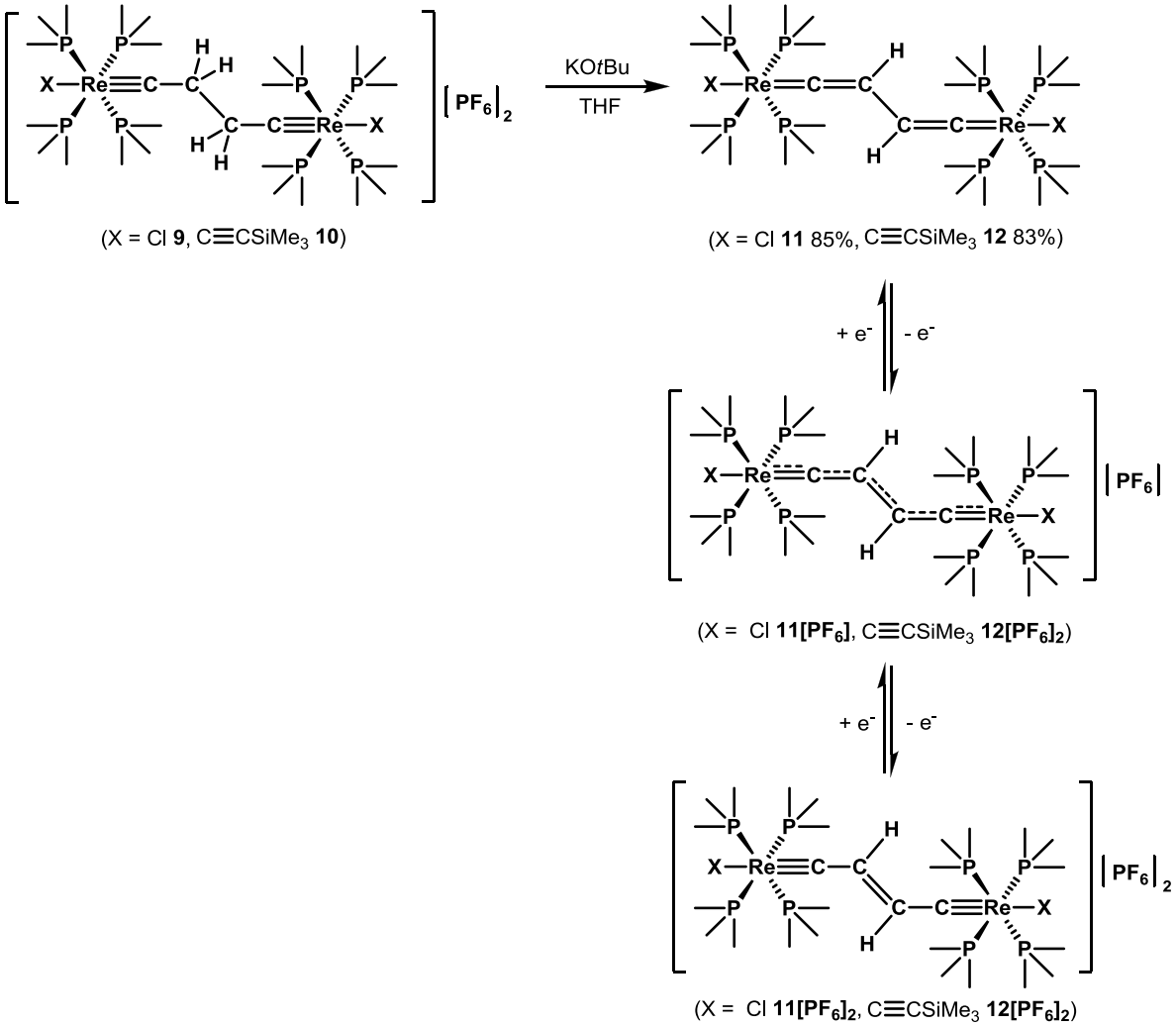

(X = Cl **9**, C≡$CSiMe_3$ **10**)

(X = Cl **11** 85%, C≡$CSiMe_3$ **12** 83%)

(X = Cl **11**[PF_6], C≡$CSiMe_3$ **12**[PF_6]$_2$)

(X = Cl **11**[PF_6]$_2$, C≡$CSiMe_3$ **12**[PF_6]$_2$)

As shown in Scheme 2, starting from the dinuclear rhenium biscarbyne complexes *trans*-$[X(PMe_3)_4Re{\equiv}C\text{-}CH_2\text{-}CH_2\text{-}C{\equiv}Re(PMe_3)_4X][PF_6]$ (X = Cl, **9**; C≡CSiMe$_3$, **10**), a family of sp^2 C_4H_2-bridged dinuclear rhenium complexes *trans*-$[X(PMe_3)_4Re{=}C{=}CH\text{-}CH{=}C{=}Re(PMe_3)_4X]$ (X = Cl, **11**; C≡CSiMe$_3$, **12**), *trans*-$[X(PMe_3)_4Re{\equiv}C\text{-}CH{=}CH\text{-}C{\equiv}Re(PMe_3)_4X][PF_6]$ (X = Cl, **11[PF$_6$]**; C≡CSiMe$_3$, **12[PF$_6$]**) and *trans*-$[X(PMe_3)_4Re{\equiv}C\text{-}CH{=}CH\text{-}C{\equiv}Re(PMe_3)_4X][PF_6]_2$ (X = Cl, **11[PF$_6$]$_2$**; C≡CSiMe$_3$, **12[PF$_6$]$_2$**) were synthesized. The neutral complexes **11** and **12** were obtained by the deprotonation of the biscarbyne complexes **9** and **10**. A stepwise oxidation of the neutral complexes with $[Cp_2Fe][PF_6]$ gave the MV complexes **11[PF$_6$]** and **12[PF$_6$]** and the dicationic complexes **11[PF$_6$]$_2$** and **12[PF$_6$]$_2$**. All the dinuclear rhenium complexes have been were characterized by NMR, IR, Raman, elemental analysis and single crystal X-ray diffraction studies. The oxidation reactions of **11** and **12** to **11[PF$_6$]$_2$** and **12[PF$_6$]$_2$** resulted in the transformation of the valence structure of the sp^2 C_4H_2 bridge from a bisvinylidene (=C=CH-CH=C=) to an ethylenylidene biscarbyne (≡C-CH=CH-C≡) form, which were verified by NMR, IR and Raman, and X-ray diffraction analyses. Cyclic voltammetry (CV), UV-vis spectroscopy for all dinuclear rhenium complexes, EPR spectroscopy and variable-temperature magnetization measurements for the MV complexes **11[PF$_6$]** and **12[PF$_6$]** were also investigated. The CV spectra of the dicationic species **11[PF$_6$]$_2$** and **12[PF$_6$]$_2$** indicated that the neutral complexes **11** and **12** were good reducing agents and give large K_c of 1.8×10^{10} and 7.1×10^7, respectively. The large K_c values revealed high thermodynamic stabilities of the MV compounds under CV conditions. The UV-vis spectra of the complexes **11**, **11[PF$_6$]**, **11[PF$_6$]$_2$**, **12**, **12[PF$_6$]**, and **12[PF$_6$]$_2$** show intense absorption bands in the visible and ultraviolet region, which were attributed to metal-to-ligand charge transfer (MLCT) transitions. In the visible and near-infrared region, an additional absorption band is observed at approximately 772 nm (ε is about 1.3×10^4 M^{-1} cm^{-1}) with a notable shoulder at ~ 700 nm for **11[PF$_6$]** and at 897 nm (ε is about 1.9×10^4 M^{-1} cm^{-1}) with an intense shoulder at ~ 800 nm for **12[PF$_6$]**. Both were assigned to the IVCT bands. The overlapping IVCT bands were deconvoluted into three Gaussian-shape bands with a feature pertaining to class III species (Robin & Day classification). The electronic coupling energy H_{ab} and the delocalization parameters Γ for the MV complexes **11[PF$_6$]** and **12[PF$_6$]** are 7068 cm^{-1} and 6100 cm^{-1}, and 0.63 and 0.59, respectively. Based on the CV and NIR spectroscopic data, **11[PF$_6$]** and **12[PF$_6$]** can be safely described as a class III MV compound. **11[PF$_6$]** and **12[PF$_6$]**

were EPR-silent at 300-30K, broad signals with reasonable intensities were only observed below 13 K without hyperfine coupling. Variable-temperature magnetic susceptibility measurements for **11[PF_6]** and **12[PF_6]** displayed a typical paramagnetic behavior.

Scheme 3

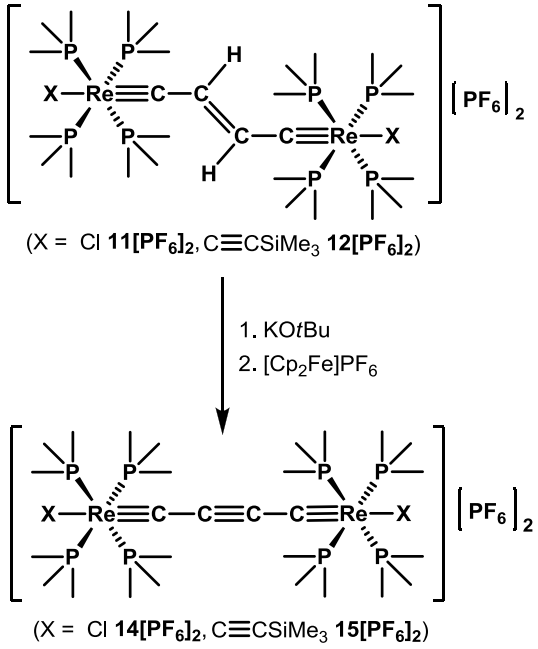

The dicationic dinuclear rhenium alkynediyl biscarbyne complexes *trans*-[$X(PMe_3)_4Re{\equiv}C$-$C{\equiv}C$-$C{\equiv}Re(PMe_3)_4X][$PF_6$]$_2$ (X = Cl, **14[PF_6]$_2$**; $C{\equiv}CSiMe_3$, **15[PF_6]$_2$**) were obtained by the deprotonations of the ethylenylidene biscarbyne complexes **11[PF_6]$_2$** and **12[PF_6]$_2$** with KO*t*Bu followed by the subsequent oxidation with [Cp_2Fe][PF_6] (Scheme 3). **15[PF_6]$_2$** was obtained as a pure product, while **14[PF_6]$_2$** was achieved as a product along with 5~10% starting material **11[PF_6]$_2$**. The neutral dinuclear rhenium cumulenic complex **15** could not be isolated from the reduction of the alkynediyl biscarbyne complex **15[PF_6]$_2$**. The neutral complex **15** is sensitive to O_2, gradually transforms into a less-defined brown mixture in solution, and decomposes immediately upon heating and in polar solvents, such as CH_2Cl_2, CH_3CN and acetone. **15** is thermodynamically less stable than the neutral bisvinylidene complex **12** probably due to a singlet/triplet spin equilibrium in **15**. The cyclic voltammetry (CV) studies on **14[PF_6]$_2$** and **15[PF_6]$_2$** displayed large K_c values of 6.4×10^9 and 4.7×10^8, respectively, revealing high thermodynamic stability of the mixed-valence (MV) complexes under CV conditions. The CV investigations also suggested that the electronic properties of the end groups have significant

influence on the K_c values and the ability to conduct electrons of the ethylenylidene biscarbyne (≡C-CH=CH-C≡) bridge and of the alkynediyl biscarbyne (≡C-C≡C-C≡) bridge might be similar.

Scheme 4

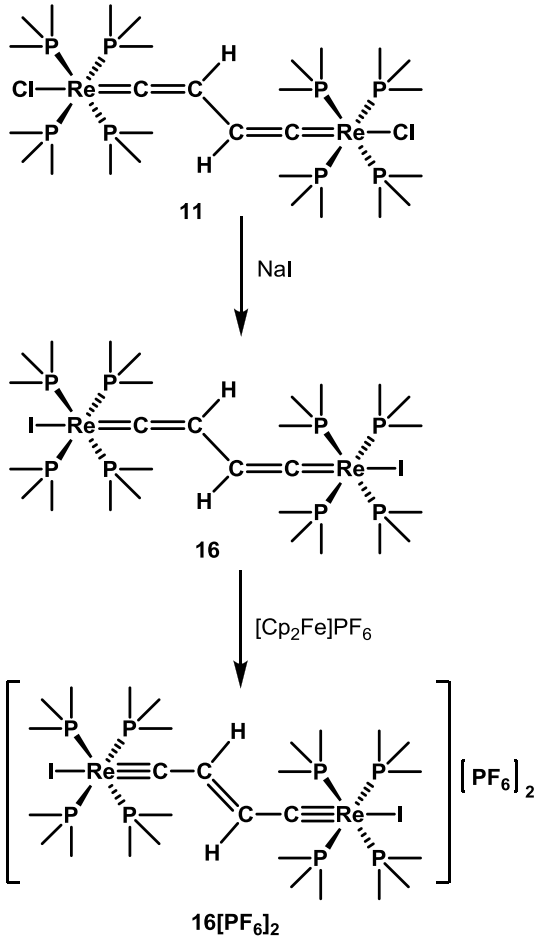

The substitution of the chloride ligands in the neutral dinuclear rhenium bisvinylidene complex *trans*-[Cl(PMe$_3$)$_4$Re=C=CH-CH=C=Re(PMe$_3$)$_4$Cl] (**11**) with the iodide ligands was carried out by the treatment with an excess of NaI in THF. The reaction resulted in the iodide substituted complex *trans*-[I(PMe$_3$)$_4$Re=C=CH-CH=C=Re(PMe$_3$)$_4$I] (**16**). The dicationic dinuclear rhenium ethylenylidene biscarbyne complex *trans*-[I(PMe$_3$)$_4$Re≡C-CH=CH-C≡Re(PMe$_3$)$_4$I][PF$_6$]$_2$ (**16[PF$_6$]$_2$**) was obtained by the oxidation of the neutral complex **16** with [Cp$_2$Fe][PF$_6$].

7. Zusammenfassung

In den vergangenen Jahren führte das Streben nach immer kleineren elektronischen Komponenten zu einer Zunahme der Forschungsaktivität im Bereich der molekularen Elektronik in der Chemie, der Physik und der Materialwissenschaft. Molekulare Drähte gehören zu den grundlegenden Komponenten eines elektronischen Schaltkreises auf molekularer Ebene. Zudem basieren viele anspruchsvolle Bausteine molekularer Elektronik auf molekularen Drähten.

Metallorganische molekulare Drähte, in welchen redox-aktive Metallzentren in starre und lineare π-konjugierte organische Gerüste eingebettet sind, gehören zu den erfolgsversprechendsten Molekülen, um lange und hoch leitfähige molekulare Drähte zu erhalten. Die elektronische Kommunikation der Metallzentren durch die organische Brücke hat einen starken Einfluss auf die chemischen und physikalischen Eigenschaften des Komplexes und ist abhängig von der Art der Metallzentren, des verbrückenden Liganden und der anderen am Metall gebundenen Liganden. Die in der vorliegenden Arbeit beschriebenen C_4-verbrückten dinuklearen Rhenium Komplexe zeigen eine ausgeprägte elektronische Kommunikation der Metallzentren. Jedoch gehören die beschriebenen Verbindungen zur Klasse der sog. „Stopper“, da weder die weitere Funktionalisierung mit Ankergruppen, welche eine Fixierung an Elektroden erlauben würde, noch die Erweiterung zu oligonuklearen Molekülen möglich ist.

Acknowledgements

First of all, I would like to thank my supervisor, Prof. Dr. Heinz Berke, for giving me the opportunity to study in his group, for having introduced me into this fascinating and challenging field and for his excellent guidance and generous support that he provided throughout this work. I would like to extend my special thanks and appreciation to Dr. Koushik Venkatesan for a great deal of interesting scientific discussions, for his stimulating and encouragement, and for all the help that he provided during my work.

I am also very grateful to Dr. Olivier Blacque for X-ray crystal structure analyses; Dr. Thomas Fox for NMR measurements especially for his tireless effort and a great patience on time consuming samples; Dr. Ferdinand Wild for MS and Raman analyses; Hanspeter for his great help to maintain the glovebox in good condition; Mr. Heinz Spring and Mrs. Barbara Spring for elemental analyses; Mr. Manfred Jöhri for his great support in computer techniques and Dr. Christian Frech for his great help in lab.

I would like to thank Dr. Sergey N. Semenov for providing tremendous support for CV, NIR, EPR and magnetic measurements.

Furthermore, I would like to extend my sincere gratitude to Ms. Beatrice Spichtig, Ms. Susanna Sprokkereef, Ms. Tanja Spörri, Ms. Nathalie Fichter and Dr. Jae Kyoung Pak for their assistance in administrative affairs and their generous help in my work and my life in Zurich during all these years.

I would like to thank my gloveboxes members Carolina Egler, Subrata Chakraborty, Dr. Yanfeng Jiang, Anne Landwehr and Dr. Alexander Dybov for the tremendous support and cooperation, especial during the time when we were fighting with ice and air in the glove box.

I also would like to thank my labmates Xianghua Yang and Dr. Chunfang Jiang for their kind help in the lab and in my life. Shiva Taghipourian and Dr. Marcello Bertolli for their guidance during the time I started working in the lab.

I would like to thank Hailin Dong and Xiaoqiong Wan for the encouragement. I also would like to thank Dr. Balz Dudle, Franziska Lissel and Michael Koch for their kind help during the time I prepared my thesis.

I am very grateful to all members of Berke group and all ACI members for the various help and cooperation, for the wonderful and memorable time that we spent together.

Financial support from the Swiss National Science Foundation, from the funds of the University of Zurich and from the graduate school of CMSZH is acknowledged.

Finally, I would like to express my gratitude to my family. My hearty thanks go to my parents and my mother-in-law and my father-in-law for their understanding and selfless love. And I greatly appreciate my beloved husband, Xiaolin Qin, for his support and encouragement. For years, it is his endless love gives me strength to overcome a variety of difficulties and setbacks. To him I dedicated this thesis.

Appendix

Crystal data and structure refinement of the complexes studied by X-ray diffraction

Table I.1. Crystal data and structure refinement for complexes *trans*-[ReCl(=C=CHSiMe$_3$)(PMe$_3$)$_4$] (**2**) and *trans*-[ReCl(=C=CH$_2$)(PMe$_3$)$_4$] (**3**)

Complexes	**2**	**3**
Empirical formula	$C_{23}H_{52}ClP_4ReSi$	$C_{14}H_{38}ClP_4Re$
Formula weight (g·mol^{-1})	702.28	551.98
Temperature (K)	183(2)	183(2)
Wavelength (Å)	0.71073	0.71073
Crystal system, space group	Monoclinic, $P2_1/c$	Tetragonal, I-42m
a (Å)	9.9893(2)	9.4806(2)
b (Å)	27.3501(5)	9.4806(2)
c (Å)	12.0368(2)	12.2198(7)
α (°)	90	90
β (°)	98.624(2)	90
γ (°)	90	90
V (Å^3)	3251.37(10)	1098.34(7)
Z, density (calculated) (mg/m^3)	4, 1.435	2, 1.669
Absorption coefficient (mm^{-1})	4.063	5.937
F (000)	1424	548
Crystal size (mm)	0.29 × 0.25 × 0.20	0.48 × 0.33 × 0.28
θ range for data collection (°)	2.54 to 30.51	2.72 to 32.56
Limiting indices	$-12 \le h \le 14$	$-14 \le h \le 12$
	$-39 \le k \le 39$	$-14 \le k \le 13$
	$-17 \le l \le 16$	$-18 \le l \le 18$

Reflections collected/unique	34655/9870 [R (int) = 0.0447]	4765/1082 [R (int) = 0.0413]
Completeness to θ	99.4% (θ = 30.51)	100.0% (θ = 32.56)
Absorption correction	Analytical	Analytical
Max. and min. transmission	0.56 and 0.44	0.31 and 0.19
Refinement method	Full-matrix least-squares on F^2	Full-matrix least-squares on F^2
Data / restraints / parameters	9870/0/278	1082/0/40
Goodness-of-fit on F^2	0.996	1.079
Final R indices [$I > 2\sigma$ (I)]	R_1 = 0.0282 wR_2 = 0.0605	R_1 = 0.0179 wR_2 = 0.0418
R indices (all data)	R_1 = 0.0438 wR_2 = 0.0630	R_1 = 0.0179 wR_2 = 0.0418
Largest diff. peak and hole (e.A^{-3})	1.064 and -0.817	1.036 and -0.805

Table I.2. Crystal data and structure refinement for complexes *trans*-[ReCl(≡C-CH_3)(PMe_3)$_4$][PF_6] (**5**) and *trans*-[Re(C≡C$SiMe_3$)(≡C-CH_3)(PMe_3)$_4$][PF_6] (**6**)

Complexes	**5**	**6**
Empirical formula	$C_{14}H_{39}ClF_6P_5Re$	$C_{19}H_{48}F_6P_5ReSi$
Formula weight ($g \cdot mol^{-1}$)	697.96	759.72
Temperature (K)	183(2)	183(2)
Wavelength (Å)	0.71073	0.71073
Crystal system, space group	Triclinic, *P*-1	Orthorhombic, $P2_12_12_1$
a (Å)	8.4391(1)	19.4556(3)
b (Å)	11.9301(1)	19.8765(2)
c (Å)	13.3966(2)	33.6182(5)
α (°)	83.710(1)	90
β (°)	82.451(1)	90
γ (°)	83.055(1)	90
V ($Å^3$)	1321.23(3)	13000.5(3)
Z, density (calculated) (mg/m^3)	2, 1.754	16, 1.553
Absorption coefficient (mm^{-1})	5.044	4.064
F (000)	688	6080
Crystal size (mm)	0.30 × 0.29 × 0.12	0.34 × 0.19 × 0.13
θ range for data collection (°)	2.42 to 30.51	2.30 to 25.68
Limiting indices	$-12 \le h \le 12$	$-20 \le h \le 23$
	$-17 \le k \le 17$	$-21 \le k \le 24$
	$-19 \le l \le 19$	$-30 \le l \le 40$
Reflections collected/unique	27508/8040 [*R* (int) = 0.0359]	67596/24381 [*R* (int) = 0.0525]
Completeness to θ	100.0% (θ = 30.51)	99.8% (θ = 25.68)
Absorption correction	Analytical	Analytical

Max. and min. transmission	0.63 and 0.29	0.668 and 0.496
Refinement method	Full-matrix least-squares on F^2	Full-matrix least-squares on F^2
Data / restraints / parameters	8040/0/257	24381/40/1176
Goodness-of-fit on F^2	1.017	0.942
Final R indices $[I > 2\sigma(I)]$	$R_1 = 0.0217$ $wR_2 = 0.0546$	$R_1 = 0.0413$ $wR_2 = 0.0834$
R indices (all data)	$R_1 = 0.0247$ $wR_2 = 0.0553$	$R_1 = 0.0614$ $wR_2 = 0.0866$
Largest diff. peak and hole ($e.A^{-3}$)	1.620 and -0.654	3.753 and -1.142

Table I.3. Crystal data and structure refinement for complexes *trans*-[X(PMe$_3$)$_4$Re≡C-CH$_2$-CH$_2$-C≡Re(PMe$_3$)$_4$X][PF$_6$]$_2$ (X = Cl, **9**; C≡CSiMe$_3$, **10**)

Complexes	**9**	**10**
Empirical formula	$C_{36}H_{88}Cl_2F_{12}N_4P_{10}Re_2$	$C_{38}H_{94}F_{12}P_{10}Re_2Si_2$
Formula weight (g·mol^{-1})	1558.13	1517.43
Temperature (K)	183(2)	183(2)
Wavelength (Å)	0.71073	0.71073
Crystal system, space group	Monoclinic, $P2_1/c$	Triclinic, P-1
a (Å)	16.7518(2)	10.1955(2)
b (Å)	16.8786(2)	10.4458(1)
c (Å)	23.6770(4)	15.8038(3)
α (°)	90	90.942(1)
β (°)	108.338(2)	108.673(1)
γ (°)	90	91.938(1)
V (Å^3)	6354.62(17)	1592.94(5)
Z, density (calculated) (mg/m^3)	4, 1.629	1, 1.582
Absorption coefficient (mm^{-1})	4.206	4.145
F (000)	3096	758
Crystal size (mm)	0.39 × 0.33 × 0.27	0.35 × 0.31 × 0.11
θ range for data collection (°)	2.56 to 30.51	2.41 to 32.58
Limiting indices	$-23 \le h \le 23$	$-15 \le h \le 15$
	$-24 \le k \le 13$	$-15 \le k \le 15$
	$-33 \le l \le 33$	$-23 \le l \le 23$
Reflections collected/unique	51907/19360 [R (int) = 0.0301]	45347/11599 [R (int) = 0.0396]
Completeness to θ	99.9% (θ = 30.51)	100.0% (θ = 32.58)
Absorption correction	Analytical	Analytical
Max. and min. transmission	0.40 and 0.27	0.717 and 0.308

Refinement method	Full-matrix least-squares on F^2	Full-matrix least-squares on F^2
Data / restraints / parameters	19360/0/623	11599/0/304
Goodness-of-fit on F^2	1.023	0.973
Final R indices $[I > 2\sigma(I)]$	$R_1 = 0.0333$ $wR_2 = 0.0784$	$R_1 = 0.0215$ $wR_2 = 0.0497$
R indices (all data)	$R_1 = 0.0536$ $wR_2 = 0.0815$	$R_1 = 0.0257$ $wR_2 = 0.0503$
Largest diff. peak and hole ($e.A^{-3}$)	1.573 and -1.438	1.510 and -1.090

Table I.4. Crystal data and structure refinement for complexes *trans*-[X(PMe_3)$_4$Re=C=CH-CH=C=Re(PMe_3)$_4$X] (X = Cl, **11**; C≡C$SiMe_3$, **12**)

Complexes	**11**	**12**
Empirical formula	$C_{61}H_{160}Cl_4P_{16}Re_4$	$C_{38}H_{92}P_8Re_2Si_2$
Formula weight ($g \cdot mol^{-1}$)	2276.05	1225.48
Temperature (K)	183(2)	183(2)
Wavelength (Å)	0.71073	0.71073
Crystal system, space group	Monoclinic, $C2/c$	Monoclinic, $P2_1/c$
a (Å)	23.8582(8)	15.5085(11)
b (Å)	16.4443(2)	9.9898(4)
c (Å)	18.8658(6)	18.9014(8)
α (°)	90.0	90
β (°)	136.406(6)	93.969(5)
γ (°)	90.0	90
V ($Å^3$)	5103.8(6)	2921.3(3)
Z, density (calculated) (mg/m^3)	2, 1.481	2, 1.393
Absorption coefficient (mm^{-1})	5.113	4.422
F (000)	2268	1236
Crystal size (mm)	0.20 × 0.11 × 0.06	0.27 × 0.17 × 0.08
θ range for data collection (°)	2.48 to 30.51	2.45 to 32.58
Limiting indices	$-34 \le h \le 33$	$-23 \le h \le 23$
	$-23 \le k \le 23$	$-15 \le k \le 15$
	$-26 \le l \le 26$	$-28 \le l \le 28$
Reflections collected/unique	48101/7793 [R (int) = 0.0306]	60610 /10640 [R (int) = 0.0534]
Completeness to θ	99.9% (θ = 30.51)	100.0% (θ = 32.58)
Absorption correction	Analytical	Analytical
Max. and min. transmission	0.753 and 0.462	0.719 and 0.412

Refinement method	Full-matrix least-squares on F^2	Full-matrix least-squares on F^2
Data / restraints / parameters	7793/7/239	8371/0/241
Goodness-of-fit on F^2	1.087	1.018
Final R indices $[I > 2\sigma(I)]$	$R_1 = 0.0202$ $wR_2 = 0.0647$	$R_1 = 0.0280$ $wR_2 = 0.0600$
R indices (all data)	$R_1 = 0.0270$ $wR_2 = 0.0656$	$R_1 = 0.0375$ $wR_2 = 0.0623$
Largest diff. peak and hole ($e.A^{-3}$)	1.152 and -0.491	1.517 and -0.899

Table I.5. Crystal data and structure refinement for complexes *trans*-[X(PMe$_3$)$_4$Re≡C-CH=CH-C≡Re(PMe$_3$)$_4$X][PF$_6$] (X = Cl, **11[PF$_6$]**; C≡CSiMe$_3$, **12[PF$_6$]**)

Complexes	**11[PF$_6$]**	**12[PF$_6$]**
Empirical formula	$C_{28}H_{74}Cl_2F_6P_9Re_2$	$C_{80}H_{192}F_{12}OP_{18}Re_4Si_4$
Formula weight (g·mol^{-1})	1246.92	2813.01
Temperature (K)	183(2)	183(2)
Wavelength (Å)	0.71073	0.71073
Crystal system, space group	Monoclinic, $C2/c$	Monoclinic, $P2_1/c$
a (Å)	23.8733(9)	10.0523(1)
b (Å)	16.3419(2)	21.4240(2)
c (Å)	17.5388(7)	30.5215(3)
α (°)	90	90
β (°)	135.308(7)	92.588(1)
γ (°)	90	90
V (Å^3)	4812.3(7)	6566.42(11)
Z, density (calculated) (mg/m^3)	4, 1.721	2, 1.423
Absorption coefficient (mm^{-1})	5.480	3.981
F (000)	2460	2828
Crystal size (mm)	0.44 × 0.08 × 0.07	0.35 × 0.19 × 0.07
θ range for data collection (°)	2.49 to 26.37	2.67 to 25.00
Limiting indices	$-29 \le h \le 29$	$-11 \le h \le 11$
	$-20 \le k \le 20$	$-25 \le k \le 25$
	$-21 \le l \le 21$	$-36 \le l \le 28$
Reflections collected/unique	26240/4900 [R (int) = 0.0327]	48173/11516 [R (int) = 0.0365]
Completeness to θ	99.8% (θ = 26.37)	99.7% (θ = 25.00)
Absorption correction	Analytical	Analytical

Max. and min. transmission	0.710 and 0.284	0.758 and 0.429
Refinement method	Full-matrix least-squares on F^2	Full-matrix least-squares on F^2
Data / restraints / parameters	4349/0/252	5860/7/564
Goodness-of-fit on F^2	1.090	0.879
Final R indices $[I > 2\sigma(I)]$	$R_1 = 0.0402$ $wR_2 = 0.1175$	$R_1 = 0.0379$ $wR_2 = 0.1145$
R indices (all data)	$R_1 = 0.0439$ $wR_2 = 0.1188$	$R_1 = 0.0649$ $wR_2 = 0.1241$
Largest diff. peak and hole (e.A^{-3})	6.437 and -0.952	3.634 and -0.520

Table I.6. Crystal data and structure refinement for complexes *trans*-[X(PMe$_3$)$_4$Re≡C-CH=CH-C≡Re(PMe$_3$)$_4$X][PF$_6$]$_2$ (X = Cl, **11[PF$_6$]$_2$**; C≡CSiMe$_3$, **12[PF$_6$]$_2$**)

Complexes	**11[PF$_6$]$_2$**	**12[PF$_6$]$_2$**
Empirical formula	$C_{36}H_{86}Cl_2F_{12}N_4P_{10}Re_2$	$C_{40}H_{96}Cl_4F_{12}P_{10}Re_2Si_2$
Formula weight (g·mol^{-1})	1556.11	1685.27
Temperature (K)	183(2)	183(2)
Wavelength (Å)	0.71073	0.71073
Crystal system, space group	Triclinic, *P*-1	Orthorhombic, *Pnnm*
a (Å)	12.7521(2)	16.0272(4)
b (Å)	16.7487(3)	15.8081(3)
c (Å)	16.8775(3)	14.4694(3)
α (°)	89.868(1)	90
β (°)	72.390(2)	90
γ (°)	68.702(2)	90
V (Å^3)	3177.56(11)	3665.96(14)
Z, density (calculated) (mg/m^3)	2, 1.626	2, 1.527
Absorption coefficient (mm^{-1})	4.206	3.752
F (000)	1544	1680
Crystal size (mm)	0.38 × 0.24 × 0.12	0.37 × 0.28 × 0.25
θ range for data collection (°)	2.55 to 30.51	2.54 to 30.50
Limiting indices	$-18 \le h \le 17$	$-22 \le h \le 20$
	$-23 \le k \le 23$	$-21 \le k \le 22$
	$-24 \le l \le 24$	$-20 \le l \le 12$
Reflections collected/unique	54153/19377 [*R* (int) = 0.0288]	18981/5804 [*R* (int) = 0.0322]
Completeness to *θ*	99.9% (*θ* = 30.51)	99.9% (*θ* = 30.50)
Absorption correction	Analytical	Analytical

Max. and min. transmission	0.738 and 0.347	0.487 and 0.379
Refinement method	Full-matrix least-squares on F^2	Full-matrix least-squares on F^2
Data / restraints / parameters	19377/30/622	5804/3/196
Goodness-of-fit on F^2	1.068	0.969
Final R indices $[I > 2\sigma(I)]$	$R_1 = 0.0308$ $wR_2 = 0.0816$	$R_1 = 0.0308$ $wR_2 = 0.0674$
R indices (all data)	$R_1 = 0.0430$ $wR_2 = 0.0836$	$R_1 = 0.0501$ $wR_2 = 0.0704$
Largest diff. peak and hole ($e.A^{-3}$)	2.053 and -1.169	0.827 and -0.679

Table I.8. Crystal data and structure refinement for complexes *trans*-[X(PMe$_3$)$_4$Re≡C-C≡C-C≡Re(PMe$_3$)$_4$X][PF$_6$] (X = Cl, **14[PF$_6$]$_2$**; C≡CSiMe$_3$, **15[PF$_6$]$_2$**)

Complexes	**14[PF$_6$]$_2$**	**15[PF$_6$]$_2$**
Empirical formula	$C_{32}H_{78}Cl_2F_{12}N_2P_{10}Re_2$	$C_{40}H_{94}Cl_4F_{12}P_{10}Re_2Si_2$
Formula weight (g·mol^{-1})	1471.98	1683.25
Temperature (K)	183(2)	183(2)
Wavelength (Å)	0.71073	0.71073
Crystal system, space group	Triclinic, *P*-1	Orthorhombic, *Pnnm*
a (Å)	16.7250(2)	16.2406(2)
b (Å)	19.2386(2)	15.7552(2)
c (Å)	22.9508(3)	14.4581(2)
α (°)	104.928(1)	90
β (°)	105.099(1)	90
γ (°)	107.392(1)	90
V (Å^3)	6336.83(16)	3699.45(8)
Z, density (calculated) (mg/m^3)	4, 1.543	2, 1.511
Absorption coefficient (mm^{-1})	4.212	3.718
F (000)	2904	1676
Crystal size (mm)	0.34 × 0.26 × 0.08	0.45 × 0.21 × 0.19
θ range for data collection (°)	2.53 to 30.51	2.59 to 30.50
Limiting indices	$-23 \le h \le 23$	$-20 \le h \le 23$
	$-27 \le k \le 27$	$-22 \le h \le 22$
	$-32 \le l \le 32$	$-20 \le h \le 16$
Reflections collected/unique	139164/38664 [*R* (int) = 0.0414]	31036/5859 [*R* (int) = 0.0409]
Completeness to *θ*	99.9% (*θ* = 30.51)	99.9% (*θ* = 30.50)
Absorption correction	Analytical	Analytical

Max. and min. transmission	0.734 and 0.346	0.570 and 0.358
Refinement method	Full-matrix least-squares on F^2	Full-matrix least-squares on F^2
Data / restraints / parameters	38664/195/1123	5859/3/189
Goodness-of-fit on F^2	0.976	0.981
Final R indices $[I > 2\sigma(I)]$	$R_1 = 0.0411$ $wR_2 = 0.1158$	$R_1 = 0.0257$ $wR_2 = 0.0657$
R indices (all data)	$R_1 = 0.0714$ $wR_2 = 0.1209$	$R_1 = 0.0383$ $wR_2 = 0.0676$
Largest diff. peak and hole ($e.A^{-3}$)	2.185 and -1.455	1.678 and -0.562

Table I.9. Crystal data and structure refinement for complexes *trans*-[I(PMe$_3$)$_4$Re≡C-C≡C-C≡Re(PMe$_3$)$_4$I][PF$_6$]$_2$ **16[PF$_6$]$_2$**

Complex	**16[PF$_6$]$_2$**
Empirical formula	$C_{38}H_{89}F_{12}I_2N_5P_{10}Re_2$
Formula weight (g·mol^{-1})	1780.07
Temperature (K)	183(2)
Wavelength (Å)	0.71073
Crystal system, space group	Monoclinic, $P2_1/n$
a (Å)	16.8475(3)
b (Å)	16.7922(2)
c (Å)	25.6311(4)
α (°)	90
β (°)	103.991
γ (°)	90
V (Å^3)	7036.1(2)
Z, density (calculated) (mg/m^3)	4, 1.680
Absorption coefficient (mm^{-1})	4.603
F (000)	3464
Crystal size (mm)	0.48 × 0.35 × 0.25
θ range for data collection (°)	2.56 to 28.28 deg.
Limiting indices	$-22 \le h \le 22$
	$-22 \le k \le 22$
	$-34 \le l \le 34$
Reflections collected/unique	111267/17463 [R (int) = 0.0358]
Completeness to θ	99.9% (θ = 28.28)
Absorption correction	Analytical

Max. and min. transmission	0.415 and 0.246
Refinement method	Full-matrix least-squares on F^2
Data / restraints / parameters	13875/135/599
Goodness-of-fit on F^2	1.069
Final R indices $[I > 2\sigma(I)]$	$R_1 = 0.0580$ $wR_2 = 0.1530$
R indices (all data)	$R_1 = 0.0725$ $wR_2 = 0.1584$
Largest diff. peak and hole ($e.A^{-3}$)	4.079 and -3.278

Curriculum Vitae

PERSONAL INFORMATIONS:

Name:	Yan Li
Sex:	Female
Date of birth:	November 10th, 1974
Marital status:	Married
Nationality:	P. R. China
E-mail:	yanli@aci.uzh.ch
Tel:	00 41 44 6354698 (Lab)
	00 41 78 9209073 (Mobile)
Address:	Flühgasse 32
	CH-8008, Zürich
	Switzerland

EDUCATION:

01/2007 – present	Anorganisch-Chemisches Institüt
	Universität Zürich
	Switzerland
	PhD candidate (Organometallic chemistry)
	Title of thesis: Syntheses and Physical Studies of Dinuclear Rhenium Complexes as Precursors for Potential Molecular Wire Applications
	Supervisor: Prof. Dr. Heinz. Berke
09/2003 – 06/2006	School of Chemistry and Chemical Engineering
	Guangxi Normal University
	P. R. China
	Master of Sicence (M.Sc, Inorganic chemistry)
	Title of thesis: Studies on Complexes of N-(2-pyridylmethyl)iminodiacetic Acid (Investigation of the influences of reaction conditions on the crystal structures and the relationship

between the structures and properties).
Supervisor: Prof. Dr. Fupei Liang
Defense: June 4th, 2006

09/1992 – 06/1996 School of Chemistry and Chemical Engineering
Guangxi University
P. R. China
Bachelor of Engineering (B.Eng, Chemical engineering)
Title of thesis: Chemical Process Design for Polyvinyl Chloride (PVC) Manufacturing
Supervisor: Prof. Lijuan Xie
Defense: June 1996

09/1989 – 06/1992 Yishan Senior High School
Guangxi
P. R. China
Senior high school student

WORKING EXPERIENCE:

2/2000 – 9/2003 Guilin Technical Secondary School of Forestry
Guangxi
P. R. China
Teacher of chemistry
Teaching Courses: Chemistry, Analytic Chemistry, Environmental Engineering, Environmental Monitoring

7/1996 – 2/2000 Liuzhou Chemical Industry Co. Ltd.
Guangxi
P. R. China
11/1998 – 2/2000 Chief of technology section of chemical subsidiary company including soda plant, methanol and formaldehyde plant and osmanthus concrete and jasmine concrete plant
7/1997 – 11/1998 Technician of methanol and formaldehyde plant
7/1996 – 7/1997 Operator of methanol and formaldehyde plant

ACADEMIC PUBLICATIONS:

1. Zilu Chen, **Yan Li**, Chunfang Jiang, Fupei, Liang, You Song, "Metal complexes with N-(2-pyridylmethyl)iminodiacetate: from discrete polynuclear compounds to 1D coordination polymers", *Dalton Trans*., **2009**, 5290-5299.
2. **Yan Li**, Fupei Liang, Chunfang Jiang, Xiaoling Li, Zilu Chen, "2D network coordination polymers of lanthanide with N-(2-pyridylmethyl)iminodiacetic acid: Hydromthermal systheses, crystal structures and luminescent properties", *Inorg. Chim. Acta*., **2008**, *361*, 219-225.
3. Chunfang Jiang, **Yan Li**, Fupei Liang, "Synthesis and crystal structure of complex $[Mn^{II}Mn_2^{III}(H_2L)_2(CH_3COO)_4(CH_3OH)_2]\cdot H_2O\cdot CH_3OH$", *Guangxi Shifan Daxue Xuebao, Ziran Kexueban*, **2008**, *26*, 66-70.
4. Chunfang Jiang, **Yan Li**, Fupei Liang, Weihong Yan, Yan Tang, "Preparation of manganese carbonate crystal through ligand's decomposition under hydrothermal condition", *Guangxi Shifan Daxue Xuebao, Ziran Kexueban*, **2007**, *25*, 58-61.
5. Chunfang Jiang, Fupei, Liang, **Yan Li**, Xiujian Wang, Zilu Chen, Hedong Bian, "Synthesis, characterization and magnetic properties of copper (II) complexes with 4-N-(2'pyridylimine)benzoic acid", *J. Mol. Struct*., **2007**, *842*, 109-116.
6. Fupei Liang. Miaoling Huang, Chunfang Jiang, **Yan Li**, Ruixiang Hu, "Syntheses, structures and magnetic properties of isonicotinate-bridged heterometallic Ln(III)-Cu(II) coordination polymers", *J. Coord. Chem*., **2007**, *60*, 2343-2350.